

This electronic thesis or dissertation has been downloaded from the King's Research Portal at <https://kclpure.kcl.ac.uk/portal/>



Improving the Sensitivity and Specificity of LC/MS to Enable Bioanalysis of Therapeutic and Endogenous Proteins and Peptides

Chambers, Erin

Awarding institution:
King's College London

The copyright of this thesis rests with the author and no quotation from it or information derived from it may be published without proper acknowledgement.

END USER LICENCE AGREEMENT



Unless another licence is stated on the immediately following page this work is licensed

under a Creative Commons Attribution-NonCommercial-NoDerivatives 4.0 International

licence. <https://creativecommons.org/licenses/by-nc-nd/4.0/>

You are free to copy, distribute and transmit the work

Under the following conditions:

- Attribution: You must attribute the work in the manner specified by the author (but not in any way that suggests that they endorse you or your use of the work).
- Non Commercial: You may not use this work for commercial purposes.
- No Derivative Works - You may not alter, transform, or build upon this work.

Any of these conditions can be waived if you receive permission from the author. Your fair dealings and other rights are in no way affected by the above.

Take down policy

If you believe that this document breaches copyright please contact librarypure@kcl.ac.uk providing details, and we will remove access to the work immediately and investigate your claim.



Improving the Sensitivity and Specificity of LC/MS to
Enable Bioanalysis of Therapeutic and Endogenous
Proteins and Peptides

A thesis submitted in partial fulfillment of the requirements
for the degree of Doctor of Philosophy

Erin E. Chambers

September 2014

Analytical and Environmental Sciences Research Division

School of Biomedical Sciences

King's College London

Dedication

For my late grandfather Walter C. Beard Jr., whose knowledge of chemistry and whose wonderful inventions have inspired me from a very young age

Acknowledgements

The author would like to acknowledge a few key individuals, without whom this research , writing, and PhD journey would not have been possible.

Dr. Robert Plumb. As my “unofficial” mentor, Robert’s constant encouragement, tireless reading of chapters, and thoughtful guidance helped make my studies and this thesis possible. Robert has been my constant coach , advocate, and guide during this process. My appreciation for his support can not be expressed enough.

My supervisors Dr. Norman Smith and Dr. Cristina Legido-Quigley. I will be forever grateful to Norman for accepting me into his lab as a PhD student. Norman has made it possible for me to complete a task I never thought possible. He and Cristina have given me the latitude and flexibility to work on my studies and thesis while working a full-time job. I can not express enough what this opportunity has meant to me personally. I would also like to thank Norman for his hilarious anecdotes, and endless positive outlook, which always showed up just when I needed encouragement the most.

Dr. Paul Rainville. Throughout my journey, I have benefitted tremendously from Paul’s help in navigating the logistics of the PhD process. I would like to thank Paul for answering countless questions and for serving as a valued colleague and mentor to me.

Dr. Diane Diehl. Diane was my supervisor when I initially decided to pursue my PhD.

Without Diane's initial support and encouragement, this PhD would not be possible. Diane has always and will continue to serve as an inspiration and role model for me in both my career and life.

Kenneth J. Fountain. As my current supervisor and supervisor for the majority of PhD studies, I would especially like to thank Ken for giving me the time and flexibility to pursue projects which both benefitted Waters and allowed me to complete my degree research.

Mary E. Lame. I would like to thank my valued friend and colleague Mary for her encouragement, support, friendship and partnership in the lab.

Waters Corporation, Dr. Michael Yelle and my colleagues Dr. Claude Mallet, Dr. Thomas Wheat, Dr. Steve Koza and the late Dr. Uwe Neue. Without Waters and Mike Yelle's approval and financial support, I would not have been able to pursue this degree. My colleagues Claude, Tom, Steve and Uwe all provided critical scientific discussions relating to chromatography, insulin analysis, and/or large molecule behaviour.

My family and my dear husband Christopher. Last, and certainly not least, I would like to thank my two sweet little girls and my dear, dear husband Chris who made it possible for me to put in all the extra time and work necessary to complete these studies. I can not express enough what it has meant to me to have their support through this process. I would

also like to thank my mother and father for their constant encouragement and for instilling in me the necessary strength, commitment and fortitude to undertake this task. I hope that in some way, I will one day be a source of inspiration for my little girls, Ava and Molly, who were born during the course of these studies.

Abstract

This thesis establishes LC/MS as a viable, robust, and attractive alternative analytical platform to ligand binding assays for the quantification of therapeutic and endogenous peptides/proteins in biological fluids. A rigorous investigation of the parameters that affect assay sensitivity, specificity and robustness revealed that a careful combination of mixed-mode solid phase extraction, reversed-phase liquid chromatography utilizing sub 2 μ m charged surface solid core stationary phases, coupled to tandem quadrupole mass spectrometry can deliver a generic platform for assay development. By extending the innovations developed in the initial work to a micro-fluidic scale it was possible to both reduce sample consumption and increase assay sensitivity by up to 20-30 fold. The value of this approach was demonstrated with subsequent validation (to FDA guidelines) of 5 separate ultra-high sensitivity assays for large hydrophobic peptides using this approach.

The initial studies focused on understanding the factors that influence LC/MS assay performance for the quantification of biotherapeutics and biomarkers in biofluids. This was divided into three discrete sections: sample preparation, liquid chromatography and mass spectrometry. This investigation produced a comprehensive set of rules and guidelines to be applied during LC/MS method development for biologics quantification. From an MS perspective, these included (but were not limited to) the recommendation to choose the highest precursor/product pairs possible, avoid immonium ions, monitor multiple MRM transitions during method development, and the importance of tuning at the chromatographic flow rate was also noted. The liquid chromatography studies revealed that

sub-2 μm superficially porous particles with larger pore size, and/or positively charged surface stationary phases, produced the highest efficiency and most sensitive separations, at flow rates that yield throughputs compatible with routine bioanalytical work. In addition, it was discovered that decreasing the flow rate, lowering the gradient slope, and increasing temperature could all reduce carryover and increase sensitivity further for many peptide analyses.

The rules derived from the basic research were then applied to the development of assays for teriparatide (an osteoporosis drug), amyloid beta peptides (putative Alzheimer's disease biomarkers) and human insulin and five analogs. Implementing a protein precipitation plasma pre-treatment step to reduce endogenous background was combined with SPE and chromatography based on a charged surface column to yield a quantification limit of 15 pg/mL teriparatide from 200 μL human plasma. A key aspect of amyloid beta measurement in human cerebrospinal fluid included a guanidine HCl pre-treatment step which eliminated aggregation and protein binding, enabling accurate and precise quantification of total amyloid beta, with a quantification limit of <40 pg/mL from 100 μL human cerebrospinal fluid. Protein precipitation and mixed-mode anion exchange SPE coupled to a multidimensional chromatographic system enabled differentiation of human insulin from Humalog even though they share many of the preferred product ions, have the same precursor masses, and co-elute. The achieved detection limit of 50 pg/mL (8.6 fmol/mL) enabled measurement of fasting insulin levels. The developed method was applied in the analysis of a cohort of Type I and Type II diabetic patients on a variety of combination therapies.

It has long been known that low-flow LC has significant advantages for high sensitivity analysis when coupled to MS. However, the lack of robustness and long analysis times associated with early hardware, limited its widespread use. The initial work on teriparatide and insulin analysis as well as additional work on endogenous and injected glucagon were adapted to a new prototype integrated micro-fluidic device, resulting in a 20-30 fold overall sensitivity improvement. In addition, analysis of small cyclic peptides was performed at both 2.1 mm ID and 150 μ m ID scale, the latter enabling quantification of desmopressin from 20 fold less sample with a quantification limit of approximately 6.5 amol on column, or 2.5 pg/mL from 25 μ L human plasma.

As a result of this work, LC/MS is now a viable alternative to traditional LBA for PK studies and biomarker validation, showing the necessary throughput, sensitivity and robustness. Added to this, the assays also have greater precision, wider dynamic range and less cross reactivity, facilitating greater confidence in the derived results, faster assay development times and the ability to distinguish subtle differences in patient populations, for example.

Table of Contents

| | |
|--|-----------|
| Dedication | 2 |
| Acknowledgements..... | 3 |
| Abstract | 6 |
| List of Figures..... | 16 |
| List of Tables | 33 |
| List of Equations | 38 |
| List of Symbols and Abbreviations..... | 40 |
| Chapter 1..... | 47 |
| Introduction | 47 |
| 1.1 Peptides and Proteins as Drugs | 48 |
| 1.1.1 Biosimilars | 50 |
| 1.1.2 Biomarkers | 52 |
| 1.2 Bioanalysis of Biopharmaceuticals and Biomarkers | 53 |
| 1.3 Pros and Cons of Traditional Quantitative Assays for Biotherapeutics | 58 |
| 1.4 Overview of Modern Liquid Chromatography (LC)..... | 59 |
| 1.4.1 Brief History of Chromatography | 60 |
| 1.4.2 LC Theory | 62 |

| | |
|---|------------|
| 1.4.3 UPLC Systems | 68 |
| 1.4.4 A Review of LC for Peptide Quantification..... | 69 |
| 1.5 Overview of Modern Mass Spectrometry | 73 |
| 1.5.1 Principles of Mass Spectrometry and Common Components..... | 73 |
| 1.5.2 MS Analyzers Most Frequently Used in Bioanalysis (BA) | 75 |
| 1.5.3 Electrospray Ionization | 77 |
| 1.6 LC/MS for Biopharmaceutical Quantification..... | 78 |
| 1.7 Identifying and Understanding Handling Considerations..... | 81 |
| 1.7.1 Solubility | 82 |
| 1.7.2 Adsorption..... | 83 |
| 1.7.3 Stability | 86 |
| 1.8 Alternative Techniques and Topics..... | 87 |
| 1.9 Research Aims..... | 90 |
| 1.10 References | 92 |
| Chapter Two | 107 |
| Investigating Sample Preparation, LC and MS for Large Molecule Quantification: Development of Basic Screening Tools and Guidelines for LC/MS Bioanalytical Assays for Biopharmaceuticals | 107 |
| 2.1 Introduction | 108 |
| 2.2 Section I. Investigation into Parameters Affecting LC of Large Molecules | 110 |

| | |
|--|------------|
| 2.2.1 Influence of Particle Size | 110 |
| 2.2.2 Influence of Ligand | 116 |
| 2.2.3 Influence of Chromatographic Pore Size | 119 |
| 2.2.4 Charged Surface and Fully Porous versus Solid Core Particles..... | 119 |
| 2.3 Recommendation for a Generic LC screening process | 127 |
| 2.4 Section II. Investigation into Mass Spectrometry in Bioanalysis of Large Molecules | 136 |
| 2.4.1 Introduction | 136 |
| 2.4.2 MS Guidelines for Peptide Quantification | 139 |
| 2.5 Section III. Peptide Extraction and Sample Preparation | 146 |
| 2.5.1 Understanding the Differences Between Sample Preparation Techniques and Impact on Results | 146 |
| 2.5.2 Proposed Peptide Extraction Screening Protocol..... | 160 |
| 2.5.3 Recommendations for Troubleshooting | 164 |
| 2.5.4 Exploring Large Pore Size SPE Sorbents | 166 |
| 2.6 Examples of Semi-validated Methods for Small Peptides | 174 |
| 2.7 Summary of Key Rules and Guidelines Established in This Chapter..... | 177 |
| 2.8 Conclusions | 180 |
| 2.9 References | 182 |
| Chapter 3..... | 186 |

| | |
|--|------------|
| Developing a High Sensitivity LC-MS/MS Method for Direct Quantification of Human Parathyroid 1-34 (Teriparatide) in Human Plasma..... | 186 |
| 3.1 Introduction | 187 |
| 3.2 Experimental | 190 |
| 3.2.1 Chemicals and Reagents..... | 190 |
| 3.2.2 Preparation of samples, calibration standards and quality control samples | 190 |
| 3.2.3 Sample Preparation | 191 |
| 3.2.4 Chromatographic Conditions | 192 |
| 3.2.5 Mass spectrometry and Software | 192 |
| 3.3 Results and Discussion..... | 193 |
| 3.3.1 Development of sample pre-treatment and solid-phase extraction | 193 |
| 3.3.2 Mass Spectrometry of Teriparatide | 198 |
| 3.3.3 Liquid Chromatography | 201 |
| 3.3.4 Human Plasma Standard Curve and Quality Control Data | 205 |
| 3.3.5 Specificity..... | 210 |
| 3.5 Conclusions | 211 |
| 3.6 References | 213 |
| Chapter 4..... | 217 |
| Quantification of Amyloid beta peptides, Putative Alzheimer’s Disease Biomarkers | 217 |

| | |
|--|------------|
| 4.1 Introduction | 218 |
| 4.2 Experimental | 222 |
| 4.2.1 Chemicals and Reagents..... | 222 |
| 4.2.2 Preparation of samples, calibration standards and quality control samples | 223 |
| 4.2.3 Solid-phase extraction conditions | 224 |
| 4.2.4 Ultra-performance liquid chromatography tandem mass spectrometry | 224 |
| 4.3 Results | 226 |
| 4.3.1 Sample pre-treatment and solid-phase extraction recoveries | 226 |
| 4.3.2 LC-MS/MS Analysis of A β Peptides | 227 |
| 4.4 Discussion | 242 |
| 4.5 Additional Investigations in Support of Candidate Reference Method Development and Progression | 247 |
| 4.6 Conclusions | 251 |
| 4.7 References | 252 |
| Chapter 5..... | 258 |
| Investigation into Intact Insulin Quantification Using Single or Multidimensional Chromatography and Reversed-phase or Mixed-mode SPE | 258 |
| Section I: Initial Proof of Concept Investigation | 260 |
| 5.1 Introduction | 260 |
| 5.2 Experimental | 266 |

| | |
|---|------------|
| 5.3 Results and Discussion..... | 269 |
| 5.4 Conclusions from Initial Proof of Concept Studies | 292 |
| Section II Improved Sensitivity and Specificity Using Multidimensional LC and Mixed-mode SPE | 294 |
| 5.5 Introduction | 294 |
| 5.6 Experimental for Improved Insulin Assay | 297 |
| 5.7 Results and Discussion..... | 302 |
| 5.8 Conclusions on the Use of Multidimensional LC and Improved Sample Preparation for Insulin Quantification..... | 322 |
| 5.9 References | 324 |
| Chapter 6..... | 332 |
| Preliminary Investigations into the Benefits of Integrated Microscale LC for Peptide Quantification | 332 |
| 6.1 Introduction | 333 |
| 6.2 Experimental | 335 |
| 6.2.1 Source of Reagents and Preparation of Stock Solutions | 335 |
| 6.2.2 Sample preparation..... | 335 |
| 6.2.3 Liquid Chromatography | 335 |
| 6.2.4 Mass Spectrometry | 338 |
| 6.2.5 Sample Preparation | 339 |

| | |
|--|------------|
| 6.3 Results and Discussion..... | 339 |
| 6.3.1 Chromatographic Method Development..... | 339 |
| 6.3.2 Sensitivity, Linearity, Accuracy and Precision | 348 |
| 6.4 Conclusions | 359 |
| 6.5 References | 360 |
| Chapter 7..... | 362 |
| Final Conclusions and Recommendations for Future Work | 362 |
| 7.1 Final Conclusions..... | 363 |
| 7.2 Recommendations for Future Work..... | 368 |
| 7.3 References | 371 |

List of Figures

| | |
|---|----|
| Figure 1.1 Important biotherapeutics coming off patent and open to biosimilars competition..... | 51 |
| Figure 1.2 Process flow for the development of novel protein biomarker candidates..... | 53 |
| Figure 1.3 Representative PK profile obtained by plotting changes in plasma drug concentrations over time..... | 55 |
| Figure 1.4 van Deemter curve with individual components..... | 68 |
| Figure 1.5 Mass spectra for the peptide bradykinin acquired under various resolution conditions..... | 76 |
| Figure 1.6 Graphical representation of the electrospray ionization process..... | 78 |
| Figure 1.7 MS spectra for the singly charged small molecule imipramine (top left) and a multiply charged peptide bivalirundin (bottom right)..... | 80 |
| Figure 1.8 Comparison of a 1D separation (A) of desmopressin and octreotide and a 2D separation (B)..... | 88 |

| | |
|---|-----|
| Figure 2.1 van Deemter plot, for theoretical compounds representing a small molecule and different sized peptides, constructed using flow rate expected for a 2.1 mm column..... | 112 |
| Figure 2.2 Calculated van Deemter plot, using flow rate, for a model peptide analyzed on a 2.1 mm column packed with 1.7 and 3.5 μm particles..... | 113 |
| Figure 2.3 Representative chromatogram of 50 ng/mL desmopressin separated on columns packed with the same stationary phase in 1.7 or 3.5 μm particles. The Table on the right summarizes results from other peptide analytes showing even greater benefits from using sub 2 μm materials..... | 115 |
| Figure 2.4 Separation of enfuvirtide on ACQUITY BEH C ₁₈ 130Å, 300Å and BEH C ₄ ... | 117 |
| Figure 2.5 Separation of teriparatide (MW 4117) on an ACQUITY UPLC CSH C ₁₈ and ACQUITY BEH 300 C ₁₈ ; the same mobile phases, sample, and gradients were used.... | 118 |
| Figure 2.6A Summary of relative peak areas for test peptides separated on either a silica hybrid C18 (BEH 300Å) or solid core charged surface silica (CORTECS C18+ 90 Å) column using either 0.5% TFA or 1% FA as the injection solvent..... | 122 |
| Figure 2.6B Summary of relative peak area for test peptides separated on the four columns in Table 2.2, using a flow rate of either 0.25 or 0.4 mL/min..... | 122 |

| | |
|---|-----|
| Figure 2.6C Summary of relative retention for test peptides separated on the four columns described in Table 2.2, using a flow rate of 0.4 mL/min and 1% FA as the injection solvent..... | 123 |
| Figure 2.6D Summary of relative peak widths for test peptides separated on the four columns described in Table 2.2, using a flow rate of 0.4 mL/min and 1% FA as the injection solvent..... | 123 |
| Figure 2.6E Summary of relative peak areas for test peptides separated on the four columns described in Table 2.2, using a flow rate of 0.4 mL/min and 1% FA as the injection solvent..... | 124 |
| Figure 2.6F Comparison of peak widths for melittin on four different columns..... | 124 |
| Figure 2.6G Comparison of peak widths for bovine insulin on four different columns... | 125 |
| Figure 2.6H Comparison of peak widths for teriparatide on four different columns..... | 125 |
| Figure 2.7 Representative separation of 5 peptide therapeutics using the proposed LC screening..... | 130 |
| Figure 2.8 The effect of column temperature on area count for amyloid beta 1-40 (MW 4330)..... | 132 |

| | |
|--|-----|
| Figure 2.9 The effect of flow rate on area count for amyloid beta 1-40 (MW 4330)..... | 132 |
| Figure 2.10 The influence of gradient slope on peak area for teriparatide (MW 4117): column temperature is 60°C and flow rate is 0.4 mL/min..... | 133 |
| Figure 2.11 A comparison of peak area for teriparatide when either 0.1% FA or 0.1% FA + 5% TFE are used in acetonitrile as the B mobile phase..... | 134 |
| Figure 2.12 The influence of the addition of rat plasma as carrier protein on the peak shape of teriparatide (2.12A) and a comparison of two carrier protein options (2.12B) | 136 |
| Figure 2.13 MS spectra for 500 pg/mL glucagon extracted from human plasma. Top panel was acquired using an MRM transition corresponding to an ammonia loss; bottom panel was acquired using an MRM transition corresponding to a specific b/y ion..... | 141 |
| Figure 2.14 Analysis of amyloid beta 1-38 using MRM transitions for the same precursor to fragment pair derived from either monitoring the 4 th (top) or 5 th (bottom) charge states... | 142 |
| Figure 2.15 MSMS analysis of insulin lispro using either a 5+ (top) or 6+ (bottom) precursor paired to a 217 fragment..... | 143 |
| Figure 2.16 MS analysis of enfuvirtide (MW 4492)..... | 144 |

| | |
|--|-----|
| Figure 2.17 MSMS of the doubly charged bivalirudin precursor at m/z 1091..... | 145 |
| Figure 2.18 Level of phospholipids remaining in elution solvents based on ACN (top) and MeOH (bottom)..... | 149 |
| Figure 2.19A Comparison of level of human albumin remaining in supernatant after 1:1 PPT with either 100 or 70% ACN..... | 150 |
| Figure 2.19B Comparison of levels of various proteins remaining in supernatant after protein precipitation with either 100 or 70% ACN..... | 150 |
| Figure 2.20 Effect of various pretreatment options on the recovery of teriparatide from human plasma..... | 151 |
| Figure 2.21 Absolute recovery (left) and matrix effects (right) for bivalirudin and desmopressin using a variety of different common sample preparation techniques.... | 157 |
| Figure 2.22 Recovery for desmopressin and bivalirudin extracted from human plasma using four mixed-mode SPE sorbents..... | 158 |
| Figure 2.23 Well design for Waters μ Elution format 96-well extraction plate..... | 161 |

| | |
|---|-----|
| Figure 2.24 Recovery for 12 test peptides extracted from human plasma using the proposed SPE screening method..... | 162 |
| Figure 2.25 SPE recovery of test proteins in final eluate from a 20 µm wide pore sorbent, a 20 µm typical pore size sorbent, and a 30 µm typical pore size sorbent..... | 168 |
| Figure 2.26 SPE recovery of test proteins in load fraction from a 20 µm wide pore sorbent, a 20 µm typical pore size sorbent, and a 30 µm typical pore size sorbent..... | 168 |
| Figure 2.27A Recovery in final SPE elution for test proteins on wide pore and standard pore size 20 µm sorbents..... | 169 |
| Figure 2.27B Recovery in SPE final elution for mouse murine IgG on wide pore and standard pore size 20 µm sorbents as well as 30 µm standard pore size sorbents..... | 170 |
| Figure 2.28 Recovery of various test proteins using different concentrations of acetonitrile in the elution solvent..... | 171 |
| Figure 2.29 Extraction recovery of proteins from either human plasma or solvent standards using a wide pore prototype (designated DWB)..... | 172 |

| | |
|--|-----|
| Figure 2.30 Extraction recovery of proteins from human plasma using a wide pore prototype (DWB-178), a comparable particle size typical pore size sorbent (HLB HT) and a commercially available 30 μ m typical pore size sorbent (Std HLB)..... | 173 |
| Figure 2.31 Extraction recovery of human serum albumin (HSA) from human plasma using a wide pore prototype (DWB-178), a comparable particle size typical pore size sorbent (HLB HT) and a commercially available 30 μ m typical pore size sorbent (Std HLB)... | 173 |
| Figure 2.32 Representative chromatograms for 1 and 5 pg/mL desmopressin extracted from 500 μ L human plasma, compared to blank extracted plasma, using the proposed generic starting methods described in this chapter..... | 175 |
| Figure 2.33 Representative chromatograms for 5 and 20 pg/mL angiotensin I extracted from 350 μ L human plasma, compared to blank extracted plasma, using the proposed generic starting methods described in this chapter..... | 175 |
| Figure 2.34 Comparison of LC-MS/MS analysis of a signature peptide from trastuzumab before (A) and after (B) SPE clean-up using a mixed-mode weak cation sorbent and generic protocol..... | 177 |
| Figure 3.1 Structure and amino acid sequence for teriparatide..... | 189 |

| | |
|---|-----|
| Figure 3.2 Comparison of MS background present in final eluates from various sample preparation techniques, relative to the retention time of teriparatide..... | 194 |
| Figure 3.3 % SPE recovery of teriparatide following different plasma pre-treatment options..... | 195 |
| Figure 3.4.1. MS spectra of teriparatide (A) and human parathyroid 1-38 (B)..... | 199 |
| Figure 3.4.2. MSMS spectra of the 5+ teriparatide precursor at m/z 824 (A), the 6+ precursor at m/z 687 (B), and the 7+ precursor at m/z 589 (C). Fragments chosen for quantification are highlighted with an asterisk and correspond to y32 ions..... | 200 |
| Figure 3.5 MS/MS analysis of teriparatide extracted from human plasma monitoring either m/z 824-> 984 (top) or m/z 824-> 159 (bottom) | 201 |
| Figure 3.6. A teriparatide 1 ng/mL neat standard chromatographed on an ACQUITY UPLC CSH C18 column at 35°C (top panel) and an ACQUITY UPLC BEH C18 300 column at 35°C (bottom panel.) Both columns are 2.1 X 50mm, 1.7 µm. The flow rate is 0.4 mL/min and the gradient is 20-65% B in 2 minutes..... | 202 |
| Figure 3.7 LC/MS analysis of teriparatide using a test gradient of 20 to 65% B over 2 minutes run at either 0.4 mL/min (top) or 0.3 mL/min (bottom) | 203 |

| | |
|--|-----|
| Figure 3.8 LC/MS analysis of teriparatide using a gradient of 15% B to 50% B over either 3.6 (top) or 1.8 (bottom) minutes..... | 204 |
| Figure 3.9. UPLC separation of teriparatide and internal standard, from a 125 pg/mL extracted plasma sample, using a 2.1 X 50mm ACQUITY UPLC CSH column and the final gradient conditions..... | 205 |
| Figure 3.10. Representative chromatograms from teriparatide extracted from blank human plasma (A) and from human plasma at 20 (B), 35 (C) and 75 (D) pg/mL..... | 208 |
| Figure 3.11. Representative standard curve of teriparatide extracted from human plasma, from 15- to 500 pg/mL..... | 209 |
| Figure 4.1 Sequence, MW and pI for amyloid beta peptides 1-38, 1-40, and 1-42..... | 220 |
| Figure 4.2 ESI+ MSMS spectra for A β ₁₋₃₈ | 228 |
| Figure 4.3 ESI+ MSMS spectra for A β ₁₋₄₀ | 228 |
| Figure 4.4 ESI+ MSMS spectra for A β ₁₋₄₂ | 229 |
| Figure 4.5 Representative chromatographic separation of amyloid beta isoforms 1-38, 1-40, and 1-42..... | 230 |

| | |
|---|-----|
| Figure 4.6 Representative standard curve for A β ₁₋₃₈ extracted from artificial CSF..... | 231 |
| Figure 4.7 Representative standard curve for A β ₁₋₄₀ extracted from artificial CSF..... | 231 |
| Figure 4.8 Representative standard curve for A β ₁₋₄₂ extracted from artificial CSF..... | 232 |
| Figure 4.9 Correlation between A β ₁₋₄₂ concentrations determined using standard curves prepared in either spiked human CSF or artificial CSF + rat plasma carrier protein..... | 233 |
| Figure 4.10 ESI- MSMS spectra for A β ₁₋₄₂ | 234 |
| Figure 4.11 Comparison of LC-MS/MS analysis of A β ₁₋₄₂ , extracted from human CSF, using negative ionization (top) and positive ionization (bottom)..... | 234 |
| Figure 4.12 Comparison of LC-MS/MS analysis of A β ₁₋₄₀ , extracted from human plasma, using negative ionization (top) and positive ionization (bottom)..... | 235 |
| Figure 4.13 Summary of basal levels of A β ₁₋₃₈ , ₁₋₄₀ , and ₁₋₄₂ extracted from three lots of pooled human CSF and a single lot of pooled monkey CSF..... | 236 |
| Figure 4.14 Representative chromatogram of A β ₁₋₄₂ extracted from 3 pooled lots of human CSF and one pooled lot of monkey CSF..... | 237 |

| | |
|---|-----|
| Figure 4.15 Comparison of 50 pg/mL A β peptides separated using either a 1D or 2D ACQUITY UPLC system; 30 μ L of sample are injected in the 2D system and 15 μ L on the 1D system..... | 250 |
| Figure 5.1 Amino acid sequences and structures for human insulin and five analogs..... | 261 |
| Figure 5.2 LC chromatograms of final SPE eluates resulting from plasma samples initially pretreated with TRIS (panel A, top) or TFA (panel B, top) prior to SPE; bottom panels are summed spectra from 5.5 to 6.25 minutes..... | 272 |
| Figure 5.3 MS spectra for human insulin at either 200 μ L/min (top) or 10 μ L/min (bottom)..... | 276 |
| Figure 5.4 MS spectra for insulin aspart (A), detemir (B), glulisine (C) and glargine (D).. | 277 |
| Figure 5.5 Representative MSMS spectra for insulin analogs..... | 278 |
| Figure 5.6 MSMS of the 7+ insulin glargine precursor using a collision energy of 18 eV (top) or 35 eV (bottom)..... | 279 |

| | |
|--|-----|
| Figure 5.7 Specificity difference for insulin glargine extracted from human plasma observed when monitoring an immonium ion fragment (top) versus the more specific sequence ion at m/z 984; inset shows a typical immonium ion structure..... | 280 |
| Figure 5.8 Chromatographic separation of bovine insulin using a traditional C18 300Å (ACQUITY UPLC BEH 300 C18) column (top) and a charged surface (ACQUITY UPLC CSH C18) column (bottom)..... | 282 |
| Figure 5.9 Change in chromatographic performance for insulin glargine from the first two injections (bottom and middle panels) and after injections of precipitated plasma (top)... | 284 |
| Figure 5.10 Chromatographic separation of insulin analogs using the final gradient conditions described in section 5.2.4..... | 285 |
| Figure 5.11A Representative chromatogram of insulin glulisine at the LOD (B) and LLOQ (C) in human plasma; blank extracted human plasma is also shown (A)..... | 289 |
| Figure 5.11B Representative chromatogram of insulin glargine at the LOD (B) and LLOQ (C) in human plasma; blank extracted human plasma is also shown (A)..... | 290 |
| Figure 5.12 ACQUITY UPLC 2D valve diagram for at-column-dilution (ACD) and trap and back elute chromatography..... | 301 |

| | |
|--|-----|
| Figure 5.13 Average insulin recovery using different precipitation and pretreatment conditions..... | 303 |
| Figure 5.14 MS spectra for human insulin; insulin lispro produces the same precursor mass profile..... | 306 |
| Figure 5.15 MSMS spectra for human insulin and insulin lispro..... | 307 |
| Figure 5.16 Effect of precursor choice on specificity of insulin lispro in extracted human plasma: m/z 1162->217 (A) and m/z 968->217 (B); arrow indicates lispro peak..... | 308 |
| Figure 5.17 Comparison of extracted ion chromatograms for insulin lispro, RT 4.27 (left) and glargine, RT 4.12 (right) from patient sample 20 (top) and an extracted insulin standard (bottom)..... | 309 |
| Figure 5.18 A representative comparison of peak areas for insulin and analogs chromatographed on sub-2 μ m solid core charged-surface C ₁₈ columns (A) versus fully porous charged-surface C ₁₈ columns (B). Peak annotation includes area and retention time..... | 310 |
| Figure 5.19 UPLC-MS/MS Chromatograms of human insulin, insulin analogs, and bovine insulin (IS)..... | 311 |

| | |
|---|-----|
| Figure 5.20 LC-MS/MS extracted ion chromatograms for insulin glargine (Lantus) in human plasma at the low QC (A) and LLOQ (B) as compared to blank extracted human plasma (C)..... | 315 |
| Figure 5.21 LC-MS/MS extracted ion chromatograms for insulin lispro (Humalog) in human plasma at the low QC (A) and LLOQ (B) as compared to blank extracted human plasma (C)..... | 315 |
| Figure 5.22 LC-MS/MS extracted ion chromatograms for insulin glulisine (Apidra) in human plasma at 100 pg/mL (A) and LLOQ (B) as compared to blank extracted human plasma (C)..... | 316 |
| Figure 5.23 Overall method workflow: contribution of individual steps to final performance..... | 323 |
| Figure 6.1 Schematic of single pump trapping configuration used in this study..... | 338 |
| Figure 6.2 Average increase in sensitivity for a group of small molecules injected (constant volume and concentration) at various chromatographic scales from 2.1 mm to 75 μ m ID Figure reproduced with permission from Waters Corporation and James Murphy.... | 341 |
| Figure 6.3 Comparison of insulin separation on 150 μ m ID columns packed with various stationary phases. The first peak in each chromatogram is insulin glargine, the second peak | |

| | |
|--|-----|
| contains human insulin and insulin lispro, aspart, and glulisine. The last peak is insulin detemir..... | 343 |
| Figure 6.4 Comparison of vasopressin (first peak) and desmopressin (second peak) separation on 150 μ m ID columns packed with two stationary phases..... | 345 |
| Figure 6.5A Comparison of a 5 μ L injection of a 5 ng/mL standard of glucagon at analytical scale (top) and microscale (bottom)..... | 346 |
| Figure 6.5B Comparison of a 5 μ L injection of a 5 ng/mL standard of insulin glargine at analytical scale (bottom) and microscale (top)..... | 347 |
| Figure 6.6 Injections of 5, 10 or 15 μ L of human plasma extract containing 50 pg/mL glucagon | 348 |
| Figure 6.7A Comparison of the analysis of a 20 pg/mL teriparatide extracted plasma sample using either analytical (bottom) or microscale (top) chromatography..... | 349 |
| Figure 6.7B Comparison of the analysis of a 25 pg/mL glucagon extracted plasma sample using either analytical (bottom) or microscale (top) chromatography..... | 350 |
| Figure 6.8A Representative chromatograms of insulin glargine at 25, 100, and 200 pg/mL compared to blank extracted plasma, separated on a 150 μ m column..... | 351 |

| | |
|--|-----|
| Figure 6.8B Representative chromatograms of insulin glulisine at 25, 100, and 200 pg/mL compared to blank extracted plasma, separated on a 150 μ m column..... | 352 |
| Figure 6.9 Separation of 2.5 pg/mL desmopressin from 25, 100, and 200 μ L human plasma..... | 353 |
| Figure 6.10A Separation of desmopressin at various concentrations, extracted from 100 μ L human plasma..... | 354 |
| Figure 6.10B Separation of vasopressin at various concentrations, extracted from 100 μ L human plasma..... | 354 |
| Figure 6.10C Separation of octreotide at various concentrations, extracted from 100 μ L human plasma..... | 355 |
| Figure 6.11A Representative standard curve for teriparatide extracted from 50 μ L human plasma, from 10-1000 pg/mL..... | 356 |
| Figure 6.11B Representative standard curve for glucagon extracted from 200 μ L human plasma, from 12.5-1000 pg/mL..... | 356 |

Figure 6.11C Representative standard curve for insulin glargine extracted from 50 μ L
human plasma, from 25-10000 pg/mL.....357

List of Tables

| | |
|--|-------|
| Table 1.1 Useful pharmacokinetic terms and their definitions..... | 56-57 |
| Table 1.2 Useful amino acid properties..... | 83 |
| Table 2.1 Diverse peptides used in chromatographic and sample preparation testing, and their relevant physiochemical properties. Not all peptides are used in all tests..... | 120 |
| Table 2.2 Characteristics of the four columns compared for peptide separations..... | 120 |
| Table 2.3 Final % SPE recovery and % matrix effects for test peptides extracted from human plasma using the proposed screening method..... | 164 |
| Table 2.4 Properties of individual amino acids and mass shifts due to modifications..... | 165 |
| Table 2.5 Test proteins for evaluation of wide pore polymeric reversed-phase SPE materials..... | 167 |
| Table 3.1. MRM transitions, collision energies, and cone voltages for teriparatide and human parathyroid 1-38 (rhPTH (1-38)), the internal standard (IS)..... | 193 |
| Table 3.2. Representative standard curve statistics for teriparatide extracted from 200 μ L human plasma..... | 206 |

| | |
|---|-----|
| Table 3.3. QC statistics from teriparatide extracted from 6 individual lots of human plasma..... | 207 |
| Table 3.4. Individual matrix factor assessments from 3 replicates each, from 6 sources of human plasma..... | 211 |
| Table 4.1 Mass spectrometry conditions for MRM transitions of the amyloid β peptides and their ^{15}N -labeled internal standards..... | 225 |
| Table 4.2A Summary of QC statistics for $\text{A}\beta$ peptides in human CSF pool 1..... | 238 |
| Table 4.2B Summary of QC statistics for $\text{A}\beta$ peptides in human CSF pool 2..... | 239 |
| Table 4.2C Summary of QC statistics for $\text{A}\beta$ peptides in human CSF pool 3..... | 240 |
| Table 4.2D Summary of QC statistics for $\text{A}\beta$ peptides in cynomolgous monkey CSF pool 1..... | 241 |
| Table 4.3 Average QC values for $\text{A}\beta$ peptides extracted from 50 μL human plasma ($N=3$ in each of two pooled lots) and detected using a Waters Xevo TQ-S MS..... | 246 |

| | |
|--|-----|
| Table 4.4 Representative standard curve statistics for A β ₁₋₄₂ from 50 to 10,000 pg/mL extracted from 50 μ L artificial CSF..... | 247 |
| Table 4.5 Summary of basal A β ₁₋₄₂ levels in human CSF, as determined from standard curves prepared in four different matrices (three surrogates compared to human CSF) and analyzed on LC/MS platforms utilizing either a 1D or a 2D LC system..... | 249 |
| Table 5.1 MS conditions for human insulin, 5 analogs, and the internal standard bovine insulin; highlighted transitions correspond to the primary quantitative transition, other transitions are confirmatory..... | 269 |
| Table 5.2 Representative standard curve statistics for insulin glulisine (A) and insulin glargine (B) from 50 pg/mL to 500 ng/mL in solvent standards..... | 286 |
| Table 5.3 Representative standard curve and QC sample statistics (n=3) for insulin detemir from 200 pg/mL to 25 ng/mL in human plasma..... | 288 |
| Table 5.4 Representative standard curve and QC statistics (n=3) for insulin glulisine from 0.2 ng/mL to 25 ng/mL in human plasma..... | 289 |
| Table 5.5 Standard curve ranges, r ² values, and mean accuracy for curve points for all compounds..... | 313 |

| | |
|---|-----|
| Table 5.6 . Inter- and intra-day accuracy and precision for QC samples for insulin glargine..... | 317 |
| Table 5.7 Inter- and intra-day accuracy and precision for QC samples for insulin Lispro..... | 317 |
| Table 5.8 Inter- and intra-day accuracy and precision for QC samples for human insulin..... | 318 |
| Table 5.9 Calculated concentrations of human insulin and/or its analogs detected in patient samples..... | 321 |
| Table 6.1A Gradient conditions for microscale analysis of glucagon | 337 |
| Table 6.1B Gradient conditions for microscale analysis of insulins..... | 337 |
| Table 6.1C Gradient conditions for microscale analysis of teriparatide..... | 337 |
| Table 6.1D Gradient conditions for microscale analysis of desmopressin, vasopressin, and octreotide..... | 337 |
| Table 6.2 Representative standard curve performance statistics for glucagon extracted from human plasma..... | 357 |

| | |
|--|-----|
| Table 6.3 Representative standard curve and QC performance statistics for insulin glargine extracted from human plasma..... | 358 |
|--|-----|

| | |
|--|-----|
| Table 6.4 Representative standard curve performance statistics desmopressin, vasopressin, and octreotide extracted from human plasma..... | 358 |
|--|-----|

List of Equations

| | |
|---|-----|
| Equation 1.1 Selectivity..... | 63 |
| Equation 1.2 Capacity/Retention factor..... | 64 |
| Equation 1.3 Efficiency/Plate Count..... | 64 |
| Equation 1.4 Resolution..... | 65 |
| Equation 1.5 Relationship between resolution and efficiency..... | 65 |
| Equation 1.6 Relationship between efficiency and particle size..... | 65 |
| Equation 1.7 Relationship between flow rate and particle size..... | 66 |
| Equation 1.8 Relationship between peak width and particle size..... | 66 |
| Equation 1.9 van Deemter equation..... | 67 |
| Equation 2.1 % SPE recovery..... | 147 |
| Equation 2.2 % matrix effects..... | 156 |

| | |
|---|-----|
| Equation 3.1 Calculation of matrix factor (MF)..... | 192 |
|---|-----|

List of Symbols and Abbreviations

| | |
|-------|---|
| A | Contribution of Eddy diffusion to band broadening or aqueous mobile phase |
| AA | Acetic acid |
| ACD | At column dilution |
| ACN | Acetonitrile |
| ADME | Absorption, distribution, metabolism, excretion |
| ADMET | Absorption, distribution, metabolism, excretion, toxicity |
| API | Atmospheric pressure ionization |
| APCI | Atmospheric pressure chemical ionization |
| AUC | Area under the curve |
| aq | Aqueous |
| API | Atmospheric ionisation |
| B | Contribution of longitudinal diffusion to band broadening or organic mobile phase |
| BEH | Bridged ethyl-hybrid |
| CI | Chemical ionisation |

| | |
|------------------|---|
| C _{max} | Maximum plasma drug concentration |
| CMFD | Ceramic microfluidic device |
| DMPK | Drug metabolism pharmacokinetics |
| dp | Chromatographic particle size |
| ELISA | Enzyme linked immunosorbent assay |
| ESI | Electrospray ionization mode |
| ESI + | Positive electrospray ionization mode |
| ESI - | Negative electrospray ionization mode |
| eV | Electron volt |
| F | Bioavailability |
| FTIR | Fourier Transform Infrared |
| GC | Gas chromatography |
| GC/MS | Gas chromatography coupled with mass spectrometry |
| GPC | Gel permeation chromatography |
| H | Plate height |
| HETP | Height equivalent to a theoretical plate |
| HLB | Hydrophilic lipophilic balance |

| | |
|----------|--|
| h | Hour |
| HPLC | High pressure liquid chromatography |
| HTCC | High temperature co-fired ceramic |
| i.d. | Internal diameter |
| IND | Investigation new drug application |
| IPA | Isopropanol |
| K | Elimination rate constant |
| k | Capacity factor, or retention factor |
| kg | Gradient retention factor |
| kV | Kilovolt |
| L | Length |
| LC | Liquid chromatography |
| L/Hr | Litres per hour |
| LC/MS | Liquid chromatography coupled to mass spectrometry |
| LC/MS/MS | Liquid chromatography coupled to triple quadrupole mass spectrometry |
| LOD | Limit of detection |
| LLOQ | Lower limit of quantification |

| | |
|-------|---|
| LC/UV | Liquid chromatography coupled with ultra violet detection |
| M | Mass |
| MALDI | Matrix assisted laser desorption ionization |
| MeOH | Methanol |
| mg | Milligram |
| min | Minute |
| mL | Millilitre |
| mm | Millimetre |
| MRM | Multiple reaction monitoring |
| MS | Mass spectrometry |
| m/z | Mass/charge ratio |
| n | Number of replicates |
| N | Efficiency |
| NaOH | Sodium hydroxide |
| NDA | New drug application |
| Nl | Nanolitre |
| nm | Nanometer |

| | |
|-------|---|
| NFT | Neuro-fibrillary tangles |
| NSB | Non-specific binding |
| Pc | Peak capacity |
| PCB | Printed circuit board |
| PD | Pharmacodynamics |
| pg | Picogram |
| PK | Pharmacokinetics |
| PL | Phospholipid |
| psi | Pressure per square inch |
| Pw | Peak width |
| Q | Single quadrupole |
| QQQ | Triple quadrupole |
| Q-Tof | Quadrupole time of flight mass spectrometer |
| R | Resolution (mass spectrometer) |
| RCF | Relative centrifugal force |
| RIA | Radio immunoassay |
| RP | Reversed-phase |

| | |
|------------------|---|
| Rs | Resolution |
| R ² | Coefficient of determination |
| s | Second |
| SIR | Single ion recording |
| S/N | Signal to noise ratio |
| SPE | Solid phase extraction |
| SRM | Selected reaction monitoring |
| tg | Gradient time |
| T _{max} | Time where C _{max} is observed |
| TOF | Time of flight |
| t ₀ | Void time |
| t _R | Retention time |
| t _{1/2} | Drug half life |
| u | Linear velocity |
| μL | Microliter |
| μm | Micrometer |
| UPLC | Ultra performance liquid chromatography |

| | |
|----------------|---|
| US FDA | United States Federal Drug Administration |
| UV | Ultraviolet |
| V | Applied voltage |
| V _o | Volume of mobile phase pumped for an unretained analyte to reach the detector |
| V _R | Volume of mobile phase pumped for a retained analyte to reach the detector |
| w | Chromatographic peak width |
| α | Selectivity |
| °C | Degree Celsius |
| ΔM | Delta M is the difference of two neighbouring m/z values |
| % | Percent |
| % v/v | Percent volume by volume |

Chapter 1

Introduction

1.1 Peptides and Proteins as Drugs

According to the World Health Organization, the global pharmaceuticals market was worth approximately \$300 billion in 2013 and expected to rise another \$100 billion within 3 years. Historically, this market was comprised primarily of small molecule drug entities that were either derived from plant extracts, synthesized based on endogenous compounds, or developed from structural activity relationships (SARs).[1] These compounds have been responsible for almost eliminating many diseases such as measles, mumps, rubella, and chicken pox, controlling such debilitating problems such as high blood pressure and finally reducing mortalities due to HIV/AIDS, and certain cancers[2]. Today, a rapidly increasing number of new pharmaceuticals, called biopharmaceuticals, are being developed which are based on biological molecules such as peptides, proteins, and oligonucleotides. This shift in interest towards large molecule therapeutics is primarily due to a number of their inherent characteristics including lower toxicity, greater specificity, and higher potency. For example, as of 2011, there were 60 peptide based medicines available, and at least another 400 in late stage clinical trials. Overall, there are over 600 biologically-based candidate pharmaceuticals in development, many of which are antibody or peptide-based. [3, 4] In fact, according to a recent study through the Peptide Therapeutics Foundation, there are approximately 17 new peptide drug entities going into clinical trials each year, and these are about twice as successful in phase III clinical trials than their small molecule counterparts.[5] Advances in the various technologies applied for drug discovery and biomolecule characterization (i.e., recombinant DNA, fermentation, proteomics, genomics,

and informatics) [6] have made it possible for drug manufacturers to successfully develop and characterize biopharmaceuticals. These types of compounds have been used to treat a variety of serious diseases such as diabetes, cancer, arthritis, and hemophilia. Perhaps the oldest, best known, and top-selling peptide therapeutic is insulin, with several analogs reaching multi-billion dollar sales, such as insulin glargine (Lantus), insulin lispro (Humalog) and insulin aspart (NovoRapid). While originally dosed by injection, current research focuses on developing nasal or transdermal dose formulations, [7] both of which will require more sensitive and selective methods than those previously employed.

Additional peptide-based drug products, including goserelin, leuprolide, and octreotide, have also reached over a billion dollars in sales treating critical health issues such as osteoporosis and prostate and other cancers.

Therapeutic peptides are typically modified or synthetic versions of substances that already exist in the body, and therefore tend to be better tolerated than many small molecule-based medicines, as they do not form toxic metabolites. In addition, by their very nature, these biological compounds are often more specific than small molecules used to treat the same disease, as they have been designed to mimic behaviour of endogenous substances and are mapped to specific receptor proteins. Relative to small molecules, other benefits of peptide drugs include greater activity and potency, lower toxicity, improved molecular recognition, no accumulation in tissues and organs, and minimal drug-drug-interactions. One example is the synthetic peptide desmopressin, a modified form of the human hormone arginine vasopressin. It is prescribed as a replacement for antidiuretic hormone (vasopressin) and is used to treat bedwetting and diabetes insipidus. Desmopressin provides several treatment benefits over recombinant vasopressin. It degrades more slowly,

enabling less frequent dosing, and it does not raise blood pressure unlike the unmodified peptide. There are also drawbacks to peptide drugs and their development. Peptide pharmaceuticals tend to have low oral bioavailability, often necessitating intravenous dosing rather than the patient preferred delivery methods such as tablets or capsules taken orally. In addition, their solubility is poor, and peptides are rapidly eliminated from the body and/or broken down by enzymatic activity, and finally, due to their hydrophilicity, it is difficult for these candidate medicines to cross biological membranes. Poor membrane transfer accounts for the fact that the majority of peptide candidate medicines are aimed at extracellular targets such as G-protein-coupled receptors[8]. A few companies however, have focused their development programs on peptide drugs for intra-cellular, or “undruggable” targets. Some of these issues have been resolved through recent research efforts [8]. For example, PEGylation, liposomal encapsulation, and conjugation to small molecules, antibodies or proteins have been shown to be effective means of improving the stability and in vivo half-life of peptide therapeutics [9].

1.1.1 Biosimilars

A biosimilar may be thought of as analogous to a generic version of a small molecule pharmaceutical. In the small molecule medicine market place 44% of all of the medicine prescribed in USA are generics and estimated to be worth \$106 billion by 2016 (<http://www.newpharmathinkers.com/wp-content/uploads/downloads/2012/07/Generic-Industry-Summary.pdf>). While small molecule generics must contain the identical active ingredient to the original reference drug, biosimilars are close, but *not identical* to the

original biologic. Biologics are created through biological systems such as cell lines, and not from stock chemical starting materials, through very complex processes that are difficult to duplicate[10]. Many of the most popular biologically based-therapies will come off patent in the 2010-2020 time frames. Figure 1.1 summarizes the US patent expiration for key biopharmaceuticals. This opens up a tremendous sales opportunity (\$200-400 billion for insulins alone)[11] for biosimilars or bio-betters research, which necessarily includes a significant quantitative analytical chemistry component.

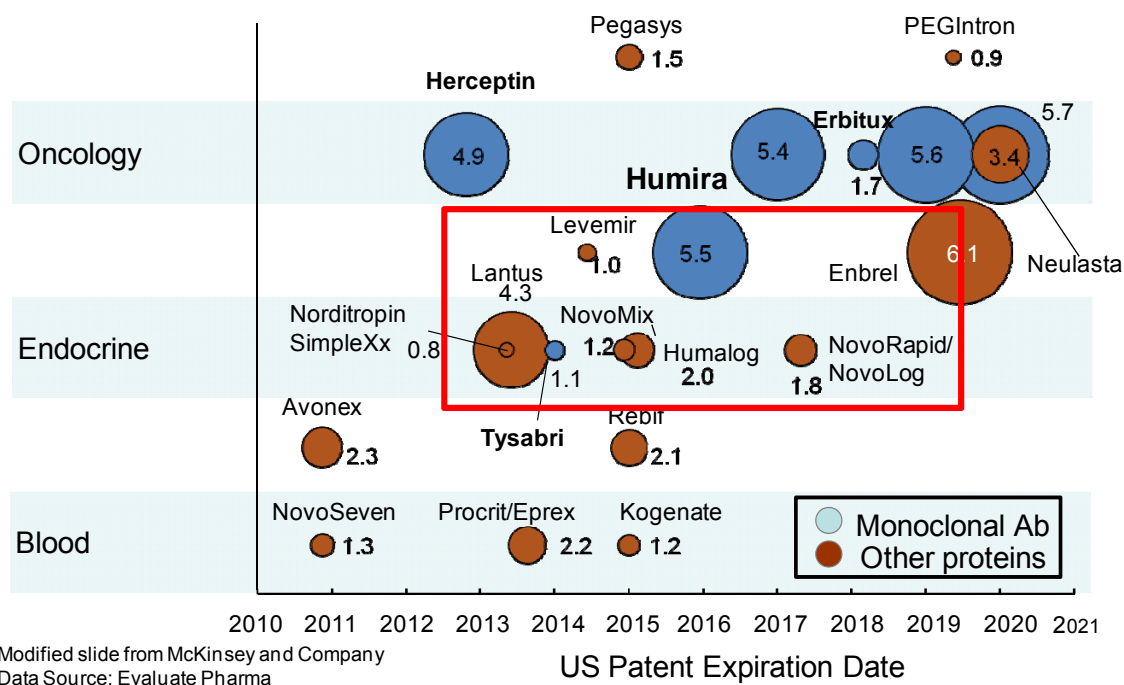


Figure 1.1 Important biotherapeutics coming off patent and open to biosimilars competition

The primary focus of bioequivalence studies for small molecule generics is the systemic exposure profile, specifically the C_{max} and T_{max} which must be the same as the reference drug when administered at a similar dose. This is described in detail in the FDA

Guidance for Industry recommendations for bioequivalence studies[12]. In addition to efficacy and PK data, biosimilars registration and regulatory acceptance will also include an assessment of immunogenicity, heterogeneity, pharmacovigilance and safety.

1.1.2 Biomarkers

In addition to development of novel therapeutics, the study and identification of peptide and/or protein biomarkers is a critical area of research. Biomarkers are used both to predict various disease states prior to onset, and also to identify targets for drug development. Peptide and protein biomarkers are endogenous compounds whose relationship to a disease state has been identified. The presence or absence of these compounds can be linked to the onset or progression of a disease. For example, amyloid beta peptides are being studied extensively in Alzheimer's Disease research[13]. Other examples include cardiac troponin for the diagnosis of myocardial infarction and brain natriuretic peptide (BNP) for congestive heart failure. Changes in biomarker concentration, sometimes subtle, can also be used to measure drug efficacy or to characterize cohort populations. Assays used to measure these minor relative changes must, therefore, be exceedingly accurate, reproducible and precise. Guidelines for these assays are prescribed by the FDA in the Guidance for Industry for Bioanalytical Method Validation[12, 14]. Research in this area encompasses several stages, including biomarker discovery- the identification and verification of a putative biomarker, and biomarker validation- where assay sensitivity, specificity and optimization are carried out. Both of these require ultra-high sensitivity quantitative or semi-quantitative assays. During the discovery phase,

metabolomics or proteomic approaches may be taken to map the biology of systems, using relative quantification to identify proteins or peptides which are differentially expressed between diseased and normal populations[15]. Throughout the process thousands of candidates (discovery) to thousands of samples (validation) are assayed, using both LC/MS and immunoassay techniques. Figure 1.2 captures the process of biomarker research and is re-printed with permission from Nature Biotechnology[15].

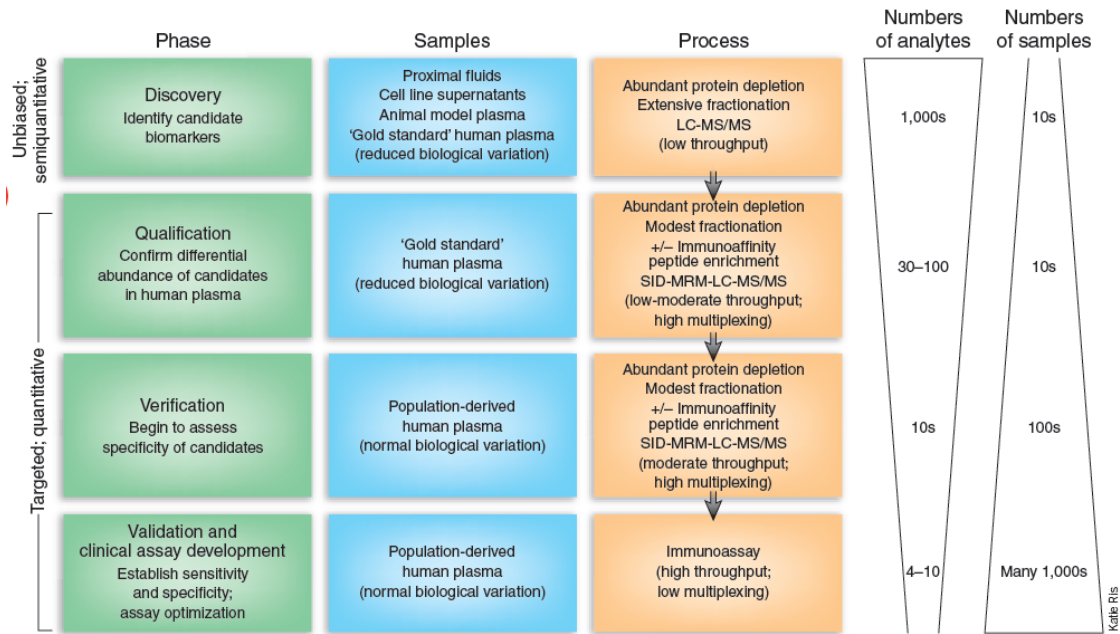


Figure 1.2 Process flow for the development of novel protein biomarker candidates

1.2 Bioanalysis of Biopharmaceuticals and Biomarkers

Bioanalysis is one of the most critical activities in the drug discovery and development process today. Bioanalytical data is used not only to make critical decisions on progression of drug candidates via the measurement of pharmacokinetic parameters, but also to

understand efficacy in human patients. The time to fully develop and launch a new drug can be as many as 15 years and can cost in the range of 100-900 million dollars[16, 17]. In typical small molecule drug development, one may start with ~1500 candidates in discovery, with an average of <1% of those progressing to phase I studies in animals[17]. The number of candidates decreases further through phase II and III human trials, yielding on average less than 2 of the original 1500 coming out of phase III and into registration[17]. Bioanalysis plays a role throughout all of these stages. The primary causes for the dramatic attrition rate are the selection of candidates that may appear promising in vitro or in phase I but lack efficacy in man, poor pharmacokinetics, and poor safety profile. Both the high cost, and the high attrition rate have driven pharmaceutical companies to try to improve the drug development process through improving both the quality of bioanalytical data and the speed with which it is obtained. Those pressures then also translate to CRO's or generic companies. It is these key factors that necessitate innovation in bioanalysis.

The most common matrices for analysis are plasma, blood, serum, urine, cerebrospinal fluid (CSF), faeces, and tissues such as brain or liver. As mentioned, bioanalytical activities are performed during both the discovery phase of drug development and during the development or regulated phase of the process and are performed to help determine the pharmacokinetics (PK) and pharmacodynamics of the drug. PK include the study of the Absorption, Distribution, Metabolism and Excretion (ADME) properties of the drug as well as a calculation of bioavailability, which is obtained by mapping changes in drug plasma concentration over time and comparing the area under the plasma time curve (AUC) for oral and IV drug dosing. Figure 1.3 is representative of stylistic PK profile data for oral and IV dosing.

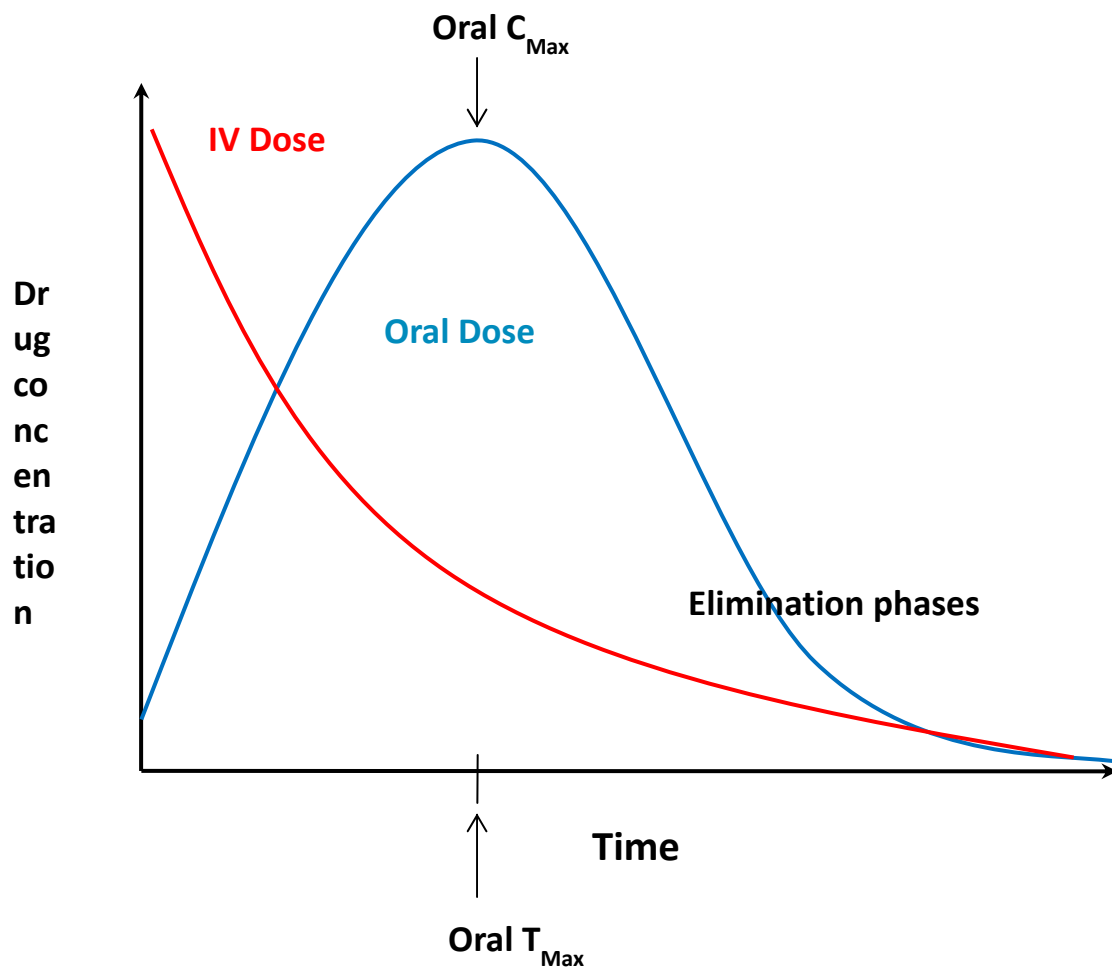


Figure 1.3 Representative PK profile obtained by plotting changes in plasma drug concentrations over time.

A table of useful PK terms and their definitions can be found in Table 1.1

| Characteristic | Description | Example value | Symbol | Formula |
|-------------------------------|--|---------------|---------------|------------------------|
| Dose | Amount of drug administered. | 500 mg | D | Design parameter |
| Dosing interval | Time between drug dose administrations. | 24 h | τ | Design parameter |
| C_{\max} | The peak plasma concentration of a drug after administration. | 60.9 mg/L | C_{\max} | Direct measurement |
| t_{\max} | Time to reach C_{\max} . | 3.9 h | t_{\max} | Direct measurement |
| C_{\min} | The lowest (trough) concentration that a drug reaches before the next dose is administered. | 27.7 mg/L | $C_{\min,ss}$ | Direct measurement |
| Volume of distribution | The apparent volume in which a drug is distributed (i.e., the parameter relating drug concentration to drug amount in the body). | 6.0 L | V_d | $= \frac{D}{C_0}$ |
| Concentration | Amount of drug in a given volume of plasma . | 83.3 mg/L | C_0, C_{ss} | $= \frac{D}{V_d}$ |
| Elimination half-life | The time required for the concentration of the drug to reach half of its original value. | 12 h | $t_{1/2}$ | $= \frac{\ln(2)}{k_e}$ |

| | | | | |
|----------------------------------|---|------------------------|----------|--|
| Elimination rate constant | The rate at which a drug is removed from the body. | 0.0578 h ⁻¹ | k_e | $= \frac{\ln(2)}{t_{1/2}} = \frac{CL}{V_d}$ |
| Infusion rate | Rate of infusion required to balance elimination. | 50 mg/h | k_{in} | $= C_{ss} \cdot CL$ |
| Area under the curve | The integral of the concentration-time curve (after a single dose or in steady state). | 1,320 mg/L·h | | $AUC_{0-\infty} = \int_0^{\infty} C \, dt$ |
| | | | | $AUC_{\tau,ss} = \int_t^{t+\tau} C \, dt$ |
| Clearance | The volume of plasma cleared of the drug per unit time. | 0.38 L/h | CL | $= V_d \cdot k_e = \frac{D}{AUC}$ |
| Bioavailability | The systemically available fraction of a drug. | 0.8 | f | $= \frac{AUC_{po} \cdot D_{iv}}{AUC_{iv} \cdot D_{po}}$ |
| Fluctuation | Peak trough fluctuation within one dosing interval at steady state | 41.8 % | $\%PTF$ | $= \frac{C_{max,ss} - C_{min,ss}}{C_{av,ss}}$ where $C_{av,ss} = \frac{1}{\tau} AUC_{\tau,ss}$ |

Table 1.1 Useful pharmacokinetic terms and their definitions

Due to the increasing number of peptide therapeutics and biomarkers, there exists an immediate need for an efficient method development workflow for the bioanalysis of peptide therapeutics as well as a comprehensive understanding of their differences with respect to small molecules. As described in previous sections, quantification of peptides is

important not only for synthetic peptide drugs, but also for peptide biomarkers and for quantification of proteins based upon measurement of unique or signature peptides.

Naturally, the determination of PK parameters and metabolic fate are as critical during the drug discovery and development process for peptide therapeutics as for small molecules.

For small molecule drug candidates, this data is typically generated by liquid chromatography/tandem mass spectrometry (LC/MS/MS) analysis of in-vitro (liver microsomes, CaCo2 cells, etc.) or in-vivo (animal or human fluids or tissues) samples. In small molecule analysis, LC/MS/MS, specifically triple quadrupole MS, has become the technique of choice for these activities due to its un-paralleled selectivity and sensitivity.

In contrast to small molecules, the gold standard for biomolecule quantification has historically been ligand binding assays (LBAs) such as enzyme-linked immunosorbent assays (ELISAs) and radioimmunoassays (RIAs). While these types of assays remain the primary and most widely accepted method of quantifying protein and antibody-based therapies, LC/MS/MS has begun to emerge as the technique of choice for quantification of synthetic peptides and is increasingly being used to analyze endogenous peptide biomarkers[18]. While ligand binding assays have high sensitivity, specificity, and rapid “plate reader” detection, they also have several shortcomings that are influencing the transition to LC/MS/MS methods.

1.3 Pros and Cons of Traditional Quantitative Assays for Biotherapeutics

LBAs do not quite meet the demands of a high throughput discovery setting where the specific biological reagents are not yet available. Not only are specific reagents

necessary, but the time required to develop these reagents may be in the order of several months to a year. Furthermore, the reproducibility and reliability of quantitative results is highly dependent on reagent quality and batch-to-batch consistency. In addition, LBAs have limited linear dynamic range (often requiring extensive dilution of samples to accommodate the concentration range of a PK study), cross reactivity (yielding erroneous or inaccurate results) and matrix interferences. LBAs also have difficulty distinguishing between the drugs and metabolites or other closely related substances. Finally, an individual assay is required for each peptide of interest, limiting multiplexing ability.

1.4 Overview of Modern Liquid Chromatography (LC)

Liquid chromatography is a technique used to separate one or more desired analytes or compounds from a sample for the purposes of identification (based on its elution time from the chromatography column), purification (through fraction collection) or quantification (through the use of calibrator and quality control sample injection, followed by detection and software processing). The components of a modern chromatographic system include one or more pumps, which deliver one or more aqueous and organic mobile phases to the column as well as carry the sample from an injector to the head of the column, an injector (which delivers the sample from a vial or plate to the column), a chromatographic column and a detector (such as ultraviolet/visible, mass spectrometric, refractive index, evaporative light scattering, electrochemical, NMR and fluorescence). Separation is primarily achieved by varying mobile phase composition, column stationary phase chemistry, temperature and gradient profile, which impact both the chemical and physical behaviour of the analyte in

the column. Generally speaking, elution of an analyte from the column is related to its preference for and partitioning between the stationary phase (particles inside the column) and solubility in the mobile phase (liquid moving through the column) at a given time.

This technique has been applied over a variety of application areas including clinical research, forensic toxicology, environmental and food safety analyses, and pharmaceutical development. Samples from matrices as diverse as blood, plasma, urine, soil, corn, milk, and waste water are all amenable to this technique once these matrices have been simplified through initial sample preparation or extraction.

1.4.1 Brief History of Chromatography

Chromatography, derived from chroma (colour) and graph (writing), had its origins in the late 1800s when scientists such as Runge, Goppelsroeder and Schonbein performed dye and other separations on filter paper[19]. In the 1900s Tswett performed experiments with an open glass cylinder and plant extracts, using different solvents to affect separation[20]. Over the next century, liquid and gas chromatography were developed and LC evolved into essentially what is now high performance liquid chromatography (HPLC). As many researchers with divergent aims were involved in the evolution of chromatography, it may be more instructive to highlight a few key individuals and their respective contributions, rather than to follow a distinct timeline. Their observations form the foundation for some of the key performance-assessing equations that shape current LC column development and separations.

Martin and Synge performed pioneering work in amino acid separations[21-23], developing an understanding of the influence of dynamic partitioning and drawing the conclusion that smaller sorbent particles and higher pressure were critical to improving resolution. They were the first to describe the concept of a theoretical plate related to partitioning of an analyte between the liquid and stationary phase, and eventually won a Nobel prize for their work. Essentially, the faster the partitioning, the more theoretical plates a column has, or the higher the efficiency of the column. This led to the description of HETP, or height equivalent to a theoretical plate (H), whose relationship is the converse- the lower the H, greater the efficiency. A simple way to describe H is column length (L) divided by plate count or efficiency (N)[24]. Further to this, they proposed three parameters which affect the magnitude of H: a partitioning coefficient, the diffusion rate, and the velocity of the mobile phase. These concepts should begin to sound familiar to any chromatographer as they form the basis for what is known as the van Deemter equation.

Incidentally, Moore and Stein came to similar conclusions during the development of a form of GPC[25] which precipitated a fruitful collaboration with James Waters and resulted in the introduction of the first commercial GPC system[26]. This research further supported two concepts affecting increased column resolution: the potential for the use of smaller particles (enabling faster flow rates) and the importance of a uniform packing bed.

van Deemter expanded the concepts proposed by Martin and Synge and delved deeper into mass transfer and diffusion, while introducing the incorporation of the physical characteristics of the packed bed[27-29].

Snyder further highlighted the importance of the interplay between the analyte and stationary phase and analyte and mobile phase, emphasizing that earlier work did not fully

exploit those parameters which could influence selectivity[30]. It was at this point that the role of column length, particle size, flow rate, and mobile phase polarity and their combined influence on chromatographic performance was reported.

The conclusions arising from these studies naturally led to a focus on the development of smaller, more uniform packing materials and smaller ID columns. This resulted in the necessary innovations in hardware capable of withstanding higher pressures and novel packing processes capable of achieving high efficiency, uniformly packed beds.

Traditional HPLC uses columns packed with stationary phase particles ranging in size from 3.5 to 10 μm with the most common particle chemistry being a silica-based C_{18} . More recently, hybrid particles were introduced which enable LC using a mobile phase pH >10. HPLC is performed in several common modes, including reversed-phase (accounting for approximately 70-80% of LC separations)[27], hydrophilic interaction chromatography (HILIC), normal phase, ion exchange, and size exclusion. As the overwhelming majority of separations for quantitative analysis of large and small molecules is performed using reversed-phase, the remainder of this section will focus on theory and practice in this mode.

1.4.2 LC Theory

1.4.2.1 Definition of Chromatographic Terms and Relevant Equations and Relationships

A few fundamental equations form the basis of current chromatographic theory and provide the tools with which HPLC performance is measured. Comprehensive understanding of the equations presented in this section provides a critical foundation for

any chromatography-based research. The concepts were utilized in this author's work to facilitate concise development and design of appropriate experiments aimed at optimizing and improving the LC component of peptide bioanalytical methods.

Selectivity is a measure of the degree of separation between two analytes under a specific chromatographic condition and is shown in equation 1.1 where k_B is the retention factor of analyte B and k_A , that of analyte A. A value of 1 essentially indicates that analytes will not be separated under the indicated conditions. This is distinct from resolution which relates to the separation of analytes at baseline.

Equation 1.1
$$\alpha = \frac{k_B}{k_A}$$

Retention time is the time it takes a peak or analyte band to travel from the injector to the detector. This is the most often reported attribute for differentiating and describing distinct peaks in a chromatogram. In general, greater retention time indicates stronger interaction between the analyte and the stationary phase. For example, in reversed-phase chromatography, hydrophobic compounds retain longer than hydrophilic compounds.

Peak asymmetry is a measure of the Gaussian nature of a peak. King[27] describes an asymmetry-squared method whereby the tail and front of the peak are measured at 4.4% of the height and this ratio is squared.

Capacity or retention factor, can be used to normalize retention in order to compare different columns and can be defined as[27, 31] in Equation 1.2:

Equation 1.2

$$k = \frac{t_R - t_0}{t_0} = \frac{V_R - V_0}{V_0}$$

In this equation, t_r is the time taken for the analyte to reach the detector and t_0 is the time for unretained analytes to reach the detector. V_r and V_0 represent the volumes required for retained and unretained analytes, respectively, to reach the detector.

Efficiency (plate count) is related to, and defines, the efficiency of the column. Practically speaking, the higher the N , the narrower and more concentrated the analyte bands are, and the more efficient the column. In the equation below, V_n is the elution volume of a peak, w is peak width, and a is a constant derived from the peak height at which the width is measured[24].

Equation 1.3

$$N = \left(\frac{V_n}{\sigma} \right)^2 = a \left(\frac{V_n}{w} \right)^2$$

Linear velocity, u , refers to the speed of the mobile phase moving through the column. It is normally expressed in centimeters per second. As these are not units used in everyday LC analyses, one may see van Deemter-like plots where LC flow rate is used instead. Linear velocity is related to flow rate, the internal ID of the column and the particle size. Linear velocity is determined by dividing the column length (L) by the retention time of an unretained compound t_0 [27, 32]. This term is particularly useful when transferring a method from a column with one internal diameter to a column of another internal diameter.

Resolution describes, in its most basic sense, the relationship between the width of two peaks relative to the distance between them. The ability to either decrease peak width or improve separation between them, increases resolution. The relationship between resolution and intra-column band spread can be summarized as follows:

Equation 1.4
$$Rs \equiv \frac{t_{R,2}-t_{R,1}}{\frac{1}{2}(w_1+w_2)} = \sqrt{\frac{N}{4}} \left(\frac{\alpha-1}{\alpha} \right) \left(\frac{k}{k+1} \right)$$

Where N is plate count (efficiency), α is the selectivity, and k is retention factor.

There are a few additional relationships central to understanding modern LC, and ultra performance liquid chromatography (UPLC), in particular. The following equations describe the relationship between particle size, flow rate, and efficiency[24] and are key to understanding the attractiveness of sub 2 μ m particle LC (UHPLC) and its widespread implementation in a broad range of application areas:

Equation 1.5
$$Rs \propto \sqrt{N}$$

Resolution is proportional to the square root of efficiency.

Equation 1.6
$$N \propto \frac{1}{d_p}$$

Efficiency (N) is inversely proportional to particle size (d_p), meaning that as the particle size decreases, efficiency improves and resolution also improves.

Equation 1.7
$$F_{opt} \propto \frac{1}{d_p}$$

Optimal flow rate for a separation is inversely proportional to particle size, meaning that smaller particles yield higher optimal flow rates and thus reduced analysis times.

Equation 1.8
$$N \propto \frac{1}{w^2}$$

Narrower peaks widths, arising from smaller particles, produce higher efficiency separations.

1.4.2.2 Band Broadening and the Van Deemter Equation

Arguably one of the most often referred to mathematical representations of chromatographic performance is the van Deemter equation and derivatives thereof.

The aforementioned description of HETP from Martin and Synge, though an accepted measure of column performance, is albeit a simplistic one. To truly characterize analyte behaviour, one must consider the degree of bandspreading. Analytes are initially introduced through the LC system as a discrete band, with Gaussian distribution with the highest concentration of analyte being in the center of the band. As analytes travel from the injector to the column, and then through the column, during this process there are ample opportunities for the analyte band to widen or broaden, this is called bandspread or dispersion. The result is a dilution effect which produces a chromatographic peak which is

broadener and less intense. Ultimately, this corresponds to decreased peak height, decreased signal to noise, and ultimately reduced sensitivity. Bandsread can be minimized by controlling both intra- and extra- column sources. Injection volume, transfer tubing ID, connections, packing material particle size, packing efficiency, and diffusion characteristics all contribute.

van Deemter expanded on the original HETP concept to include a more comprehensive analysis of three simultaneous diffusion related processes that an analyte molecule undergoes as it travels through a column as well as expressing the dependence of HETP on linear velocity[28, 33]. Specifically, van Deemter's equation (Equation 1.9 , below) includes a parameter to describe what is called eddy diffusion (the "A term"), longitudinal diffusion (the "B term"), and mass transfer (the "C term"). Eddy diffusion is generally the movement of analyte molecules to the surface of a particle and around it and is related largely to particle size, while longitudinal diffusion corresponds to analyte movement within the mobile phase on the stationary phase and tends to decrease with increasing linear velocity. Mass transfer relates to the facility of analyte movement in and out of chromatographic pores and is affected by linear velocity and the square of particle size[24]. A generic van Deemter plot, including a plot of the individual terms of the van Deemter equation, appears in Figure 1.4. Another additional equation worthy of mention is the Knox Equation, which is a useful way to assess the quality of a column.

Equation 1.9

$$HETP = a(dp) + \frac{b}{u} + c(dp)^2u$$

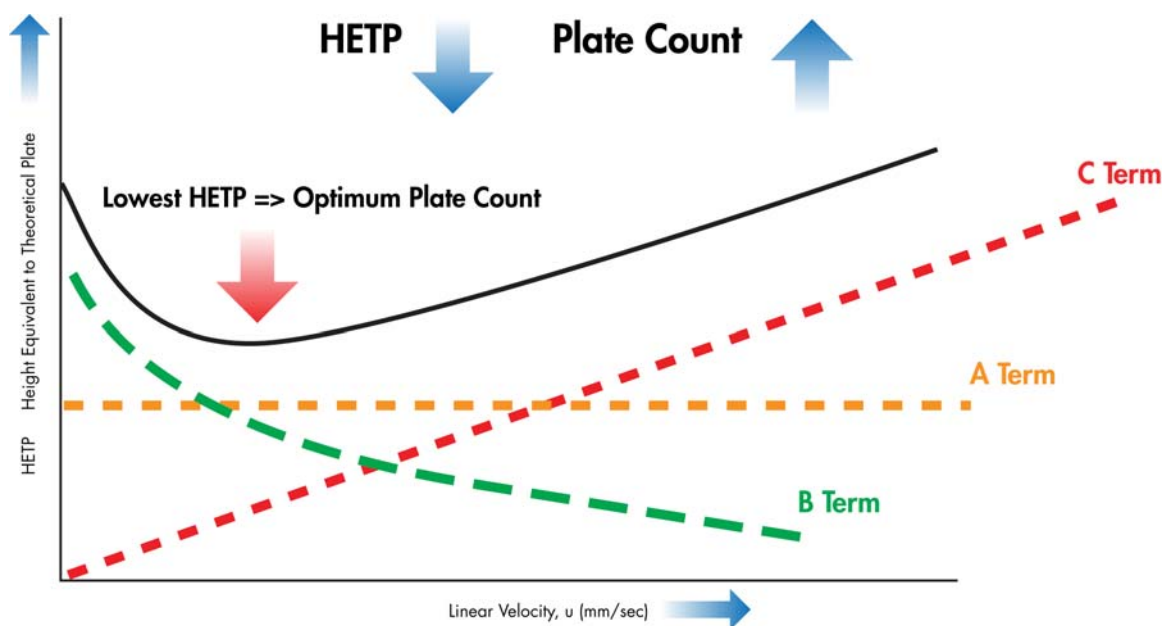


Figure 1.4 van Deemter curve with individual components

1.4.3 UPLC Systems

The complexity of sample composition and the need for greater sensitivity and analysis speed (throughput) stretched the limits of traditional HPLC systems. As theory and practice so amply demonstrated, the use of even smaller particles and higher flow rates should provide the needed improvements. Work published by MacNair and Jorgenson[34] highlighted the difficulties associated with sub- $2\mu\text{m}$ particles and the associated pressures and paved the way for the introduction of Ultra Performance Liquid Chromatography (UPLC) in 2004 and the associated columns packed with $1.7\mu\text{m}$ particles. UPLC systems were designed to minimize system and column bandspread while enabling operation at pressures up to 15,000 psi. These two key hardware attributes finally allowed the full realization of the benefits of sub- $2\mu\text{m}$ separations. Subsequent introductions of other sub-

2 μ m particle columns and systems capable of operating at pressures up to 9000 psi broadened this chromatographic area into what we now call UHPLC, or Ultra High Pressure Liquid Chromatography. Practically speaking, since particle size is directly related to efficiency and flow rate, use of sub-2 μ m particles in a minimally dispersive system results in higher efficiency separations, faster. Since their introduction, these types of systems have become quite common in bioanalytical laboratories [35-67].

1.4.4 A Review of LC for Peptide Quantification

The challenges associated with chromatography of peptides stem in part from the diversity of this class of compounds. As a class, they span a broad range of sizes, molecular weights, isoelectric points (pI), three-dimensional structures, and polarity. Although a high degree of diversity is present, peptide composition is actually heavily conserved- there are only a finite number of amino acids which comprise their sequences, ensuring the presence of multiple closely related species. Peptides are present in samples across an extensive linear dynamic range, 4-5 orders of magnitude or more. Whether derived from a protein digest or present as a naturally existing or synthetic peptide, peptides in biological matrices will need to be separated from numerous closely related interferences. For example, missed cleavages and secondary cleavages in protein digests result in peptides that are nearly identical to the target peptides. Chromatography of peptides is further complicated by other additional factors. These large molecules have multiple points of interaction with chromatographic surfaces, meaning that different parts of the molecule can interact in different ways, possibly yielding poor peak shape or peaks which elute in two places. In

addition, larger molecules such as peptides and proteins exhibit slower diffusion properties, and undergo secondary interactions with stationary phases, both which can result in poor peak shape and/or carryover under conditions traditionally used in bioanalysis.

Although LC separation of peptides has been well documented in the context of proteomic analyses or peptide mapping for qualitative work, LC conditions for that type of research differ significantly from what is required for a bioanalytical workflow. Peptide mapping studies commonly utilize long, shallow gradients (60-120 minutes), low flow rates (relative to small molecule analyses) or nanoflow systems, and ion pairing agents such as TFA. These conditions are not particularly attractive for a bioanalytical laboratory where throughput and MS sensitivity are key aspects of method development. LC systems for peptide quantification in these types of laboratories must use MS compatible buffers and additives, run times should be between 2 to 10 min maximum, if possible, while selectivity from endogenous interferences must be obtained. In addition, peak shapes for small and large peptides alike should be as Gaussian and narrow as possible (to improve signal-to-noise) and the LC system should use sub 2 μm particles, which have been shown to minimize the potential for matrix effects caused by co-elutions [68].

Several reviews have been published over the past 3 years on the topic of LC conditions for peptide bioanalysis. Surveying well over 250 journal articles, the most common set of conditions found consisted of C₁₈ chromatographic columns with aqueous acetonitrile mobile phases, most frequently modified with formic acid.

Acidic conditions are typically used as the carboxyl groups on peptides are neutral at low pH, improving chromatographic retention and minimizing secondary interactions. Those peptides having a strong basic quality (containing several arginine or lysine residues)

may not exhibit ideal chromatographic behaviour under these conditions, therefore, ion-pairing reagents such as TFA may be employed to improve chromatographic peak shape. TFA however, is known to cause significant ion suppression under electrospray conditions and so it is desirable to avoid its use where possible. The suppression observed is due to both the formation of strong ion pairs (which cannot be ionized) and the reduction in signal as a result of high droplet surface tension and conductivity [69].

In 2005, Garcia [70] published a thorough review of the impact of various modifiers on the sensitivity and resolution of peptides and proteins. Though many buffers and alternate volatile ion-pairing reagents were assessed, none were suitable replacements for TFA when peptide chemistry necessitated its use. The MS suppression experienced in the presence of TFA was outweighed by the resolution improvement it afforded. A recent review by Ewles and Goodwin [71] describes their findings with respect to balancing the drawbacks and benefits of TFA and optimal conditions. In their work it appears that low concentrations of TFA (0.01 – 0.05%) in both organic and aqueous mobile phases might provide the desired ion-pairing without the degree of suppression associated with higher levels. In addition, mixtures of low concentrations of TFA with more standard MS modifiers and buffers (i.e., formic acid or ammonium formate) might provide both the peak shape and resolution benefits without the concomitant decrease in sensitivity that usually accompanies the use of TFA. The exact nature and composition of the mobile phase will be highly dependent on the peptide and its sequence as well as the desired retention, resolution, or sensitivity.

On rare occasion, the use of high pH mobile phases has been reported either to neutralize basic groups or to provide improved solubility of the peptide.

For the majority of peptide separations, acetonitrile is the organic solvent of choice, although Giorgianni et al [72] reported improved detection limits for several peptides using methanol. On most modern LC systems, it is straightforward to screen ACN and MeOH, and should perhaps be considered as part of routine method development for peptides.

Acetone was also examined as an alternative to ACN [73]. Retention order for a set of test peptides remained the same. However acetone resulted in wider peaks, increased tailing, and decreased retention relative to ACN. Peptide response by MS however, was similar.

With respect to peptide chromatography, the final topic worthy of mention is the use of Hydrophilic Interaction Chromatography (HILIC). In HILIC separations, acetonitrile is typically the weak solvent and water the strong solvent. It is important to note that HILIC may only be used successfully for those peptides soluble in higher percentages of acetonitrile. Although its use for peptides has been reviewed in the past [74, 75], very few quantitative applications have been reported. One very recent example combines both HILIC SPE and HILIC chromatography to successfully quantify several arginine-containing hexapeptides[76]. HILIC was also employed by Zhan [77] to quantify a tetrapeptide in plasma. In general, peptide separation by HILIC is employed successfully only for smaller, more polar peptides.

The use of end-capped silica-based or hybrid C₁₈ stationary phases is most common for quantitative peptide applications[78]. Naturally, materials which minimize interactions with surface silanols are normally used, primarily to improve peak shape. The relatively recent (1999) introduction of hybrid particles has enabled separations to be carried out over a broader pH range and with significantly reduced surface silanol interactions observed than with traditional silica particles.

1.5 Overview of Modern Mass Spectrometry

1.5.1 Principles of Mass Spectrometry and Common Components

Mass spectrometry is one of the most important and widely used analytical techniques today in many application areas. It is fair to say that in bioanalysis specifically, LC/MS is the dominant and preferred option for both quantitative and qualitative measurements.

Separation of various compounds occurs on the basis of the mass (m) to charge (z) ratio (m/z) of the analyte. Simplistically, mass spectrometry relies on transfer of analyte molecules from a liquid to the gas phase and ionization. Analytes are then separated by m/z , in a vacuum, using electric fields. Finally, analyte ions are measured at a detector.

The primary components of any mass spectrometer consist of a sample inlet, an ion source, a mass analyzer, a detector, a pumping system (to create and maintain vacuum) and a data collection system[79]. There are variations on several of these components, and only those that are most relevant to this work are described in any detail herein. Furthermore, some of the most powerful and flexible MS systems have arisen out of combining multiples of a given component. Examples include triple quadrupole (QQQ) and hybrid quadrupole time-of-flight (QTof) instruments, Electrostatic FTIR MS (Orbitrap) and linear ion traps.

In bioanalysis, the most common way to introduce a sample into an MS system is through atmospheric pressure ionization (API) due to its compatibility with LC sample

introduction and the fact that it can be used to ionize a broad range of analytes efficiently without overly extensive fragmentation in the source, often known as soft ionization. The two ionization modes associated with API are electrospray ionization (ESI) and atmospheric pressure chemical ionization (APCI.) Common mass analyzers used in bioanalysis include quadrupole mass filters, time-of-flight (ToF), and ion traps. In ToF analysis, analyte m/z is determined by flight time in a vacuum, with smaller analytes reaching the detector first. Common detectors include photomultipliers, electron multipliers and multichannel plate detectors. Ion traps operate by accumulating ions in “traps” of varying geometries, and then ejecting specific ions to be measured. The first traps were quadrupole ion traps, with poor linear dynamic range, which limited their use in quantitative applications. These were followed by linear ion traps that had greater ion storage capacity and reduced charging effects compared to their predecessors. Perhaps the most interesting and relevant ion traps are orbitraps, which are essentially an accurate mass version of an ion trap. The orbitrap geometry consists of an outer and inner electrode between which ions spin and are confined by RF and voltage. The combination of angular momentum and RF yields high resolution. Since the resolution is proportional to the time spent in the trap, the highest resolution is not achievable within the sampling rates required for fast separations. Introduction of the C-trap timed the injection of ions into the orbitrap, allowing for more efficient use of the duty cycle and improved resolution for narrow chromatographic peaks.

1.5.2 MS Analyzers Most Frequently Used in Bioanalysis (BA)

Most quantitative bioanalytical applications are performed on triple quadrupole instruments, although recent increases in sensitivity of accurate mass instrumentation have resulted in a rise in their presence in routine BA labs. High sensitivity quantification is frequently carried out on QQQs using multiple-reaction-monitoring (MRM) mode whereby one or more precursor ions are selected in the first quadrupole, fragmented in a collision cell, and one or more products are selected in the second quadrupole for detection. Qualitative analysis is often performed on accurate mass instruments such as a QToF or orbitrap due to the wealth of additional information that can be gleaned about a sample, such as structural elucidation, unambiguous identification based on mass accuracy, or by monitoring a broad mass range to obtain an overall profile of sample components.

Currently, triple quadrupoles operating in MRM mode are the most sensitive platform for quantification and are typically capable of achieving 3-5 orders of magnitude linear dynamic range. In MRM mode, these instruments enjoy an approximate 5-10X sensitivity advantage over comparable vintage accurate mass platforms[80]. Mass accuracy on a QQQ is approximately ± 0.1 - 0.5 m/z and is considered sufficient for most quantitative applications. Accuracy at this level is described as “nominal mass measurement.” In contrast, “accurate mass” instruments utilizing time-of-flight (ToF) or orbitrap analyzers are capable of accuracy to within ± 1 -5 ppm. In what might be described as “full scan mode” (even though ToF instruments are not scanning instruments), ToF platforms provide significantly greater sensitivity than QQQs when a comprehensive snapshot of the sample components is desired, in the region of 100 to 1000-fold.

Tandem quadrupole and accurate mass platforms differ perhaps most markedly in the mass resolution they are capable of delivering. For QQQ, TOF, and orbitraps, resolution is defined as the molecular weight (MW) of a compound divided by the peak width at half height (FWHM). QQQs normally operate under unit-mass resolution conditions, which means that they can distinguish singly charged ions with a valley between the peaks of approximately 10-30% depending on instrument tuning. For a compound of MW 600, this would mean a resolution of 850-1000, the exact value being dependent on tuning. In contrast, accurate mass platforms routinely operate at resolutions of 5000-50,000 or more, thus readily enabling visualization of complex multiply charged species such as peptides or proteins. Figure 1.5 demonstrates the comparison of spectra for bradykinin acquired under various resolution conditions.

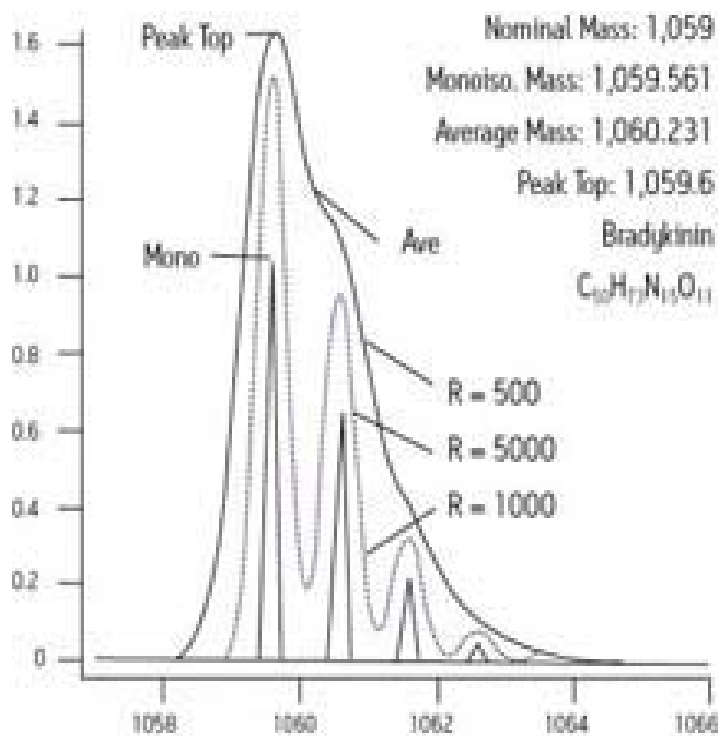


Figure 1.5 Mass Spectra for the peptide bradykinin acquired under various resolution conditions.

1.5.3 Electrospray Ionization

Although MS systems are capable of operating in a number of different ionization modes, such as ESI, APCI, and CI, this discussion will focus on ESI as it is the predominant technique for large molecules. ESI is compatible with analytes of a wide polarity range and is desirable as the precursor ion is often left intact. Though Malcolm Dole is credited with the initial idea of electrospray[81], its development into a commercially viable technique is generally attributed to John Fenn[82].

In electrospray ionization, ions are generated in the solution phase, inside the MS source. The solvent is then evaporated off (desolvation) and gas-phase ions enter the MS. In one common source/probe geometry, LC effluent passes through a metal capillary in the MS probe to which DC voltage is applied, inducing ionization. There are several theories on ion desorption. In one accepted ionization mechanism, during desolvation, opposite charges repel each other within the droplet causing “coulombic repulsion”[81, 83, 84]. Aided by evaporation of the liquid through heating, smaller and smaller droplets are formed, whose charge density increases until ions are ejected from the droplet. Figure 1.6 illustrates this process. In addition, electrospray ionization may occasionally produce $(M-H)^+$ ions as well.

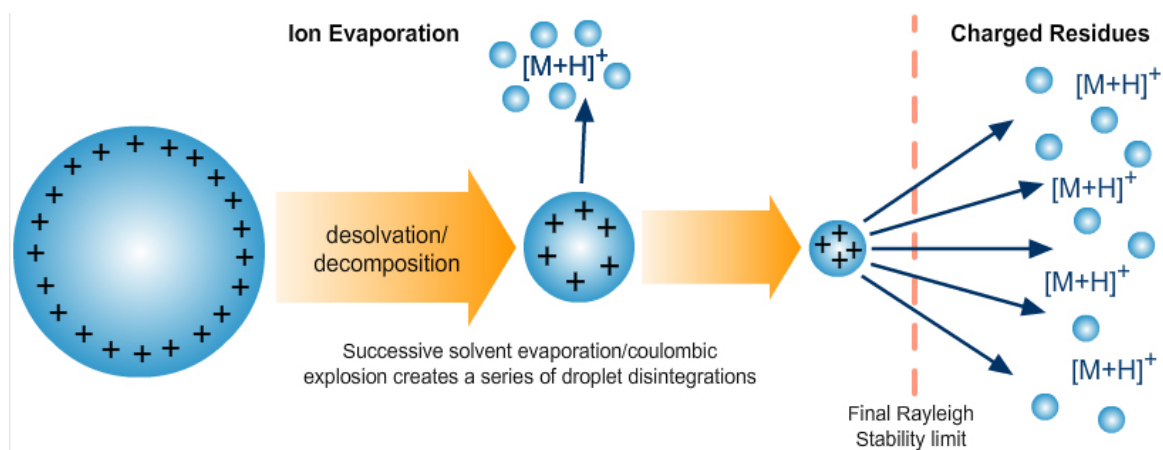


Figure 1.6 Graphical representation of the electrospray ionization process.

1.6 LC/MS for Biopharmaceutical Quantification

Due to the increasing number of biopharmaceuticals and biosimilars in development, LC/MS is increasingly being considered as a replacement for traditional LBAs. LC/MS/MS is an attractive alternative to LBAs because it is characterized by short method development times, broad linear dynamic range, a higher degree of accuracy and precision (reflected in more stringent regulatory guidelines)[14], high specificity, and the ability to simultaneously quantify multiple peptide therapeutics within a single injection and/or method (multiplexing). In addition, LC/MS/MS is already widely used in most bioanalytical laboratories, thus making it accessible to those skilled with the technology.

Development of LC/MS/MS assays (including sample extraction prior to analysis) for peptides is not without its challenges, however. There are those challenges related specifically to the nature and handling of peptides, and there are others related to evolving regulatory guidelines and our growing understanding of the possible limitations of LC/MS/MS. For example, bioanalytical methods have historically relied on the selectivity

of triple quadrupole mass spectrometry to generate acceptable data. Reliance on MS selectivity was so strong in fact, that ballistic LC gradients and simple quick and dirty sample preparation techniques such as protein precipitation became commonplace. The evolution of regulatory guidelines since 2007 now requires that scientists develop more selective and reliable bioanalytical methods[85, 86]. Discussions relating to acceptable results from incurred sample reanalysis (ISR) impact not only assay reproducibility but bring a new focus to analyte stability in various matrices (i.e., plasma, blood, urine). New guidelines for the acceptable variability of matrix effects will require the most selective bioanalytical method possible, placing renewed focus on the bioanalytical method as a whole. These guidelines force bioanalytical scientists to consider the chromatography, mass spectrometry, and extraction protocol with equal importance to provide accurate and reproducible results.

LC/MS faces a few important and persistent hurdles when being considered as a replacement for a previously existing LBA or for new methods. Guidelines for validation of LBA methods are less stringent than for chromatographic assays[14]. LC/MS still struggles to obtain the sensitivity of LBAs, and more specifically achieve similar detection limits with the same volume of sample. LBAs can provide sensitivity in the pg/mL range, consuming only 20-50 μ L of sample or less.

Furthermore, from a handling and analysis standpoint, physiochemical properties of peptides differ from small molecules in many ways. In many instances, conventional well-established “small molecule” LC/MS techniques and strategies may not be directly applicable to the analysis of peptides, necessitating potentially extensive staff training and/or time to acquire the necessary experience. One of the aforementioned differences is

other peptides and high abundance proteins in biological samples, increases the complexity of the method development process.

A review of almost 200 articles in the literature[87] shows that many different combinations of LC, MS, and sample preparation conditions have been used for bioanalysis of peptide therapeutics, making it challenging to identify a common starting point for method development. In addition, many of the published references utilize non-selective sample preparation methods such as protein precipitation (PPT) and reversed-phase solid phase extraction (RP SPE). These techniques are often used either because they are inexpensive or require little to no method development. Though common in small molecule analysis, the use of less selective sample clean-up for peptides may not only necessitate the use of longer chromatographic runs to eliminate the co-elution of endogenous materials with the analyte but may also result in methods which fail matrix effects or ISR criteria. Of these challenges, perhaps the greatest difficulties in developing LC/MS-based methods which use non-affinity extraction, arise during peptide handling. Adsorption, stability, and solubility are critical parameters to understand and control during the method development process.

1.7 Identifying and Understanding Handling Considerations

Prior to discussing the utility of specific sample preparation techniques, one must first understand how the behaviour of peptides, and the challenges associated with it, impact the successful development of an extraction method. From the moment the peptide standard is dissolved (if it is in lyophilized powder form), one must address the issues of

solubility and adsorption. In general, peptide solubility is not resolved in the same manner as for small molecules, and many adsorb to the walls of vials, collection plates, LC surfaces, etc. This is particularly true for larger, more hydrophobic peptides. During method development, heavy emphasis must be placed on identifying the condition under which the peptide exhibits optimal solubility as this impacts every aspect of method development and forms the foundation for successful development of a reproducible, sensitive bioanalytical assay. In addition, failure to address adsorption/NSB can be likewise detrimental to the method as a whole and therefore must be assessed prior to extraction and preparation of test solutions.

1.7.1 Solubility

Peptide solubility is heavily dependent on its specific amino acid sequence, in particular the hydrophobicity and acidity or basicity. There exist many sets of guidelines for solubilizing peptides, and all seem to agree on a few key points and rely on the use of well understood characteristics of amino acids to help predict peptide solubility. Several good sets of guidelines, summarized below, can be found on web pages from Sigma-Aldrich, Thermo Scientific, GenScript, and Pierce. Table 1.2 summarizes the relevant amino acid properties.

| Property | Amino Acid |
|---|---|
| Hydrophobic | A, F, I, L, M, P, V, W, Y |
| Moderate | C, G |
| Hydrophilic | D, E, H, K, N, Q, R, S, T, pyro-glutamic acid |
| Positive Charge | K, R, H, N-terminus |
| Negative Charge | D, E, Y, C-terminus |
| Degradation likely | M, W |
| Prone to de-amidation, dehydration, cyclization to pGlu | N, Q, C-terminal amides, N-terminal Q |
| Prone to oxidation under mild conditions | C, M |

Table 1.2 Useful amino acid properties

1. If a peptide is very small, < 5 residues, it will likely dissolve in aqueous solutions unless the sequence is entirely comprised of hydrophobic residues.
2. Peptides containing >25% charged residues and < 25% hydrophobic residues generally dissolve in aqueous solutions.
3. If the peptide is basic, acidic solutions (formic acid or TFA) with a low % organic (5%) often work well. The converse is true for acidic peptides, try solubilizing in basic solutions (1-5% NH₄OH for example) with a low % organic.
4. Peptides containing >50% hydrophobic residues may be only slightly soluble or insoluble in aqueous solutions. Hydrophobic peptides are best solubilized in DMSO, DMF, strong acid solutions (TFA, formic, acetic), or isopropanol. For cysteine-containing peptides, use DMF instead of DMSO.
5. Guanidine HCl or urea may be necessary for those peptides that tend to aggregate and can later be removed during sample preparation.
6. Peptides which contain >75% of S, T, E, D, K, R, H, N, Q or Y may form intramolecular hydrogen bonds and form gels in aqueous solutions. These peptides should be treated in the same manner as hydrophobic peptides (#4).

1.7.2 Adsorption

In addition to solubility, every effort must be made to minimize or eliminate adsorption. Peptides bind to vials, collection plates, pipette tips and other surfaces. Many researchers have reported significant peptide losses, particularly to pipette tips, during solution preparation or sample handling [88-90]. This may be mitigated by “pre-treating” the tips through aspiration of the peptide solution up and down in the pipette tip prior to dispensing into the final vessel. Other factors that may influence adsorption include solvent composition, container material, temperature, and pH. Adsorption occurs primarily in solvent standards rather than extracts of biological matrices, although matrices with low protein/lipid content such as CSF or urine may still exhibit adsorption. Most biological matrices contain residual proteins or other peptides at higher levels which can act as carriers, binding preferentially to surfaces rendering them “inert” to the low level peptides of interest. Relative to vial/tube/plate composition, side chains of basic peptides can readily interact with surface silanols on glass and hydrophobic peptides may bind through hydrophobic interactions with polypropylene or other plastic surfaces. This effect is more pronounced at low peptide concentrations. Complete loss of peptide during serial dilution often results in loss at the low end of the calibration curve, or even absence of the peptide peak during analysis of low level solvent standards. For this reason, it is generally recommended that when preparing standard curves, one should spike directly into plasma from the peptide stock solution (in which adsorption losses are negligible) and then prepare

subsequent dilutions for the lower concentration points by diluting the plasma spiked with the peptide stock solution with additional plasma.

Issues related to adsorption are further exacerbated by inappropriate solvent choice. Peptide losses occur readily in aqueous solutions. Adsorption can, in part, be ameliorated using the proper solvent composition. Any information gathered during solubility testing should be applied to all subsequent solution preparation. For example, if the addition of acid, base, or organic solvent improves solubility, the appropriate action should be taken to include these modifiers in dilutions of the concentrated standard. Peptides are naturally more soluble in aqueous solutions if they are charged, and conversely, more soluble in organic solutions when uncharged. For particularly hydrophobic peptides, or low concentration aqueous solutions of peptides, one might also consider the addition of a commercially available protein such as serum albumin to help eliminate non specific binding (NSB) to surfaces by blocking adsorption sites. This is not typically necessary for plasma or serum extracts. However, urine or cerebrospinal fluid (CSF) extracts may require the same treatment as solvent-based solutions. Finally, concentration by evaporation and reconstitution should be avoided if at all possible as this frequently results in significant losses. Several options exist for addressing this problem. Addition of a small volume of a viscous solvent such as dimethyl sulfoxide (DMSO) or glycerol prior to evaporation prevents complete dry down. Alternatively, certain SPE formats exist which enable up to 15 fold concentration of the sample without evaporation. This option has the additional benefits of not only increasing throughput by eliminating time consuming evaporation, but also of reducing the number of handling steps whilst ensuring that the sample is in a solution which

not only provides good solubility for the peptide (if SPE method development has been performed properly) but also an injection solvent which is chromatographically compatible.

1.7.3 Stability

Another common concern is possible peptide instability or degradation occurring in-vivo or ex-vivo. Reubsaet et al [91, 92] describe instability as falling into two categories: physical and chemical instability. Physical instability is primarily associated with unfolding (caused by temperature, pH extremes, or guanidine HCl or urea denaturation) and aggregation (primarily due to hydrophobic interactions between partially unfolded species). Chemical instability is related to modifications in amino acids which can occur through oxidation, reduction, deamidation, hydrolysis, arginine conversion, β -elimination, and racemisation [91]. It is important to control conditions which may result in modification during all phases of method development. For example, the use of protease inhibitors to improve matrix stability has been widely accepted. Ewles and Goodwin [71] report testing numerous protease inhibitors. They concluded that 20 mM diisopropylfluoro phosphate (DFP) or Pefabloc® (Roche Diagnostics, West Sussex, UK) were among the best options. In addition, it was noted that simple addition of acid (formic or hydrochloric) was often adequate to inhibit protease activity.

Chemical instability is primarily caused by hydrolysis, oxidation, pyroglutamic acid formation and de-amidation. Peptides containing D (Asp) are most likely to undergo acid catalyzed hydrolysis. De-amidation occurs under base catalyzed conditions in the presence of N-G (Asn-Gly) or Q-G (Gln-Gly.) Cysteine and methionine easily undergo oxidation,

which is accelerated at high pH. The presence of an N-terminal Gln will most certainly result in pyroglutamic acid formation. It is important to note the sequence of the peptide you are working with and assess the potential for any chemical modifications that may occur either as a result of the storage or extraction conditions. It may be necessary to eliminate extreme high pH or low pH conditions during an experiment depending on the specific amino acid composition. A recent development is the increased use of dried blood spots (DBS) in bioanalytical assays[93-107]. In addition to the obvious benefits with respect to low sample volumes and less expensive storage and shipping, DBS has shown promise in stabilizing unstable compounds. This technique was successfully employed by Kehler et al [108] for the analysis of the large peptide Exendin-4.

1.8 Alternative Techniques and Topics

The use of more advanced techniques such as 2D-LC and nano-flow LC have been documented in cases where the required detection limits could not be reached with conventional approaches[109-112]. This is typically due to ultra-low levels in study samples or the presence of closely related endogenous and/or isobaric interferences that could not be resolved using more traditional instrumentation.

Common configurations of 2D LC systems include trap and back elute, trap and forward elute, 2 column approaches (RP-RP, RP-HILIC, etc.), parallel column regeneration, at column dilution and heart cutting [113]. Trap and elute configurations enable one to load more sample at higher flow rates, focus the sample using a trapping column, and flush salts and other interferences to waste. Heart cutting configurations maximize resolution by

allowing one to take a narrow chromatographic band containing the peak of interest and “cut” it from the first column followed by loading of this greatly simplified sample onto the second column for further separation. An example of the benefit of 2D LC for the separation of desmopressin and octreotide is shown in Figure 1. 8. In the 2D separation, phospholipids were removed when the chromatographic band containing octreotide and desmopressin was heart-cut and transferred to a second column. The Figure was reproduced with permission from PPD Pharma.

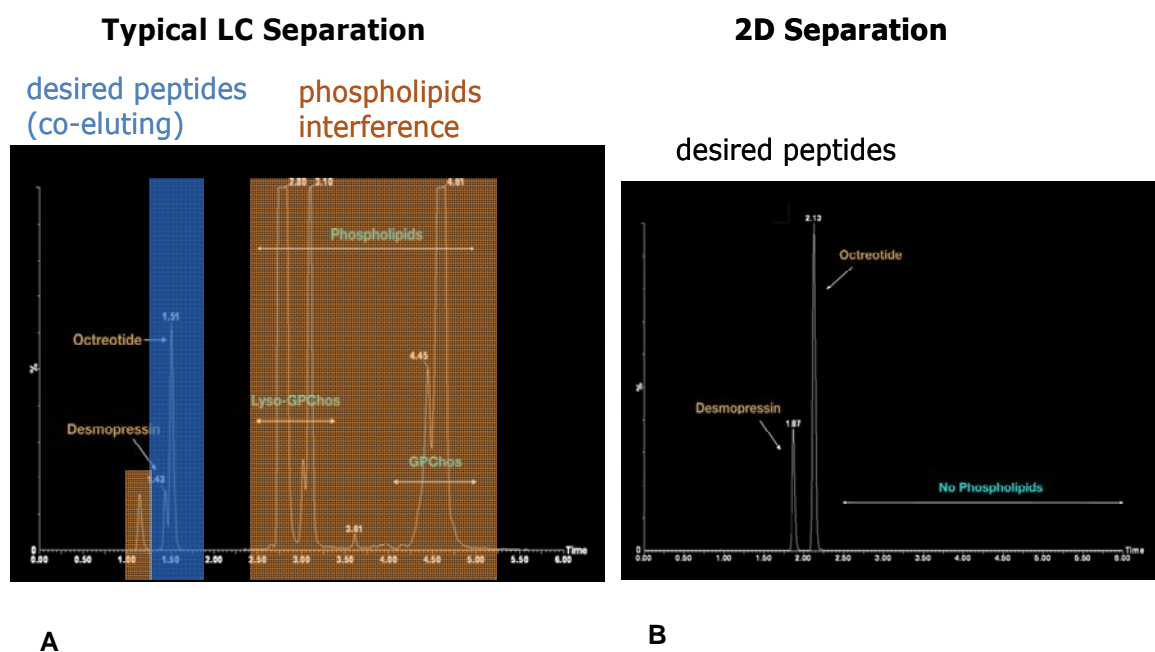


Figure 1.8 Comparison of a 1D separation (A) of desmopressin and octreotide and a 2D separation (B)

A recent publication by Zhang et al [112] details the development of a sensitive method for endogenous oxytocin, which reaches an LLOQ of 1 pg/mL in human plasma using SPE and 2D LC. RP was used in both dimensions. Oxytocin was eluted with a

gradient on the first column, the peak was then heart cut to the second column and eluted under isocratic conditions.

The low flow rates used in nano-LC can provide significant improvements in MS ionization efficiency, resulting in dramatic sensitivity gains due in part to improved ionization efficiency. However, nano-flow systems are often perceived as having poor robustness, requiring a very skilled operator and as being somewhat of an “art.” The narrow diameter columns (typically 75-300 μm), sensitivity to integrity of connections and tubing cuts, and “finicky” nature of the spray from various tip types contribute to this perception and to the limited use of nano-flow in routine bioanalytical laboratories. In addition, the low flow rates required result in long chromatographic run times, severely restricting throughput.

Methods which include highly selective isolation and enrichment techniques based on affinity purification of peptides, such as immunoprecipitation (IP), prior to analysis can achieve even greater specificity. Li et al [114] described such an approach for the quantification of amyloid peptides during the 2009 AAPS meeting. Columns packed with anti-peptide antibodies have also been used to selectively enrich target peptides. This was successfully applied by Neubert et al [111] to enrich signature tryptic peptides of pepsin/pepsinogen for protein quantification. Though in more widespread use currently, these approaches are limited by the availability of commercial reagent kits or the internal resources needed to develop the highly specialized reagents or columns required.

1.9 Research Aims

This research projects aims to overcome the identified short comings of LC/MS as it pertains to its adoption for quantification of large molecules, endogenous and therapeutic peptides in particular. Specifically, this work will endeavour to increase the sensitivity and specificity of LC/MS assays for peptides and ultimately to couple this with a reduction in required sample volume.

The research will be carried out in several steps:

Phase 1: Develop an understanding of factors influencing LC and MS sensitivity and specificity for peptides and propose rules and guidelines for MS method development as well as a starting LC screening protocol. Similarly, various sample preparation techniques will be evaluated on the basis of recovery, selectivity, and compatibility with the required LC mobile phase. A starting sample preparation protocol will also be proposed.

Phase 2: Apply the fundamental handling issues and proposed resolutions learned in phase 1 to develop an LC/MS method to quantify amyloid beta peptides, putative Alzheimer's Disease biomarkers, in human CSF. This method is intended to replace IP/LC/MS methods and ELISAs. We will also explore and contrast various surrogate matrices to the standard

addition approach for quantification in CSF. Finally, 1D and 2D LC strategies will be evaluated.

Phase 3: Investigate a multi-stage sample preparation scheme to develop an assay for the osteoporosis drug teriparatide with specificity and sensitivity equivalent to the traditional RIA.

Phase 4: Investigate multi-dimensional LC coupled to two-stage high-throughput sample preparation to simultaneously quantify human insulin and five commonly dosed analogs. Demonstrate performance improvements relative to more generic approaches.

Phase 5: Investigate the use of microscale LC and an integrated microfluidic column to further improve sensitivity and reduce sample volume required in assays for teriparatide, glucagon, multiple insulins and a selection of endogenous and therapeutic cyclic peptides.

1.10 References

1. Swinney, D. and J. Anthony, *How were new medicines discovered?* Nature Reviews Drug Discovery, 2011. 10: p. 507-519.
2. EFPIA, *The Pharmaceutical Industry in Figures*. 2013.
3. Reichart, J., et al., *Development Trends for Peptide Therapeutics: a Comprehensive quantitative analysis of peptide therapeutics in clinical development*, 2010.
4. Vlieghe, P., et al., *Synthetic Therapeutic Peptides: Science and Market*. Drug Discovery Today, 2010. 15: p. 40-56.
5. Berkrot, B. *Success rates for experimental drugs falls: study*. 2011.
6. Ho, R. and M. Gibaldi, *Biotechnology and Biopharmaceuticals* 2003, New Jersey: Wiley and Sons.
7. Edwards, C., M. Cohen, and S. Bloom, *Peptides as Drugs*. QJM, 1999. 92: p. 1-4.
8. Thayer, A., *Improving Peptides*. Chemical and Engineering News, 2011. 89(22): p. 13-20.
9. Werle, M. and A. Bernkop-Schnürch, *Strategies to improve plasma half life time of peptide and protein drugs*. Amino Acids, 2006. 30(4): p. 351-367.
10. Amgen, *Biologics and Biosimilars: an Overview*. 2014.
11. Rotenstein, L., *Opportunities and Challenges for Biosimilars: What's on the Horizon in the Global Insulin Market?* Clinical Diabetes, 2012. 30(4): p. 138-150.
12. FDA and CDER, *Guidance for Industry*

Bioequivalence Studies with Pharmacokinetic Endpoints for Drugs Submitted Under an ANDA. 2013.

13. Hardy, J. and D.J. Selkoe, *The amyloid hypothesis of Alzheimer's disease: progress and problems on the road to therapeutics*. Science, 2002. 297: p. 353-356.
14. FDA, *Guidance for Industry: Bioanalytical Method Validation*, C.a. CVM, Editor 2001.
15. Rifai, N., M.A. Gillette, and S.A. Carr, *Protein biomarker discovery and validation: the long and uncertain path to clinical utility*. Nat Biotech, 2006. 24(8): p. 971-983.
16. Wang, S.S., *Researchers Aim to Speed Cures to Patients*, in *Wall Street Journal* 2013.
17. Wang, J. and L. Urban, *The impact of early ADME profiling on drug discovery and development strategy*. Drug Discovery World, 2004.
18. Nowatzke, W., et al., *Unique challenges of providing bioanalytical support for biological therapeutic pharmacokinetic programs*. Bioanalysis, 2011. 3(5): p. 509-521.
19. Touchstone, J.C., *History of Chromatography*. Journal of Liquid Chromatography, 1993. 16(8): p. 1647-1665.
20. Ettre, L., *Tswett and the Invention of Chromatography*. LCGC North America, 2003. 21(5): p. 458-467.
21. Martin, A.J. and R.L. Synge, *A new form of chromatogram employing two liquid phases: A theory of chromatography. 2. Application to the micro-determination of the higher monoamino-acids in proteins*. Biochemistry Journal, 1941. 35(12): p. 1358-1368.

22. Syngé, R.L., *Experiments on amino-acids: The partition of acetamino-acids between immiscible solvents*. Biochemistry Journal, 1939. 33(12): p. 1913-1917.
23. Martin, A.J. and R.L. Syngé, *Separation of the higher monoamino-acids by counter-current liquid-liquid extraction: the amino-acid composition of wool*. Biochemistry Journal, 1941. 35(1-2): p. 91-121.
24. Grumbach, E., J. Arsenault, and D. McCabe, *Beginners Guide to UPLC Ultra-Performance Liquid Chromatography* 2009, Milford, MA: Waters Corporation.
25. Moore, J.C., *Gel permeation chromatography. I. A new method for molecular weight distribution of high polymers*. Journal of Polymer Science Part A: General Papers, 1964. 2(2): p. 835-843.
26. Ettre, L.S. and J. Waters, *The development of GPC and the first HPLC instruments*. LCGC NORTH AMERICA, 2005.
27. Neue, U., *HPLC Columns Theory, Technology and Practice* 1997, New York: John Wiley and Sons.
28. van Deemter, J.J., F.J. Zuiderweg, and A. Klinkenberg, *Longitudinal diffusion and resistance to mass transfer as causes of nonideality in chromatography*. Chemical Engineering Science, 1956. 5(6): p. 271-289.
29. Cazes, J.S., *Chromatographic Theory* 2002, New York: Marcel Dekker.
30. Snyder, L.R., *Maximum resolution per unit time in liquid-solid adsorption chromatography. Separation on column vs. thin layers*. Analytical Chemistry, 1967. 39(7): p. 705-709.
31. Kromidas, S., *HPLC Made to Measure* 2006, Germany: Wiley-VCH.

32. Majors, R. and P. Carr, *Glossary of HPLC/LC Separation Terms*. LCGC Europe, 2008.
33. Ettre, L.S. and K.I. Sakodinskii, *M. S. Tswett and the discovery of chromatography II: Completion of the development of chromatography (1903–1910)*. *Chromatographia*, 1993. 35(5-6): p. 329-338.
34. MacNair, J.E., K.C. Lewis, and J.W. Jorgenson, *Ultrahigh-Pressure Reversed-Phase Liquid Chromatography in Packed Capillary Columns*. *Analytical Chemistry*, 1997. 69(6): p. 983-989.
35. Chen, J.P., et al., *Ultra-high-performance liquid chromatography tandem mass spectrometry method for the determination of gambogenic acid in dog plasma and its application to a pharmacokinetic study*. *Biomed Chromatogr*, 2014. 7(10).
36. Chen, J.Z., et al., *Development of a sensitive and rapid UPLC-MS/MS method for the determination of koumine in rat plasma: application to a pharmacokinetic study*. *Biomed Chromatogr*, 2013. 27(6): p. 736-40.
37. Chen, L., et al., *Quantitative determination of azithromycin in human plasma by ultra performance liquid chromatography-electrospray ionization mass spectrometry and its application in a pharmacokinetic study*. *J Chromatogr B Analyt Technol Biomed Life Sci*, 2007. 855(2): p. 255-61.
38. Chen, M., et al., *Determination of Rutin in Rat Plasma by Ultra Performance Liquid Chromatography Tandem Mass Spectrometry and Application to Pharmacokinetic Study*. *J Chromatogr Sci*, 2014. 16.
39. Du, P., et al., *Development and validation of a rapid and sensitive UPLC-MS/MS method for determination of total docetaxel from a lipid microsphere formulation in*

- human plasma*. J Chromatogr B Analyt Technol Biomed Life Sci, 2013. 926: p. 101-7.
40. Gao, H., et al., *Determination of Pseudoginsengenin DQ in rat plasma by UPLC-MS/MS and application of the method in a pharmacokinetic study*. J Chromatogr B Analyt Technol Biomed Life Sci, 2013. 933: p. 1-7.
 41. Hu, M.L., M. Xu, and Q. Ye, *Quantitative Determination of Ketoconazole by UPLC-MS/MS in Human Plasma and its Application to Pharmacokinetic Study*. Drug Res, 2014. 22: p. 22.
 42. Huang, C., W. Wang, and L. Miao, *Determination of Cefaclor by UPLC-MS-MS for a Chinese Pharmacokinetic Study*. J Chromatogr Sci, 2014. 52(7): p. 636-40.
 43. Iqbal, M., et al., *Development and validation of ultra-performance liquid chromatographic method with tandem mass spectrometry for determination of lenalidomide in rabbit and human plasma*. Chem Cent J, 2013. 7(1): p. 7-7.
 44. Kan, X., S.L. Zheng, and C.Y. Zhou, *UPLC-MS/MS Determination of Phentolamine in Human Plasma and its Application to a Pharmacokinetic Study*. Drug Res, 2014. 22: p. 22.
 45. Kay, R.G., et al., *High-throughput ultra-high-performance liquid chromatography/tandem mass spectrometry quantitation of insulin-like growth factor-I and leucine-rich alpha-2-glycoprotein in serum as biomarkers of recombinant human growth hormone administration*. Rapid Communications in Mass Spectrometry, 2009. 23: p. 3173-3182.

46. Li, G., et al., *Development and application of a UPLC-MS/MS method for the pharmacokinetic study of 10-hydroxy camptothecin and hydroxyethyl starch conjugate in rats*. J Pharm Biomed Anal, 2014. 88: p. 345-53.
47. Lin, X., et al., *Determination of alprostadil in rat plasma by ultra performance liquid chromatography-electrospray ionization-tandem mass spectrometry after intravenous administration*. J Pharm Biomed Anal, 2009. 49(4): p. 983-8.
48. Liu, Y., et al., *Ultra-performance liquid chromatography-tandem mass spectrometry method for the determination of nitrendipine in dog plasma and its application to a pharmacokinetic study of a solid self-emulsifying pellet formulation*. Arzneimittelforschung, 2011. 61(12): p. 674-80.
49. Liu, Z., et al., *Simultaneous determination of pimpinellin, isopimpinellin and phellopterin in rat plasma by a validated UPLC-MS/MS and its application to a pharmacokinetic study after administration of Toddalia asiatica extract*. J Chromatogr B Analyt Technol Biomed Life Sci, 2012. 892: p. 102-8.
50. Qin, F., et al., *Determination of nimodipine in human plasma by ultra performance liquid chromatography-tandem mass spectrometry and pharmacokinetic application*. J Pharm Biomed Anal, 2008. 46(3): p. 557-62.
51. Tang, Y., et al., *[Determination of sitagliptin phosphate in rat plasma by ultra high performance liquid chromatography-tandem mass spectrometry]*. Se Pu, 2011. 29(6): p. 475-80.
52. Vuppala, P.K., et al., *Development and validation of a UPLC-MS/MS method for the determination of 7-hydroxymitragynine, a mu-opioid agonist, in rat plasma and its*

- application to a pharmacokinetic study. Biomed Chromatogr, 2013. 27(12): p. 1726-32.*
53. Wang, D., et al., *Determination of lovastatin in human plasma by ultra-performance liquid chromatography/electrospray ionization tandem mass spectrometry. Biomed Chromatogr, 2008. 22(5): p. 511-8.*
 54. Wang, X., et al., *Development and validation of UPLC-MS/MS method for determination of domperidone in human plasma and its pharmacokinetic application. Biomed Chromatogr, 2013. 27(3): p. 371-6.*
 55. Wang, X.S., et al., *Determination of cephalomannine in rat plasma by gradient elution UPLC-MS/MS method. J Chromatogr B Analyt Technol Biomed Life Sci, 2014. 963: p. 70-4.*
 56. Wang, Y., et al., *Simultaneous determination of neochlorogenic acid, chlorogenic acid, cryptochlorogenic acid and geniposide in rat plasma by UPLC-MS/MS and its application to a pharmacokinetic study after administration of Reduning injection. Biomed Chromatogr, 2014. 20(10).*
 57. Wang, Z., et al., *UPLC-MS/MS determination of voriconazole in human plasma and its application to a pharmacokinetic study. Biomed Chromatogr, 2014. 13(10).*
 58. Yan, C., et al., *Determination of xanthatin by ultra high performance liquid chromatography coupled with triple quadrupole mass spectrometry: application to pharmacokinetic study of xanthatin in rat plasma. J Chromatogr B Analyt Technol Biomed Life Sci, 2014. 948: p. 57-61.*

59. Yang, S., et al., *Determination of palonosetron in human plasma by ultra performance liquid chromatography-tandem mass spectrometry and its application to a pharmacokinetic study*. J Pharm Biomed Anal, 2012. 57: p. 13-8.
60. Ying, X., et al., *Determination of vitexin-2''-O-rhamnoside in rat plasma by ultra-performance liquid chromatography electrospray ionization tandem mass spectrometry and its application to pharmacokinetic study*. Talanta, 2007. 72(4): p. 1500-6.
61. Yuan, H., et al., *Determination of lovastatin in human plasma by ultra-performance liquid chromatography-electrospray ionization tandem mass spectrometry and its application in a pharmacokinetic study*. J Pharm Biomed Anal, 2008. 46(4): p. 808-13.
62. Zhang, L., et al., *Simultaneous determination of Guanfu base G and its active metabolites by UPLC-MS/MS in rat plasma and its application to a pharmacokinetic study*. J Chromatogr B Analyt Technol Biomed Life Sci, 2014. 957: p. 1-6.
63. Zhang, W., et al., *Simultaneous determination of vitexin-4''-O-glucoside, vitexin-2''-O-rhamnoside, rutin and vitexin from hawthorn leaves flavonoids in rat plasma by UPLC-ESI-MS/MS*. J Chromatogr B Analyt Technol Biomed Life Sci, 2010. 878(21): p. 1837-44.
64. Zhang, W.M., et al., *UPLC-MS/MS method for determination of avicularin in rat plasma and its application to a pharmacokinetic study*. J Chromatogr B Analyt Technol Biomed Life Sci, 2014. 20: p. 107-111.
65. Zhang, Y., et al., *Simultaneous determination of three bufadienolides in rat plasma after intravenous administration of bufadienolides extract by ultra performance*

- liquid chromatography electrospray ionization tandem mass spectrometry*. Anal Chim Acta, 2008. 610(2): p. 224-31.
66. Zhou, W., et al., *Simultaneous determination of phenolic acids by UPLC-MS/MS in rat plasma and its application in pharmacokinetic study after oral administration of Flos Lonicerae preparations*. J Pharm Biomed Anal, 2013. 86: p. 189-97.
 67. Zhou, W., et al., *Simultaneous determination of caffeic acid derivatives by UPLC-MS/MS in rat plasma and its application in pharmacokinetic study after oral administration of Flos Lonicerae-Fructus Forsythiae herb combination*. J Chromatogr B Analyt Technol Biomed Life Sci, 2014. 950: p. 7-15.
 68. Chambers, E., et al., *Journal of Chromatography B*, 2007. 852(1-2): p. 22-34.
 69. Apffel, A., et al., *Enhanced sensitivity for peptide mapping with electrospray liquid chromatography-mass spectrometry in the presence of signal suppression due to trifluoroacetic acid-containing mobile phases*. Journal of Chromatography A, 1995. 712(1): p. 177-190.
 70. Garcia, M.C., *The effect of the mobile phase additives on sensitivity in the analysis of peptides and proteins by high-performance liquid chromatography-electrospray mass spectrometry*. Journal of Chromatography B, 2005. 825: p. 111-123.
 71. Ewles, M. and L. Goodwin, *Bioanalytical approaches to analyzing peptides and proteins by LC-MS/MS*. Bioanalysis, 2011. 3(12): p. 1379-1397.
 72. Giorgianni, F., et al., *LC-MS/MS Analysis of peptides with methanol as organic modifier: improved limits of detection*. Analytical Chemistry, 2004. 76: p. 7028-7038.

73. Keppel, T., M. Jacques, and D. Weis, *the Use of Acetone as a substitute for acetonitrile in analysis of peptides by liquid chromatography/electrospray ionization mass spectrometry*. Rapid Communications in Mass Spectrometry, 2010. 24: p. 6-10.
74. Zhu, B., C. Mant, and R. Hodges, *Mixed-mode hydrophilic interaction chromatography rivals reversed-phase liquid chromatography for the separation of peptides*. Journal of Chromatography, 1992. 594: p. 75-86.
75. Yoshida, T., *Peptide Separation by Hydrophilic interaction chromatography: a review*. Journal of Biochemistry and Biophysical Methods, 2004. 60: p. 265-280.
76. Zhou, W., et al., *Rapid and simultaneous determination of hexapeptides (Ac-EEMQRR-amide and H2N-EEMQRR-amide) in anti-wrinkle cosmetics by hydrophilic interaction liquid chromatography–solid phase extraction preparation and hydrophilic interaction liquid chromatography with tandem mass spectrometry*. Journal of Chromatography A, 2011. 1218(44): p. 7956-7963.
77. Zhan, Y., X. Chen, and D. Zhong, *Quantifying Tetrapeptide SS-20 in rat plasma using hydrophilic interaction liquid chromatography coupled with electrospray ionization mass spectrometry*. Journal of Chromatography B, 2011. 879: p. 3353-3359.
78. Ewles, M. and L. Goodwin, *Bioanalytical approaches to analyzing peptides and proteins by LC–MS/MS*. Bioanalysis, 2011. 3(12): p. 1379-1397.
79. Rossi, D. and M. Sinz, *Mass Spectrometry in Drug Discovery* 2002, New York, Basel: Marcel Dekker.

80. Plumb, R., et al., *Comparison of the quantification of a Therapeutic protein using nominal and accurate mass MS/MS*. Bioanalysis, 2012. 4(5).
81. Daas, C., *Fundamentals of Contemporary Mass Spectrometry* 2007, New York: John Wiley and Sons.
82. Yamashita, M. and J.B. Fenn, *Electrospray Ion Source. Another Variation on the Free-Jet Theme*. J. Phys. Chem. , 1984. 88: p. 4451-4459.
83. Kebarle, P. and L. Tang, *Analytical Chemistry*, 1993(65): p. 972A-986A.
84. de Hoffmann, E., *Mass Spectrometry Principles and Applications* 2002, New York: John Wiley and Sons.
85. Viswanathan, C.T., et al., *Workshop/Conference Report-Quantitative Bioanalytical Methods Validation and Implementation: Best Practices for Chromatographic and Ligand Binding Assays*. The AAPS Journal, 2007. 9(1): p. Article 4.
86. Fast, D.M., et al., *Workshop Report and Follow-up- AAPS Workshop on Current Topics in GLP Bioanalysis: Assay Reproducibility for Incurred Samples- Implications of Crystal City Recommendations*. The AAPS Journal, 2009.
87. Van den Broek, I., et al., *Quantitative bioanalysis of peptides by liquid chromatography coupled to (tandem) mass spectrometry*. Journal of Chromatography B, 2008. 872: p. 1-22.
88. Granvogl, B., M. Plösch, and L. Eichacker, *Sample preparation by in-gel digestion for mass spectrometry-based proteomics*. Analytical and Bioanalytical Chemistry, 2007. 389(4): p. 991-1002.

89. Rappsilber, J., M. Mann, and Y. Ishihama, *Protocol for micro-purification, enrichment, pre-fractionation and storage of peptides for proteomics using StageTips*. Nat. Protocols, 2007. 2(8): p. 1896-1906.
90. Speicher, K., S. Harper, and D. Speicher, *Systematic Analysis of Peptide Recoveries from In-Gel Digestions for Protein Identifications in Proteome Studies*. Journal of Biomolecular Techniques, 2000. 11: p. 74-86.
91. Reubsaet, J.L.E., et al., *Analytical techniques used to study the degradation of proteins and peptides: chemical instability*. Journal of Pharmaceutical and Biomedical Analysis, 1998. 17(6-7): p. 955-978.
92. Reubsaet, J.L.E., et al., *Analytical techniques used to study the degradation of proteins and peptides: physical instability*. Journal of Pharmaceutical and Biomedical Analysis, 1998. 17(6-7): p. 979-984.
93. Al-Dirbashi, O.Y., et al., *Analysis of Methylcitrate in Dried Blood Spots by Liquid Chromatography-Tandem Mass Spectrometry*. JIMD Rep, 2014. 6: p. 6.
94. Barcenas, M., et al., *Tandem Mass Spectrometry Assays of Palmitoyl Protein Thioesterase 1 and Tripeptidyl Peptidase Activity in Dried Blood Spots for the Detection of Neuronal Ceroid Lipofuscinoses in Newborns*. Anal Chem, 2014. 14: p. 14.
95. Crimmins, E., et al., *Validation of blood-based assays using dried blood spots for use in large population studies*. Biodemography Soc Biol, 2014. 60(1): p. 38-48.
96. de Bruin, E., et al., *Evolution of an influenza pandemic in 13 countries from 5 continents monitored by protein microarray from neonatal screening bloodspots*. J Clin Virol, 2014. 30(14): p. 00253-4.

97. Heath, A.K., et al., *Measurements of 25-hydroxyvitamin D concentrations in archived dried blood spots are reliable and accurately reflect those in plasma*. J Clin Endocrinol Metab, 2014. 2.
98. Held, P.K., et al., *Development of an assay to simultaneously measure orotic acid, amino acids, and acylcarnitines in dried blood spots*. Clin Chim Acta, 2014. 2: p. 149-154.
99. Jager, N.G., et al., *Use of dried blood spots for the determination of serum concentrations of tamoxifen and endoxifen*. Breast Cancer Res Treat, 2014. 146(1): p. 137-44.
100. Ma, W.L., et al., *Analysis of polychlorinated biphenyls and organochlorine pesticides in archived dried blood spots and its application to track temporal trends of environmental chemicals in newborns*. Environ Res, 2014. 23: p. 204-210.
101. Mannu, R.S., P.E. Turpin, and L. Goodwin, *Alternative strategies for mass spectrometer-based sample dilution of bioanalytical samples, with particular reference to DBS and plasma analysis*. Bioanalysis, 2014. 6(6): p. 773-84.
102. Nageswara Rao, R., *Emerging liquid chromatography-mass spectrometry technologies improving dried blood spot analysis*. Expert Rev Proteomics, 2014. 11(4): p. 425-30.
103. P, S.S., et al., *Development of an LC-MS/MS method for determination of bicalutamide on dried blood spots: application to pharmacokinetic study in mice*. Biomed Chromatogr, 2014. 19(10).

104. Ramesh, T., P.N. Rao, and R.N. Rao, *Development of LC-MS/MS method for the determination of dapiprazole on dried blood spots and urine: application to pharmacokinetics*. Biomed Chromatogr, 2014. 28(5): p. 615-20.
105. Rhoden, L., et al., *Simple procedure for determination of valproic acid in dried blood spots by gas chromatography-mass spectrometry*. J Pharm Biomed Anal, 2014. 96: p. 207-12.
106. Tran, C., et al., *Stable isotope dilution microquantification of creatine metabolites in plasma, whole blood and dried blood spots for pharmacological studies in mouse models of creatine deficiency*. Clin Chim Acta, 2014. 28: p. 160-168.
107. Tretzel, L., et al., *Use of dried blood spots in doping control analysis of anabolic steroid esters*. J Pharm Biomed Anal, 2014. 96: p. 21-30.
108. Kehler, J., et al., *Application of DBS for quantitative assessment of the peptide Exendin-4; comparison of plasma and DBS method by UHPLC-MS/MS*. Bioanalysis, 2010. 2(8): p. 1461-1468.
109. Chambers, E., et al., *Multidimensional LC-MS/MS Enables Simultaneous Quantification of Intact Human Insulin and 5 Recombinant Analogs in Human Plasma*. Analytical Chemistry, 2014. 86(1): p. 694-702.
110. Houbart, V., et al., *Development of a nano-liquid chromatography on chip tandem mass spectrometry method for high-sensitivity hepcidin quantitation*. J Chromatogr A, 2011. 1218(50): p. 9046-54.
111. Neubert, H., J. Gale, and D. Muirhead, *Online High-Flow Peptide Immunoaffinity Enrichment and Nanoflow LC-MS/MS: Assay Development for Total Salivary Pepsin/Pepsinogen*. Clinical Chemistry, 2010. 56(9): p. 1413-1423.

112. Zhang, G., et al., *Ultra sensitive quantitation of endogenous oxytocin in rat and human plasma using a two-dimensional liquid chromatography–tandem mass spectrometry assay*. Analytical Biochemistry, 2011. 416(1): p. 45-52.
113. Vooght-Johnson, D., *The Waters Bioanalysis World Tour*. Bioanalysis, 2010. 2(12): p. 1931-1942.
114. Li, W., et al., *Development of a Sensitive, High-throughput Immunoaffinity-LC-Tandem Mass Spectrometry Method for the Quantification of Amyloid β Peptides ($A\beta$) in Biological Matrices*, in *American Association of Pharmaceutical Scientists* 2009.

Chapter Two

Investigating Sample Preparation, LC and MS for Large Molecule Quantification: Development of Basic Screening Tools and Guidelines for LC/MS Bioanalytical Assays for Biopharmaceuticals

2.1 Introduction

Chapter 1 established that the ideal platform for quantification of both small molecules and peptides is LC/MS. Within that realm, the most common LC conditions for small molecules employ reversed-phase stationary phases. Sample prep for small molecules is typically protein precipitation, liquid-liquid extraction (for lipophilic molecules), or SPE which has the advantages of being easy to automate, offering a wide variety of stationary phases, and the ability to finely tune the wash and elution solutions to obtain specificity. It would seem logical to quantify peptides using the same techniques. However, with respect to LC, peptides elute in a very narrower window of organic composition relative to small molecules. As this thesis focuses on analysis in *biological* matrices, thousands of other peptides can coincidentally elute within that same organic composition window, making LC separation particularly challenging. In addition, peptides are zwitterionic, further complicating LC method development. From a sample preparation perspective, protein precipitation extracts are often too dirty to enable low level peptide quantification while liquid-liquid extraction uses solvents which are not compatible with peptide solubility. From a mass spectrometry perspective there are several key factors that make peptide analysis more complicated than that of small molecules. Peptides are multiply charged and therefore the precursor ion current is distributed across several different species, each potentially containing its own isotope envelope. This means that not only is the parent signal decreased relative to small molecules (in general), but one must also optimize the conditions for multiple precursors, and subsequently find a way to identify the most specific of these. In addition, attempted collision induced dissociation (CID) of the various precursors may

result in either minimal or overly extensive fragmentation (into many low abundance species), and in fewer cases, the desired production of several well defined fragment candidates. As a result, sensitivity is further reduced relative to small molecules either due to the production of many singly *or* multiply charged fragments or when little to no fragmentation occurs. Again, one must now identify a way to choose the most specific of the many possible fragments available from each of the possible precursors.

Whilst the obvious starting point for peptide bioanalytical research would be that used for small molecules, one must recognize that because the morphology and chemical nature of peptides is so different from their small molecule counterparts, this approach is not likely adequate for high sensitivity peptide quantification. Therefore, the work described in this chapter is aimed at identifying the best possible starting conditions for peptide bioanalytical method development. From this, a series of rules and guidelines for high sensitivity peptide quantification will be derived. This chapter and the learnings therein will form the foundation upon which all subsequent chapters will be based.

This chapter will be presented in three segments: liquid chromatography, mass spectrometry, and sample preparation. Each segment will identify key parameters for consideration when using these techniques for peptides, potential pitfalls, and differences relative to small molecule analysis. The studies described within each section will result in the generation of fundamental rules and guidelines to be applied in Chapters 3-6. Following the successful identification of recommendations from each of the three sections: LC, MS, and sample preparation, a logical, stepwise, and routine strategy to bioanalytical method development for peptides will be proposed. Finally, a critical aspect of this work will be the development of rules and guidelines which produce more selective, sensitive and

reproducible methodologies and ensure their validity with respect to current and evolving (future) regulatory requirements.

2.2 Section I. Investigation into Parameters Affecting LC of Large Molecules

A review of over 200 published methods for peptide quantification[1] validates the use of reversed-phase C18 LC for peptide analysis as this condition is employed in the overwhelming majority of instances. Furthermore, acetonitrile is the organic solvent of choice, representing the optimal condition for the bulk of peptide separations. Finally, this same review establishes formic acid as the ideal modifier. Therefore, the focus of this section will be limited primarily to ascertaining and distinguishing the important subtleties and attributes within this set of conditions which render *optimal* separation of peptides possible. Only a minimal discussion of other modifiers, stationary phases, and organic options will be presented.

2.2.1 Influence of Particle Size

It is clear that resolution from closely related endogenous constituents, speed, and sensitivity are all absolutely critical for effective, reliable and efficient analysis/separation of peptides in bioanalysis. Sub-2 μm porous particle LC, or UHPLC, has been used extensively in both small molecule and peptide bioanalytical applications specifically for the benefits it provides in terms of these exact parameters [2-12]. As valuable as these characteristics are to small molecule analysis, they can be even more critical to successful

peptide analysis. Peptide drugs are often modified versions of substances already in the body, meaning that there will almost always be a closely related interference present in the sample. The drug desmopressin and the endogenous hormone vasopressin upon which it is based, are a good example of this. Desmopressin differs from human vasopressin by the loss of an amino group. Thus, the resolving power of the chromatography system used for this separation is critical, and sub-2 μm LC has demonstrated improvements in resolution and detection limits that are significantly better than conventional HPLC [2-4, 6-12].

It is important to understand the differences between small and large molecules as it pertains to the use of UHPLC. A van Deemter plot was constructed using flow rate instead of linear velocity to demonstrate how the theoretical plate height for large molecules degrades much more rapidly than for small molecules at the higher flow rates that typically dominate most bioanalytical laboratory operations today (Figure 2.1). The figure was developed using the van Deemter equation below, where u = flow rate rather than the more traditional linear velocity. In the below equation HETP is equal to the Height Equivalent to a Theoretical Plate.

$$\text{HETP} = 1.5 (3.5) + 0.5/u + 0.1666 (3.5)^2 u$$

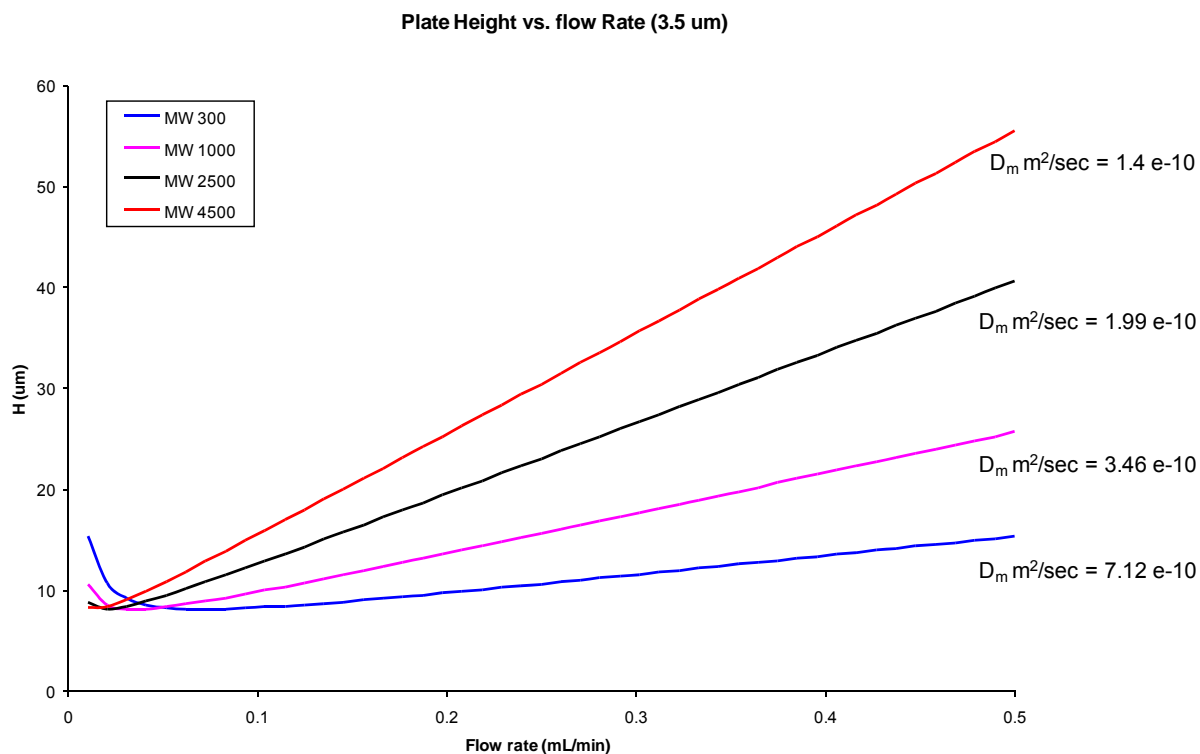


Figure 2.1 van Deemter plot, for theoretical compounds representing a small molecule and different sized peptides, constructed using flow rate expected for a 2.1 mm column

The plot clearly highlights how for small molecules the chromatographic performance is conserved at a much higher flow rate (linear velocity) than that for larger molecules. The data displayed in the plot shows that as the flow rate is increased from 0.1 to 0.5 mL/min the HETP is only increased from 10 to 15 for small molecules and changes from 12 to 35 for a large peptide, As such small molecules can be analyzed with much higher flow rates without a significant loss in separation quality and efficiency versus larger molecules like peptides, which must be analyzed using lower flow rates in order to achieve the required performance. This is primarily due to the lower diffusion rates of peptides in and out of the pores of the stationary phase. However, for high throughput applications

such as bioanalysis, it is not practical to use the very low flow rates needed for peptide separations, nor is it typically practical to use isocratic separations. due to the complexity of the matrix, speed required to effect a challenging separation and the throughput required in a routine bioanalytical environment.

In order to compensate for the slower diffusion of peptides, smaller particle sizes can be used. Figure 2.2 shows the calculated van Deemter plots for a 2500 MW peptide analysed on 2.1 mm diameter columns packed with both 1.7 and 3.5 μm particles.

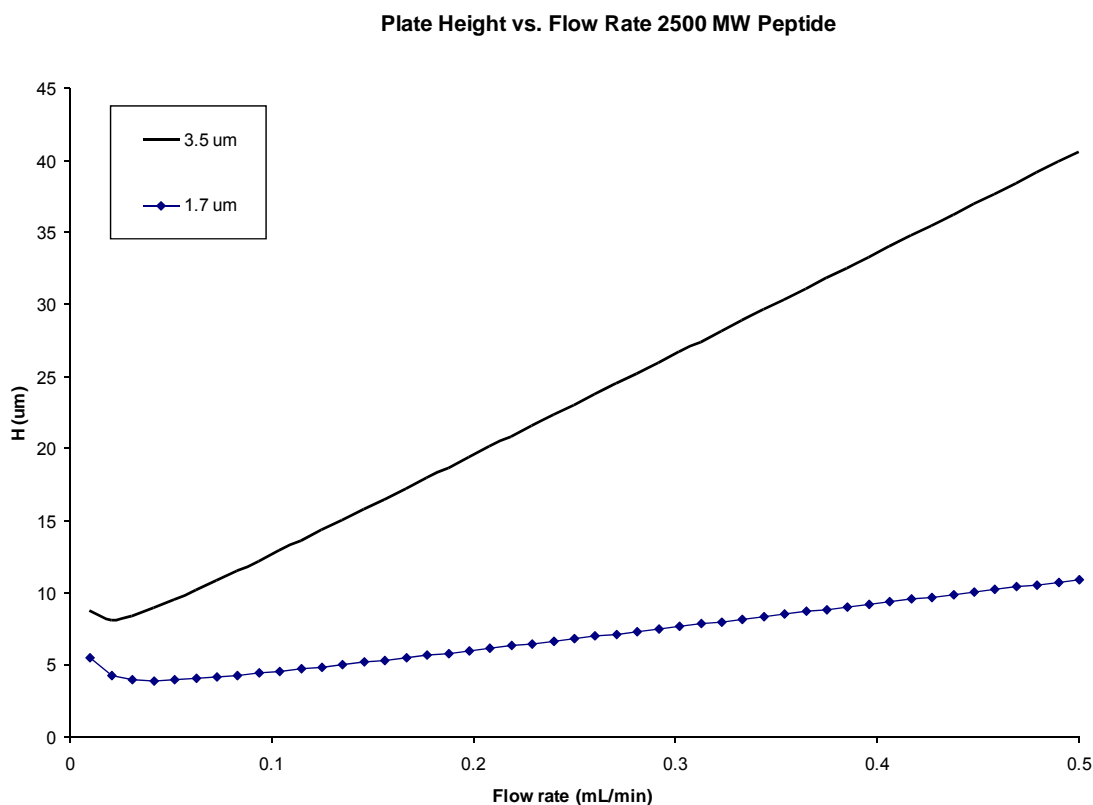
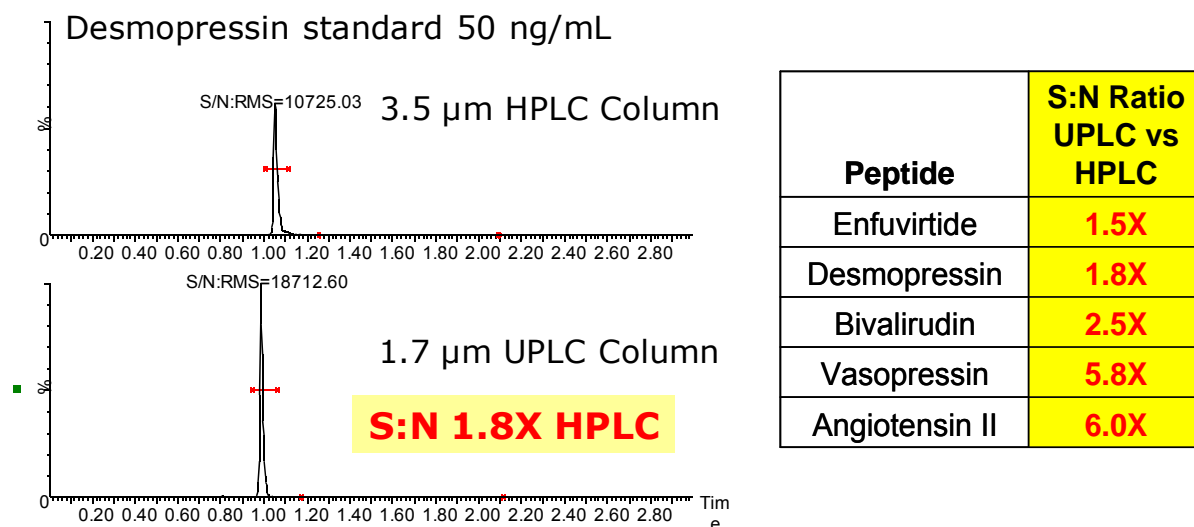


Figure 2.2 Calculated van Deemter plot, using flow rate, for a model peptide analyzed on a 2.1 mm column packed with 1.7 and 3.5 μm particles

While the optimum flow rate for this peptide is similar on both particles ($\sim 25 - 50$ $\mu\text{L/min}$), the separation performance of the 3.5 μm particle column degrades much more

rapidly than the 1.7 μm particle column as the flow rate increases. From an implementation standpoint, this means that better resolution and peak shape can be obtained on sub-2 μm particles at higher flow rates. At a typical bioanalytical flow rate of 0.4 mL/min the column packed with 3.5 μm particles has a 5X increase in plate height compared to its optimum, whereas the column packed with 1.7 μm particles exhibits only a 2X increase in plate height. This clearly indicates that the use of smaller particles is preferred for high throughput bioanalysis of peptides.

From a practical standpoint, however, peptides are typically analyzed using a gradient rather than isocratic methods in order to reduce analysis times and to facilitate the separation of complex, diverse mixtures with a wide range of hydrophobicities. To illustrate the benefit of using small particles for peptide separations, 3.5 μm and 1.7 μm columns packed with the same stationary phase were compared (Figure 2.3).



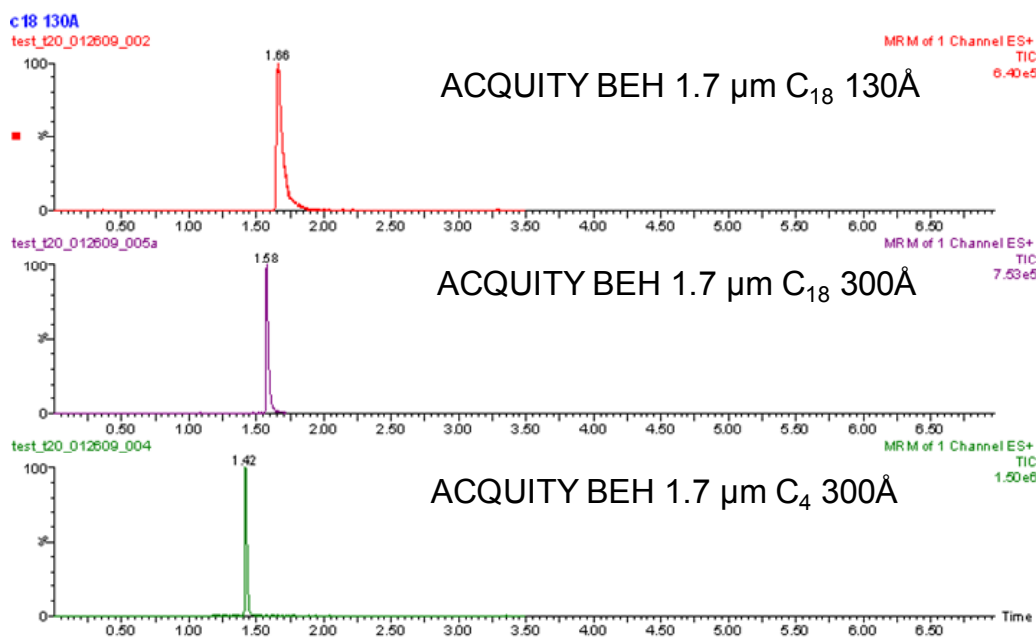
Note: Both columns tested on a low dispersion system

Figure 2.3 Representative chromatogram of 50 ng/mL desmopressin separated on columns packed with the same stationary phase in 1.7 or 3.5 µm particles. The Table on the right summarizes results from other peptide analytes showing even greater benefits from using sub 2 µm materials.

Both columns were of a 2.1 X 50 mm geometry, using the same BEH C₁₈ stationary phase operated at 0.4 mL/min using a formic acid and acetonitrile mobile phase gradient. These columns have the same base particle and differ only in particle size. Both were run on a low dispersion chromatography system capable of operating up to 15,000 psi. (ACQUITY UPLC system) using the same flow rate and gradient. The peptides analysed on the 1.7 µm particle column consistently elute as sharper, more efficient peaks, which translated into a higher signal-to-noise value (peak-to-peak or RMS) and the ability to achieve lower limits of detection. These data correlate well with the previous findings by Gilar et. al, who demonstrated a marked increase in peak capacity for peptides using 1.8 µm particles compared to either 3.5 or 5 µm particles [5].

2.2.2 Influence of Ligand

Though C₁₈ seems to be the preferred ligand for the majority of reversed-phase separations, in our experiments, the use of shorter ligands may occasionally prove advantageous for particularly large or hydrophobic peptides. Figure 2.4 illustrates the improvement in peak shape and signal intensity that was obtained on a C₄ column for the HIV fusion inhibitor enfuvirtide when analyzed on columns having identical base chemistry, with two different pore sizes (130 and 300Å) and either C₄ or C₁₈ ligands. Enfuvirtide is a very hydrophobic peptide, having an HPLC index of 155, therefore it is not surprising that a better peak shape is obtained on a less retentive column. From Figure 2.4, it is clear that the peak width is greatly improved when larger pore sizes are used (300 versus 130 Å). Peak width narrows even further as the ligand is changed from C₁₈ to C₄ (0.4 min versus 0.6 min wide at base) and peak area and intensity are greater (25560 area counts versus 15900) on the C₄ column. Although other large, hydrophobic peptides were also tested on C₄ columns, they did not all exhibit the same peak shape improvements.



Enfuvirtide: MW 4492

Figure 2.4 Separation of enfuvirtide on ACQUITY BEH C₁₈ 130Å, 300Å and BEH C₄.

More recently, C18 columns with a positively charged surface were introduced and also tested. Initially, such columns were developed to improve performance for basic small molecules in low-ionic strength mobile phases, such as formic acid. This is achieved by minimizing undesired secondary interactions with the stationary phase, resulting in reduced tailing and increased loading capacity. Though originally designed with small molecule performance in mind, studies by McCalley[13, 14] suggest that this type of column might provide an advantage for peptides. His studies demonstrated that ionic species such as peptides exhibit poor peak shape at orders of magnitude lower concentrations than neutral species. This behaviour is exacerbated when low ionic strength mobile phases are used (i.e. formic acid). The effect could be mitigated through the use of ion pair reagents such as TFA, however, this is not compatible with MS detection. Since the charged surface column

tested was designed to mitigate these exact shortcomings, it was a good candidate for peptide chromatography. Figure 2.5 demonstrates the peak shape improvement for teriparatide provided by a Waters Charged Surface Hybrid (CSH) column when compared to analysis on a traditional, uncharged BEH C18 hybrid particle. This is interesting since the BEH particle actually has 300 Å pores, while the CSH is characterized by 130 Å pores. The improved performance shown in Figure 2.5 may be attributed to the ability of the positively charged surface to minimize secondary interactions with the stationary phase and reduce NSB, resulting in narrower chromatographic peaks.

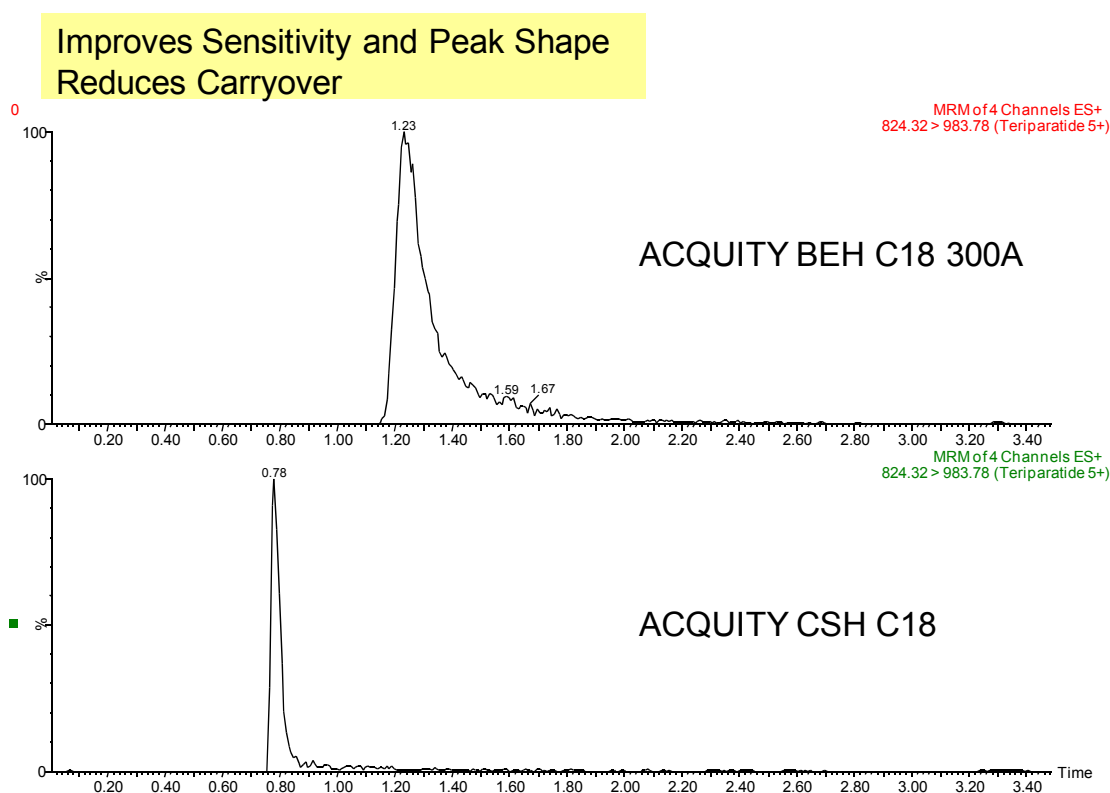


Figure 2.5 Separation of teriparatide (MW 4117) on an ACQUITY UPLC CSH C₁₈ and ACQUITY BEH 300 C₁₈; the same mobile phases, sample, and gradients were used.

2.2.3 Influence of Chromatographic Pore Size

The influence of pore size was discussed in the previous section. No concrete rule currently exists as to which pore size to use for peptides of a particular size, which means columns packed with particles of different pore sizes need to be evaluated to determine the effect on peak shape. From the data collected in this study using a screening approach based on a single column, a larger pore size column gives superior peak shape, and results in better signal-to-noise and lower detection limits, particularly for larger peptides. Smaller peptides generally perform equally well on columns with either a 130 or 300Å pore size. The data shown above suggests that larger pores may mitigate some of the loss in efficiency observed for peptides at higher flow rates.

2.2.4 Charged Surface and Fully Porous versus Solid Core Particles

Reports by Wagner, Stefano and Kirkland[15-17] demonstrated a superior mass transfer and thus significantly improved peak performance for large molecules using solid-core particles, making these columns an obvious candidate for evaluation.

On an individual case basis, the data collected suggests that pore size and presence or absence of surface charge could influence the chromatographic peak shape for peptides. To evaluate the effect of particle porosity a more comprehensive comparison of columns including a set of test peptides with diverse properties was designed. Test peptides and their properties are summarized below in Table 2.1. Table 2.2 details the specific columns tested and some of their relevant characteristics. All columns were 2.1 X 50mm.

| Peptide | MW | pI | Residues | HPLC Index* |
|-----------------|------|------|----------|-------------|
| RASG-1 | 1000 | 9.3 | 10 | 0.4 |
| Angiotensin II | 1046 | 7.4 | 8 | 38.3 |
| Bradykinin | 1060 | 12.0 | 9 | 47.8 |
| Vasopressin | 1084 | 9.1 | 9 | 7.6 |
| Goserelin | 1270 | 7.3 | 10 | 31.7 |
| Angiotensin I | 1296 | 7.5 | 10 | 56.2 |
| Somatostatin | 1638 | 10.4 | 14 | 52.6 |
| Neurotensin | 1673 | 8.9 | 13 | 44.4 |
| Renin Substrate | 1758 | 7.6 | 14 | 81 |
| Enolase T35 | 1872 | 7.3 | 16 | 113.3 |
| Bivalirudin | 2180 | 3.9 | 20 | 46.2 |
| Enolase T37 | 2827 | 4.0 | 23 | 100.2 |
| Melittin | 2846 | 12.1 | 26 | 124.4 |
| BNP | 3464 | 12.0 | 32 | 15.9 |
| Teriparatide | 4118 | 9.1 | 34 | 90.4 |
| Enfuvirtide | 4492 | 4.1 | 36 | 155.9 |
| Bovine Insulin | 5734 | 5.3 | 51 | |

Table 2.1 Diverse peptides used in chromatographic and sample preparation testing, and their relevant physiochemical properties. Not all peptides are used in all tests.

* HPLC index is used as a measure of *relative* hydrophobicity. A low value indicates a more polar peptide, a high value indicating a more hydrophobic peptide.

| Column | Pore Size Å | Surface Charge | Porous/Solid core | Particle Size µm | Description |
|-----------------------------------|-------------|----------------|-------------------|------------------|--------------|
| Silica Hybrid C18 | 130 | none added | Porous | 1.7 | BEH C18 130 |
| Silica Hybrid C18 | 300 | none added | Porous | 1.7 | BEH C18 300 |
| Charged Surface silica | 130 | + | Porous | 1.7 | CSH C18 |
| Solid core charged surface silica | 90 | + | Solid core | 1.6 | CORTECS C18+ |

Table 2.2 Characteristics of the four columns compared for peptide separations.

All columns were analysed on the same low dispersion chromatographic system (ACQUITY UPLC) using a generic gradient elution profile from 5 to 75% acetonitrile at a flow rate of either 0.25 or 0.4 mL/min.

The primary goals of the study were as follows:

- to compare efficiency at different flow rates,
- compare superficially porous to fully porous charged surface columns,
- to compare different pore sizes on the same chemistry stationary phase,
- to compare different stationary phase chemistries,
- and to compare injection solvents.

The stationary phases were compared for analyte retention, peak shape, and analyte peak area. Different flow rate conditions were compared to better understand the relationship between linear velocity and mass transfer. The hypothesis under evaluation was that the influence of flow rate on chromatographic efficiency would be greater for larger peptides on traditional fully porous columns, than on solid-core stationary phases. A similar hypothesis was made regarding larger pore size stationary phases, chiefly that peak shape and intensity would suffer less at higher linear velocities when larger pore size stationary phases were employed.

In addition, peptide standards were prepared in solutions containing carrier protein (0.05% by volume rat plasma) and either 1% formic acid, or 0.5% TFA. This was carried out to address both the potential solubility differences as well as to assess whether the presence of an ion pairing reagent would influence peak shape and sensitivity. Both peak area and peak width were measured under all conditions. Summaries of the results of these experiments and representative data are found in Figures 2.6 A-H.

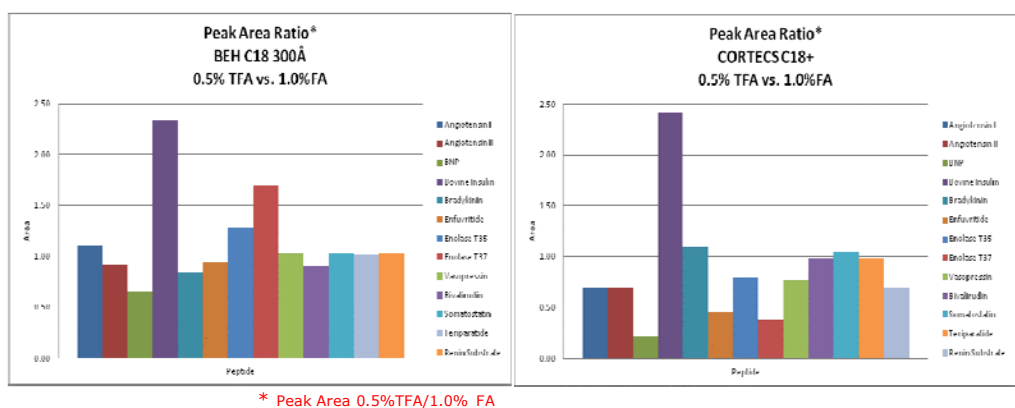


Figure 2.6A Summary of relative peak areas for test peptides separated on either a silica hybrid C18 (BEH 300Å) or solid core charged surface silica (CORTECS C18+ 90 Å) column using either 0.5% TFA or 1% FA as the injection solvent.

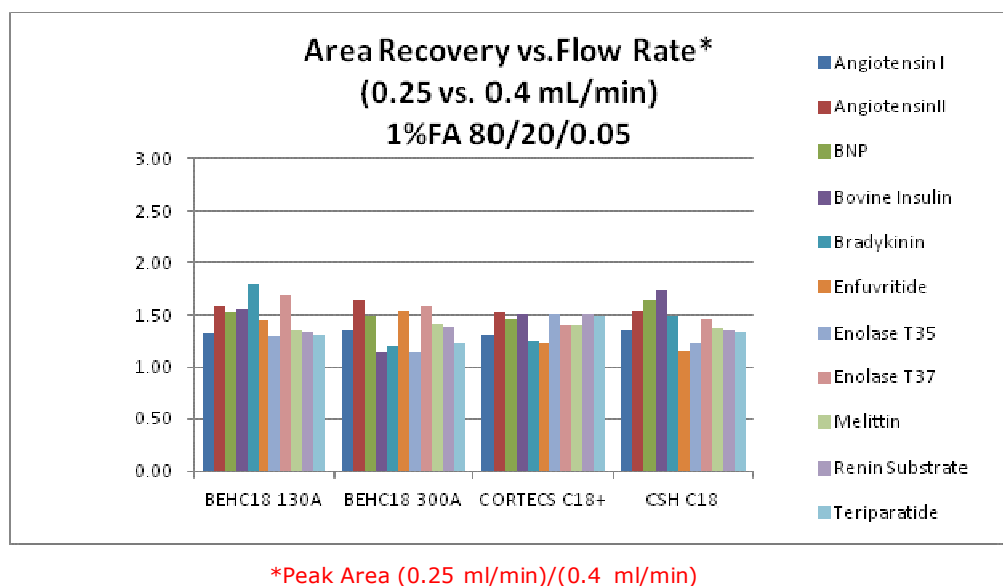


Figure 2.6B Summary of relative peak area for test peptides separated on the four columns in Table 2.2, using a flow rate of either 0.25 or 0.4 mL/min.

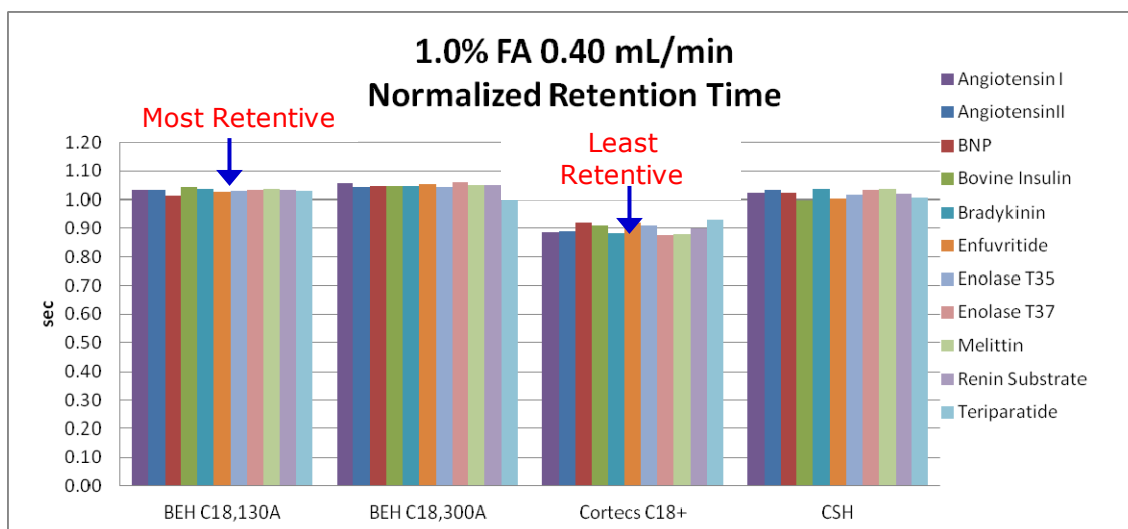


Figure 2.6C Summary of relative retention for test peptides separated on the four columns described in Table 2.2, using a flow rate of 0.4 mL/min and 1% FA as the injection solvent.

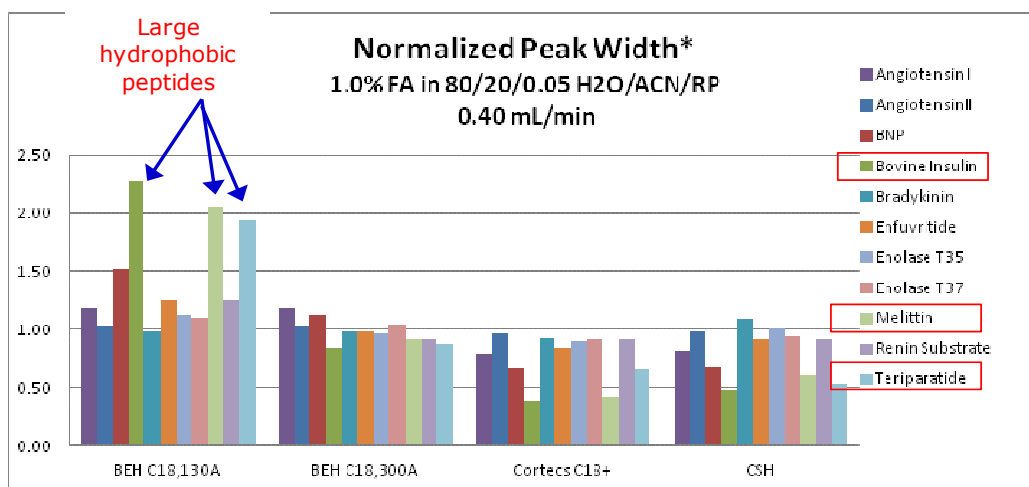
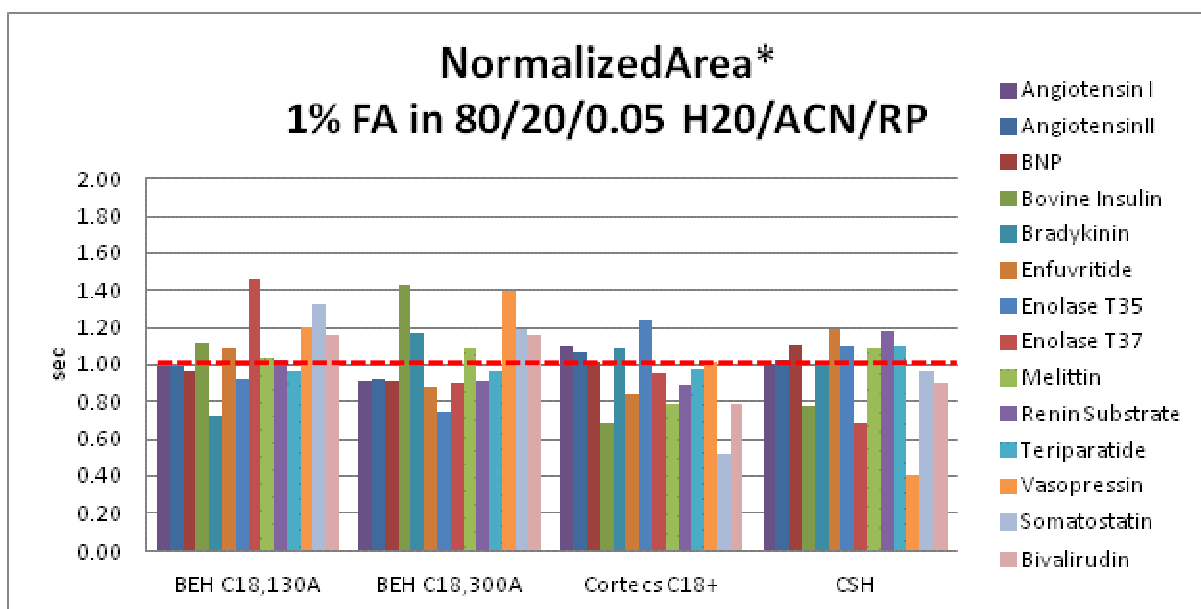


Figure 2.6D Summary of relative peak widths for test peptides separated on the four columns described in Table 2.2, using a flow rate of 0.4 mL/min and 1% FA as the injection solvent.



* Normalized to average area of peptide across the 4 columns

Figure 2.6E Summary of relative peak areas for test peptides separated on the four columns described in Table 2.2, using a flow rate of 0.4 mL/min and 1% FA as the injection solvent.

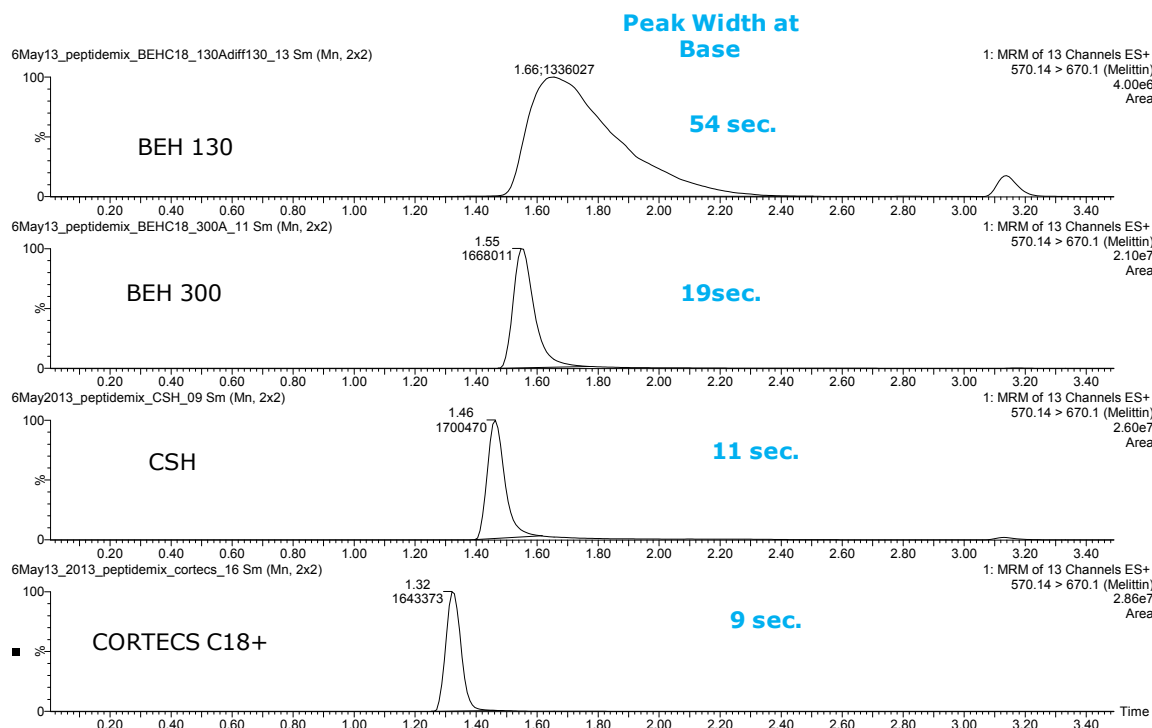


Figure 2.6F Comparison of peak widths for melittin on four different columns.

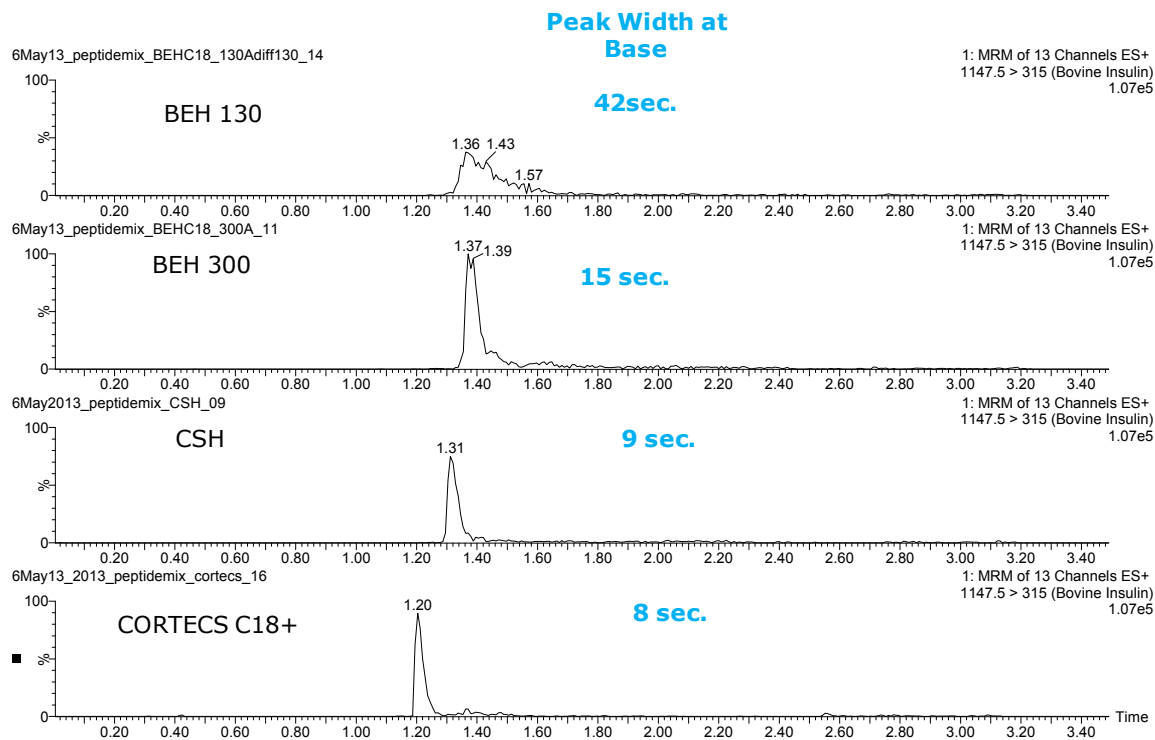


Figure 2.6G Comparison of peak widths for bovine insulin on four different columns.

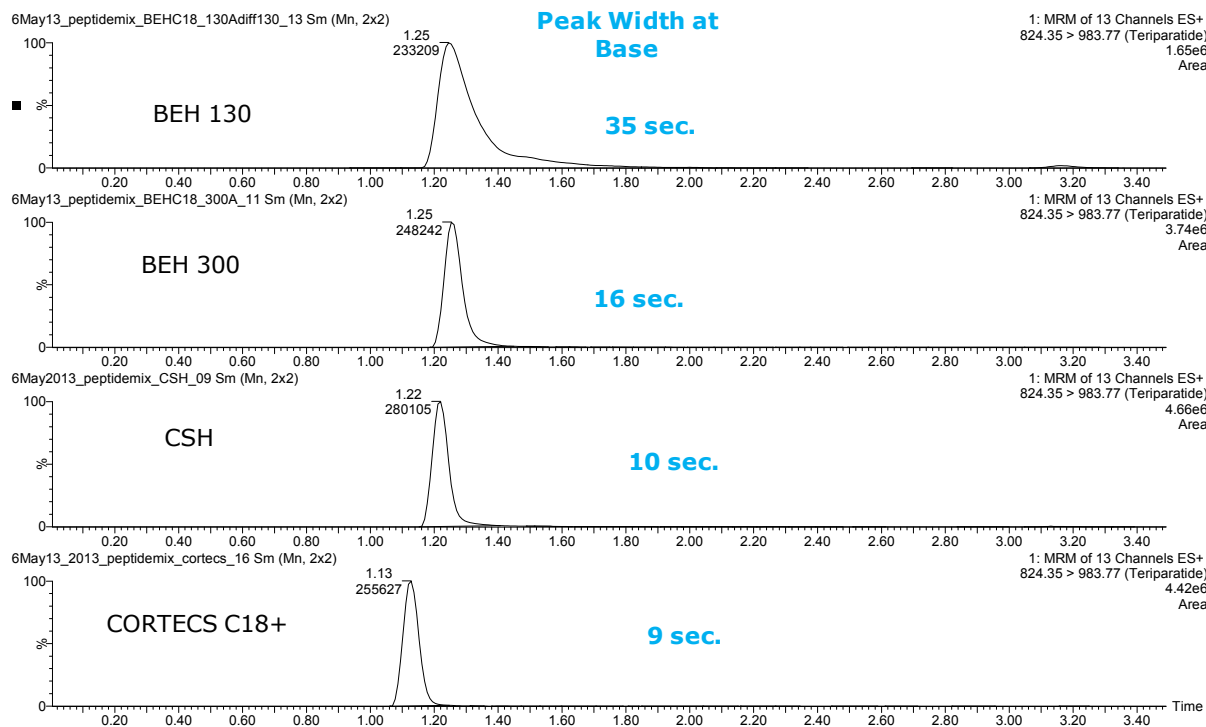


Figure 2.6H Comparison of peak widths for teriparatide on four different columns.

Although it was hypothesized that one could use the properties of a peptide to choose the best column, the data prove otherwise. Furthermore, insulin appears to be an outlier in many tests and will be the subject of a more thorough assessment and comprehensive method development in Chapter 5. From these data, there are, however some conclusions and generalizations that can be made. Figure 2.6A indicates that, in general, peak areas on the silica hybrid with 300 Å pores (BEH 300) column are roughly equivalent whether aqueous trifluoroacetic acid (TFA) or aqueous formic acid (FA) are used as the injection solvents. In contrast, using aqueous TFA as the injection solvent on the superficially porous charged surface silica column (CORTECS C18+) generally yields lower peak areas. Those that suffer most in the presence of TFA, enfuvirtide, the T37 tryptic peptide of enolase, and brain natriuretic peptide (BNP), are diverse in that some are acidic, some basic, some polar and some quite non-polar. The only common property that might link them is their size as all are >2800 MW and could be considered “large”. This is the first instance where insulin is a clear outlier, preferring TFA under either column condition. It is presumed that this is primarily due to solubility. Figure 2.6B demonstrates clearly that, regardless of column selection, peak areas are on average 25-50% greater at 0.25 mL/min than observed at 0.4 mL/min. In cases where absolute sensitivity is not critical, the higher flow rate may be advantageous as it yields improved throughput. Figure 2.6C summarizes relative retentivity of the various columns and establishes that the CORTECS C18+ (the only superficially porous column tested here) is the least retentive, conversely, the porous charged surface column provided a modest 10% increase in retention. Not surprisingly, both traditional C18 columns offer the greatest peptide retention. Figure 2.6D examines peak

widths and in fact supports the theory that, using a traditional C18 stationary phase broader peaks may be observed for larger hydrophobic peptides such as insulin, teriparatide, and melittin. The narrowest peaks are typically observed using charged surface columns. (Figures 2.6F-H provide additional detail that may not be clear when looking at the averaged bar graph in Figure 2.6D.) Figure 2.6E summarizes peak areas across all columns tested and, for insulin, highlights that the greatest area is achieved on the large pore size C18, but at the expense of peak width (Figure 2.6D), which is significantly narrower on either of the charged surface columns. Other large peptides such as BNP, T37, enfuvirtide, and teriparatide do not follow this trend. A more detailed examination of chromatograms exposes an obvious trend. Figures 2.6F-H compare the chromatographic performance for melittin, insulin, and teripartide, respectively. It is clear that peak widths for all three of these large hydrophobic peptides exhibit the same trend. Narrowest peaks are found on the solid core charged surface column (CORTECS C18+), and become increasingly broad as one progresses to the fully porous charged surface (CSH), fully porous silica hybrid with 300 Å pores (BEH 300), and finally, the broadest peaks are observed on a fully porous silica hybrid with 130 Å pores (BEH 130.)

Monolith columns were not examined in this study as they do not provide adequate resolution in lengths that are practical for the application.

2.3 Recommendation for a Generic LC screening process

The investigation of particle diameter, pore size, and stationary phase chemistry suggests that choice of optimal column for achieving maximum sensitivity for a specific peptide may not be predictable based on the peptide properties. Rather, it must be determined through a series of simple screening experiments. However, from the data presented above, the following set of guidelines for LC method development have been derived. Initial method development for peptide chromatography should consist of screening 3 columns, all C₁₈, packed with <2 µm particles, and in 2.1 X 50 mm dimension. Specifically, our data indicates that a C₁₈ column with 300Å pores, a fully porous charged surface hybrid C₁₈ column, and a superficially porous, or solid core, C₁₈ with a positively charged surface should be evaluated. The use of a 2.1 x 50 mm column provides both the throughput required and adequate separation, especially if used in conjunction with selective sample preparation. If improved separation is needed, longer columns should be used. A gradient from 15% to 75% acetonitrile should be employed as an initial screening regime as it brackets the typical elution window for peptides with a broad range of hydrophobicities. It is important to note that during gradient elution, gradient conditions should be set to ensure the elution of the peptide within the above defined window. The use of ballistic gradients, common in small molecule analysis, which could cause elution at very high percentages of organic, may result in precipitation of the peptide on the column. Once a peptide has precipitated on the chromatographic column, it may be very difficult to remove, and may result in poor chromatography (broad/split peaks, carry-over) in subsequent runs and ghost peaks.

An optimal flow rate of 0.4 mL/min on a 2.1 mm diameter column correlates with our own data and previously published findings [18] and represents a starting point which

balances speed with sensitivity arising from resolution and peak shape. Although the parameters defined here represent an appropriate starting point, they may be optimized during method development to achieve the desired resolution, run time, and limit of detection for a particular assay.

In order to evaluate the feasibility and utility of the proposed chromatographic starting point for peptide bioanalysis, a subset of therapeutic or endogenous peptides (listed in Table 2.1) were selected for analysis. The peptides were chosen based on their diversity in molecular weights, acidity/basicity, and hydrophobicity. Throughout these studies, HPLC index is used as a measure of *relative* hydrophobicity. A low value indicates a more polar peptide, a high value indicating a more hydrophobic peptide.

A separation of 5 representative therapeutic/endogenous peptides using the UHPLC screening conditions recommended above is shown in Figure 2.7. All peptides elute within the specified organic composition window, despite their divergent hydrophobicities, size and pI. Each exhibits a Gaussian peak shape and elutes in a narrow chromatographic band, having peak widths ~ 2 seconds wide at base. Furthermore, the separation power is such that vasopressin (human antidiuretic hormone), peak 1, and desmopressin, peak 3, are baseline resolved using the proposed screening method. These compounds are analogous to each other, differing only in the loss of an amino group (in desmopressin), making this separation particularly challenging. The presence of highly similar endogenous peaks in an extracted sample is expected to be quite common in real world bioanalytical studies, therefore such selectivity is highly attractive.

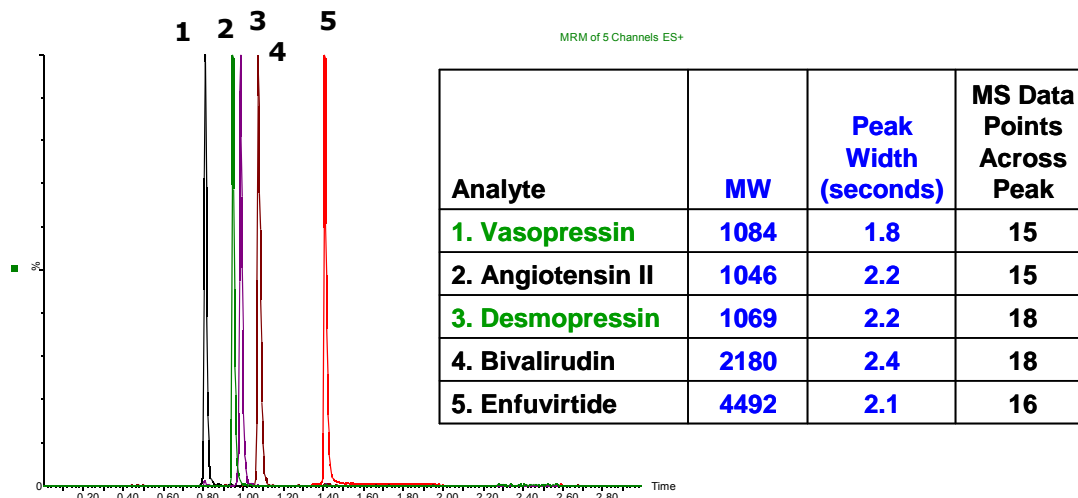


Figure 2.7 Representative separation of 5 peptide therapeutics using the proposed LC screening.

The method above is proposed simply as an LC screening method or starting point. It should be recognized that optimization and/or troubleshooting may be necessary upon examination of initial results. Therefore the following recommendations for subsequent steps in separation optimization are proposed. These are derived from experiences gained during this research.

In addition to the challenges already addressed (selectivity, resolution, throughput, and peak shape), other common pitfalls encountered when analyzing peptides include analyte carryover, adsorption, and issues related to peptide solubility in the mobile phase and the injection solvent. In particular, solubility and adsorption problems can manifest themselves as any of the following: carryover, poor peak shape, poor linearity, poor reproducibility and loss of sensitivity at low concentrations. In the case of suspected carryover, one needs to first determine if the carryover is occurring in the chromatographic column or in the LC instrument itself (i.e. tubing, injector port, sample needle.)

A simple test to determine the source of carryover involves performing an internal gradient. In other words, the gradient is repeated within the same run without performing a separate injection. If a peak appears in the second gradient at the expected retention time of the peptide of interest, then the carryover is suspected to be due to incomplete elution of the peptide from the stationary phase in the first gradient. This can be resolved in several ways. Column carryover (also called memory effect) is due to the inability of the chromatographic conditions to fully elute the peptide during the run, either due to slow and incomplete diffusion in and out of the chromatographic stationary phase pores and/or poor solubility in the mobile phase with the modifier and flow rate being used. To improve solubility in the mobile phase, the separation temperature can be increased. In addition, flow rate may be decreased to allow more time for diffusion into the mobile phase. These changes often not only decrease carryover, but also increase peak area as more of the peptide is effectively solubilized in the mobile phase and/or speed of partitioning increased. Figures 2.8 and 2.9 demonstrate significant improvements in area counts for an amyloid beta peptide (MW 4330). Specifically, at higher temperature the data show a ~50% increase in area, and at lower flow rate, an incremental ~50% increase in area.

52% increases in area counts at higher temperature, reduces carryover

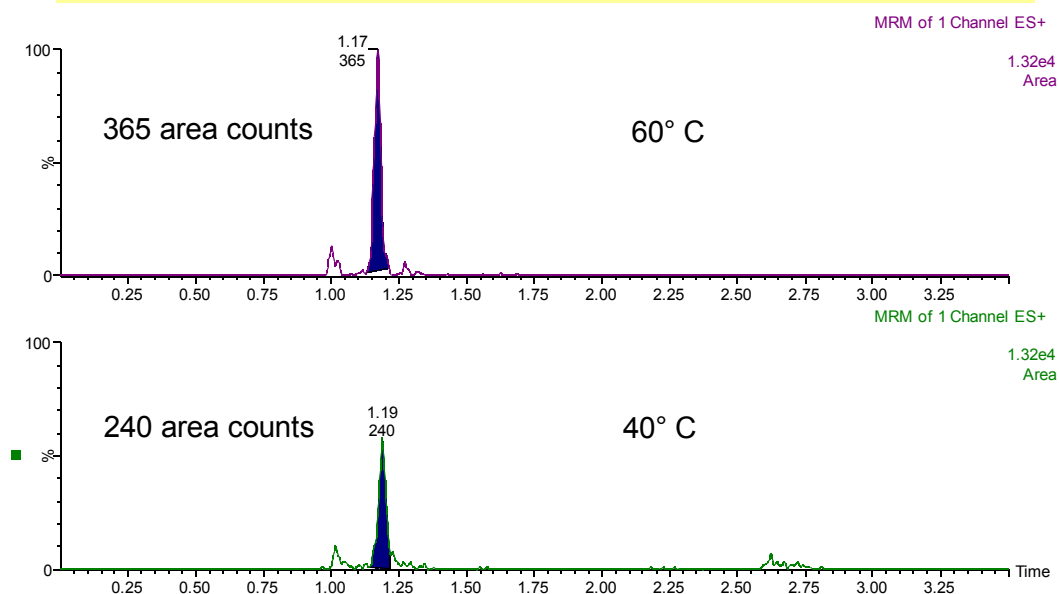


Figure 2.8 The effect of column temperature on area count for amyloid beta 1-40 (MW 4330)

Lower flow rate increases area 48% and reduces carryover

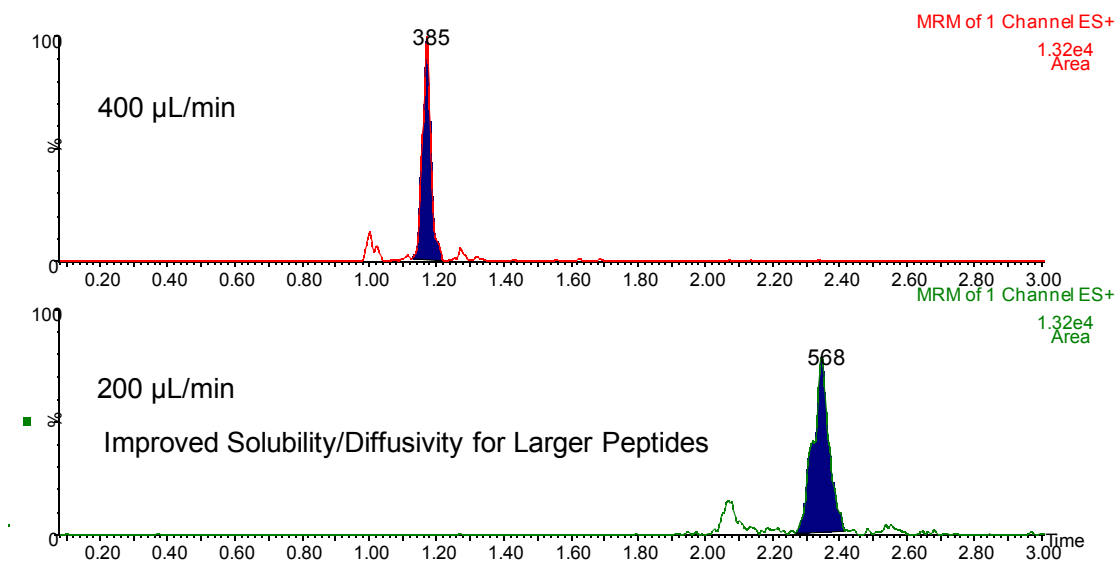


Figure 2.9 The effect of flow rate on area count for amyloid beta 1-40 (MW 4330)

Reducing the gradient steepness can also have a similar effect, as highlighted in the separation for teriparatide in Figure 2.10. In this case, the shallower gradient allows more time for the peptide to diffuse into the mobile phase, thus improving its recovery and ultimately area counts and sensitivity. In addition, a higher strength or higher percentage of the mobile phase additive can be used (i.e. increasing % of formic acid.)

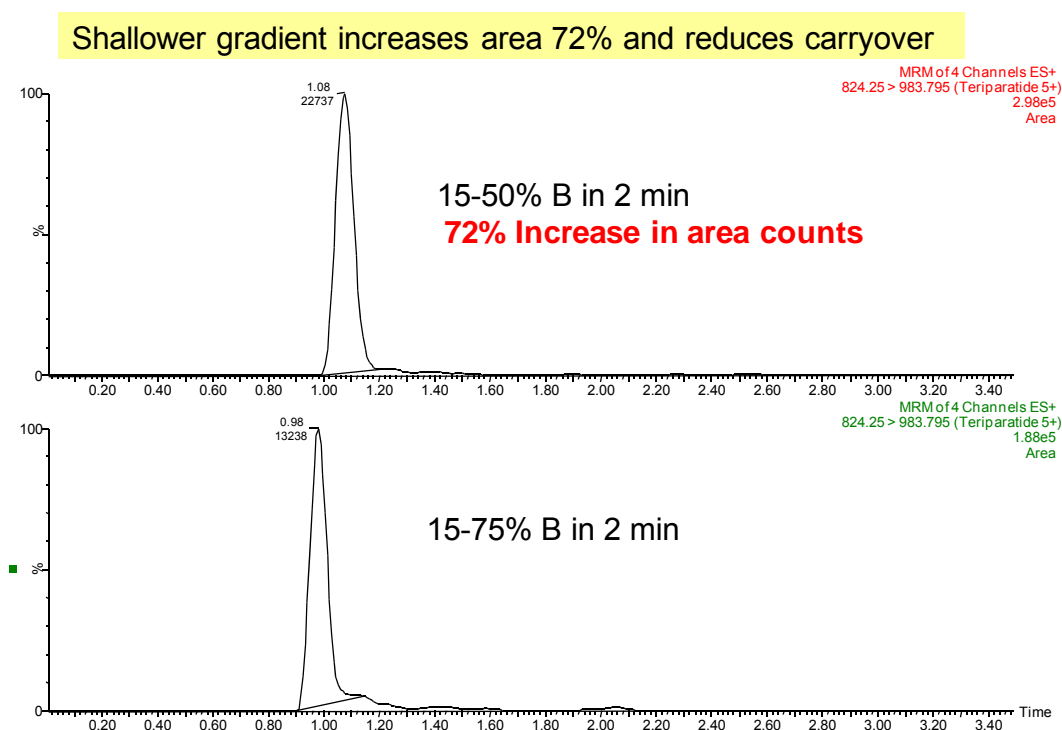


Figure 2.10 The influence of gradient slope on peak area for teriparatide (MW 4117): column temperature is 60°C and flow rate is 0.4 mL/min.

If the internal gradient test does not show carryover due to incomplete elution from the stationary phase, then the carryover is occurring in the injection fluidics, and adjustment of the needle washes and/or injection solvents may be required. In a recent paper by Mitulovic et al [9] the authors identified an efficient wash solvent using several percent

trifluoroethanol (TFE) to clean not only the autosampler, but also a trap column if used. Based on this data, it could be hypothesized that TFE might also be added to mobile phases for additional column cleaning for particularly troublesome peptides. Figure 2.11 demonstrates the increased area counts for the large peptide teriparatide when 5% TFE is added to mobile phase B, which consisted of 0.1% formic acid in acetonitrile. This suggests that teriparatide recovery is improved in the presence of TFE due to improved solubility.

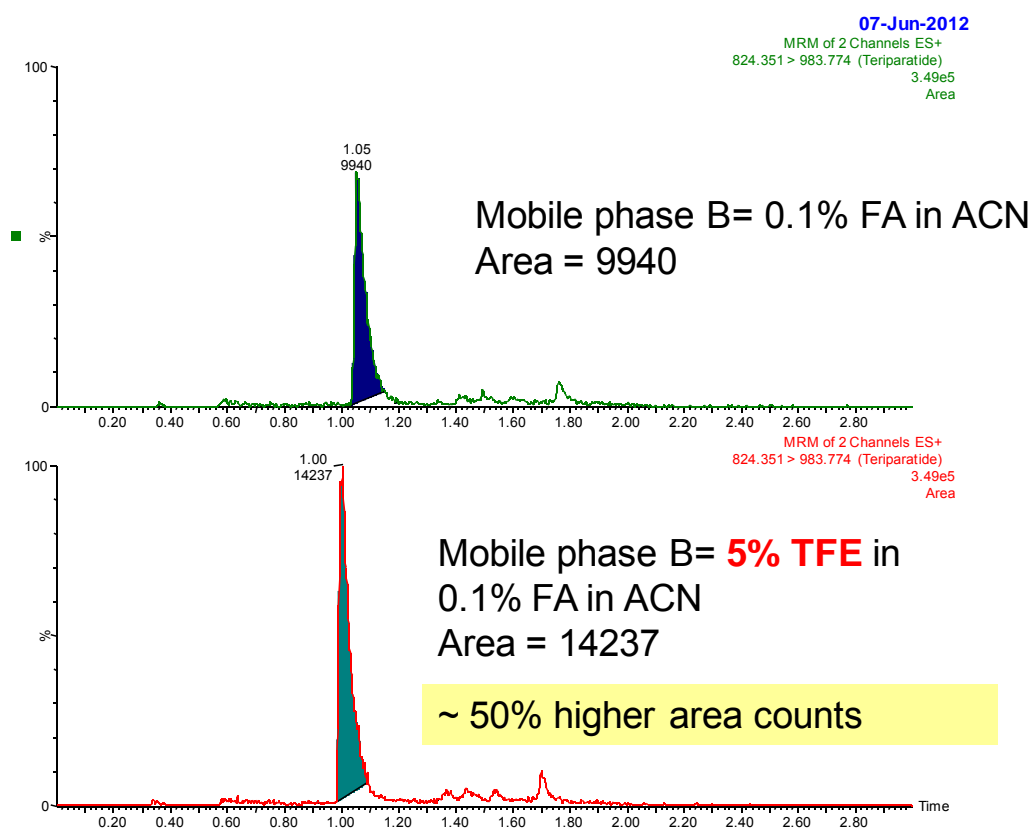


Figure 2.11 A comparison of peak area for teriparatide when either 0.1% FA or 0.1% FA + 5% TFE are used in acetonitrile as the B mobile phase.

An injection solvent that does not contain a sufficient concentration of organic solvent and modifier may also cause carryover, as peptides can precipitate out of solution during the injection process and deposit on the connecting tubing and other components in the system, resulting in adsorption and non-specific binding (NSB). Adsorption and NSB represent perhaps the greatest difficulty encountered when handling peptides and must be assessed as early in method development as possible, as they can affect not only the LC method but also the sample preparation. Care must be taken when choosing LC vials or plates. In general plastic is better than glass, especially for basic peptides as they can interact with surface silanols in glass vials and plate inserts via ionic attraction. Recently, so-called “low binding” tubes and plates have been introduced by such manufacturers as Eppendorf. These tubes and plates are now widely used in peptide and protein analysis due to the significantly reduced binding.

As a result of the findings above some general comments can be made regarding peptide analysis: in general peptide solutions should be dissolved in an aqueous solution containing a minimum of 5% organic (v/v) and 0.1% formic acid or 0.05% TFA (v/v), both of which help to keep target peptides in solution. It is prudent to add a carrier protein to all solvent standards and stock solutions, even if NSB is not predicted. Either 0.05% plasma (by volume) or 40 µg/mL bovine serum albumin (BSA) have shown to exhibit an equivalent effect, and can not only reduce binding to containers, but may also reduce unwanted secondary interactions with the column stationary phases. Figure 2.12 shows the equivalence of the two carrier protein options (Figure 2.12B), and also demonstrates the peak shape improvement that results from this addition (Figure 2.12A).

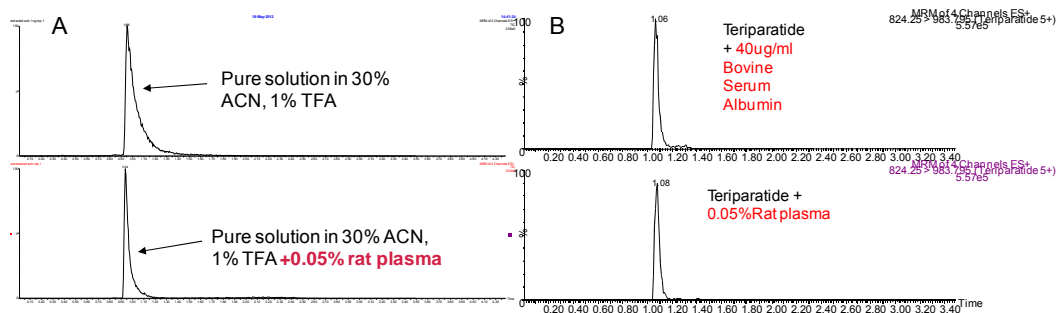


Figure 2.12 The influence of the addition of rat plasma as carrier protein on the peak shape of teriparatide (2.12A) and a comparison of two carrier protein options (2.12B)

It may be advantageous to employ injection solvents with even higher concentrations of organic solvent and acid / base modifier in order to maintain solubility throughout the duration of an overnight analytical run and autosampler stability tests. The data displayed in Chapter 4 on the quantitation of amyloid β peptides[19] demonstrate this concept quite nicely. For the analysis of amyloid peptides, the final injection solvent consisted of ~40% organic solvent and ~5% NH_4OH , both of which were essential for maintaining solubility and minimizing adsorptive losses for these incredibly hydrophobic class of peptides.

2.4 Section II. Investigation into Mass Spectrometry in Bioanalysis of Large Molecules

2.4.1 Introduction

Chapter 1 established that triple quadrupole (QQQ) or ion trap MS are the best options for high sensitivity quantification. TOF MS was not used as it currently does not yet have the sensitivity of QQQ in the MRM mode, and MALDI is only semi-quantitative and

lacks the upfront LC separation necessary to resolve the peptides of interest from endogenous compounds in the complex matrices associated with bioanalysis.

The vast majority of quantitative analysis in bioanalytical laboratories is performed on triple quadrupole mass spectrometers due to their specificity and selectivity resulting in highly sensitive analytical assays. This section will focus on the use of triple quadrupoles (QQQs) as they represent the instrument configuration in most widespread use, though ion traps and quadrupole time of flight instruments are also employed. Recent advances in MS instrument design have resulted in the increased use of hybrid-TOF instruments, but reduced sensitivity versus QQQs in multiple reaction monitoring (MRM) mode have limited their use as a platform for ultra-low level peptide quantification. At the present moment in time triple quadrupole instruments, operated in MRM mode, still offer the highest sensitivity for targeted analyses, and are the platform of choice for both small molecule and peptide quantitative applications.

Mass spectrometric analysis of peptides differs significantly from that of small molecules in that the overall signal obtained for peptides is often lower than for small molecules for a similar molarity or analyte concentration. There are several reasons for this. Firstly, peptides are multiply charged species whereas small molecules are typically singly charged, and second, there may be several different multiply charged precursors present, both of which dilute the overall ion intensity across several species. Furthermore, peptides tend to form many low abundance fragments rather than one or two intense ones, reducing overall signal for MRM experiments. An even greater loss of signal can be observed for large peptides that are not as efficiently transferred into the gas phase during ionization as are small molecules. It may be advantageous to sum transitions to either improve signal

intensity or reduce variability if the relative abundance of a specific precursor changes during the analysis. Clearly, one not only needs to consider the sensitivity of the MS specifically for large molecules, but also any additional aspects of the method (LC, sample concentration during extraction, etc.) that can be used to improve assay sensitivity.

During analyte signal optimization in the mass spectrometer, it is common to see several different precursor ions due to multiple charging. Whereas small molecules gain or lose a single proton, large biomolecules have multiple protonation sites and therefore can gain or lose several or many protons, generating what are called “multiply charged” species. For example, the N terminus and the various amino acid side chains of peptides are common sites of protonation. If one considers that mass spectral detection is performed on the basis of the mass to charge (m/z) ratio, the following equations can be used to calculate the expected m/z for the various possible multiply charged precursors a peptide may produce: Singly charged = $M + H/1$, doubly charged $M + 2/2$, triply charged = $M + 3/3$, and so on, corresponding to double, triple, quadruple, and even higher charge states.

The most common mode of MS analysis for peptides is electrospray positive ionization mode, and in this mode of analysis peptides fragment in a very predictable manner. Primary fragmentation yields a series of ions corresponding to cleavage at the amide (or peptide) bonds between the amino acids that comprise the peptide sequence. If the charge is retained on the N-terminal fragment, the ions are classified as b ions; if the charge is retained on the C terminus, the ions are classified as y. There are other internal cleavage ions and immonium ions, but b and y ions are the most frequently observed [20]. Coincidentally, these are also good choices for quantification as they tend to be inherently specific for the peptide of interest. The final point related to fragmentation is that the most

complete and the most useful fragmentation is typically obtained when the highest possible charge state is fragmented [20]. This reinforces the importance of tuning on multiple precursors.

2.4.2 MS Guidelines for Peptide Quantification

As a result of the experiences gained in this research the following conclusions can be drawn on the optimization of the mass spectrometer for peptide quantification. Firstly, the source conditions should be tuned for maximum transmission of the precursor without in-source fragmentation. As mentioned, it is good practice to tune and optimize several different MRM transitions. These may be multiple fragments from a single precursor or the same or different fragments from different precursors. These transitions can be used for both confirmation as well as to provide options for obtaining the best specificity and sensitivity, particularly for biological samples that contain many endogenous interferences. It is important to note that a transition that appears to be most intense during tuning of solvent standards may not be the transition with the highest signal for an extracted sample. This is due to the potential for isobaric and co-eluting matrix interferences which may either suppress the analyte signal or increase the background so much as to obscure low levels of analyte.

When performing MS/MS tuning and optimization of the precursor ion signal intensity using collision induced dissociation (CID), one must consider that fragments from multiply charged precursors may be multiply *or* singly charged. This requires MS/MS to be performed across a broad mass-to-charge range, often up to the maximum range of the

quadrupoles. This can vary from 1000 m/z to 3000 m/z depending on the manufacturer and model. Careful choice of both precursor and fragment ions can be the critical factor in developing a robust and reliable MS method for peptide therapeutics. The following guidelines can be employed in choosing the optimal peptide fragment for analysis. The choice of fragment ion is fairly straightforward in the case of small molecule therapeutics, where the most intense fragments are most often chosen for quantitation. Conversely, the most intense *peptide* fragments may not always be the most specific. In addition to non-specific water losses, it is quite common to see intense peptide fragments at low m/z values such as m/z 136, 110, 129, etc. These specific fragments correspond to immonium ions, a result of secondary fragmentation, arising from individual amino acids in the sequence. The m/z ratios of 136, 120, 129, 110, and 86 indicate the presence of tyrosine, phenylalanine, arginine, histidine, and leucine/isoleucine, respectively. Transitions based on this type of fragment are often non-specific, resulting in increased baseline noise and multiple peaks from other isobaric peptides present in biological extracts, and should be avoided if possible. In a similar manner, high intensity ammonia losses are commonly observed. These also often prove to be significantly less specific in extracted samples. Figure 2.13 demonstrates this quite clearly for 500 pg/mL glucagon extracted from human plasma. In this example, although the glucagon peak arising from an ammonia loss is 10X higher in absolute signal intensity, the signal to noise is equivalent to the peak obtained when monitoring the fragment at m/z 940. Furthermore, the background is significantly lower in the latter case.

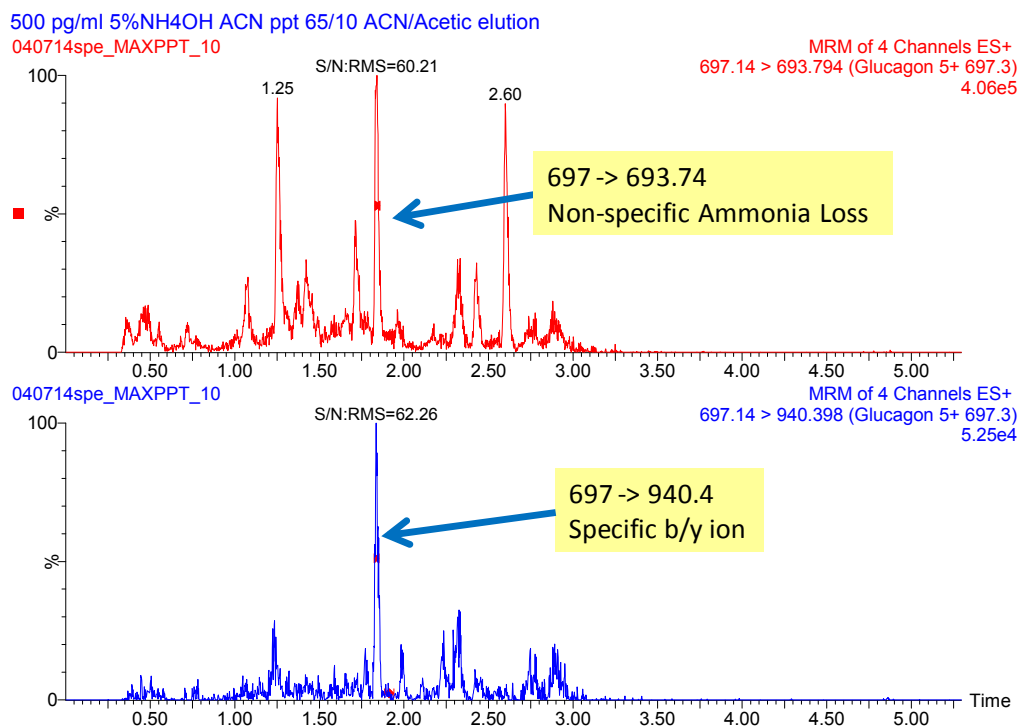


Figure 2.13 MS spectra for 500 pg/mL glucagon extracted from human plasma. Top panel was acquired using an MRM transition corresponding to an ammonia loss; bottom panel was acquired using an MRM transition corresponding to a specific b/y ion.

Occasionally, when a peptide does not fragment well (either no fragments are generated or too many low abundance fragments result, the so called “all or nothing” phenomenon), the use of SIR, where both quadrupoles are set to the same precursor m/z value, may be required. This approach may require extensive sample preparation and/or multidimensional LC to separate isobaric interferences that are not distinguished by unit mass resolving mass spectrometers such as quadrupoles. The ideal fragments for reliable, reproducible quantitation are b or y sequence ions.

An additional consideration for both precursor and fragment ion choice is the use of higher m/z ions, for example using a 4^+ instead of a 5^+ precursor and/or the use of a fragment present at higher m/z than alternative choices. Transitions based on higher m/z ion

pairs often benefit from reduced chemical noise relative to the equivalent pair (i.e. the same compound, same fragment, but different charge state) from a higher charge state present at lower m/z values. This is illustrated in Figure 2.14 in which two separate transitions for an amyloid β peptide with a molecular weight of 4132 are monitored during analysis of a human plasma extract. The transitions represent quadruply (4^+) or quintuply (5^+) charged versions of the same precursor to fragment pair. These data clearly show that reduced background and improved signal to noise can be obtained if the highest precursor/fragments pairs possible are chosen for quantitative analysis.

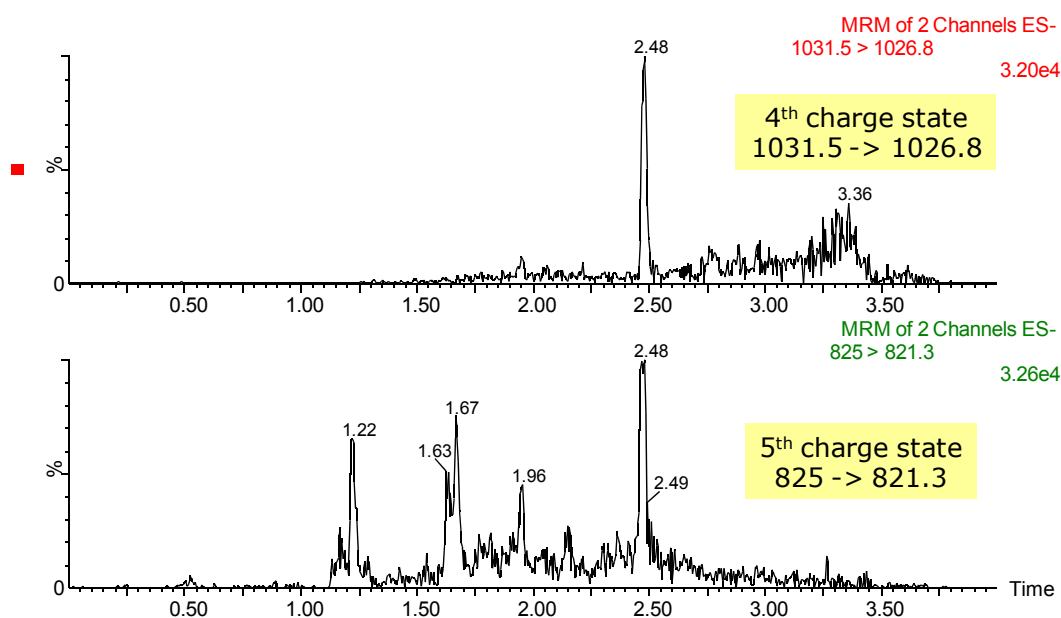


Figure 2.14 Analysis of amyloid beta 1-38 using MRM transitions for the same precursor to fragment pair derived from either monitoring the 4th (top) or 5th (bottom) charge states.

In another example, absolute sensitivity of insulin lispro in solvent standards is approximately 2X higher when monitoring a transition which includes the 5+ precursor at m/z 969 than when the 6+ precursor at m/z 1163 is chosen (Figure 2.15). However, the

signal to noise (S:N) is actually about 3X better for the ostensibly “less sensitive” 1163 transition. This again demonstrates the specificity advantage of using precursor/fragments at the highest m/z possible which still provides adequate sensitivity.

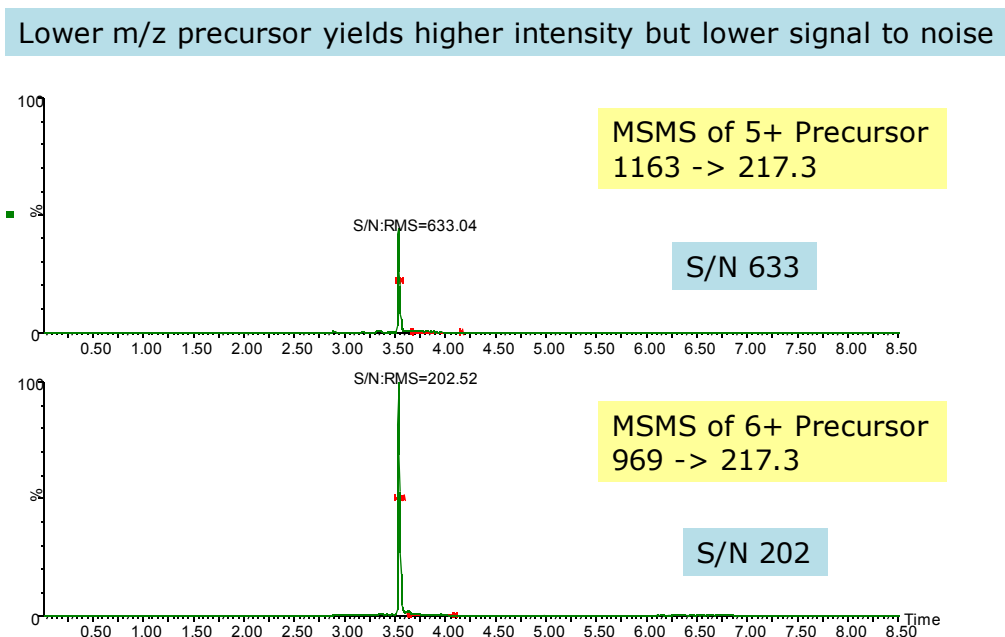


Figure 2.15 MSMS analysis of insulin lispro using either a 5+ (top) or 6+ (bottom) precursor paired to a 217 fragment.

An important aspect of MRM analysis of peptides is the mass range of the first and second quadrupoles. For example, the MS infusion of enfuvirtide (MW 4492) produced a dominant 3^+ precursor at approximately m/z 1498, requiring an instrument with a mass range of at least 1500 (Figure 2.16). Similarly, the MS/MS analysis of the 2^+ precursor of bivalirudin (MW 2180) at m/z 1091 produced two major singly charged fragments at m/z 650 and m/z 1531 (Figure 2.17), again demonstrating the need for adequate mass range. A mass range of ≥ 2000 Dalton on both quadrupoles allows the use of higher mass precursors and fragments which have less chemical noise (Figures 2.13, 2.14 and 2.15), resulting in

greater signal to noise and improved detection limits for peptides. Although TQ instruments with limited mass range quadrupoles (i.e. 1000, 1200 or 1500 amu, for example) provide higher transmission for small molecules and hence high sensitivity for those species, transmission and sensitivity for larger molecules may suffer.

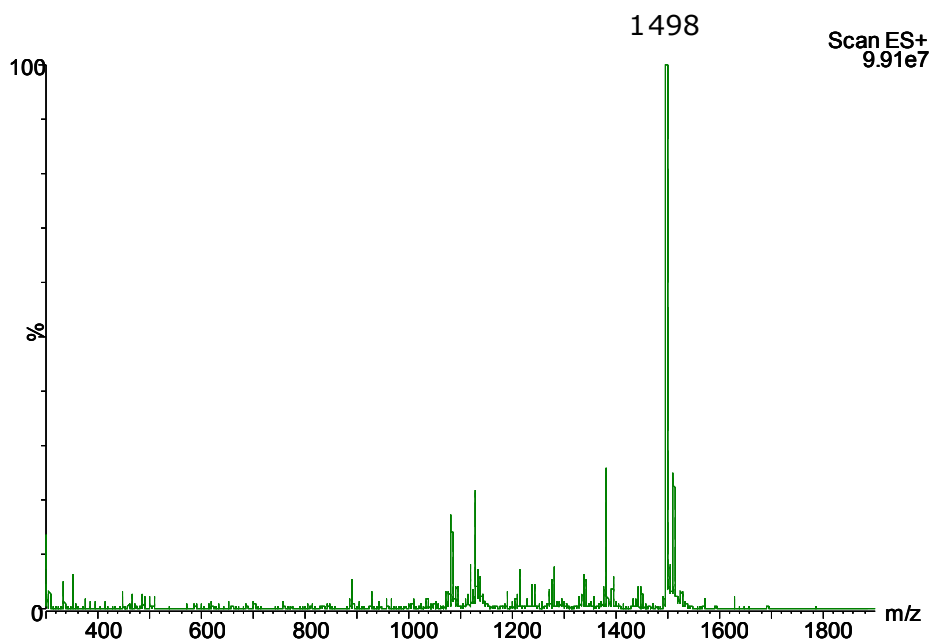


Figure 2.16 MS analysis of enfuvirtide (MW 4492)

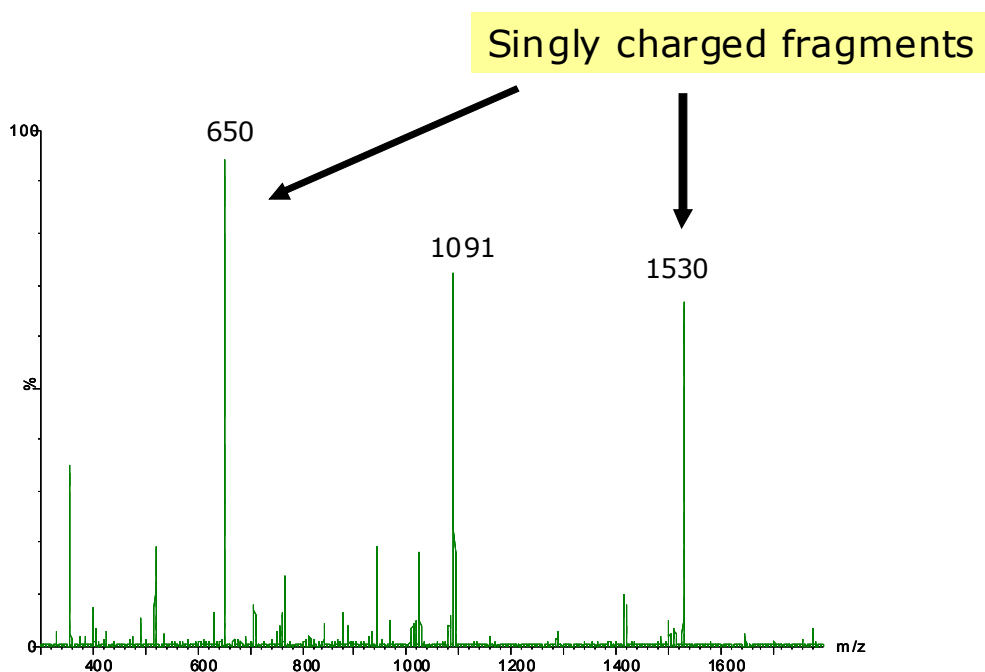


Figure 2.17 MSMS of the doubly charged bivalirudin precursor at m/z 1091

There are various factors that influence the nature and relative abundance of peptide precursors formed in the MS source. Chief among these are mobile phase flow rate, pH and concentration of the mobile phase modifier. It is not uncommon, for example, to observe different charge state precursors dominating at different flow rates. A recent publication [21] on the quantitation of angiotensin II describes the predominance of a triply charged precursor at 700 $\mu\text{L}/\text{min}$ and that of the doubly charged under nanoflow conditions (250 nL/min). One possible explanation for this phenomenon is that the turbulence between the solvent stream and the injection bolus would cause dilution at the boundaries between the two, leading to small changes in concentrations, ultimately resulting in changes in the observed protonation envelopes. This theory is one that fits the observed data.

Another well studied [22-24] phenomenon is the relationship between charge state distribution and analyte concentration. Wang and Cole [25] demonstrated that the charge

state envelope shifts toward lower values as the peptide concentration increases. For example, one might observe more doubly charged species than triply charged at higher analyte concentrations. This observation further supports the recommendation that one should monitor transitions from several charge states during method development and assess any potential impact on quantification.

2.5 Section III. Peptide Extraction and Sample Preparation

2.5.1 Understanding the Differences Between Sample Preparation Techniques and Impact on Results

Once the issues of solubility, adsorption, and instability have been addressed, an extraction technique must be developed in order to isolate a peptide from a complex biological sample containing many closely related interferences. There are three main extraction techniques used in bioanalysis: protein precipitation (PPT), solid phase extraction (SPE), and liquid-liquid extraction (LLE), with SPE figuring most prominently in the peptide literature [1]. The following section will review the pros and cons of each technique and then propose a broadly applicable screening method. In addition, due to the recent introduction of additional regulatory criteria that must be met during bioanalytical method validation (e.g., matrix effects, incurred sample reanalysis), a strong emphasis must be placed on selectivity of the various methods and their role in facilitating meeting evolving regulatory guidelines.

Depending on the specific matrix, components that must be separated include but are not limited to phospholipids, salts, proteins, other peptides, formulation agents and dosing media, amongst others. This discussion will focus primarily on plasma and serum as these are the most common matrices in bioanalytical laboratories.

Prior to the extraction itself, it is essential that the binding between the therapeutic or endogenous peptides and proteins present in the biological matrix is disrupted. This binding may be stronger than the binding between small molecules and endogenous proteins, necessitating additional pre-treatment alternatives. Common means of disrupting protein binding include pretreatment with acid (4% phosphoric, formic, 1-10% TFA, or TCA) or base (5% NH_4OH), or for particularly hydrophobic peptides, denaturation with guanidine HCl or urea may be necessary. These reagents can later be removed during solid phase extraction without concern for peptide losses. Protein binding problems typically manifest themselves as apparent “low recovery” during the extraction process. Peptides that are bound to proteins in the matrix either co-precipitate along with endogenous proteins during PPT or pass through an SPE device during sample loading. An easy test to confirm the presence of protein binding is to prepare a set of spiked samples in both the study matrix and in phosphate buffered saline (PBS). Recovery should be calculated according to equation 2.1 below. If recovery is higher in the PBS samples, then protein binding is likely.

Equation 2.1

% SPE recovery= (average peak area in pre-spiked extracted samples/average peak area in post-spiked extracted samples)*100

In plasma, 22 proteins make up 99% of the total protein content. Of these, albumins (MW ~65 kDa) make up about 45% of the total protein content, and are present at tens of mg/mL. Immunoglobulins (MW ~150 kDa) make up another 15-30% [26]. These proteins are present at many orders of magnitude higher concentration than peptide therapeutics and biomarkers, and are often even less soluble.

In addition to high levels of proteins, plasma phospholipids (PLs) are a major source of concern for both small and large molecule bioanalytical assays. The presence of high levels of residual PLs in sample extracts is particularly concerning considering their role in matrix effects. Bennet and Van Horne identified PLs as the major source of matrix effects in plasma in 2003 (AAPS posters, 2003) and discussions relating to their removal continue to dominate industry-related conferences. A thorough investigation of various sample preparation techniques and their influence specifically on phospholipid removal clearly demonstrated several important differences between the techniques [27].

Overall, PPT is universally regarded as a quick, inexpensive technique. However, with respect to removal of the various aforementioned interferences, the resultant extract is exceedingly “dirty” due to the entirely non-specific nature of the procedure. As long as the protein binding is disrupted, most high abundance plasma proteins (typically proteins >~40 kDa) can be precipitated or separated using PPT. However, PPT has several serious drawbacks. For example, it does not precipitate phospholipids (PLs), salts, other peptides, metabolites, or dosing media and formulation agents, therefore they remain in high concentrations in the supernatant that is used for analysis. PLs are less soluble in ACN, it is preferred both as a precipitation solvent and as an SPE elution solvent. Figure 2.18 demonstrates the increase in phospholipids present when a methanolic final eluate was used.

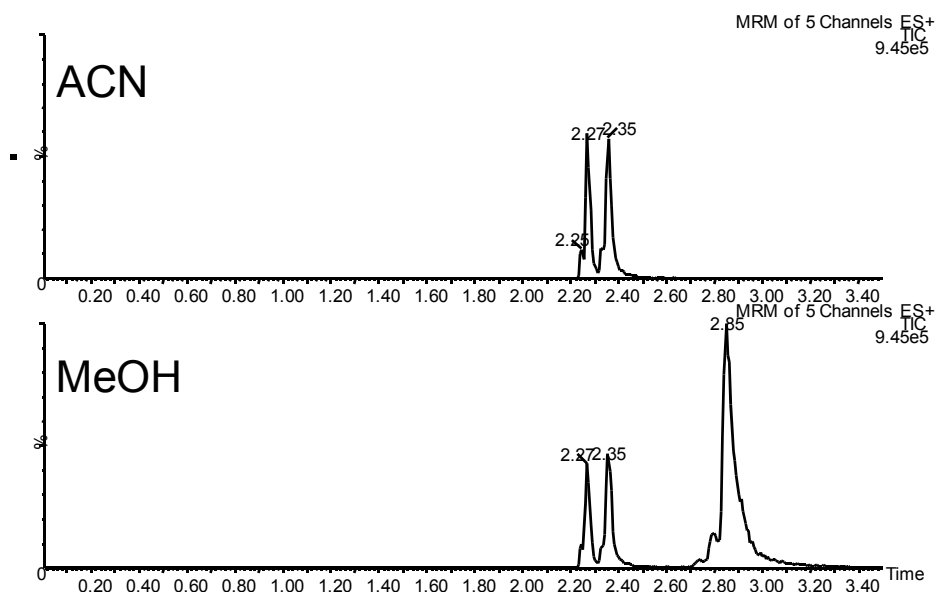


Figure 2.18 Level of phospholipids remaining in elution solvents based on ACN (top) and MeOH (bottom)

If ACN is to be used for PPT of a sample containing a peptide analyte, one must carefully choose the ratio of organic to plasma as peptides precipitate if the organic concentration is too high. Optimization of the final organic composition and the nature of the organic used in the precipitation solvent and sample may balance precipitation of unwanted proteins with peptide solubility and hence peptide recovery. The addition of TFA or trichloroacetic acid (TCA) may help in cases where peptide solubility in the precipitation solvent is limited. In order to better understand the utility of PPT as a selective pretreatment step several mini-studies were performed. Plasma samples were precipitated 1:1 with either 100% ACN or 70% ACN, resulting in final sample compositions of 50 or 35% organic, respectively. The recovery of proteins of MWs ranging from ~6000 (insulin) to ~77,000 (apo-transferrin) was calculated in each supernatant, and is summarized in Figures 2.19A and 2.19B. Recovery was calculated using the post-extracted spike method.

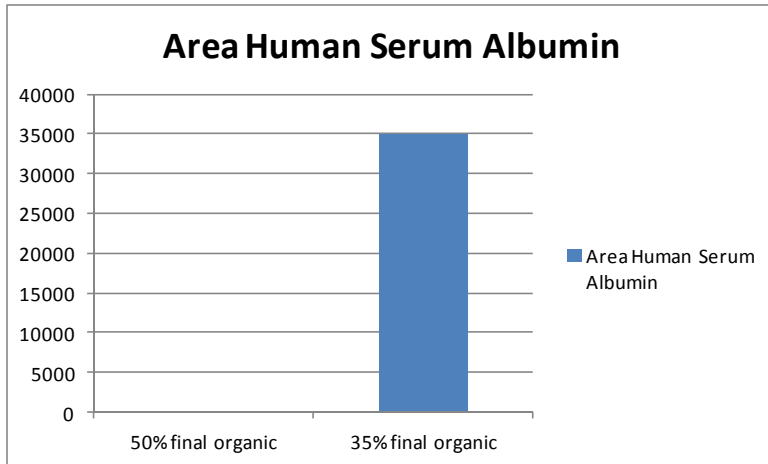


Figure 2.19A Comparison of level of human albumin remaining in supernatant after 1:1 PPT with either 100 or 70% ACN.

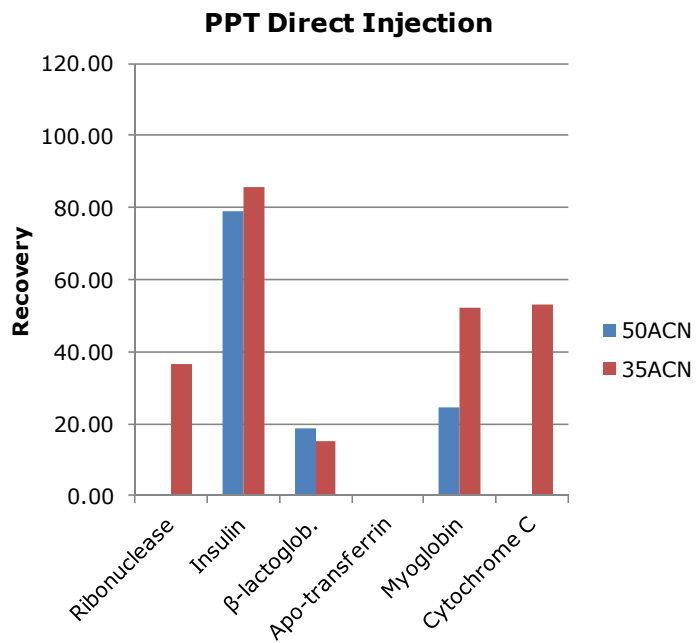
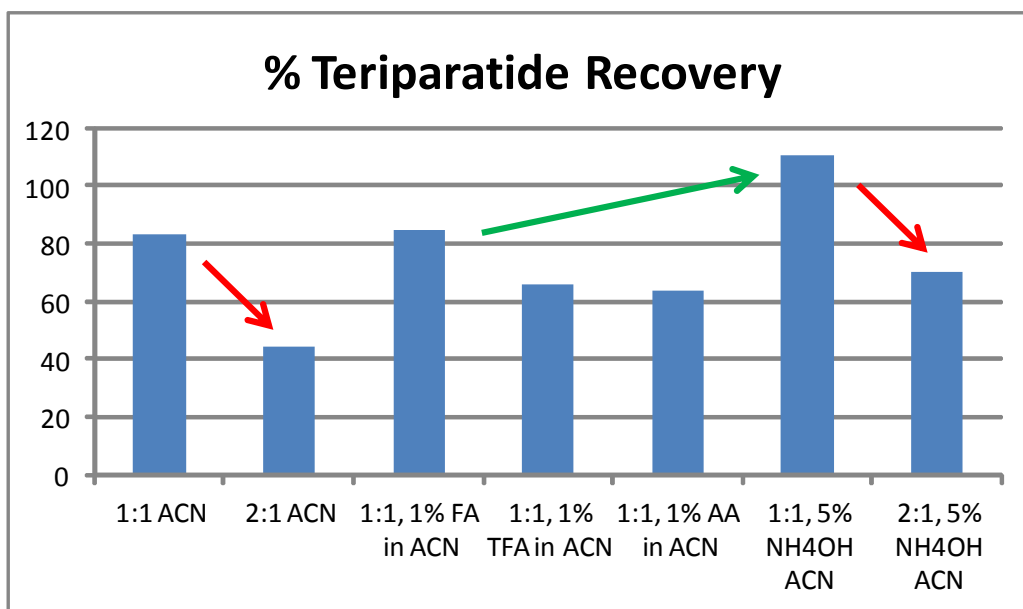


Figure 2.19B Comparison of levels of various proteins remaining in supernatant after protein precipitation with either 100 or 70% ACN.

The data presented highlighted several important results. First, 1:1 precipitation with ACN essentially eliminates human serum albumin (HSA) from the extracts (2.19A). Presumably, larger proteins such as IgGs, are also eliminated. This is supported by the absence of apo-transferrin (MW ~77,000) in either extract (Figure 2.19B). Second, smaller proteins such as insulin are preserved in both cases. Proteins in the 10-20 kD range are present with ~40-50% recovery in the 35% (final organic concentration) extract and to a much lesser extent or not at all in the 50% (final organic concentration) extract. These data suggest that a type of pseudo-fractionation, or depletion of high abundance proteins, may be performed using PPT in the proper ratio, without loss of smaller peptides. A higher final organic solvent composition and the addition of modifiers were also tested during pretreatment of teriparatide in human plasma, prior to SPE. Results are shown in Figure 2.20.



Too much organic causes peptide loss, pH impacts recovery

Figure 2.20 Effect of various pretreatment options on the recovery of teriparatide from human plasma

From this data, one can conclude that teriparatide is partially precipitated when the organic content is too high, for example when a 2:1 ratio of organic to plasma is used versus 1:1. The data in Figure 2.20 also suggest that teriparatide may be more soluble under basic conditions than acidic as recovery is higher in the presence of aqueous ammonia versus formic acid, TFA, or acetic acid.

It should be noted that the non-specificity which characterizes PPT as a stand-alone technique, often leads to severe matrix effects which cause variability, poor robustness and poor reproducibility in the final assay. For this reason, our studies utilize PPT primarily as a pre-treatment option and not as the primary mode of peptide isolation.

As established in Figure 2.20, it is clear that when a 2:1 ratio of organic to plasma is used versus a 1:1 ratio, recovery for teriparatide decreases significantly this is due to the fact that teriparatide is precipitated with plasma proteins under the higher organic conditions. In addition, modifying the solvent pH with a base results in increased recovery for teriparatide over acid modification as a result of improved solubility or disruption of protein binding, or both.

The use of LLE to extract peptides from plasma has been reported only a handful of times, and with lower than desired recovery. In general, the ionic nature of peptides and their poor solubility in very apolar solvents severely restricts the utility of this approach. Furthermore, typical LLE solvents such as methyl tertiary butyl ether (MTBE), hexane, ethyl acetate, etc. also extract lipids efficiently, yielding final extracts saturated with phospholipids. LLE also does little to separate peptides of interest from other peptides present in the sample or many of the other common interferences. Separation of a target peptide from other peptides in the sample is most readily accomplished by SPE, where

manipulation of both organic content and nature and concentration of modifier can result in very selective final eluates[27]. Neither protein precipitation nor liquid-liquid extraction possess the degree of resolving power necessary to accomplish this as both rely on simple separation mechanisms: either physical precipitation only, or distribution between aqueous and organic layers. Historically with SPE, silica-based C18 and more recently polymer-based reversed-phase (RP) or mixed-mode (having both RP and ion exchange retention mechanisms) sorbents, seem to be the method of choice for peptide extraction[1]. There are many reasons for the popularity of SPE for selective peptide isolation. In general, one can load aqueous solutions rather than working with organic solutions which may cause precipitation. In contrast to other techniques, any reagents used to disrupt protein binding, such as denaturants, acids, bases, etc. will be eliminated during the process through a series of wash steps. In addition, the majority of unwanted proteins are eliminated during the sample loading step of an SPE method due primarily to their exclusion from the chromatographic pores of the sorbent. Dosing media and formulation agents may not be efficiently removed by protein precipitation or liquid-liquid extraction, but may, once again, be removed using SPE and judicious choice of wash and elution steps.

Most SPE methods can be automated or converted to on-line protocols such as that recently described by Calderon-Santiago et al [28]. While on-line extraction methods eliminate many of the manual components of performing an extraction, extraction times of 7-12 minutes *per sample* (prior to LC) are commonplace. Method development may be more challenging when using on-line systems as risk of carryover increases with multi-use cartridges and recovery and matrix effects are more difficult to determine. For these reasons, this research focuses on optimizing off-line SPE.

Extraction by SPE can be used with polar, non-polar, acidic and basic samples, for both large and small peptides, making it an attractive platform for a universal method development approach. Solid phase extraction, specifically mixed-mode SPE, is identified as the technique that provides the most selective final eluates [27]. A recent review of techniques specifically for peptide bioanalysis [29] also concluded that mixed-mode sorbents in conjunction with RP chromatography is the ideal platform for this application. Mixed-mode SPE sorbents typically contain both a reversed-phase backbone functionalized with a strong or weak cationic or anionic moiety. This allows analytes or interference molecules to bind to the solid support by either reversed-phase or ion exchange interactions, providing dual orthogonal mechanisms with which to perform a separation. Furthermore, one can manipulate the organic content within each wash or elution step to further improve the selectivity and cleanliness of the final elution(s). Finally, extraction of peptides using the ion exchange elution step and subsequent LC separation in the reversed-phase dimension imparts orthogonality of the bioanalytical method as a whole. Selective sample preparation in conjunction with a high resolution chromatographic separation are critical as tandem quadrupole MS systems operated at unit mass resolution and cannot differentiate between two isobaric peptides sharing an isobaric fragment ion. Unfortunately, this instance occurs more frequently than we would like due to the highly conserved chemical nature of peptide composition. There are only 20 naturally occurring amino acids that make up all of the peptides and proteins in the body, making separation challenging, and thus requiring a multidimensional approach such as the one described herein which uses mixed-mode SPE to complement RP LC.

Properties such as pI may be useful in choosing an SPE sorbent and/or in optimizing wash and elution solvents. Additionally, the pH of wash and elution solutions as well as the specific nature of the SPE sorbent can be manipulated or changed to facilitate separation from other peptides based on knowledge of pI. For example, basic peptides such as desmopressin (pI 8.6) or octreotide (pI 8.3) are expected to bind to a mixed-mode (MM) cation exchange sorbent whereas an acidic peptide such as bivalirudin (pI 3.9) should bind to a (MM) anion exchange sorbent. Depending on the exact concentration of organic required to elute the target peptide, wash solvents should contain as much organic as possible without eluting the peptide as this will effect elution of many of the endogenous peptides in the sample. The elution solvent should also contain the minimum concentration of organic required to elute the peptide in order to minimize the presence of more hydrophobic interferences in the extract. Not only can peptides of opposite ionic nature be separated from each other, but peptides of similar pI's can also be separated from each other through judicious choice of the organic solvent content in the wash and elution solutions. Using different wash and elution solvents allows for refinement of the SPE method to sequentially and systematically optimize the organic composition such that the elution window of the peptide is tightly controlled. Finally, utilizing a small volume elution SPE device can eliminate the need for an evaporation and reconstitution step, which frequently results in peptide losses due to adsorption to the plates or tubes used for evaporation or insolubility in the reconstitution solvent. This low elution volume format can effectively concentrate a sample up to 15 fold through well-researched plate designs which allow the loading of several hundred μL of sample and elute in as little as 25 μL [Waters product literature].

To further reinforce the benefits of mixed-mode SPE for peptide extraction, studies were performed to compare traditional sample preparation methods (PPT, LLE, and RP SPE) and ultimately highlight their shortcomings relative to mixed-mode SPE. Initially this was performed using the two peptides desmopressin and bivalirudin. Analyte recovery was calculated to compare and contrast extraction efficiency using generic methods for each technique and matrix effects calculations (Equation 2.2) were used to reflect sample cleanliness and as a representative measure of selectivity of the extraction types. Regulatory guidelines for bioanalytical method development[30-32] recommend that matrix effects be assessed and controlled. Specifically, it is recommended that the CV of matrix factors (a subset of equation 2.2) in multiple sources of matrix not exceed 15%. Once the limitations of these techniques were characterized and understood, the next step was to develop a simple screening method for the extracted peptide solution.

In these studies, equation 2.1 (previously described) was used to calculate the recovery of each peptide from human plasma.

Matrix effects were calculated according to equation 2.2 below.

Equation 2.2

$$\% \text{ Matrix Effects (ME)} = \left(\left(\frac{\text{Response}_{\text{Post-Extracted Spiked Sample}}}{\text{Response}_{\text{Solvent Standard}}} \right) - 1 \right) * 100$$

(2)

Results from the initial characterization experiments, which accentuate the low recovery and/or high matrix effects associated with traditional techniques are shown in Figure 2.21.

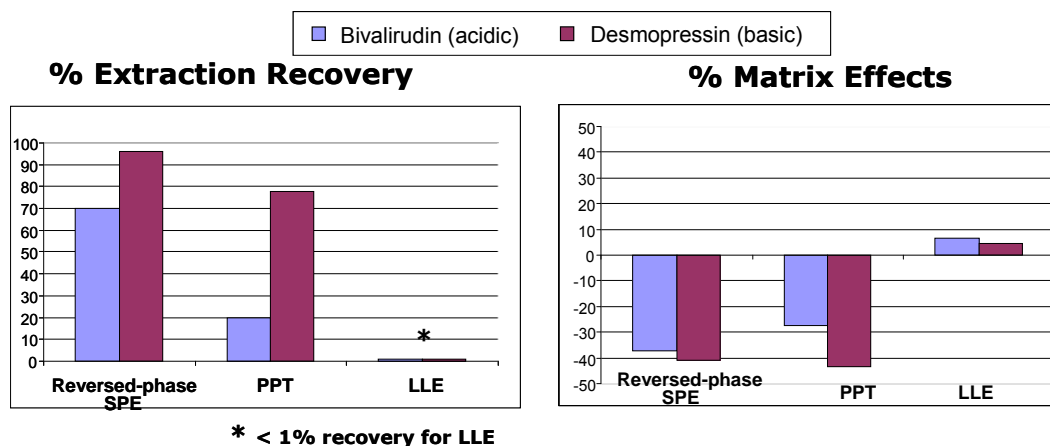


Figure 2.21 Absolute recovery (left) and matrix effects (right) for bivalirudin and desmopressin using a variety of different common sample preparation techniques

While recovery for the two peptides was highest using reversed-phase SPE or protein precipitation, both produced extracts with an unacceptable level of matrix effects. Although liquid-liquid extraction was capable of eliminating matrix effects, recovery was <2%, rendering it completely unsuitable for this purpose.

The data shows that none of the techniques provided both the high recovery required to meet challenging detection limits and low matrix effects (which would indicate improved removal of interferences and greater specificity). In addition to the benefits previously described, mixed-mode SPE has been shown to reduce matrix effects to a greater extent than other sample preparation techniques while still providing high analyte recovery [27]. Due to their zwitterionic nature, the behaviour of peptide therapeutics under various SPE conditions can be difficult to predict. Therefore, initial proof-of-concept studies were performed on 4 different mixed-mode sorbents, using a generic set of conditions originally developed for small molecule screening [27]. As each sorbent consists of a moiety that imparts reversed-phase behaviour as well as an ion exchange group (strong or weak cation

or anion exchange) for additional selectivity and therefore is capable of producing 2 elutions: one that contains compounds bound by reversed-phase (elute 1) and a second containing compounds bound by ion-exchange (elute 2). Recovery was calculated for both elute 1 and elute 2 fractions on all four of the mixed-mode sorbents and is summarized in Figure 2.22.

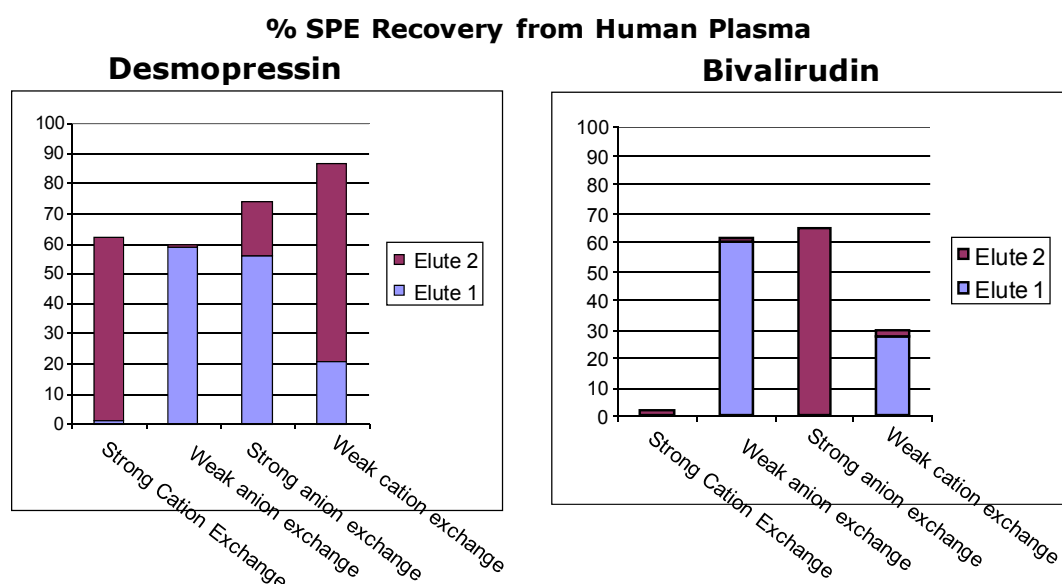


Figure 2.22 Recovery for desmopressin and bivalirudin extracted from human plasma using four mixed-mode SPE sorbents.

A careful inspection of the data in Figure 2.22 shows that using protocols designed for small molecules, recovery for test peptides was split between the two elutions and was on average <60%, whereas these same protocols typically yield recoveries for small molecules that are >80% on average. It was clear that knowledge and application of general peptide physiochemical properties was needed if the advantages of these mixed-mode SPE sorbents were going to be successfully applied to develop a generic approach to peptide

extraction. Conventional “small molecule” thinking and protocols incorporate steps and solvents used in a manner that yields poor results for peptides. For example, if one considers maximizing the recovery for small molecules, the elution window is quite broad ranging from 0-5% organic required to elute very polar compounds to 100% organic for the most hydrophobic small molecules. Generic SPE protocols for small molecules often use 100% organic in the elution to ensure the highest recovery, even for many small molecules of potentially diverse properties. In contrast, if one considers peptides as a class, the elution window is much tighter, with most peptides eluting between approximately 20 to 55% acetonitrile. This basic information should be applied during extraction method development as application of solutions containing higher than optimal organic content often result in peptide precipitation onto the SPE cartridges. It is also common to include modifiers such as formic acid in wash and elution steps for small molecules. However, stronger acids may be required if maximum solubility, and thus recovery, of peptides is to be obtained.

Further experimentation with additional peptides and examination of the resultant data was performed in order to formulate a hypothesis for a peptide screening protocol. The data indicated that strong anion exchange and weak cation exchange sorbents produced higher recoveries on average in the ion exchange elutions for the therapeutic peptides tested. Subsequently, changes were made to the original small molecule protocols, including optimization of wash and elution solutions, to generate a protocol developed specifically for peptides which incorporates basic knowledge of peptide hydrophobicity, solubility, and their zwitterionic nature. Among these changes were to use a 75% organic elution as opposed to a 100% organic elution. In addition, TFA was added to improve solubility of hydrophobic

peptides. TFA showed a significant improvement in recovery for larger, more hydrophobic peptides over formic acid without deleterious effects to sensitivity. The concentration of TFA employed was equally as important. Several concentrations in the final elution were tested, and 0.1 or 0.5% TFA were found to be inadequate in providing high recovery values for some of the larger or more hydrophobic peptides. A final concentration of 1% TFA provided the optimal recovery for a diverse set of peptides. It is concluded that a combination of improved solubility in the organic solvent and ion-pairing to reduce secondary interactions are responsible for the recovery increases. The elution solvent composition described has the advantages of providing optimal solubility for a wide range of peptides, eliminating the majority of phospholipids (which typically require higher organic to elute and are thus retained on the extraction column) and producing an eluate ready for injection onto an LC/MS/MS system without further manipulation.

2.5.2 Proposed Peptide Extraction Screening Protocol

This section describes the method details for a universal screening protocol optimized for the mixed-mode SPE extraction of peptides from biological matrices. It is derived from the results of the previous section of this chapter. The methodology screens two complementary SPE sorbents (strong anion exchange and weak cation exchange) simultaneously to rapidly identify the best starting conditions on either the mixed-mode SAX (strong anion exchange) or WCX (weak cation exchange) plates. Although one may be able to predict the appropriate sorbent for a peptide based on pI, the data collected in this

study suggests that it is not always a definitive indication. The location of charged residues in the sequence and their accessibility to the sorbent influence retention and may result in unpredictable behaviour vis a vis pI and sorbent type. For example, two peptides with similar pI's may interact differently with the same SPE sorbents, reinforcing the need for a screening protocol. Based on experimentation and resultant conclusions discussed above, the following general screening protocol is suggested.

Sorbents to be screened are weak cation exchange and strong anion exchange, and the format recommended is 96-well μ Elution (2 mg sorbent/well). The μ Elution format was chosen as it facilitates concentration without evaporation thus minimizing the potential for peptide losses due to adsorption during dry-down which would lead to an erroneous result. A schematic of the well design is shown in Figure 2.23. The sorbent bed is taller and narrower than traditional formats, acting more like a column than a flat disk. It is this geometry that enables elution in smaller volumes.

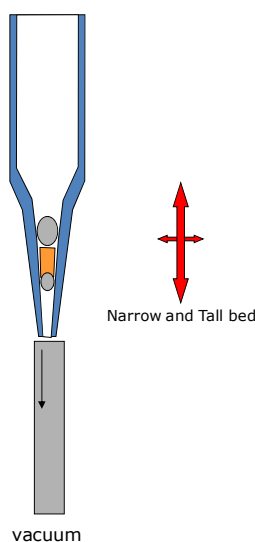


Figure 2.23 Well design for Waters μ Elution format 96-well extraction plate

Proposed Screening Method for Mixed-mode Weak Cation and Strong Anion Exchange Sorbents:

1. Condition with 200 μL MeOH.
2. Equilibrate with 200 μL H_2O .
3. Load diluted, pretreated sample.
4. Wash with 200 μL 5% NH_4OH in H_2O .
5. Wash with 200 μL 20% ACN in H_2O .
6. Elute with 1 or 2 \times 25 μL 1% TFA in 75/25 ACN/ H_2O .
7. Dilute with 25 or 50 μL H_2O if necessary.

This proposed screening protocol was tested against a panel of twelve diverse therapeutic and endogenous peptides having pI values from 3.9 to 12, ranging in size from \sim 1000 to 4500 Da, and varying from very polar to very non-polar. SPE extraction recovery for these twelve peptides, using this protocol is summarized in Figure 2.24.

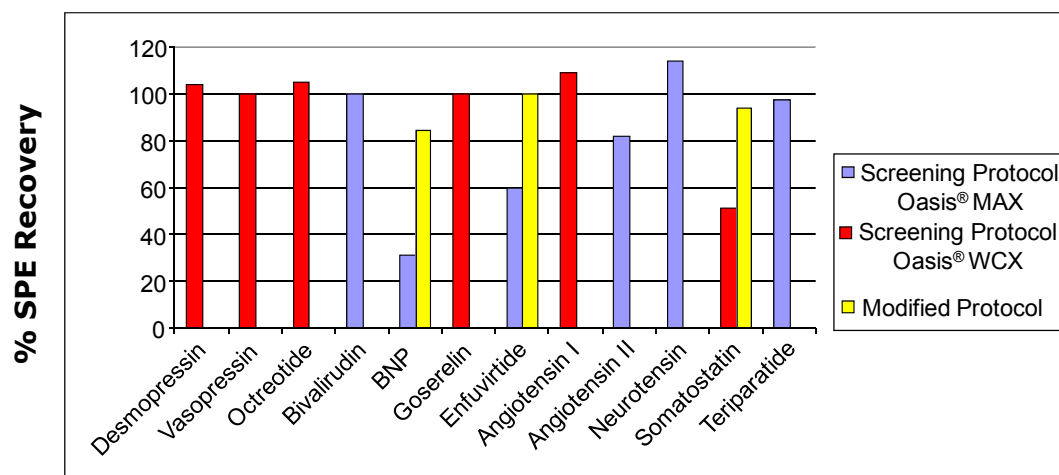


Figure 2.24 Recovery for 12 test peptides extracted from human plasma using the proposed SPE screening method

Recovery for 9 out of the 12 peptides was deemed acceptable (>80% recovery) on a first pass using the screening method, this result clearly indicates that a single SPE platform can be successfully used for peptide method development. Minor modifications to the method (described below) were made to improve recovery for BNP, somatostatin, and enfuvirtide. Brain Natriuretic Peptide (BNP) is very polar, as indicated by HPLC index of 15.9. It could be theorized that it is due to the polar nature of the molecule that the recovery was low, as it was not being retained on the sorbent during loading when applied at low pH. To address this the BNP samples were diluted with ammonium hydroxide at (5% v/v) instead of 4% H₃PO₄ to change the initial binding behaviour. Another compound with low recovery, enfuvirtide, suffers the opposite problem in that it is extremely non-polar, as indicated by an HPLC index of 155.9. Its chromatographic behaviour and retention (Figure 2.4) are also representative of its sticky nature. These factors are excellent predictors of possible high protein binding. If an analyte exhibits high or strong protein binding, it may pass through the sorbent during the loading step. In this case, more aggressive pre-treatment with TFA resulted in reduced protein binding and increased recovery. Upon further investigation, it was discovered that somatostatin was labile at high pH. The high pH wash step in the generic protocol was exchanged for a pH 6 buffer. The buffer ensures that both the Oasis[®] WCX sorbent and analyte are charged, increasing ion-exchange retention capacity as well as eliminating conditions under which somatostatin was not stable. Final SPE recovery and matrix effect values from this approach are summarized in Table 2.3.

| Peptide | pI | MW | % SPE Recovery | % Matrix Effects |
|----------------|------|------|----------------|------------------|
| Octreotide | 9.3 | 1019 | 88 | <10% |
| Angiotensin II | 7.35 | 1046 | 82 | 8% |
| Desmopressin | 8.6 | 1069 | 104 | <11% |
| Vasopressin | 9.1 | 1084 | 100 | -3% |
| Goserelin | 7.3 | 1270 | 100 | -2% |
| Angiotensin I | 7.51 | 1296 | 109 | * |
| Somatostatin | 10.4 | 1638 | 94 | * |
| Neurotensin | 8.93 | 1673 | 114 | 6% |
| Bivalirudin | 3.87 | 2180 | 100 | 10% |
| BNP | 12 | 3464 | 84 | * |
| Teriparatide | 9.1 | 4118 | 97 | 9% |
| Enfuvirtide | 4.06 | 4492 | 102 | * |

*= data not obtained

Table 2.3 Final % SPE recovery and % matrix effects for test peptides extracted from human plasma using the proposed screening method

2.5.3 Recommendations for Troubleshooting

The minor modifications to the screening protocol necessary for three of the peptides serve here to highlight areas for troubleshooting should peptide recovery be low using the described screening protocol. In general, there are a few primary reasons for actual or apparent low peptide recovery from a biological matrix: protein binding, inadequate solubility in the final elution solvent, chemical modification/instability (which changes the mass, rendering the original MRM incapable of quantifying the modified peptide), incomplete ionization of the peptide and sorbent during loading, non-specific binding, and insufficient solvent strength. In general, the larger and more hydrophobic a peptide is, the

greater the likelihood of encountering one of these issues. In addition, one should examine the amino acid content of the target peptide and refer to Table 2.4 to identify any possible chemical modifications that could occur during processing or conditions which could cause instability.

| Property | Amino Acid |
|---|---|
| Hydrophobic | A, F, I, L, M, P, V, W, Y |
| Moderate | C, G |
| Hydrophilic | D, E, H, K, N, Q, R, S, T, pyro-glutamic acid |
| Positive Charge | K, R, H, N-terminus |
| Negative Charge | D, E, Y, C-terminus |
| Degradation likely | M, W |
| Prone to de-amidation, dehydration, cyclization to pGlu | N, Q, C-terminal amides, N-terminal Q |
| Prone to oxidation under mild conditions | C, M |

| Modification | Residue | MW change |
|--------------|----------|-----------|
| Oxidation | C, M | +16 or 32 |
| Cyclization | N-term E | -17 |
| Deamidation | N, Q | +1 |

Table 2.4 Properties of individual amino acids and mass shifts due to modifications

As a first step toward improving recovery and/or determining the cause of low recovery, the following optional experiments may be performed:

1. Extract the sample in PBS + 10 µg/mL bovine serum albumin (BSA) and compare recovery to the target matrix. If recovery in the PBS solution is higher, this may indicate poor disruption of protein binding in the target matrix, indicating that a change in pre-treatment is required. If the generic acid pre-treatment is inefficient, higher concentrations of acid or base, or denaturation with guanidine HCl or urea may be necessary.

2. Increase the concentration of TFA in the final elution to 5% or 10%. This may improve solubility for larger or more hydrophobic peptides. Do not increase the organic % in the final elution, this often results in precipitation. 75% acetonitrile is sufficient. Alternatively, different modifiers such as acetic acid, may be assessed.
3. Exchange 10 mM ammonium acetate (pH ~6) for the NH_4OH wash in the generic protocol if using weak cation exchange. This may improve the ionization of the sorbent and peptide, facilitating complete binding upon sample loading. This modification also eliminates high pH steps from the protocol, allowing one to accommodate base-labile peptides without loss.
4. For acid-labile basic peptides, a strong cation exchange sorbent may be used with the ammonium acetate wash described in option 3 and the standard high pH elution.

2.5.4 Exploring Large Pore Size SPE Sorbents

Improved peak shape and column recovery, especially for larger peptides, was observed during this study when using 300Å versus 130Å chromatographic particles in UPLC separations. This led to questioning whether this same benefit could be realized during SPE, if sorbent pore size was similarly increased. To that end, SPE employing a prototype polymeric reversed-phase sorbent with an average pore diameter (APD) of 80-100Å was compared to the equivalent particle with an APD of approximately 400-600Å. Both particle substrates were 18-20 μm polymeric reversed-phase SPE material. Although the recommendation for peptides is to use mixed-mode sorbents, it was thought that starting with reversed-phase only sorbents for this test would simplify data interpretation.

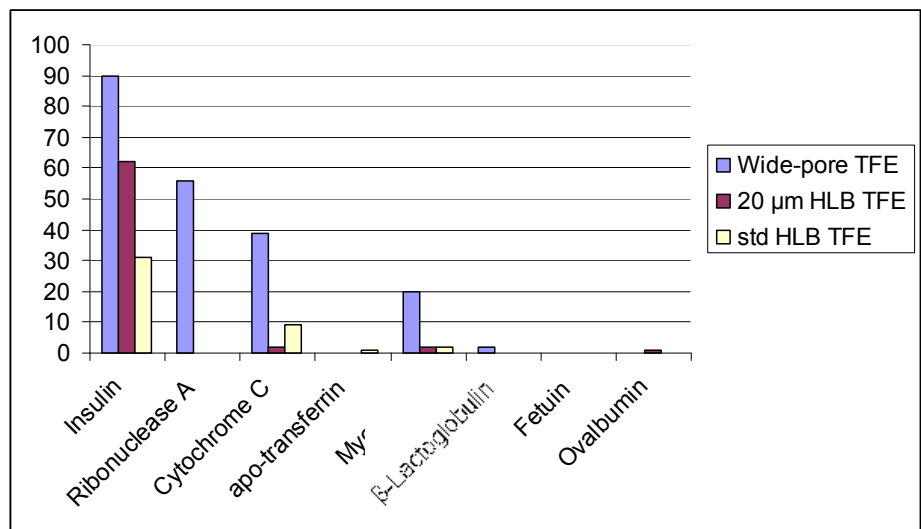
Specifically, if mixed-mode sorbents were used, one would have to consider dual retention mechanisms, ionic interactions and other variables. The experiment was considered to be better controlled and more focused on pore size influence when the retention mechanism was limited to reversed-phase. These were further compared to a commercially available 30 μm product of the same base reversed-phase polymer. For these experiments, 96-well $\mu\text{Elution}$ format plates were packed with 2 mg sorbent per well. An initial set of test proteins is described in Table 2.5. For the first set of experiments, proteins were diluted in aqueous solutions to test and compare recovery based on sorbent pore size.

| Protein | Size (approx. MW) |
|------------------------|--------------------------|
| Insulin | 5734 |
| Cytochrome C | 12384 |
| Ribonuclease A | 13700 |
| Myoglobin | 16951 |
| β -Lactoglobulin | 18270 |
| Ovalbumin | 44280 |
| Fetuin | 68000 |
| apo-Transferrin | 78000 |

Table 2.5 Test proteins for evaluation of wide pore polymeric reversed-phase SPE materials

A simple generic set of extraction conditions were applied to both plates packed with small or large pore sorbent material. The sorbent was conditioned with 200 μL MeOH, equilibrated with 200 μL water, and then 100 μL diluted protein standard was applied. Samples were washed with 200 μL 5% methanol in water and finally eluted with 2 x 25 μL 75% methanol in water, with or without 1% TFE. Final eluates were diluted with water prior to injection. As these were aqueous standards and not plasma extracts, UV detection at wavelength 254 was employed. A summary of protein recovery in the final eluates and in

the load fractions from the various sorbents are shown in Figures 2.25 and 2.26, respectively.



*Fetuin data difficult to quantify, will replace with alternate protein

Figure 2.25 SPE recovery of test proteins in **final eluate** from a 20 µm wide pore sorbent, a 20 µm typical pore size sorbent, and a 30 µm typical pore size sorbent.

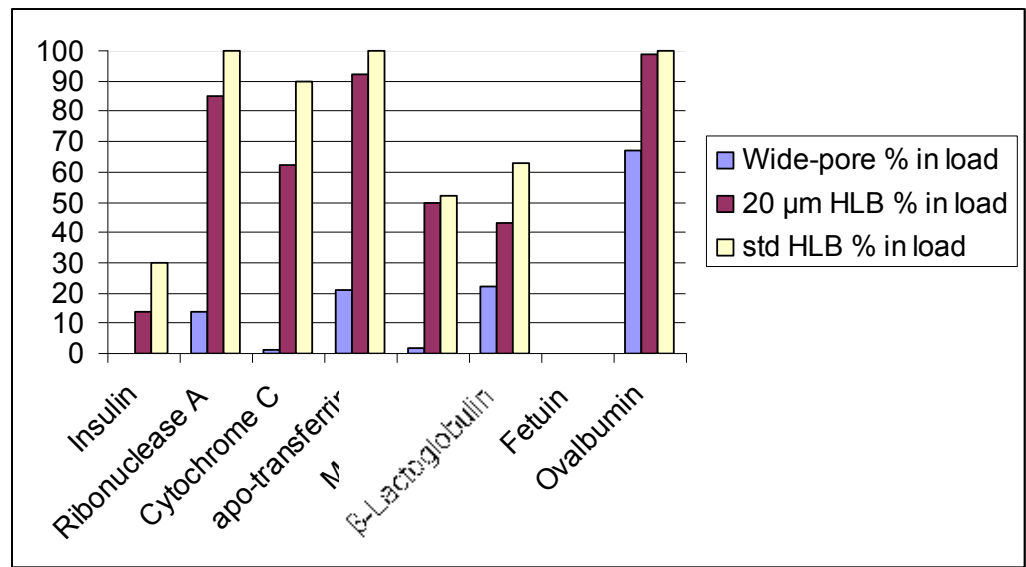


Figure 2.26 SPE recovery of test proteins in **load fraction** from a 20 µm wide pore sorbent, a 20 µm typical pore size sorbent, and a 30 µm typical pore size sorbent.

While insulin (the smallest protein) was recovered on all sorbents, some of the larger proteins were only recovered to any appreciable degree on the wide pore sorbent (Figure 2.25). Furthermore, when one looks at the presence of proteins in the load fraction (Figure 2.26), it is clear that the overwhelming majority of the protein in passing through on the load step when either of the smaller pore size sorbents is used. Although recovery is not high for *all* proteins in the final eluate on the wide-pore prototype, the proteins do appear to be at least partially retained. The assumption is that because proteins are not in the load step on the wide-pore sorbent, they are retained. Therefore, the extraction method will be modified to improve protein recovery. The elution solution was changed to 75% acetonitrile in water + 5% TFA. This method was applied to the initial set of test proteins as well as to a 200 μ L sample of 250 μ g/mL mouse murine IgG. The resultant improved recovery for all proteins in the final eluates is captured in Figures 2.27A and B.

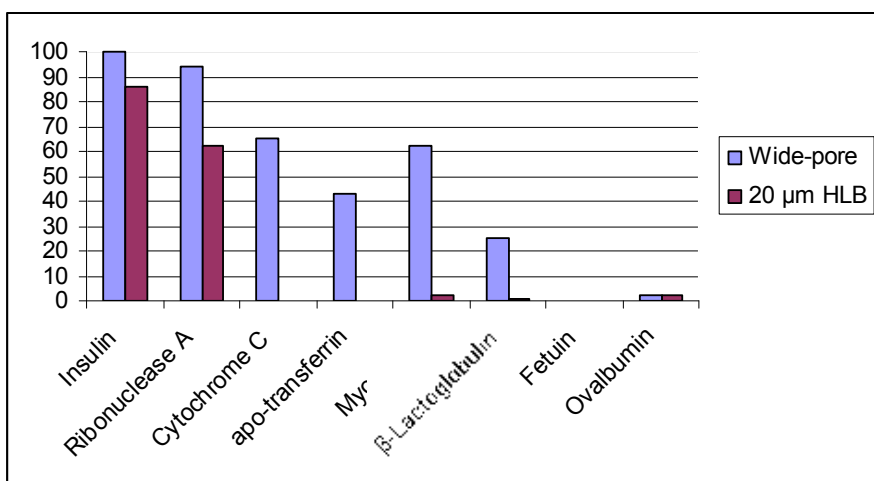


Figure 2.27A Recovery in final SPE elution for test proteins on wide pore and standard pore size 20 μ m sorbents

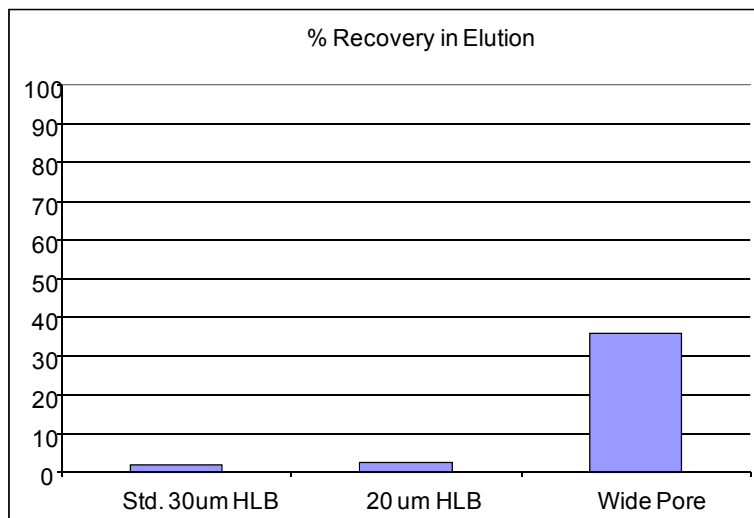


Figure 2.27B Recovery in SPE final elution for mouse murine IgG on wide pore and standard pore size 20 μm sorbents as well as 30 μm standard pore size sorbents

This data would appear to suggest that there is a clear advantage for retaining large proteins using a larger pore size SPE sorbent material. Figure 2.27A indicates that even a 77KDa protein such as transferrin can be recovered with reasonable efficiency on the wide pore sorbent. Other proteins in the 10-18KDa range, while not retained at all on typical pore size sorbents are well retained and recovered using this wide pore counterpart. It was also encouraging to see that a 150KDa IgG can also be retained and recovered, though to a lesser extent as ~50% is still found in the load fraction, using this prototype material.

As a follow up experiment, the influence of different organic solvent concentration in the final eluate was investigated, hypothesizing that fractionation might be possible based on acetonitrile %. Recovery is detailed in Figure 2.28.

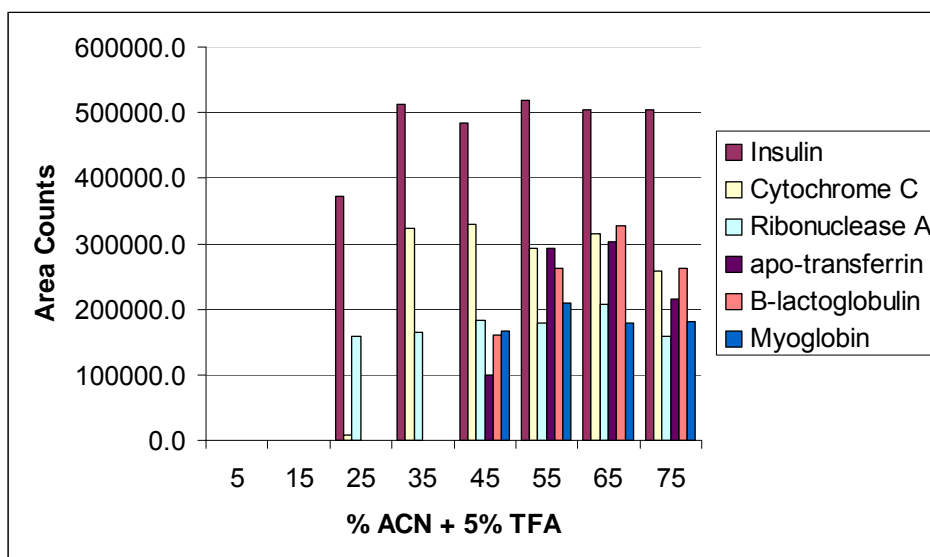


Figure 2.28 Recovery of various test proteins using different concentrations of acetonitrile in the elution solvent

The maximum recovery was achieved for insulin and ribonuclease A with only 25-35% ACN, indicating that these 2 proteins could be isolated from the others. Optimal recovery for the remaining proteins was obtained in 55-65% organic solutions, indicating that fractionation amongst those proteins was not possible under the current conditions.

The next step was to test this approach with proteins in human plasma. Using the wide pore prototype (DWB), recovery for test proteins was calculated in both human and in solvent standards (Figure 2.29). The data shows that the recovery was significantly lower when proteins were extracted from human plasma compared to that in solvent. This was expected due to the high levels of endogenous proteins present in the sample which would be expected to compete for sorbent capacity on the stationary phase. Plasma recovery across the three test sorbents was also compared, Figure 2.30. Whereas in solvent standards, the wide pore prototype showed a clear recovery advantage, particularly for proteins in the 10-18KDa range, this was not observed in plasma extracts. This result can be explained by the

fact that at high concentration (~60-80 mg/mL) human serum albumin (HSA), could be preferentially binding, in part due to its gross excess in plasma solutions, and significantly reducing the available binding sites for other proteins. To test this theory the recovery for HSA was calculated, Figure 2.31. The data clearly supports the theory, as the wide pore prototype retains significantly more HSA than either the 20 or 30 μm material with typical pore sizes.

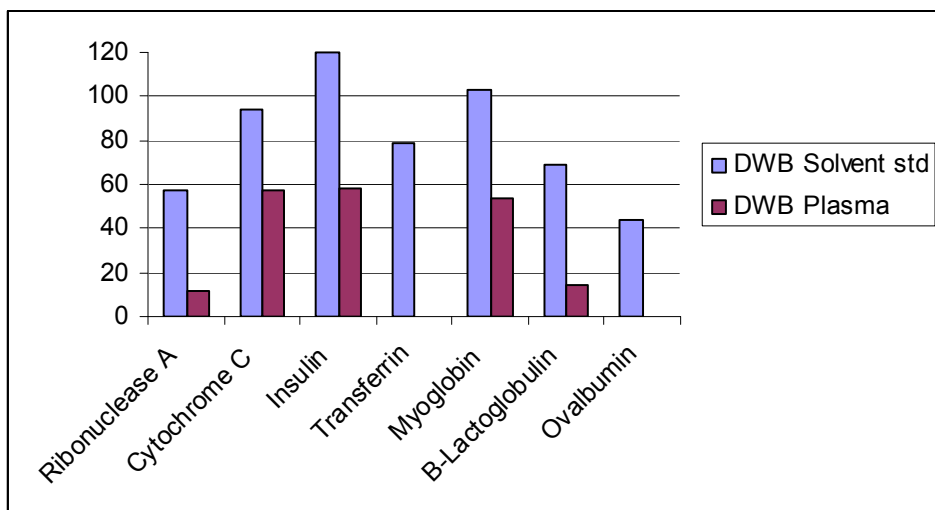
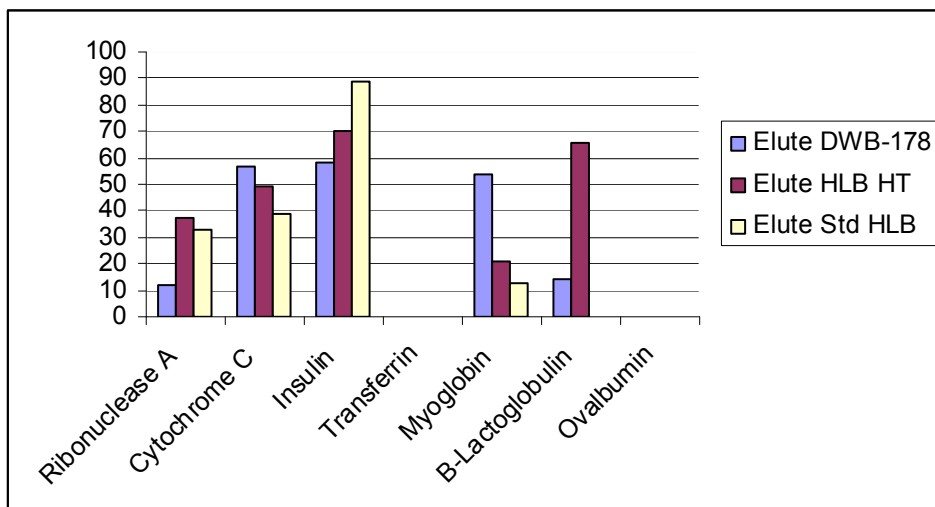


Figure 2.29 Extraction recovery of proteins from either human plasma or solvent standards using a wide pore prototype (designated DWB)



High endogenous levels of transferrin impede quantitation;
ovalbumin levels too low and peak too broad for accurate MS quantitation

Figure 2.30 Extraction recovery of proteins from human plasma using a wide pore prototype (DWB-178), a comparable particle size typical pore size sorbent (HLB HT) and a commercially available 30 μm typical pore size sorbent (Std HLB)

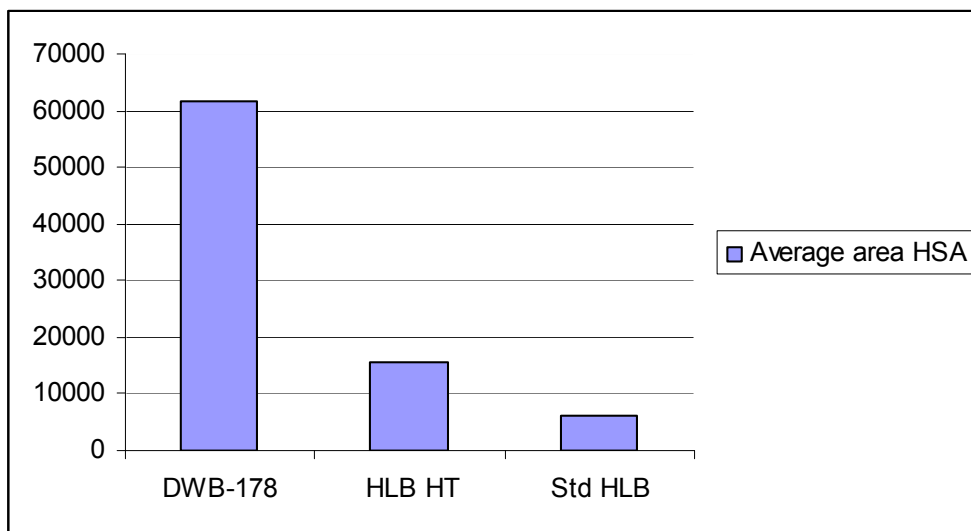


Figure 2.31 Extraction recovery of human serum albumin (HSA) from human plasma using a wide pore prototype (DWB-178), a comparable particle size typical pore size sorbent (HLB HT) and a commercially available 30 μm typical pore size sorbent (Std HLB)

From the data shown above it can be concluded that although wide pore prototypes provided a clear benefit in terms of retaining large proteins in plasma, such as HSA, it was not going to be viable for our bioanalytical experiments aimed at isolating other key proteins or peptides while eliminating albumins, and therefore was not pursued further.

2.6 Examples of Semi-validated Methods for Small Peptides

The generic LC and SPE conditions described in this chapter were used to quantify several therapeutic peptides in human plasma. Detection limits in extracted human plasma were determined for a subset of the test peptides. Blank human plasma and samples prepared at 0.001, 0.005, 0.01, 0.02, 0.05, and 0.1 ng/mL (approximately 1 to 100 fmol/mL) and were extracted according to the generic screening method. Chromatographic results were evaluated to determine limit of detection (LOD) and Lower Limit of Quantification (LLOQ). In bioanalytical assays, the LOD is defined as the level that is three times that of a extracted blank matrix sample; similarly, LLOQ is defined as five times the level of the blank[30, 31, 33].

Resulting representative chromatograms are shown in Figures 2.32 and 2.33, for desmopressin and angiotensin I, respectively, demonstrating the successful application of this combination of techniques to attain detection limits in the single pg/mL range. Naturally, the exact detection limits achievable are dependent on many factors including size and hydrophobicity of the peptide, ionization and extraction efficiency, specificity of

MS transition, chromatographic behaviour, volume of sample used and sensitivity of MS instrumentation employed, amongst others.

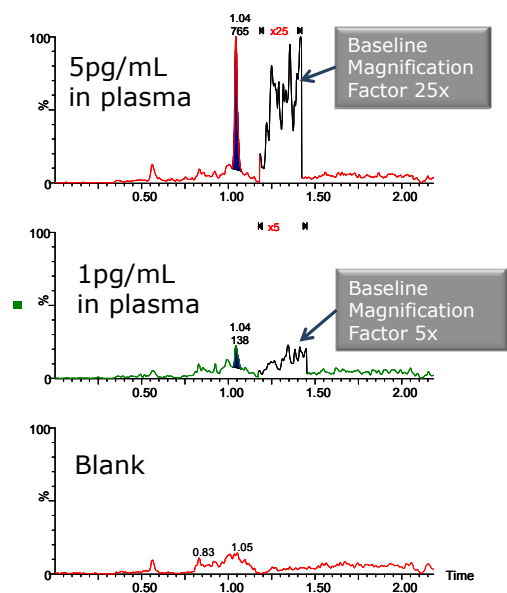


Figure 2.32 Representative chromatograms for 1 and 5 pg/mL desmopressin extracted from 500 µL human plasma, compared to blank extracted plasma, using the proposed generic starting methods described in this chapter

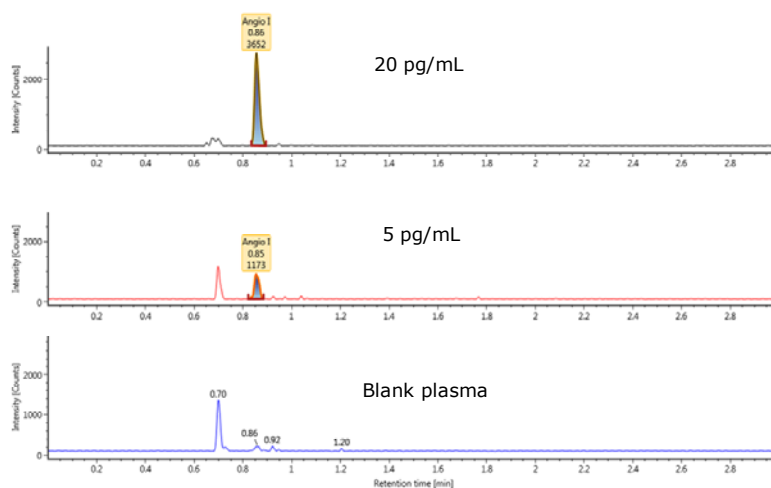


Figure 2.33 Representative chromatograms for 5 and 20 pg/mL angiotensin I extracted from 350 µL human plasma, compared to blank extracted plasma, using the proposed generic starting methods described in this chapter

This platform and approach was also successfully applied in the development of a flexible, sensitive, and selective method for β -amyloid peptides, putative biomarkers for Alzheimer's disease, and will be the subject of Chapter 4 [19]. β -amyloid peptides are considered one of the more difficult peptide classes to analyze due to their hydrophobicity, poor solubility, propensity to aggregate, high degree of non-specific binding, low circulating levels, poor MS sensitivity, and protein binding. Each aspect of peptide handling and each step of the extraction process were evaluated and optimized as per the recommendations in this chapter, ultimately yielding a method which overcame the inherent challenges faced. Lessons learned from this problematic group of peptides may be applied to other challenging peptides as well.

Although this chapter focuses on therapeutic peptides, the extraction techniques described, and to a certain extent, the chromatography, can be applied to the more elaborate application area of protein quantification using signature peptides once digestion of the protein has been accomplished. Surfactants, denaturation, reduction, and alkylation reagents as well as digestion enzymes and other peptides can be removed during SPE of the digest mixture (Figure 2.34).

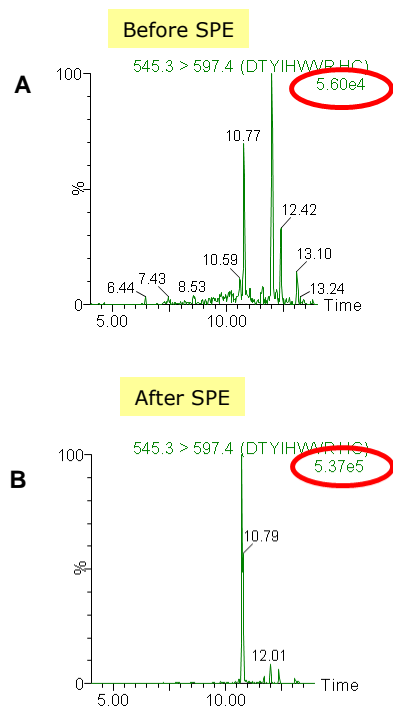


Figure 2.34 Comparison of LC-MS/MS analysis of a signature peptide from trastuzumab before (A) and after (B) SPE clean-up using a mixed-mode weak cation sorbent and generic protocol

Figure 2.34 demonstrates the potential benefit of mixed-mode SPE clean up for a signature peptide from trastuzumab. Not only are many background peaks removed and the spectra simplified, but signal intensity for the target peptide increased significantly as result of clean up using mixed-mode SPE. Recovery for the signature peptide was ~83%. In this case, the extraction protocol also provided a 5-fold concentration of the sample, which was diluted during addition of the various reagents without evaporation.

2.7 Summary of Key Rules and Guidelines Established in This Chapter

Liquid Chromatography

- C18 stationary phases provide optimal performance for most separations

- Larger pore size sorbents may improve peak shape for larger peptides
- Superficially porous and charged surface stationary phases may improve peak shape for peptides
- Reducing flow rate, increasing temperature, and shallowing gradient slope may all improve peak shape, reduce carryover, and increase sensitivity for peptides
- Always use carrier protein when working with solvent standards
- Ballistic gradients may result in peptide precipitation and loss
- TFE can be used in wash solvents and mobile phase B to reduce carryover
- Passivation of the chromatographic column with precipitated plasma prior to use may be required

Mass Spectrometry

- Choose the highest m/z precursor and fragments possible for greatest specificity
- Avoid immonium ions, water losses and ammonia losses where possible
- Choose b/y sequence ion fragments where possible
- MRM transitions wherein the fragment m/z is higher than the precursor m/z are preferred
- Positive ion mode should be used where possible rather than negative ion
- LC flow rate can influence the nature and relative abundance of specific precursors
- Always tune peptides at the chromatographic flow you will be using
- The highest sensitivity fragments may not be the most specific
- Monitoring of several MRM transitions in method development is important to ensure that the most specific of these is identified

- Choose an MS system with a mass range of ~2000 amu on both quadrupoles to allow selection of and enable highest sensitivity of higher m/z precursors and fragments

Sample Preparation and Peptide Handling

- Mixed-mode SPE provides the greatest specificity for peptide isolation
- Protein precipitation may be used as a pre-treatment step to further improve specificity
- Peptide solubility must be carefully considered when protein precipitation is used
- Increasing the % of acid/base in an elution solution can improve peptide recovery
- Organic composition of the SPE elution solution should not exceed 75%
- Screening both mixed-mode anion and mixed-mode cation sorbents most readily identifies conditions of greatest recovery and highest specificity
- pI can help predict optimal solubility
- HPLC index predicts relative hydrophobicity and can help predict non-specific binding and protein binding
- Avoid evaporation of extracts if possible
- TFE can be used to improve SPE recovery
- Changing the pH of sample diluents prior to SPE may improve binding and/or reduce interferences

2.8 Conclusions

The growing market for biotherapeutic peptides and the development of quantitative methods for those analytes has brought to light the challenges facing the analysis of this broad range of compounds. Regulatory requirements are encouraging development of methodologies that are time- and cost-effective, while still producing assays that are sensitive enough to cope with biological matrices. This chapter identifies and discusses the challenges in detail, provides potential solutions and then proposes a generally applicable platform to peptide bioanalysis method development. The generalized strategy incorporates an understanding of peptide morphology and chemistry to enable more efficient development of methods which readily achieve the robustness, speed and specificity required of a generally-applicable quantitative peptide assay. This was subsequently demonstrated using a relevant panel of therapeutic and endogenous peptides extracted from a biologically-relevant matrix. Highly targeted, specific assays can be developed individually for each of these peptides, but an approach aimed at a diverse set of peptides serves to examine the multiple factors that need to be considered in detail for assay development. Overall, the data in this chapter suggests that bioanalysis studies for peptide therapeutics are amenable to a platform-based approach to methods development when knowledge of peptide chemistry is carefully applied. Such standardized approaches for determining optimal SPE enrichment and MRM-based LC/MS analysis should permit a reduction in method development timelines and shorten time-to-market for peptide drugs. Where needed, advanced analytical techniques can provide the additional selectivity and/or sensitivity needed for exceedingly difficult or unique assays such as quantitation of certain

endogenous biomarkers or low level protein analysis through targeted enrichment and isolation of signature peptides.

Subsequent chapters in this thesis will examine, through real world quantitative applications, implementation of the principles uncovered in this fundamental research and cases where significant further method development and innovation were required.

2.9 References

1. Van den Broek, I., et al., *Quantitative bioanalysis of peptides by liquid chromatography coupled to (tandem) mass spectrometry*. Journal of Chromatography B, 2008. 872: p. 1-22.
2. de Bruijn, P., et al., Journal of Pharmaceutical and Biomedical Analysis, 2010. 51: p. 934-941.
3. Denooz, R., et al., Journal of Analytical Toxicology, 2010. 35: p. 280-286.
4. Discenza, L., et al., Journal of Chromatography B, 2010. 878: p. 1583-1589.
5. Gilar, M. and e. al, Journal of Separation Science, 2005. 28: p. 1694-1703.
6. Jemal, M., Z. Ouyang, and Y. Xia, Biomedical Chromatography, 2010. 24: p. 2-19.
7. Kay, R., et al., Rapid Communications in Mass Spectrometry, 2007. 21: p. 2585-2593.
8. Kay, R.G., et al., *High-throughput ultra-high-performance liquid chromatography/tandem mass spectrometry quantitation of insulin-like growth factor-I and leucine-rich alpha-2-glycoprotein in serum as biomarkers of recombinant human growth hormone administration*. Rapid Communications in Mass Spectrometry, 2009. 23: p. 3173-3182.
9. Mitulovic, G. and e. al, Analytical Chemistry, 2009. 81: p. 5955-5960.
10. Pedraglio, S., et al., Journal of Pharmaceutical and Biomedical Analysis, 2007. 44: p. 665-673.

11. Plumb, R., et al., *Journal of Proteome Research*, 2009. 8: p. 2495-2500.
12. Shen, J., et al., *Journal of Pharmaceutical and Biomedical Analysis*, 2006. 40: p. 689-706.
13. McCalley, D.V., *Effect of buffer on peak shape of peptides in reversed-phase high performance liquid chromatography*. *J Chromatogr A*, 2004. 4: p. 1-2.
14. McCalley, D.V., *Study of overloading of basic drugs and peptides in reversed-phase high-performance liquid chromatography using pH adjustment of weak acid mobile phases suitable for mass spectrometry*. *J Chromatogr A*, 2005. 20: p. 1-2.
15. Kirkland, J.J., et al., *Fused-Core Particle Technology in High-Performance Liquid Chromatography: An Overview*. *Journal of Pharmaceutical Analysis*, (0).
16. Destefano, J., et al., *Performance characteristics of new superficially porous particles*. *Journal of Chromatography A*, 2012. 1258: p. 76-83.
17. Wagner, B.M., et al., *Superficially porous silica particles with wide pores for biomacromolecular separations*. *Journal of Chromatography A*, 2012. 1264(0): p. 22-30.
18. Gilar, M., et al., *Journal of Chromatography A*, 2004. 1061: p. 183-192.
19. Lame, M., E. Chambers, and M. Blatnik, *Quantitation of Amyloid Beta Peptides A β 1-38, A β 1-40, and A β 1-42 in human CSF by ultra-performance liquid chromatography tandem mass spectrometry*. *Analytical Biochemistry*, 2011. 419: p. 133-139.
20. Kinter, M. and N.E. Sherman, *Protein Sequencing and Identification Using Tandem Mass Spectrometry*. Wiley-Interscience Series on Mass Spectrometry, ed. D. Desiderio and N. Nibbering 2000, USA: John Wiley and Sons, Inc.

21. Hunter, C. and L. Basa, *Detecting a Peptide Biomarker for Hypertension in Plasma*. Applied Biosystems Proteomics Technology Note.
22. Cole, R.B. and A.K. Harrata, *Solvent effect on analyte charge state, signal intensity, and stability in negative ion electrospray mass spectrometry; implications for the mechanism of negative ion formation*. Journal of the American Society for Mass Spectrometry, 1993. 4(7): p. 546-556.
23. John B, F., *Ion formation from charged droplets: roles of geometry, energy, and time*. Journal of the American Society for Mass Spectrometry, 1993. 4(7): p. 524-535.
24. Kebarle, P. and L. Tang, *From ions in solution to ions in the gas phase - the mechanism of electrospray mass spectrometry*. Analytical Chemistry, 1993. 65(22): p. 972A-986A.
25. Wang, G. and R.B. Cole, *Mechanistic Interpretation of the Dependence of Charge State Distributions on Analyte Concentrations in Electrospray Ionization Mass Spectrometry*. Analytical Chemistry, 1995. 67(17): p. 2892-2900.
26. Chemical Reviews, 2007. 107(8): p. 3605.
27. Chambers, E., et al., Journal of Chromatography B, 2007. 852(1-2): p. 22-34.
28. Calderón-Santiago, M., et al., *Analytical platform for verification and quantitation of target peptides in human serum: Application to cathelicidin*. Analytical Biochemistry, 2011. 415(1): p. 39-45.
29. Ewles, M. and L. Goodwin, *Bioanalytical approaches to analyzing peptides and proteins by LC-MS/MS*. Bioanalysis, 2011. 3(12): p. 1379-1397.

30. FDA, *Guidance for Industry: Bioanalytical Method Validation*, C.a. CVM, Editor 2001.
31. FDA and CDER, *Guidance for Industry Bioequivalence Studies with Pharmacokinetic Endpoints for Drugs Submitted Under an ANDA*. 2013.
32. Bansal, S. and A. DeStefano, *Key elements of bioanalytical method validation for small molecules*. The AAPS Journal, 2007. 9(1): p. E109-E114.
33. Fast, D.M., et al., *Workshop Report and Follow-up- AAPS Workshop on Current Topics in GLP Bioanalysis: Assay Reproducibility for Incurred Samples- Implications of Crystal City Recommendations*. The AAPS Journal, 2009.

Chapter 3

Developing a High Sensitivity LC-MS/MS Method for Direct Quantification of Human Parathyroid 1-34 (Teriparatide) in Human Plasma

This chapter is based on the following publication:

High Sensitivity LC-MS/MS Method for Direct Quantification of Human Parathyroid 1-34 (Teriparatide) in Human Plasma

Erin E. Chambers, Mary E. Lame, Jon Bardsley, Sally Hannam, Cristina Legido-Quigley, Norman Smith, Kenneth J. Fountain , Eileen Collins, and Elizabeth Thomas

Journal of Chromatography B, 938 (2013), pages 96– 104

3.1 Introduction

Osteoporosis is a major global health problem, responsible for 1.5 million bone fractures a year. In 2005 alone, the estimated cost for osteoporosis-related fractures was approximately \$19 billion[1]. One of the most common treatments for osteoporosis includes bisphosphonate drugs, which reduce bone turnover, increase bone mass and mineralization through osteoclast inhibition[2]. Teriparatide, however, is the first treatment for osteoporosis that stimulates new bone formation. It is an anabolic drug that acts to build up bones and has the potential to improve skeletal micro architecture and increases bone density[3-6].

Teriparatide (FORTEO[®]) is a recombinant form of a fragment of human parathyroid hormone, used in the treatment of osteoporosis. It is the smallest fragment of the full length (1-84) parathyroid hormone with the desired biological activity[7]. Specifically, teriparatide is comprised of the first 34 amino acids (the biologically active region) of the 84-amino acid human parathyroid hormone (PTH), and is also referred to as, rhPTH (1-34).

These types of biologics have historically been quantified using ligand binding assays (LBAs), but there are several reasons for the analysis of large molecules to be carried out by LC-MS/MS[8]. As previously mentioned in Chapter 1, LBAs can suffer from significant cross-reactivity issues and lack of standardization. For example, manufacturers of LBAs for the same analyte often use different capture reagents with different affinities for the target analyte as well as different cross reactivities[9]. This leads to significant differences in reported results as well as inaccurate results. In fact, in some instances, entire studies have been devoted to the standardization of peptide immunoassays[10]. LC-MS/MS has the advantage of shorter development times, greater accuracy and precision, the ability to

multiplex, and can readily distinguish between closely related analogues, metabolites or endogenous interferences. Furthermore, studies have shown that both ELISA and RIA assay accuracy can be significantly impacted by the stability of protein standards used or undetected peptide degradation[11]. In the latter case, an MS assay produced an analyte concentration that was 5% less than the Radio Immuno Assay (RIA). The RIA could not differentiate between the intact and degraded peptide of interest, and therefore was over-reporting the peptide concentration. Most published assays for teriparatide have been performed using RIA for quantification or other affinity-based methods[3, 6, 12, 13], therefore there is a requirement for an analogous and more specific LC-MS/MS method to be developed. One of the major hurdles one faces in developing an LC-MS assay, however, is in achieving detection limits that are similar to immunoassay. For teriparatide, an assay LOQ of between 10 and 50 pg/mL was shown to be clinically relevant[3, 14]. Using LC-MS, this quantification level is particularly difficult to achieve, especially for large peptides such as teriparatide. The primary challenge for MS sensitivity when using MRM quantification for large peptides comes from dilution of the primary precursor ion signal (from several different multiply charged species) and either poor collision induced product ion formation or further dilution of product ion signal due to extensive fragmentation. In addition, MS sensitivity is reduced due to poor analyte transfer into the gas phase. Teriparatide, like other large hydrophobic peptides [8], displays significant non-specific binding and poor solubility, making chromatography and sample preparation method development challenging.

The pharmacokinetics of teriparatide are characterized by rapid absorption within 30 minutes and rapid elimination with a half-life of 1hr, resulting in a total duration of

exposure to the peptide of approximately 4 hours[14]. At the practical clinical dose of 20 µg, typical teriparatide levels are ~50 pg/mL, further reinforcing the need for a very high sensitivity method.

The data presented below provides a single, simple LC-MS/MS method for the quantification of teriparatide (Figure 3.1) in human plasma.

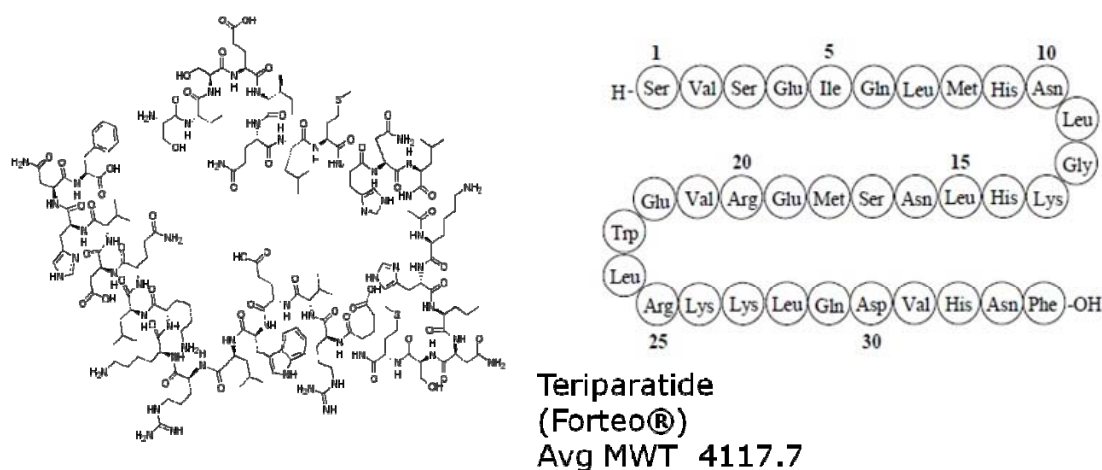


Figure 3.1 Structure and amino acid sequence for teriparatide

The method uses analytical scale sub-2µm LC and fast, selective sample preparation in a 96-well format to achieve an LOD of 10 pg/mL and a clinically relevant dynamic range of 15-500 pg/mL in human plasma.

3.2 Experimental

3.2.1 Chemicals and Reagents

Teriparatide acetate was purchased from ChemPep (Wellington, FL). Human parathyroid 1-38 (rhPTH 1-38) was purchased from American Peptide Company (Sunnyvale, CA) and rat parathyroid hormone 1-34 was purchased from Sigma-Aldrich (St. Louis, MO). The teriparatide sequence is depicted in Figure 3.1. Normal, non-diseased human plasma was purchased from Biological Specialty Corporation (Colmar, PA). Rat plasma was purchased from Equitech Bio (Kerrville, TX). Water for mobile phase and sample preparation was obtained from a Milli-Q lab water system (Millipore, Billerica, MA). Acetonitrile, methanol, and formic acid (concentrated solution, 99%) were purchased from Fisher Scientific (Fair Lawn, NJ). All other chemicals and reagents were purchased from Sigma (St. Louis, MO) unless otherwise stated.

3.2.2 Preparation of samples, calibration standards and quality control samples

Concentrated stock solutions were prepared by dissolving lyophilized teriparatide and rhPTH 1-38 powders in DMSO, each to a concentration of 1 mg/mL. A working solution of teriparatide at 10 µg/mL was prepared by dilution from the DMSO stock in 80/19/1 water/acetonitrile/formic acid containing 0.05% rat plasma. RhPTH 1-38 was used as the internal standard (IS) and was prepared in the above diluent at a concentration of 2 ng/mL to be used for spiking. For standard curve and quality control (QC) samples, spiking solutions of teriparatide were made through serial dilution of the 10 µg/mL stock in the above diluent containing formic acid, ACN, and rat plasma. All stock, working, and spike solutions were prepared in Lo-Bind tubes (Eppendorf.) For each intended standard curve point and QC level, 1 mL of control human plasma was spiked with an appropriate volume

of the appropriate concentration of analyte spiking solution. Standard curve points were prepared at 0.01, 0.015, 0.03, 0.04, 0.06, 0.08, 0.1, 0.2, 0.4, 0.5, and 1 ng/mL in human plasma. Quality control samples were prepared in human plasma at 0.02, 0.035, 0.075, 0.125, and 0.25 ng/mL. Blank human plasma samples were also analyzed for determination of limit of detection (LOD.) A 200 μ L aliquot of each sample was extracted as described in section 3.2.3 using a protein precipitation pretreatment followed by SPE.

3.2.3 Sample Preparation

Pretreatment: Protein Precipitation (PPT)

20 μ L of internal standard solution (2 ng/mL) was added to 200 μ L human plasma (standard curve point, QC or sample) and mixed. The final IS concentration was 200 pg/mL. Samples were precipitated in a 1 mL 96-well plate with 200 μ L acetonitrile containing 5% ammonium hydroxide, and centrifuged for 15 minutes at 4000 rpm.

The supernatant was transferred to a 2 mL 96-well plate containing 1 mL of water and mixed.

Solid phase extraction (SPE): Oasis® HLB μ Elution 96-well plate

Wells of the SPE plate were first conditioned with 200 μ L methanol, followed by equilibration with 200 μ L water. The entire diluted PPT supernatant (~1.4 mL) was loaded onto the extraction plate in two steps of approximately 700 μ L each using an electronic 8-channel pipettor. The wells were then washed with 200 μ L 5% methanol in water. Teriparatide and the IS were eluted sequentially with two 25 μ L aliquots of 60/34/5/1 ACN/water/TFE/TFA. Eluates were diluted with 50 μ L water and 30 μ L was injected onto the LC system.

Matrix factors (MF) were calculated according to Equation 3.1.

Equation 3.1 Calculation of matrix factor (MF)

$$\text{MF} = (\text{peak area of post-extracted spiked samples})/(\text{peak area of solvent standards})$$

3.2.4 Chromatographic Conditions

The SPE eluate was injected onto an ACQUITY UPLC CSH C18 column (2.1 x 50 mm, 1.7 μm , 130Å) using a Waters ACQUITY UPLC system equipped with a 50 μL fixed loop autosampler. Samples were kept cooled at 10°C and column temperature was maintained at 60°C. Mobile phase A consisted of 0.1% formic acid (by volume) in water and mobile phase B consisted of 0.1% formic acid (by volume) in acetonitrile. After an initial 0.2 minute hold, teriparatide and the IS were eluted using a linear gradient from 15% B to 50% B over 3.6 min at 0.4 mL/min, which was directly introduced into the MS, without splitting. Mobile phase B was then ramped from 50 to 98% over 0.1 min and held for 0.5 min to clean the column. This was followed by an equilibration at initial conditions. Total cycle time was 6 minutes.

3.2.5 Mass spectrometry and Software

For teriparatide and the IS, collision induced dissociation (CID) products of multiply charged precursors were detected in positive ion multiple reaction monitoring (MRM) mode using a Waters Xevo™ TQ-S mass spectrometer (Milford, MA). The electrospray voltage, source temperature, desolvation temperature and desolvation gas flow rate were 3.0 kV, 150 °C, 600 °C and 1000 L/Hr, respectively. MRM transitions and charge states for teriparatide and the IS as well as their respective cone voltages and collision energies are summarized in Table 3.1.

| Peptide | MRM Transition | Cone Voltage (V) | Collision Energy (eV) |
|-----------------------------|-----------------|------------------|-----------------------|
| Teriparatide | 687.05 > 787.26 | 45 | 18 |
| | 824.25 > 983.79 | 45 | 25 |
| Human Parathyroid 1-38 (IS) | 637.58 > 712.61 | 45 | 10 |
| | 892.22 > 854.80 | 45 | 22 |

Table 3.1. MRM transitions, collision energies, and cone voltages for teriparatide and human parathyroid 1-38 (rhPTH (1-38)), the internal standard (IS)

MassLynx instrument control software version 4.1 was used for data acquisition. All peak area integration, regression analysis and sample quantification was performed using TargetLynx.

3.3 Results and Discussion

3.3.1 Development of sample pre-treatment and solid-phase extraction

As mixed-mode SPE has been shown to yield the most selective extractions in our previous work [15, 16], it provided the optimal starting point for extraction method development. An experimental comparison between SPE and protein precipitation (PPT) confirmed that the endogenous background from PPT samples was too high to allow quantification at the sub-ng/mL level (Figure 3.2). It can be seen from the data in this figure that the background at the teriparatide retention time is significantly reduced when samples are processed by SPE following acetonitrile precipitation (bottom panel) relative to precipitation alone (top panel). Furthermore, precipitation with acetonitrile rather than zinc sulphate prior to SPE also results in a cleaner background. As a result, not only do we conclude that SPE is absolutely necessary, but also that pretreatment by acetonitrile

precipitation is preferred over zinc sulphate for background reduction. Sample preparation development focused on the use of a low sorbent bed-mass SPE format as a means to allow for sample concentration without evaporation, as evaporation of extracts containing peptides often results in significant peptide loss due to adsorption to surfaces and inefficient re-solubilization [8, 17].

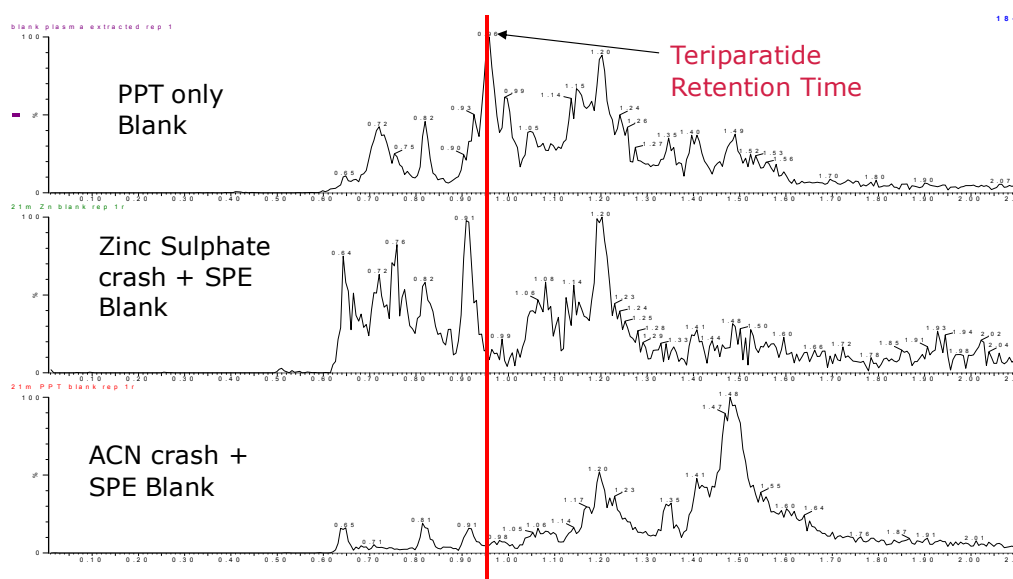


Figure 3.2 Comparison of MS background present in final eluates from various sample preparation techniques, relative to the retention time of teriparatide

Initial recovery experiments, using generic peptide extraction protocols [16] on mixed-mode strong anion exchange and weak cation exchange sorbents yielded recoveries of approximately 50%. Previous reports have shown that apparent “low extraction recovery” arises from several distinct possible sources: non-specific binding (NSB), protein binding, chemical instability, incomplete elution due to choice of elution solvent, or insufficient capacity in the extraction device[18]. Each of these possibilities was examined and tested.

The starting SPE method called for dilution of the plasma with 4% aqueous H_3PO_4 . It can be hypothesized that this may not be sufficient to disrupt any protein binding that could occur between teriparatide and plasma proteins. To address this issue alternate dilution options were assessed prior to SPE extraction, including dilution with TRIS base, 5% NaOH, 10% H_3PO_4 , guanidine HCl denaturation, zinc sulphate precipitation and organic precipitation. Figure 3.3 summarizes these findings.

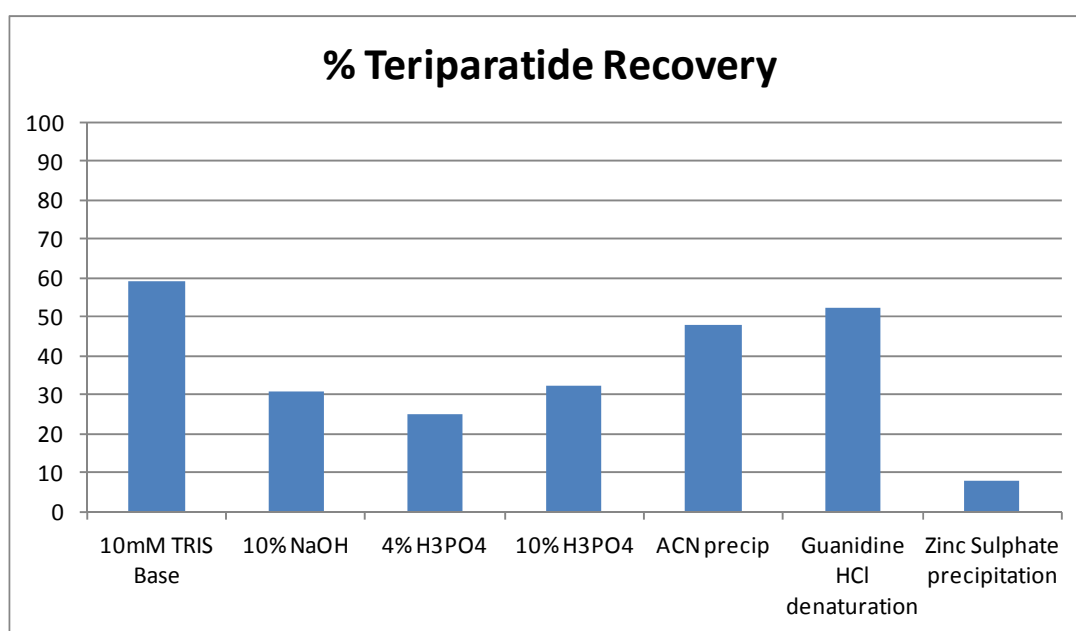


Figure 3.3 % SPE recovery of teriparatide following different plasma pre-treatment options

It can be seen from this data that organic precipitation, TRIS or Guanidine increased recovery by approximately 10%, whereas all other options resulted in negligible changes. Thus it was concluded that protein binding was not the primary cause of low recovery. Although instability in human plasma was not thought to be an issue[19], it was investigated nonetheless through the addition of a protease inhibitor however there was no improvement

in recovery. Next, the loading capacity of the plate was tested to eliminate the possibility of sample loss due to insufficient capacity. There was no increase in recovery when the sample size was reduced from 200 μ L to 50 μ L, indicating that the plate capacity was sufficient for the 200 μ L sample load. Elution solvents were also optimized through the addition of varying percentages of acidic and basic modifiers, as well as varying types and mixtures of organic solvent (ACN, MeOH, IPA), and with and without the addition of trifluoroethanol (TFE), which has been proven to improve solubility of peptides and proteins[20]. These modifications to the elution solvent did not improve recovery significantly, though the addition of TFE did increase MS area counts for teriparatide, perhaps indicating improved solubility. Finally, a rudimentary test for NSB was conducted. In one instance, the SPE plate was pre-conditioned with crashed plasma supernatant (to coat any surfaces available to bind teriparatide) and in another instance, TWEEN-20 (0.02%) was added to the samples, again to aid in coating surfaces. Neither treatment improved recovery significantly.

At this point, a more fundamental assessment of teriparatide recovery from plasma was performed using PPT alone, simply to confirm that high recovery could be obtained using the simplest approach possible. Both 2:1 and 1:1 ratios of modified and unmodified acetonitrile to plasma were tested. Recovery using a 1:1 ratio versus 2:1 ratio of organic solvent to plasma yielded approximately two-fold higher recovery. (The complete data summary from this experiment was previously shown in Chapter 2, in Figure 2.20). Thus for a larger peptide such as teriparatide, one must balance peptide recovery with precipitation of high abundance, unwanted plasma proteins. When the 2:1 ratio is used, it can be concluded that teriparatide is partially precipitated, resulting in low recovery (30-50%). This supposition is based on findings from Ewles et al[21] where they demonstrated that higher

percentages of organic are necessary to precipitate peptides of decreasing size, while larger peptides require much less organic. In addition, base-modified ACN yielded higher recovery than acid-modified ACN, due to a combination of improved solubility and more efficient disruption of protein binding. Precipitation with ACN was more efficient than MeOH or IPA. Final precipitation conditions adding 1:1 ACN + 5% NH₄OH to plasma yielded recovery in excess of 95% for teriparatide.

Once it was determined that teriparatide could be almost completely recovered using PPT whilst simultaneously reducing background high abundance proteins such as albumin, the focus returned to refining the subsequent SPE step in order to obtain adequate specificity for the assay. In this investigation a reversed-phase SPE sorbent was chosen for evaluation together with the mixed mode phase sorbents previously tested. Generic SPE methods described in Chapter 2 were modified to reflect what had been learned from the precipitation and pre-treatment experiments for teriparatide, as well as to eliminate any steps that might encourage NSB (such as 100% aqueous washes). The protein precipitation experiments demonstrated a higher recovery using ACN-based solutions, and higher peak areas when TFE was added to the elution solvent, with an average recovery greater than 90% of that obtained from the PPT step. The PPT conditions were then incorporated into the SPE method, specifically acid- and base-modified elution solutions containing ACN and TFE were tested first. Reversed-phase recovery was 89%, while maximum recovery on mixed-mode sorbents was approximately 50%.

Modification with acid or base provided little advantage in terms of recovery. However, elution with acid was chosen over basic elution to provide a degree of retention orthogonality relative to the basic loading conditions. Finally, tests were performed to

determine the minimum concentration of organic required to maximize teriparatide recovery, thus creating the most selective elution conditions possible when combined with the pH switch. In addition, low organic % in the elution solvent ensures that phospholipids and other more hydrophobic endogenous interferences are retained on the SPE plate. Elimination of 100% aqueous wash steps coupled to an elution solution comprised of 60% ACN, 5% TFE, and 1% TFA yielded >90% recovery on Oasis HLB with <2.5% matrix effects. The highest recovery was achieved on the reversed-phase only sorbent, therefore this sorbent was selected for teriparatide extraction. Normally it is preferred to use mixed-mode SPE as specified in Chapter 2. However, extraction recovery for teriparatide was 50% less on the mixed-mode versus reversed-phase only sorbent. Attempts to increase recovery on the mixed-mode sorbent were unsuccessful. Finally, it was decided that this particular application would have to be performed using reversed-phase only SPE. The addition of a protein precipitation pre-treatment step helped to improve specificity and facilitate the use of reversed-phase SPE for this particular case.

3.3.2 Mass Spectrometry of Teriparatide

While a single precursor is typically used to generate fragments for small molecule analyses, there are advantages to selecting multiple precursors to evaluate fragmentation of a peptide. Not only do the various charge states fragment differently, but it can be difficult to predict the specificity of a particular MRM transition in a sample derived from a biological matrix. Therefore having several precursors to choose from allows a degree of selection during the method development process. Several multiply charged precursors were

observed for teriparatide and human parathyroid hormone 1-38 (IS); the full scan MS spectra are shown in Figure 3.4.1.

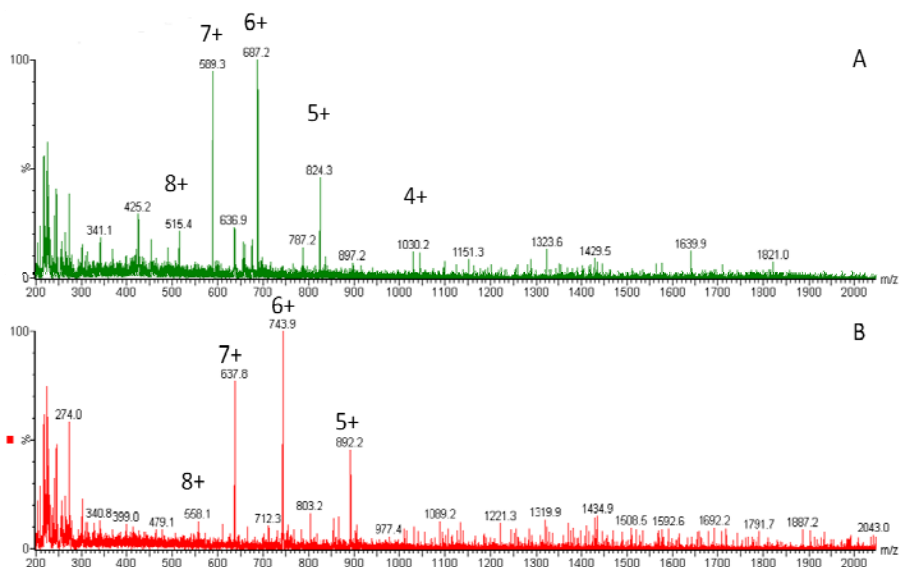


Figure 3.4.1. MS spectra of teriparatide (A) and human parathyroid 1-38 (B)

The 6+ and 7+ charge states of teriparatide at m/z 687 and 589, respectively, were observed to be the most intense ions. The 5+ precursor at m/z 824 was about half the intensity of the others. Fragmentation of m/z 687 produced a selective product ion at m/z = 787 (Figure 3.4.2B), corresponding to a 5+ y₃₂ ion. This was chosen as the primary transition used for quantitative analysis. The 7+ precursor at m/z 589 did not yield any usable product ions (Figure 3.4.2C). Fragmentation of the less intense m/z 824 precursor (Figure 3.4.2A) produced fragment ions, including a 4+ y₃₂ ion at m/z 984, of sufficient intensity only to be used for confirmatory purposes. MSMS spectra obtained at the optimized collision energies are shown in Figure 3.4.2. Fragments chosen for quantification are highlighted with an asterisk. A low intensity 4+ precursor was observed at m/z 1030, which yielded a 3+ y₂₉

fragment at m/z 1201. This mass pair, though specific, did not yield sufficient intensity for quantitative purposes.

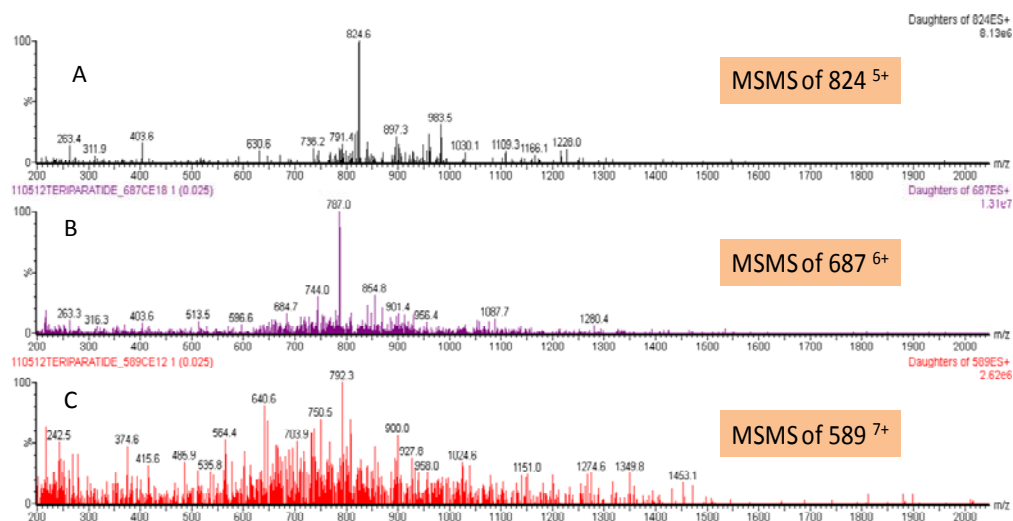


Figure 3.4.2. MSMS spectra of the 5+ teriparatide precursor at m/z 824 (A), the 6+ precursor at m/z 687 (B), and the 7+ precursor at m/z 589 (C). Fragments chosen for quantification are highlighted with an asterisk and correspond to y_{32} ions.

In addition, it is good practice to avoid any fragments below m/z 200. Although many peptides produce intense fragments in this range, these ions (often immonium ions) result in high background in extracted samples due to their lack of specificity. This was demonstrated in a recently published insulin assay[8]. The 5+ precursor at m/z 824 actually produces a high intensity fragment at m/z 159, which may be as much as 10X more intense in solvent standards. However, in an extracted plasma sample, Figure 3.5 demonstrates that although the 159 fragment is more intense than the 984 fragment used for quantification, the signal to noise is significantly lower. In this teriparatide assay, the use of y ion fragments above $m/z = 700$ yielded significantly improved specificity, facilitating the use of simple LC

and extraction methodologies which ultimately achieve detection limits similar to that of RIAs and ELISAs.

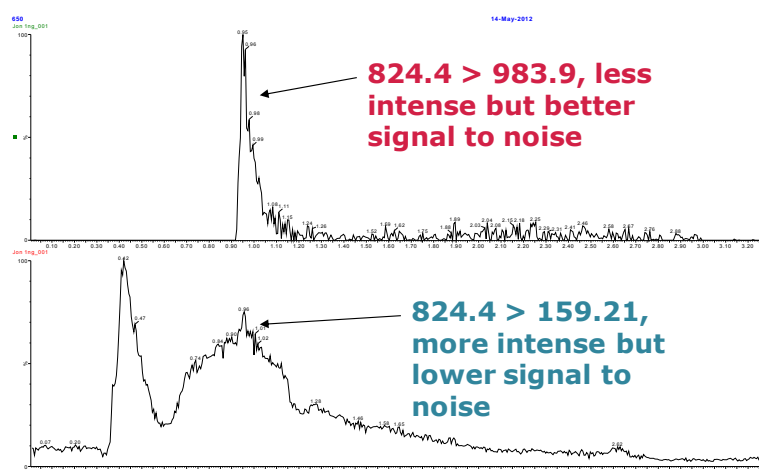


Figure 3.5 MS/MS analysis of teriparatide extracted from human plasma monitoring either m/z 824- \rightarrow 984 (top) or m/z 824- \rightarrow 159 (bottom)

3.3.3 Liquid Chromatography

The value of 300Å pore size LC columns for the separation of peptides has been documented previously[21, 22] and was established in Chapter 2. These columns were shown to significantly improve peak shape, particularly for large peptides, relative to more standard pore size (i.e., 90-130Å) columns. Unexpectedly, and specifically for teriparatide, a 300Å bridged-ethyl hybrid (BEH) column produced peaks characterized by severe tailing and widths of approximately 6-8 seconds wide at base (Figure 3.6, bottom panel). Several intact insulins demonstrated similar behaviour [8], which was resolved through the use of a column containing BEH particles modified with a low level, positively charged moiety (also referred to as Charged Surface Hybrid, or CSH). It is believed that these peptides interacted

with the uncharged, hydrophobic C18 surface of the conventional BEH 300 Å columns to a greater degree than other peptides and as such, diffusion in and out of the chromatographic pores was not efficient, resulting in the observed broad peaks and tailing. Due to the low level positive charge on the particle surface of the CSH phase, peak shape under formic acid conditions was improved. Figure 3.6 (top panel) demonstrates the improved peak shape for teriparatide obtained on a CSH versus the BEH 300Å C18 column.

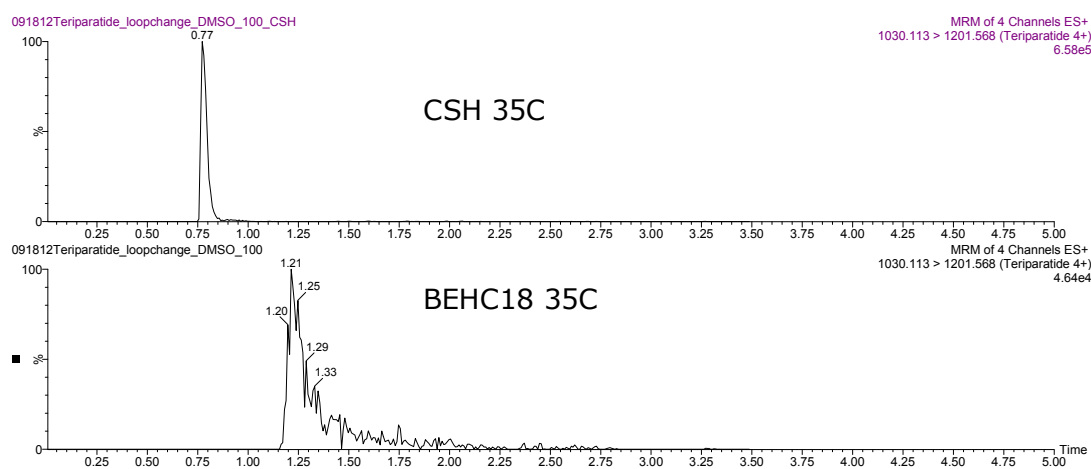


Figure 3.6. A teriparatide 1 ng/mL neat standard chromatographed on an ACQUITY UPLC CSH C18 column at 35°C (top panel) and an ACQUITY UPLC BEH C18 300 column at 35°C (bottom panel.) Both columns are 2.1 X 50mm, 1.7 µm. The flow rate is 0.4 mL/min and the gradient is 20-65% B in 2 minutes

The isoelectric point (pI) for teriparatide is approximately 9.1, making it positively charged under the low pH mobile phase conditions employed. Improved peak shape could be due to the positive charge on the stationary phase minimizing secondary interactions. During method development, flow rate, temperature, gradient, organic modifier, and the addition of TFE to mobile phase B were all evaluated. Experiments determined that

teriparatide follows similar trends to other large peptides with respect to temperature and gradient slope. Strangely, a lower flow rate, 0.3 versus 0.4 mL/min, produced an unexpected decrease in signal as shown in Figure 3.7. We then hypothesized that an even faster flow rate might further increase teriparatide signal. However, an experiment was run using a flow rate of 0.6 mL/min and not only did the teriparatide signal decrease, but carryover was observed. We believe that teriparatide either begins to precipitate and/or not enough time is allowed for efficient diffusion, when the faster flow rate is used. These observations serve to highlight the balance that must be achieved between speed, sensitivity, and diffusion/solubility of the peptide in the mobile phase.

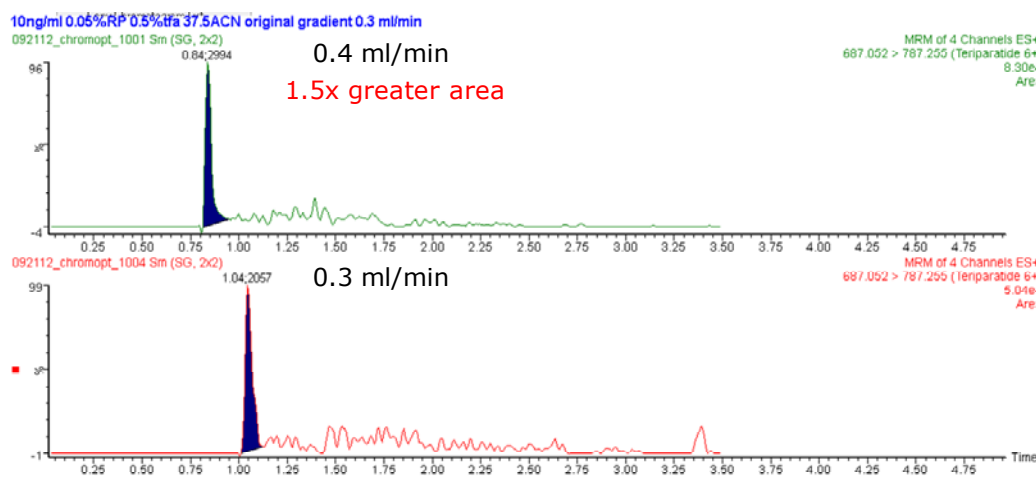


Figure 3.7 LC/MS analysis of teriparatide using a test gradient of 20 to 65% B over 2 minutes run at either 0.4 mL/min (top) or 0.3 mL/min (bottom)

Shallower gradient slopes produced the expected effect of increasing area counts. For example, a gradient of 15-50% B in 3.6 minutes versus a steeper gradient from 15-50% B over 1.8 minutes increased area counts by approximately 2X (Figure 3.8).

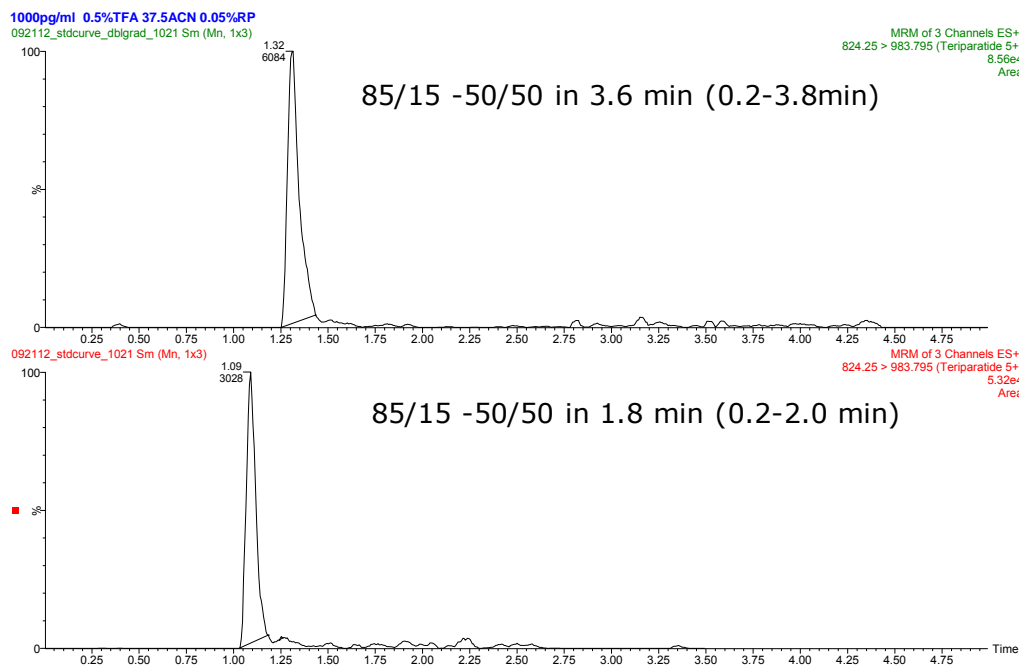


Figure 3.8 LC/MS analysis of teriparatide using a gradient of 15% B to 50% B over either 3.6 (top) or 1.8 (bottom) minutes

Increasing temperature from 35 to 60° C also increased area counts and reduced carryover, likely due to increased mass transfer, and this is consistent with previously reported work [23]. The use of ACN in mobile phase B versus MeOH or IPA resulted in 2X higher area counts. Although adding 5% TFE to mobile phase B also increased area counts for teriparatide (see Figure 2.11, Chapter 2), it resulted in an equal increase in background,

and therefore was not included. TFE was used in the needle wash, however, to further reduce any remaining carryover.

A representative chromatogram of the separation using the final gradient conditions described in the experimental section is shown in Figure 3.9.

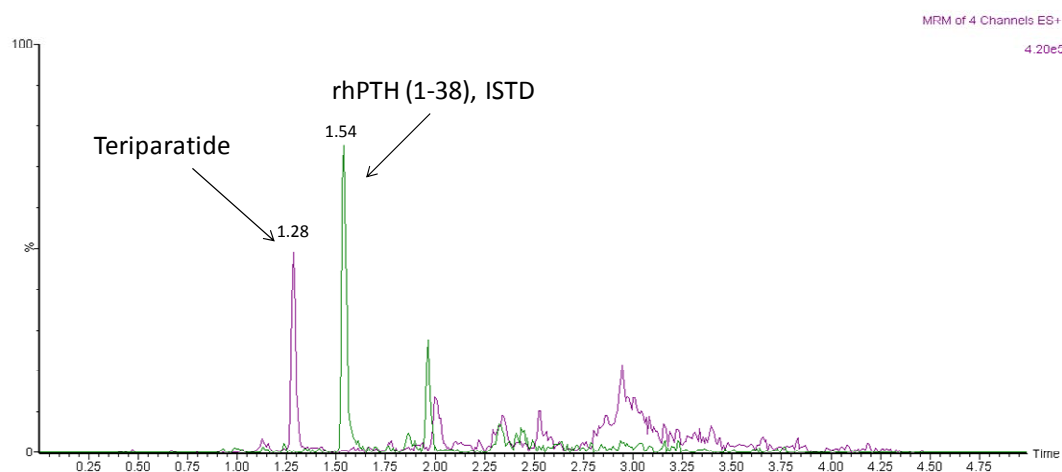


Figure 3.9. UPLC separation of teriparatide and internal standard, from a 125 pg/mL extracted plasma sample, using a 2.1 X 50mm ACQUITY UPLC CSH column and the final gradient conditions

3.3.4 Human Plasma Standard Curve and Quality Control Data

Dynamic range and assay accuracy and precision were determined using standard curves and quality control (QC) samples prepared in human plasma spiked with teriparatide and a constant concentration of the IS (final concentration 200 pg/mL). Peak area ratios (PARs) of teriparatide and the internal standard were determined and calibration curves generated. Teriparatide concentrations in QC samples were calculated from their PARs against their respective calibration lines. Calibration standards used for quantification of teriparatide ranged from 0.01 to 1 ng/mL. Using a 1/x weighting and quadratic fit, the r^2

values for all curves were found to be in the range > 0.998. The average CV of all points on 3 independent standard curves was 4% and average accuracy was 101%, indicating a very reproducible and accurate method. Statistics from a representative standard curve are summarized in Table 3.2.

| Human Plasma Lot# X1793C (Biological Specialty Corp.) | Std. Conc. (pg/mL) | Mean Calculated Conc. (pg/mL) | Std. Deviation | %CV | Number of Replicates Passed | Mean Accuracy |
|--|-------------------------------|--|-----------------------|------------|------------------------------------|----------------------|
| 15pg/ml | 15 | 16.65 | 0.64 | 3.9 | 3/3 | 111.0 |
| 30pg/ml | 30 | 30.48 | 1.39 | 4.6 | 3/3 | 101.6 |
| 40pg/ml | 40 | 41.09 | 1.95 | 4.8 | 3/3 | 102.7 |
| 60pg/ml | 60 | 62.78 | 5.20 | 8.3 | 3/3 | 104.6 |
| 80pg/ml | 80 | 75.38 | 1.56 | 2.1 | 3/3 | 94.2 |
| 100pg/ml | 100 | 94.39 | 2.78 | 2.9 | 3/3 | 94.4 |
| 200pg/ml | 200 | 202.60 | 10.63 | 5.2 | 3/3 | 101.3 |
| 400pg/ml | 400 | 401.90 | 10.86 | 2.7 | 3/3 | 100.5 |
| 500pg/ml | 500 | 498.47 | 10.36 | 2.1 | 3/3 | 99.7 |

Table 3.2. Representative standard curve statistics for teriparatide extracted from 200 µL human plasma

QC samples were prepared in triplicate in 6 sources of human plasma at 0.02, 0.035, 0.075, 0.125, and 0.25 ng/ml. The mean accuracies for all QC samples, in all sources of matrix, ranged from 90-106%, and mean precision for all levels ranged from 0.7 to 7.7%. Representative QC statistics from 6 individual sources (Biological Specialty Corporation lot #s) of human plasma are presented in Table 3.3.

| Human Plasma Lot# (Biological Specialty Corp.) | Gender | QC Conc. (pg/mL) | Mean Calculated Conc. (pg/mL) | Std. Deviation | %CV | Number of Replicates Passed | Mean Accuracy |
|---|---------------|-----------------------------|--|-----------------------|------------|------------------------------------|----------------------|
| X1793C | Mixed | 20 | 20.25 | 1.50 | 7.3 | 3/3 | 102.2 |
| 82111 | Female | 20 | 33.38 | 1.75 | 8.6 | 3/3 | 102.2 |
| 57298 | Male | 20 | 18.30 | 0.67 | 3.7 | 3/3 | 91.5 |
| 82740 | Female | 20 | 20.74 | 1.59 | 7.7 | 3/3 | 103.7 |
| 57901 | Male | 20 | 19.67 | 0.60 | 3.0 | 3/3 | 98.3 |
| X1803C | Mixed | 20 | 21.27 | 0.96 | 4.5 | 2/3 | 106.4 |
| Human Plasma Lot# (Biological Specialty Corp.) | Gender | QC Conc. (pg/mL) | Mean Calculated Conc. (pg/mL) | Std. Deviation | %CV | Number of Replicates Passed | Mean Accuracy |
| X1793C | Mixed | 35 | 33.35 | 1.99 | 6.0 | 2/3 | 95.3 |
| 82111 | Female | 35 | 34.48 | 1.84 | 5.3 | 3/3 | 98.5 |
| 57298 | Male | 35 | 31.64 | 1.81 | 5.7 | 3/3 | 90.4 |
| 82740 | Female | 35 | 33.29 | 1.73 | 5.2 | 3/3 | 95.1 |
| 57901 | Male | 35 | 34.71 | 0.30 | 0.9 | 3/3 | 99.2 |
| X1803C | Mixed | 35 | 34.24 | 2.66 | 7.8 | 3/3 | 97.8 |
| Human Plasma Lot# (Biological Specialty Corp.) | Gender | QC Conc. (pg/mL) | Mean Calculated Conc. (pg/mL) | Std. Deviation | %CV | Number of Replicates Passed | Mean Accuracy |
| X1793C | Mixed | 75 | 75.07 | 1.17 | 1.6 | 3/3 | 100.1 |
| 82111 | Female | 75 | 73.29 | 4.23 | 5.8 | 3/3 | 97.7 |
| 57298 | Male | 75 | 71.92 | 3.50 | 4.9 | 3/3 | 95.9 |
| 82740 | Female | 75 | 70.34 | 5.14 | 7.3 | 2/3 | 93.8 |
| 57901 | Male | 75 | 72.30 | 5.28 | 7.3 | 3/3 | 96.4 |
| X1803C | Mixed | 75 | 69.63 | 3.25 | 4.7 | 3/3 | 92.8 |
| Human Plasma Lot# (Biological Specialty Corp.) | Gender | QC Conc. (pg/mL) | Mean Calculated Conc. (pg/mL) | Std. Deviation | %CV | Number of Replicates Passed | Mean Accuracy |
| X1793C | Mixed | 125 | 131.21 | 2.73 | 2.1 | 3/3 | 105.0 |
| 82111 | Female | 125 | 130.01 | 1.67 | 1.3 | 3/3 | 104.0 |
| 57298 | Male | 125 | 125.82 | 1.42 | 1.1 | 3/3 | 100.7 |
| 82740 | Female | 125 | 117.34 | 6.94 | 5.9 | 3/3 | 93.9 |
| 57901 | Male | 125 | 115.21 | 5.42 | 4.7 | 3/3 | 92.2 |
| X1803C | Mixed | 125 | 113.70 | 4.92 | 4.3 | 3/3 | 91.0 |
| Human Plasma Lot# (Biological Specialty Corp.) | Gender | QC Conc. (pg/mL) | Mean Calculated Conc. (pg/mL) | Std. Deviation | %CV | Number of Replicates Passed | Mean Accuracy |
| X1793C | Mixed | 250 | 262.26 | 5.14 | 2.0 | 3/3 | 104.9 |
| 82111 | Female | 250 | 265.24 | 1.77 | 0.7 | 3/3 | 106.1 |
| 57298 | Male | 250 | 244.54 | 15.75 | 6.4 | 3/3 | 97.8 |
| 82740 | Female | 250 | 221.83 | 5.72 | 2.6 | 3/3 | 88.8 |
| 57901 | Male | 250 | 235.72 | 12.22 | 5.2 | 3/3 | 93.0 |
| X1803C | Mixed | 250 | 226.60 | 2.93 | 1.3 | 3/3 | 90.7 |

Table 3.3. QC statistics from teriparatide extracted from 6 individual lots of human plasma.

Representative chromatograms of an extracted plasma blank and teriparatide at various low level concentrations are shown in Figures 3.10A-D. A representative standard curve is shown in Figure 3.11.

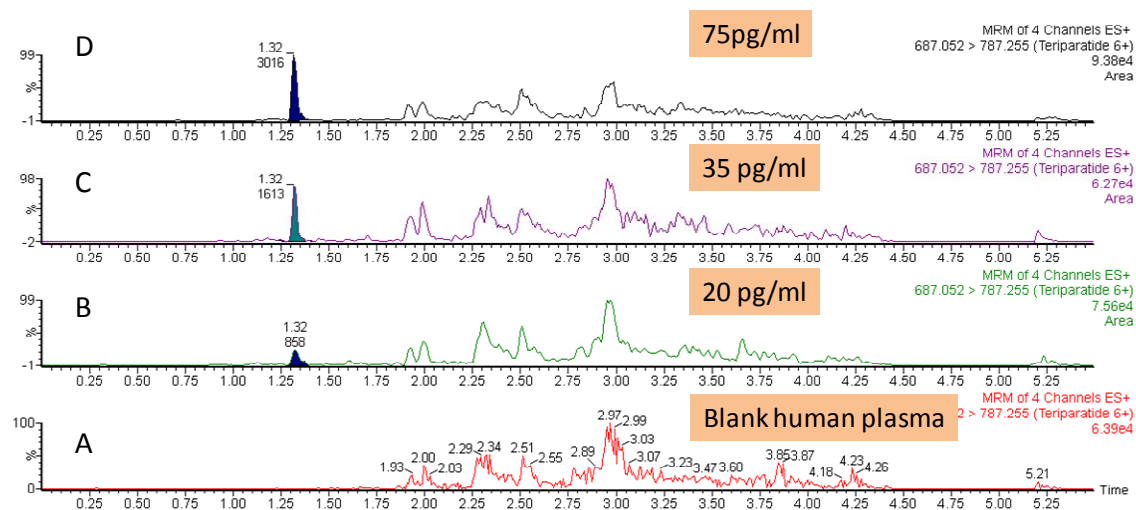


Figure 3.10. Representative chromatograms from teriparatide extracted from blank human plasma (A) and from human plasma at 20 (B), 35 (C) and 75 (D) pg/mL.

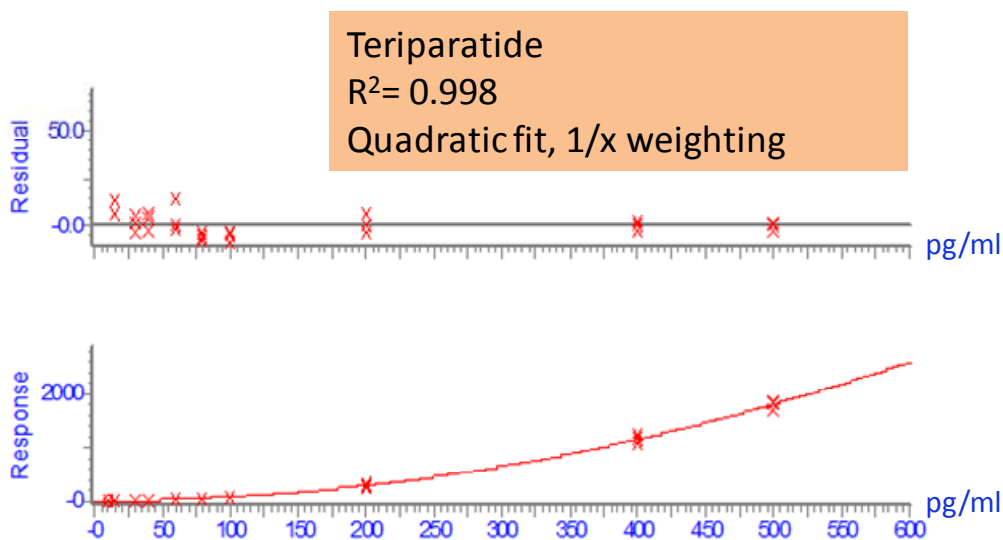


Figure 3.11. Representative standard curve of teriparatide extracted from human plasma, from 15- to 500 pg/mL.

The necessity for the use of a quadratic fit was explored from various angles. Human plasma blanks from all lots were free from interference at the teriparatide retention time. Focus on IS performance revealed that IS area counts were consistent across the concentration range and across various lots of human plasma. Furthermore, there was no interference between the IS and teriparatide in samples containing IS only. Both the nature and concentration of the IS were tested with little effect. Rat PTH 1-34, when tested as an alternative IS, yielded variable MS background with no change in linearity. An additional hypothesis relating to the use of a quadratic fit was that teriparatide might be gradually building up on the column and then leaching out slowly, due to inadequate peptide solubility. To test this theory, column temperature was increased to 80°C with no impact on performance. Another possibility is that a shift in the charge state distribution occurred with increasing analyte concentration. Data was examined and we found that no shift occurred.

Finally, the gradient steepness was further reduced in an attempt to uncover any previously undetected interferences/co-elutions. None were detected. Assay accuracy and precision met accepted criteria for a validated assay[24] , with no CV >8% for any QC level, in any source of plasma and an average accuracy of 97.5% for all QC samples. These data suggest that, although the calibration curve had this non-linear character, the data fit a weighted quadratic function well and the demonstrated accuracy and precision over the assay range were within conventional criteria for a validated assay.

3.3.5 Specificity

Matrix factors were calculated in six sources of human plasma with a CV across the various lots of 5.0 %, easily meeting recommended regulatory criteria[25]. Matrix factors for individual lots (N=3 analysis) were 1.24, 1.16, 1.18, 1.24, 1.15, and 1.31. Data for individual replicates is presented in Table 3.4. In addition, six sources of plasma were assessed for interferences in the blank samples present at the retention time of teriparatide. All extracted plasma blanks were found to be free from interference. Accuracy and precision of the lowest QC samples (fortified at 20 pg/mL or 4.85 fmol/mL) in 6 sources of human plasma confirms specificity with an average CV of 5.8% and an average accuracy of 100.7%

| Plasma Lot # | Prep 1 | Matrix Factor | Prep 2 | Matrix Factor | Prep 3 | Matrix Factor |
|-------------------------|---------------|--------------------------|---------------|--------------------------|---------------|--------------------------|
| x1793c | 26813.4 | 1.22 | 28284.6 | 1.28 | 26785.7 | 1.22 |
| x1803c | 27198.2 | 1.23 | 24787.4 | 1.13 | 24745.8 | 1.12 |
| 57298 | 26619.8 | 1.21 | 26493.7 | 1.20 | 24550.6 | 1.11 |
| 57901 | 28961.7 | 1.31 | 26002.6 | 1.18 | 27012.8 | 1.23 |
| 82111 | 26610.4 | 1.21 | 26007.4 | 1.18 | 23306.2 | 1.06 |
| 82740 | 29942.9 | 1.36 | 28104.5 | 1.28 | 28307.1 | 1.28 |

Table 3.4. Individual matrix factor assessments from 3 replicates each, from 6 sources of human plasma

3.5 Conclusions

With the global incidence of osteoporosis-related fractures expected to increase by 50% by 2025 [1], it is reasonable to also expect that the interest in development of treatment and monitoring options, and thus the identification and quantification of teriparatide, will be increasingly important to the scientific community. Not only is the interest in teriparatide specifically likely to increase, but the trend toward increasing development of peptide therapeutics and, interestingly, increasing size of peptide therapeutics[26], makes understanding and addressing the specific challenges associated with bioanalysis of large peptides particularly relevant. There are many distinct advantages to quantifying teriparatide by LC-MS/MS, and this analysis overcame many analytical hurdles including non-specific binding, poor chromatographic peak shape, carry-over, poor linearity, poor reproducibility, protein binding and poor MS sensitivity. This chapter presents a novel method for differentiating and quantifying teriparatide using μ Elution SPE and UPLC-

MS/MS, and highlights the tools and techniques for understanding, identifying, and addressing the challenges associated with large molecule analysis by LC-MS in the routine bioanalytical laboratory. The combination of a simple, yet highly selective, two-step 96-well extraction which concentrates without evaporation, chromatography using novel charged-surface columns, and detailed investigation of MS transition were key elements required to address these issues. The method described herein achieves a quantification limit of 15 pg/mL (3.6 fmol/mL) from 200 μ L of human plasma, providing the necessary sensitivity for analysis of PK studies as well as clinical trials. Accuracy and precision measurements all meet FDA criteria for method validation [27] with all CVs for QC samples <8%, and average accuracy at all levels of 97.5%. Matrix factor assessment also meet industry recommendations for validated assays[25], with a 5% CV of matrix factors across 6 lots. To the best of the authors' knowledge this is the first LC-MS/MS method for teriparatide with detection limits in the range of RIAs, ideal for highly specific and accurate teriparatide quantification.

3.6 References

1. Burge, R., et al., *Incidence and Economic burden of Osteoporosis-Related Fractures in the United States, 2005-2025*. Journal of Bone and Mineral Research, 2007. 22(3): p. 465-475.
2. Reszka, A. and G. Rodan, *Bisphosphonates Mechanism of Action*. Current Rheumatology Reports, 2003. 5(1): p. 65-74.
3. Hammerle, S.P., et al., *The single dose pharmacokinetic profile of a novel oral human parathyroid hormone formulation in healthy postmenopausal women*. Bone, 2012. 50(4): p. 965-73.
4. Neer, R.M., et al., *Effect of Parathyroid Hormone (1-34) on Fractures and Bone Mineral Density in Postmenopausal Women with Osteoporosis*. New England Journal of Medicine, 2001. 344(19): p. 1434-1441.
5. Quattrocchi, E. and H. Kourlas, *Teriparatide: a review*. Clin Ther, 2004. 26(6): p. 841-54.
6. Seibel, M.W., et al., *Validation and application of an immunoradiometric assay for the determination of human parathyroid hormone fragment 1–34 in dog plasma following subcutaneous and intravenous administration*. Journal of Pharmaceutical and Biomedical Analysis, 1996. 14(12): p. 1699-1707.
7. Kimmel, D.B., et al., *The effect of recombinant human (1-84) or synthetic human (1-34) parathyroid hormone on the skeleton of adult osteopenic ovariectomized rats*. Endocrinology, 1993. 132(4): p. 1577-84.

8. Chambers, E.E., et al., *Development of a fast method for direct analysis of intact synthetic insulins in human plasma: the large peptide challenge*. *Bioanalysis*, 2012. 5(1): p. 65-81.
9. Glenn, C. and A. Armston, *Cross-reactivity of 12 recombinant insulin preparations in the Beckman Unicel DxI 800 insulin assay*. *Annals of Clinical Biochemistry*, 2010. 47(3): p. 264-266.
10. Rodríguez-Cabaleiro, D., et al., *Pilot Study for the Standardization of Insulin Immunoassays with Isotope Dilution–Liquid Chromatography/Tandem Mass Spectrometry*. *Clinical Chemistry*, 2007. 53(8): p. 1462-1469.
11. Kay, R.G. and A. Roberts, *Bioanalysis of biotherapeutic proteins and peptides: immunological or MS approach?*. *Bioanalysis*. 2012 May;4(8):857-60. doi: 10.4155/bio.12.66.
12. Hu, Z., et al., *Recombinant human parathyroid hormone 1-34: pharmacokinetics, tissue distribution and excretion in rats*. *Int J Pharm*, 2006. 317(2): p. 144-54.
13. Sukovaty, R.L., et al., *Quantification of recombinant human parathyroid hormone (rhPTH(1-84)) in human plasma by immunoassay: Commercial kit evaluation and validation to support pharmacokinetic studies*. *Journal of Pharmaceutical and Biomedical Analysis*, 2006. 42(2): p. 261-271.
14. Satterwhite, J., et al., *Pharmacokinetics of Teriparatide (rhPTH[1–34]) and Calcium Pharmacodynamics in Postmenopausal Women with Osteoporosis*. *Calcified Tissue International*, 2010. 87: p. 485-492.

15. Chambers, E., et al., *Systematic and comprehensive strategy for reducing matrix effects in LC/MS/MS analyses*. Journal of Chromatography B, 2007. 852(1–2): p. 22–34.
16. Chambers, E.E., D. Diehl, and J. Wheaton, *Simplifying Peptide Bioanalysis*. LCGC Chromatography Online, 2010.
17. Pezeshki, A., et al., *Adsorption of peptides at the sample drying step: Influence of solvent evaporation technique, vial material and solution additive*. Journal of Pharmaceutical and Biomedical Analysis, 2009. 49(3): p. 607–612.
18. Chambers, E., *Protein and Peptide Therapeutics: Addressing Bioanalytical Demands of Complicated Peptides*
Tips and Tricks for Troubleshooting and Optimization During Method Development, B. Journal, Editor 2013.
19. MacNeill, R., et al., *LC–MS/MS quantification of parathyroid hormone fragment 1–34 in human plasma*. Bioanalysis, 2013. 5(4): p. 415–422.
20. Mitulović, G., et al., *Preventing Carryover of Peptides and Proteins in Nano LC-MS Separations*. Analytical Chemistry, 2009. 81(14): p. 5955–5960.
21. Ewles, M. and L. Goodwin, *Bioanalytical approaches to analyzing peptides and proteins by LC–MS/MS*. Bioanalysis, 2011. 3(12): p. 1379–1397.
22. Chambers, E., D. Diehl, and J. Wheaton, *Simplifying Peptide Bioanalysis*. LCGC: chromatography online, 2010. The Application Notebook.
23. Dolan, J.W., *Temperature selectivity in reversed-phase high performance liquid chromatography*. J Chromatogr A, 2002. 965(1–2): p. 195–205.

24. FDA, C., CVM, *Guidance for Industry Bioanalytical Method Validation*, C. FDA, CVM, Editor 2001: Rockville, MD.
25. Bansal, S. and A. DeStefano, *Key elements of bioanalytical method validation for small molecules*. The AAPS Journal, 2007. 9(1): p. E109-E114.
26. Reichart, J., et al., *Development Trends for Peptide Therapeutics: a Comprehensive quantitative analysis of peptide therapeutics in clinical development*, 2010.
27. *Guidance for Industry Bioanalytical Method Validation*, C. FDA, CVM, Editor 2001: Rockville, MD.

Chapter 4

Quantification of Amyloid beta peptides, Putative Alzheimer's Disease Biomarkers

This chapter is based on the following publication by this author:

Quantitation of Amyloid Beta Peptides A β ₁₋₃₈, A β ₁₋₄₀, and A β ₁₋₄₂ in human CSF by ultra-performance liquid chromatography tandem mass spectrometry

Mary E. Lame, Erin E. Chambers* and Matthew Blatnik

Analytical Biochemistry, 419 (2011), pages 133-139

4.1 Introduction

The impact of Alzheimer's disease in terms of mortality rate and cost cannot be underestimated financially both on the healthcare system and on the individual. This disease currently affects over 35 million individuals worldwide and is expected to affect 115 million by 2050[1]. In the US, it is responsible for 500,000 deaths a year and is the 6th cause of death in the USA. The cost of Alzheimer's disease is by far the most expensive in the US, with the direct costs to Americans totaling an estimated \$214 billion in 2014. Of this, \$150 billion are costs to Medicare and Medicaid. In fact, 20% of all Medicare dollars spent is on Alzheimer's related care. Additionally, it is predicted that Alzheimer's will cost the USA, alone, approximately \$1.2 trillion (in 2014 dollars) in 2050[2], a staggering number. It is no surprise that Alzheimer's research is one of the top focus areas worldwide in academia and the pharmaceutical industry.

One of the main medical challenges centres around the early diagnosis and differentiation of Alzheimer's disease (AD) from various other forms of Mild Cognitive Impairment (MCI). While post-mortem analysis remains the definitive determinant of cause of death, significant progress has been made in identifying early predictors or markers of the disease. An accumulation of research has led to current acceptance that the core indicators of AD are tau proteins, hyper-phosphorylated tau, and the amyloid beta peptide₁₋₄₂[3-8]. Recent publications by a group at Georgetown University also indicate that a panel of ten blood-based lipids *may* be early indicators of AD[9]. A very recent article in the Alzheimer's and Dementia journal identifies 10 plasma proteins that predict the progression from prodromal disease to dementia[10]. The availability of a fast, reliable, easy to deploy

test for these marker compounds could significantly benefit Alzheimer's diagnosis and treatment.

The work in this chapter focuses specifically on the development of an assay for the quantification of three key amyloid beta peptides, including one of the core Alzheimer's markers, amyloid beta ($A\beta$)₁₋₄₂. The method developed and described herein has subsequently formed the basis for a joint effort between the Global Biomarker Standardization Committee (GBSC) and the Alzheimer's Association (AA) to develop a candidate reference method for LC/MS-based $A\beta$ ₁₋₄₂ measurement[11, 12]. In fact, Dr. Mattsson of the neurochemistry laboratory at the Sahlgrenska University Hospital in Sweden describes it as the "first use of selective reaction monitoring quantification of $A\beta$ ₁₋₄₂ in human cerebral spinal fluid" in his review of approaches to reference measurement procedures for this biomarker[12]. Furthermore, this method is referenced in many of the current publications describing LC/MS based $A\beta$ ₁₋₄₂ quantification [5, 7, 11-19].

The pathogenesis of Alzheimer's is marked by formation and deposition of insoluble protein aggregates in the brain[20]. Proteinaceous plaque formation in Alzheimer's is a combination of amyloid beta peptides ($A\beta$), derived from action of β and γ secretases on the amyloid precursor protein, and formation of intracellular neurofibrillary tangles (NFT's) whose major constituent is the microtubule-binding protein tau. $A\beta$ peptides are found in both plasma and cerebral spinal fluid (CSF)[21], are 43 amino acids or less in length and can polymerize to form long insoluble fibrils consisting of parallel-aligned hydrogen-bonded β -sheets[22]. The amyloid peptide $A\beta$ ₁₋₄₀ forms the insoluble β -sheet but is seeded by $A\beta$ ₁₋₄₂. Amino acid sequence, MW and pI for amyloid peptides studied in this chapter are shown in Figure 4.1.

| |
|--|
| <p>Amyloid β 1-38 DAEFRHDSGYEVHHQKLVFFAEDVGSNKGAIIGLMVGG MW 4132 PI 5.2</p> |
| <p>Amyloid β 1-40 DAEFRHDSGYEVHHQKLVFFAEDVGSNKGAIIGLMVGGV MW 4330 PI 5.2</p> |
| <p>Amyloid β 1-42 DAEFRHDSGYEVHHQKLVFFAEDVGSNKGAIIGLMVGGVIA MW 4516 PI 5.2</p> |

Figure 4.1 Sequence, MW and pI for amyloid beta peptides 1-38, 1-40, and 1-42

The deposition of these insoluble aggregates from extracellular A β deposits as well as intracellular NFT's in the brain are considered the critical event in the development and pathology of Alzheimer's, making A β peptides appealing biomarkers of disease severity[23, 24].

Therapeutic intervention focuses on modifying the biochemical processes that deposit insoluble A β plaques in an attempt to slow disease progression or to delay its onset. Based on post-mortem examinations, formation of insoluble A β deposits are considered the critical event in Alzheimer's progression. Therefore, monitoring A β peptide concentrations during disease progression or during therapeutic intervention may be an appropriate strategy for monitoring therapeutic efficacy of a pharmacological treatment [25, 26]. Current methods to quantify amyloid peptides have led to somewhat inconclusive results in Alzheimer's programs due to a combination of non-specificity, lack of selectivity, and the inability to multiplex easily. In addition, many different methods have been used, with

dramatically different quantitative results [27]. Therefore there is a critical need for a more accurate and precise, single standardized methodology for the quantification of A β species in blood samples, and for monitoring ratios of the various isoforms in Alzheimer's programs to elucidate biological processes.

Enzyme-linked immunosorbant assays (ELISA), western blots or immunoaffinity enrichment followed by liquid chromatography mass spectrometry (LC-MS) are the most popular assays for A β quantitation [28-30]. While immuno assays are sensitive, antibody selectivity and various sample handling protocols have created contradictory A β findings and low throughput assays. Even with newer analytical technologies in place, A β quantitation by LC-MS is challenging due to low endogenous concentrations, their propensity to aggregate and even selecting the appropriate biological matrix for monitoring A β levels.

The findings detailed in Chapter 2 provided not only a fundamental understanding of the challenges associated with LC-MS of peptides, but also elucidated solutions for many of those problems. This knowledge was then applied herein to the quantification of these critical Alzheimer's disease biomarkers.

Investigators have measured A β levels in both plasma and CSF as diagnostic or pathogenic biomarkers of Alzheimer's but, prior to 2014, there was no clear correlation between plasma A β levels and Alzheimer's pathology[31, 32]. The work described by Mapstone et al[9], however, has now shown that certain lipids may also be appropriate biomarkers. Plasma is a more appealing matrix than CSF for clinical measurements because blood collection poses significantly less risk of infection to patients and can be sampled over long-term studies. However, Alzheimer's severity is associated with the inability to

clear specific A β peptides from the brain that aggregate into plaque deposits[33]. Because the brain compartment has reduced A β clearance, CSF is likely a more appropriate matrix for monitoring A β concentrations in the degree of Alzheimer's severity or during therapeutic intervention. Furthermore, at the time of writing, a confident correlation between plasma and CSF levels and the relationship to Alzheimer's progression had not yet been definitively established.

Below is described an alternative sample preparation procedure for A β species enrichment in CSF without relying upon antibodies. This SPE method had greater than 80% extraction efficacy and eliminates selectivity issues associated with antibody based analysis. When used in conjunction with the described ultra performance liquid-chromatography tandem mass-spectrometry (UPLC-MS/MS) assay, it was possible to accurately and reproducibly quantify A β_{1-38} , A β_{1-40} , and A β_{1-42} from human CSF at the level of 50 pg/mL or 0.011 nMol. Enhanced analytical methodologies like the one described herein may provide greater insight into amyloid diseases, their progression and therapeutic approaches to intervention.

4.2 Experimental

4.2.1 Chemicals and Reagents

Human amyloid-beta synthetic peptides A β_{1-38} , A β_{1-40} , and A β_{1-42} were purchased from American Peptide (Sunnyvale, CA). Nitrogen-15 isotopically labeled human amyloid-beta peptides [$^{15}\text{N}_{51}$]-A β_{1-38} , [$^{15}\text{N}_{53}$]-A β_{1-40} , and [$^{15}\text{N}_{55}$]-A β_{1-42} were purchased from rPeptide (Athens, GA). Normal, non-diseased human cerebrospinal fluid (CSF) was purchased from Biological Specialty Corporation, Colmar, PA (pool 2) and Lampire

Biological Labs, Pipersville, PA (pools 1 and 3). Artificial CSF perfusion fluid was purchased from Tocris Bioscience (Ellisville, MO). Water for mobile phase and sample preparation was obtained from a Milli-Q lab water system, (Millipore, Billerica, MA). Acetonitrile, methanol, and ammonium hydroxide (concentrated solution, 28-30%) were purchased from Fisher Scientific (Fair Lawn, NJ). All other chemicals and reagents were purchased from Sigma (St. Louis, MO) unless otherwise stated.

4.2.2 Preparation of samples, calibration standards and quality control samples

A β peptides and their isotopically labeled internal standards were corrected for purity and prepared at 1 mg/ml in dimethyl sulfoxide (DMSO). Standards were diluted to 50 μ g/ml in DMSO, divided into aliquots for single use and stored at -80 C in 0.5 ml polypropylene micro centrifuge tubes (Axygen Scientific; Union City, CA). On the day of sample analysis, aliquots of the 50 μ g/ml stock of each non-labeled peptide were pooled and diluted to 500 ng/ml in 50/50 acetonitrile/water (ACN/H₂O) +1% ammonium hydroxide (NH₄OH), ¹⁵N labeled peptides were treated similarly. The internal standard (IS) spiking solution was prepared by diluting the 500 ng/ml ¹⁵N stock to 20 ng/ml in 50/50 ACN/H₂O containing 1% NH₄OH. For standard and quality control (QC) samples, working solutions of pooled A β peptides, that were 25X the desired final concentration were made through serial dilution of the 500 ng/ml stock. For each intended standard curve point and each QC level, 1 ml of artificial CSF containing 5% rat plasma or human CSF was spiked with 40 μ l of the appropriate concentration of analyte working solution and 50 μ l IS spiking solution. Quality control samples were prepared in human and artificial CSF matrices at 0.2, 0.8, 2, and 6 ng/ml. After addition of standards and prior to extraction, human CSF, calibration and quality control samples were equilibrated at room temperature for 30 min. A 200 μ l aliquot

of each was diluted with 200 μ l of 5 M guanidine hydrochloride, shaken at room temperature for 45 min and diluted further with 200 μ l 4% phosphoric acid (H_3PO_4) in water. The resultant 600 μ l sample was extracted by SPE.

4.2.3 Solid-phase extraction conditions

Samples were extracted using an Oasis MCX μ Elution plate (Waters Corp., Milford, MA). The plate was conditioned with 200 μ l of methanol followed 200 μ l of 4% H_3PO_4 in water. The 600 μ l pretreated CSF, standards and quality control samples were loaded onto the SPE plate and washed with 200 μ l of 4% H_3PO_4 in water followed by 200 μ l of 10% acetonitrile. Amyloid beta peptides were eluted with two 25 μ l aliquots (collected together) of 75/15/10 (v/v/v) ACN/ H_2O /concentrated NH_4OH solution. Samples were then diluted with 25 μ l of water and placed in the autosampler for analysis.

4.2.4 Ultra-performance liquid chromatography tandem mass spectrometry

A 10 μ l aliquot was injected onto an ACQUITY UPLC BEH300 C18 column (2.1 x 150 mm, 1.7 μ m) using a Waters ACQUITY UPLC system. The column temperature was 50°C. The chromatography system was operated in reversed-phase gradient mode where mobile phase A consisted of 0.3% NH_4OH (by volume) in water and mobile phase B consisted of 90/10(v/v) acetonitrile/mobile phase A. After an initial 1 minute hold, A β peptides were eluted using a linear gradient from 10% B to 45% B over 5.5 min at 0.2 ml/min, which was directly introduced into the MS, without splitting. For each peptide and IS, collision induced dissociation (CID) products of 4+ precursors were detected in positive ion multiple reaction monitoring (MRM) mode using a Waters Xevo™ TQ mass

spectrometer (Milford, MA.) The electrospray voltage, source temperature, desolvation temperature and desolvation gas flow rate were 2.5 kV, 120 °C, 450 °C and 800 L/Hr, respectively. MRM transitions and charge states for each peptide and IS as well as their respective cone voltages and collision energies are summarized in Table 4.1. MassLynx instrument control software was used for data acquisition. All peak area integration, regression analysis and sample quantification was performed using TargetLynx. Peak area ratios (PARs) of the A β peptides and their isotopically labeled internal standards were determined and calibration curves for each of the A β peptides were constructed using PARs of the artificial CSF calibration standards. A β concentrations in CSF were determined from their PARs against their respective calibration line.

| Peptide Name | Precursor Ion 4+ | Product Ion 4+ | Product Ion ID | Cone voltage (V) | Collision energy (eV) |
|---|------------------|----------------|----------------|------------------|-----------------------|
| A β ₁₋₃₈ | 1033.5 | 1000.3 | b 36 | 33 | 23 |
| [¹⁵ N ₅₁]-A β ₁₋₃₈ | 1046.0 | 1012.5 | | 30 | 22 |
| A β ₁₋₄₀ | 1083.0 | 1053.6 | b 39 | 33 | 25 |
| [¹⁵ N ₅₃]-A β ₁₋₄₀ | 1096.0 | 1066.5 | | 35 | 22 |
| A β ₁₋₄₂ | 1129.0 | 1078.5 | b 40 | 28 | 30 |
| [¹⁵ N ₅₅]-A β ₁₋₄₂ | 1142.5 | 1091.5 | | 35 | 28 |

Table 4.1 Mass spectrometry conditions for MRM transitions of the amyloid β peptides and their ¹⁵N-labeled internal standards

4.3 Results

4.3.1 Sample pre-treatment and solid-phase extraction recoveries

During early method development using artificial CSF as a surrogate matrix, lower A β recovery was observed relative to that in human CSF (though neither was optimal) and characterized as non-specific binding. Subsequently, A β peptide standards were diluted in artificial CSF containing 5% rat plasma to act as a carrier in order to address this issue and decrease non-specific binding. Rat plasma was chosen as a carrier because rat A β peptides differ in amino acid composition by substitution at arginine-5, tyrosine-10 and histidine-13 for glycine, phenylalanine and arginine, resulting in different molecular weights from human A β species, thus eliminating any possible cross talk. Although the addition of carrier protein improved recovery in general, absolute recovery from both the artificial CSF + rat plasma and spiked human CSF were still lower than desired (<50%). Earlier studies in Chapter 2 and the HPLC index of these peptides led to the suspicion that protein binding was occurring. In addition, the knowledge that A β ₁₋₄₂ aggregates necessitated an especially aggressive approach to eliminating this binding. Therefore, for standard, quality control, and samples in human CSF matrix, a final concentration of 5 M guanidine hydrochloric acid was used as a denaturant to further reduce non-specific interactions between proteins and A β species as well as aggregation, which improved the assay reproducibility. Analyte retention on the SPE sorbent was enhanced by adding 4% H₃PO₄ to the samples prior to loading.

After loading samples onto the SPE plate, varying percentages of acetonitrile were examined as wash solutions to reduce matrix interferences. A 10% acetonitrile (ACN) wash was incorporated to remove matrix interferences without sacrificing amyloid beta peptide recovery. Increasing the wash solution to 20% ACN decreased A β ₁₋₃₈ recovery, being the

least hydrophobic of the amyloid peptides investigated. Optimum A β recovery was obtained using 75% ACN containing 10% NH₄OH as the eluting solution. This provided *both* the elutropic strength and the required solubility to fully elute A β ₁₋₄₂, the least soluble and most hydrophobic of these 3 peptides. Reducing the organic and the basic modifier percentages to 65% ACN and 5% NH₄OH decreased recovery for both A β ₁₋₄₀ and A β ₁₋₄₂. When the organic solvent was increased to 75% ACN with 5% NH₄OH the elutropic strength was sufficient to improve the recovery for A β ₁₋₄₀ but not for A β ₁₋₄₂. The need for 10% base to fully elute A β ₁₋₄₂ may be explained several ways. It is possible that aggregation occurs during SPE processing and a higher concentration of base is able to disrupt aggregation whereas the lower concentration cannot. Alternatively, higher base content may disrupt additional protein binding and/or ionic bonding. SPE extraction efficiency was determined by comparing average areas from a 1 ng/ml mixture of peptides in matrix taken through the described extraction procedure to average area counts from a blank extracted matrix which was then spiked post-extraction at 1 ng/ml. Recovery of A β ₁₋₃₈, A β ₁₋₄₀, A β ₁₋₄₂ standards in artificial CSF without rat plasma were approximately 60%. Recoveries of A β ₁₋₃₈, A β ₁₋₄₀, A β ₁₋₄₂ in artificial CSF containing 5% rat plasma were 94, 92 and 90% and for human CSF (using Guanidine HCl denaturation) were 88, 92, and 80%, respectively. Higher recovery leads to greater confidence in results and improved accuracy due to increased signal to noise.

4.3.2 LC-MS/MS Analysis of A β Peptides

Linear dynamic range and assay precision were determined using A β standard curves prepared in artificial CSF as described and quality control samples spiked into human CSF. The (M+H)⁴⁺ precursor to b⁴⁺-ion fragment transitions of A β ₁₋₃₈, A β ₁₋₄₀, and

A β_{1-42} that were chosen for quantification were based on relative intensity and specificity, with “b” ions being chosen in all cases. Although 5+ precursors were present, the chemical background was significantly lower when the 4+ precursors were used (see Figure 2.14). Therefore transitions based on fragmentation of the 4+ precursors were used in this assay. The highest intensity product ion was selected for use as the primary quantitative transition, although other products were also detected (Figures 4.2-4.4), namely a series of b sequence ions including b31 through b40, corresponding to sequential cleavage of amino acids from the N-terminus.

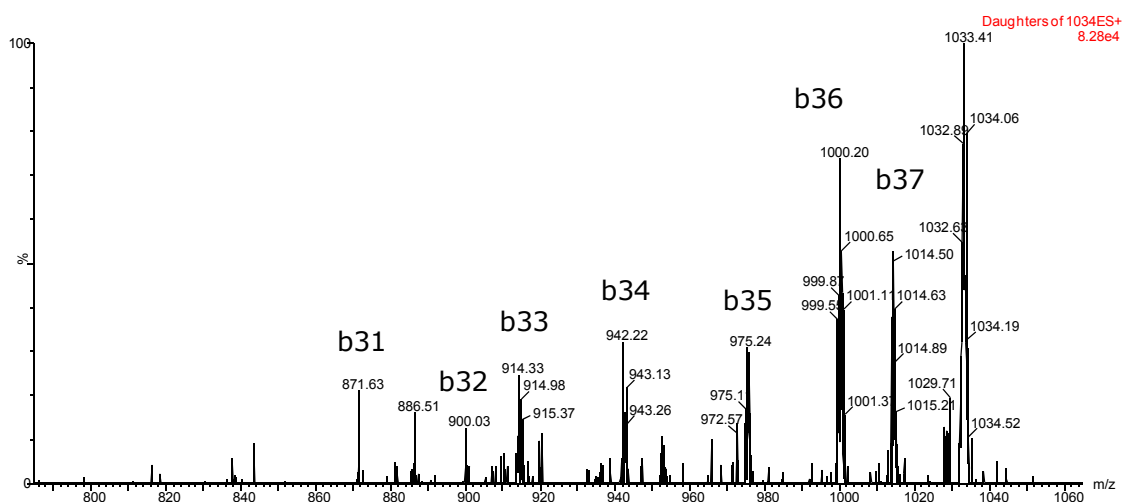


Figure 4.2 ESI+ MSMS spectra for A β_{1-38}

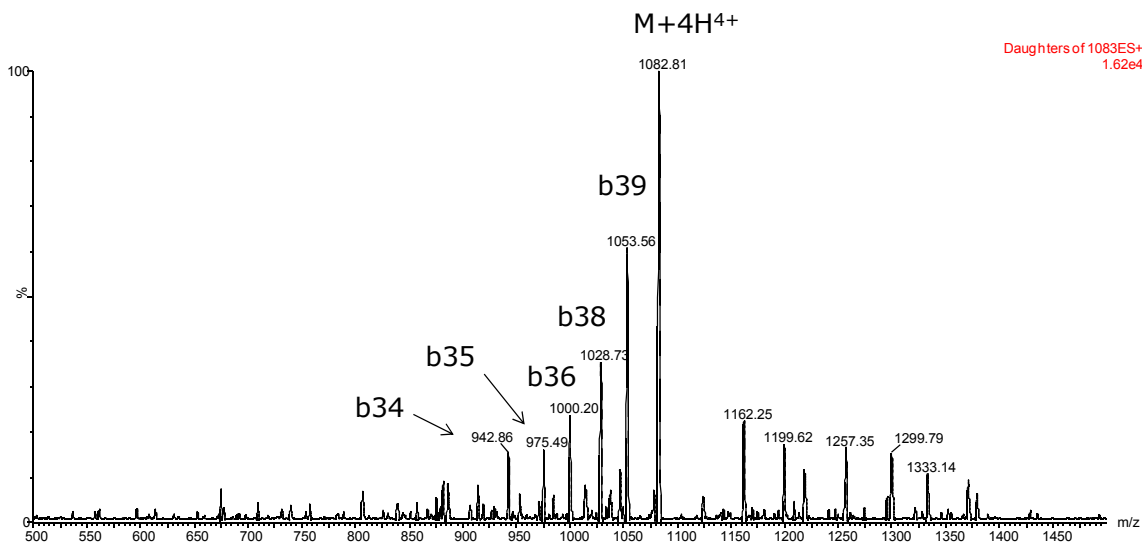


Figure 4.3 ESI+ MSMS spectra for A β ₁₋₄₀

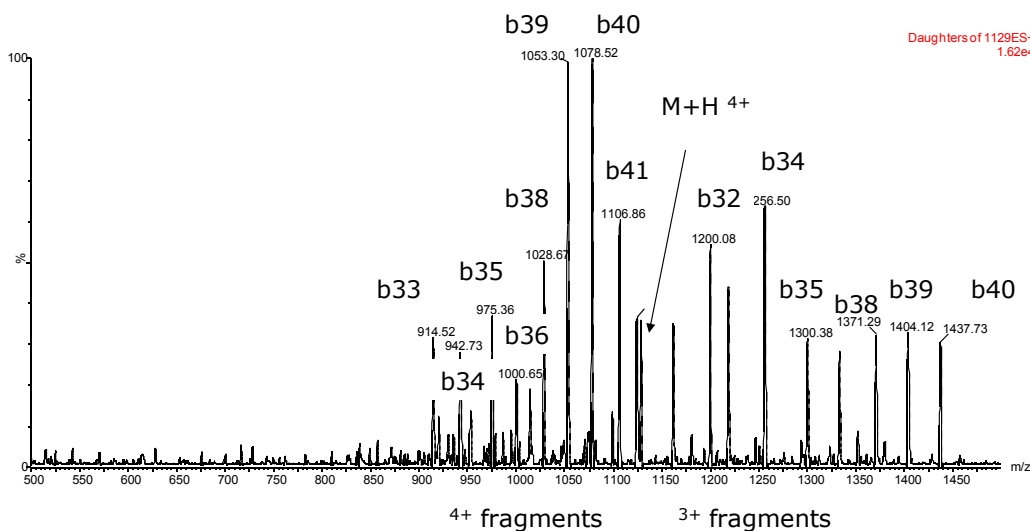


Figure 4.4 ESI+ MSMS spectra for A β ₁₋₄₂

Chromatographic retention times for A β ₁₋₃₈, A β ₁₋₄₀, and A β ₁₋₄₂ were 5.6, 5.85 and 6.03 minutes and the peptides were easily quantified in control CSF (Figure 4.5). Gaussian peaks were obtained and peak widths were 2-3 seconds wide at base. The amyloid peptides were baseline separated from each other. Peak intensity suffered at lower temperature,

higher flow rate, and/or when a steeper gradient was used. In addition, the use of a 150 mm length column was necessary to remove co-elution with endogenous interferences.

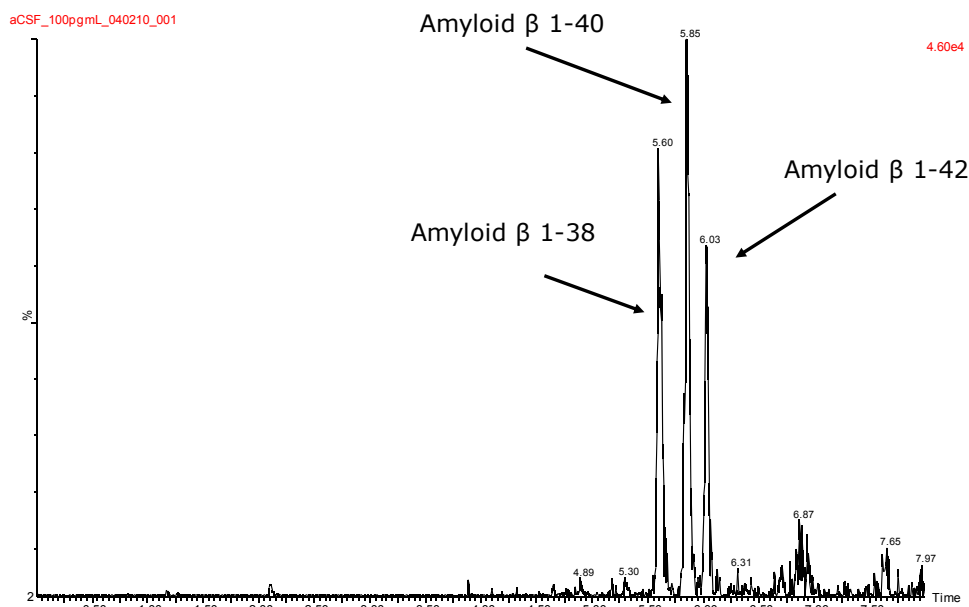


Figure 4.5 Representative chromatographic separation of amyloid beta isoforms 1-38, 1-40, and 1-42

Calibration standards used for quantification of $A\beta_{1-38}$, $A\beta_{1-40}$, and $A\beta_{1-42}$ were from 100 to 10,000 pg/ml. The r^2 values for all curves, for all amyloid peptides were > 0.98 . For standard curves prepared in artificial CSF with rat plasma (Figures 4.6-4.8), the average percent deviation for all standard curve points was 3.8%, 3.2%, and 7.2% for $A\beta_{1-38}$, $A\beta_{1-40}$, and $A\beta_{1-42}$ respectively.

Compound name: 1-38
 Correlation coefficient: $r = 0.996956$, $r^2 = 0.993921$
 Calibration curve: $0.333755 * x + -0.0119724$
 Response type: Internal Std (Ref 2), Area * (IS Conc. / IS Area)
 Curve type: Linear, Origin: Exclude, Weighting: 1/x, Axis trans: None

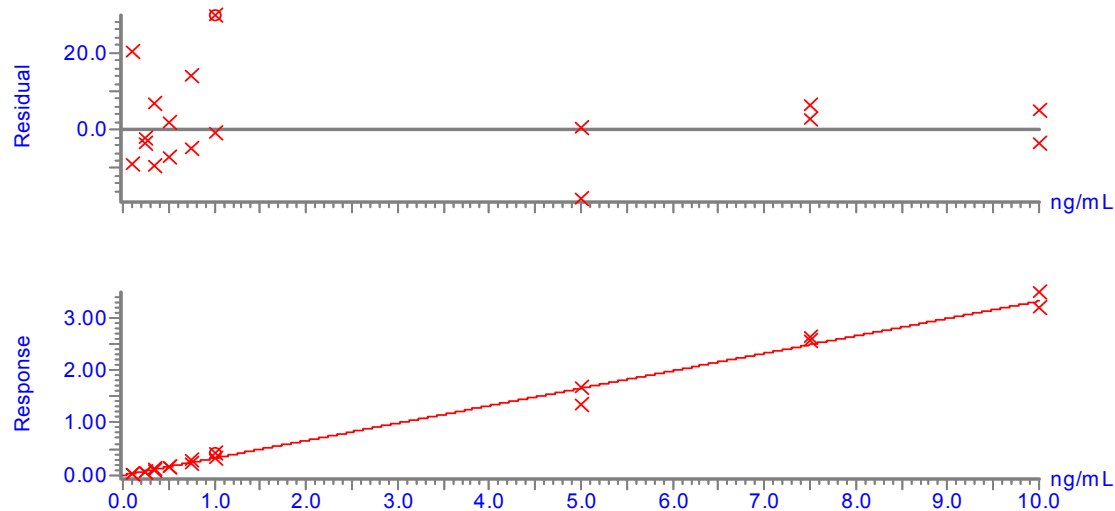


Figure 4.6 Representative standard curve for $A\beta_{1-38}$ extracted from artificial CSF

Compound name: 1-40
 Correlation coefficient: $r = 0.993003$, $r^2 = 0.986055$
 Calibration curve: $0.60165 * x + -0.0184937$
 Response type: Internal Std (Ref 2), Area * (IS Conc. / IS Area)
 Curve type: Linear, Origin: Exclude, Weighting: 1/x, Axis trans: None

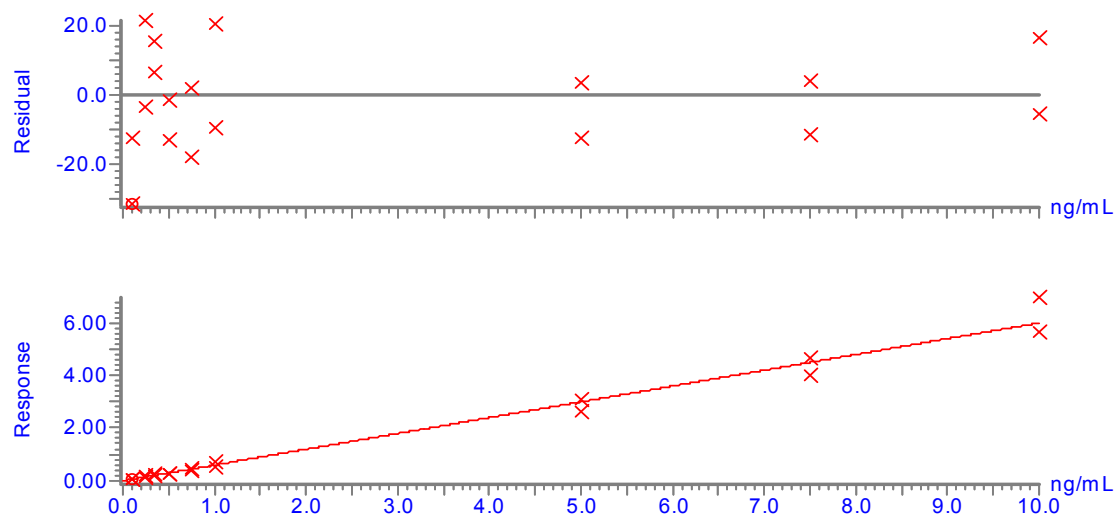


Figure 4.7 Representative standard curve for $A\beta_{1-40}$ extracted from artificial CSF

Compound name: 1-42
 Correlation coefficient: $r = 0.992169$, $r^2 = 0.984360$
 Calibration curve: $0.449201 * x + -0.0167964$
 Response type: Internal Std (Ref2). Area * (18 Conc. /18 Area)
 Curve type: Linear. Origin: Excludes. Weighing: 1/x. Axis trans: None

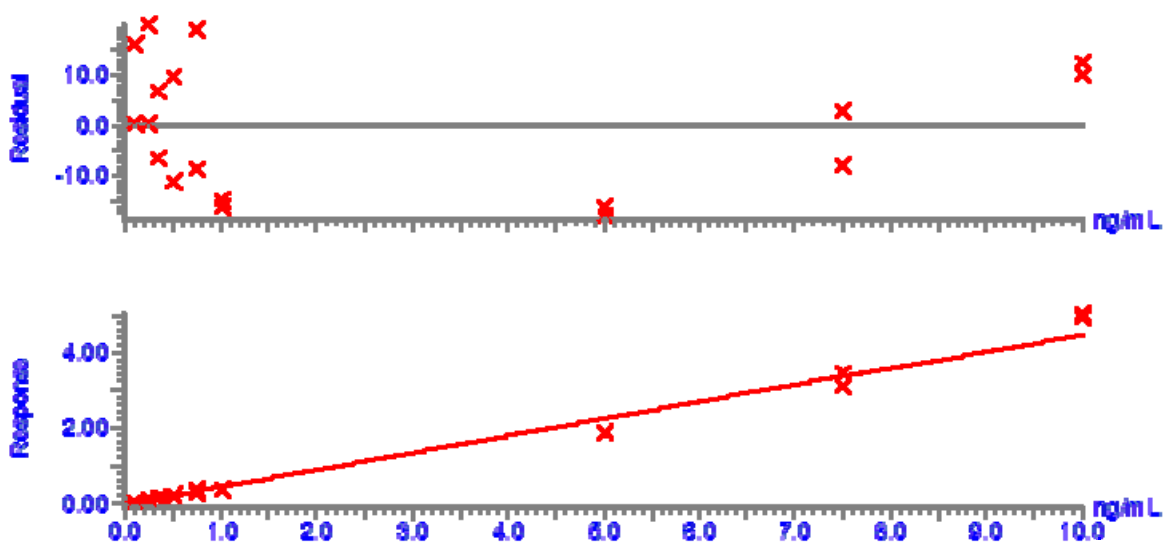


Figure 4.8 Representative standard curve for $A\beta_{1-42}$ extracted from artificial CSF

For standard curves prepared in human CSF, the average % deviation for all standard curve points was 6.1%, 2.2%, and 2.8% for $A\beta_{1-38}$, $A\beta_{1-40}$, and $A\beta_{1-42}$ respectively. To demonstrate parallelism and to confirm that artificial CSF (+ rat plasma) was a suitable surrogate matrix, a comparison of $A\beta_{1-42}$ prepared in artificial vs. human CSF was performed. The data correlated with an r^2 of 0.99 and slope of 1.1 (data for $A\beta_{1-42}$ shown in Figure 4.9); this was also true for the two additional peptides of interest. Artificial CSF was chosen as a surrogate matrix for CSF because of lower cost and higher availability. The parallelism study demonstrated that it did not negatively influence $A\beta$ quantification.

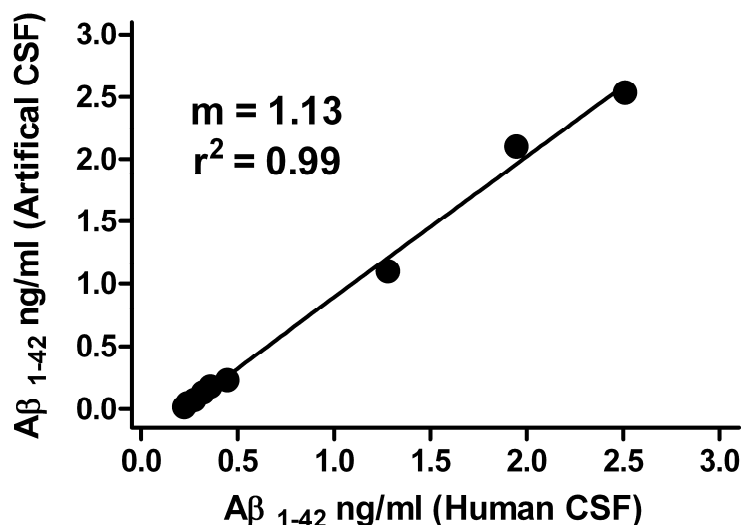


Figure 4.9 Correlation between $A\beta_{1-42}$ concentrations determined using standard curves prepared in either spiked human CSF or artificial CSF + rat plasma carrier protein

During method development, positive ion electrospray MS was compared to negative ion electrospray for CSF extracted $A\beta$ peptides. Although fragmentation in negative ion produces a very intense water loss as shown in Figure 4.10, studies in extracted human CSF highlighted the lack of specificity of such an approach. As evident with the $A\beta_{1-42}$ species, negative ion mode produced a signal 1.6-fold higher than positive but was characterized by significant matrix interferences (Fig 4.11). This was also observed with the other $A\beta$ species of interest. Though plasma was not the matrix of interest for this study, the difference in specificity is even more pronounced, as in the example of $A\beta_{1-40}$ shown in Figure 4.12. Regardless, intensity of positively charged ions was more than sufficient to accurately quantify $A\beta$ species in human CSF.

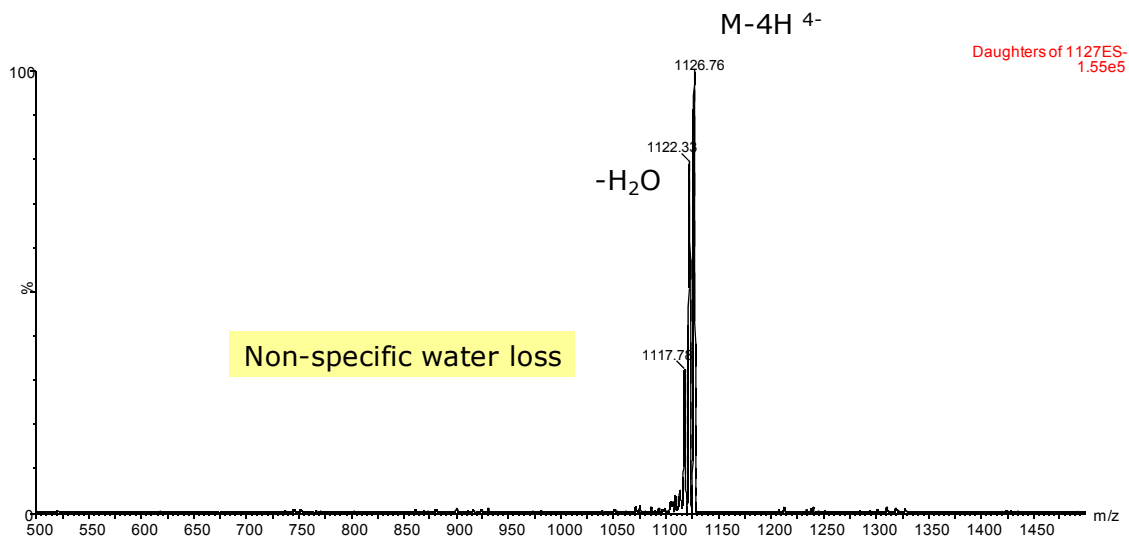


Figure 4.10 ESI- MSMS spectra for $A\beta_{1-42}$

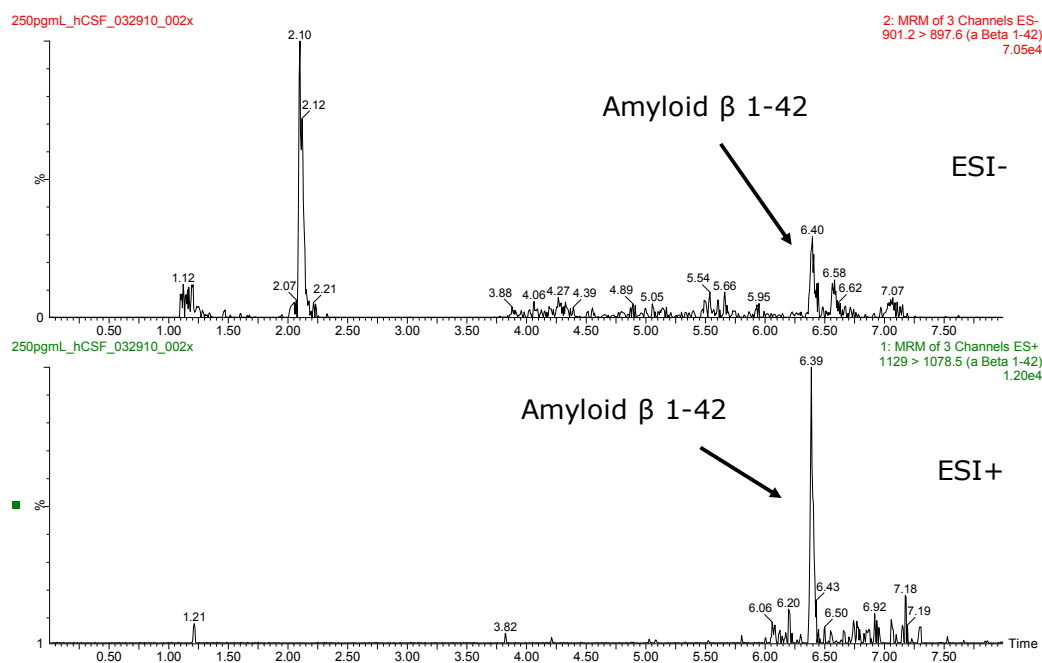


Figure 4.11 Comparison of LC-MS/MS analysis of $A\beta_{1-42}$, extracted from human CSF, using negative ionization (top) and positive ionization (bottom)

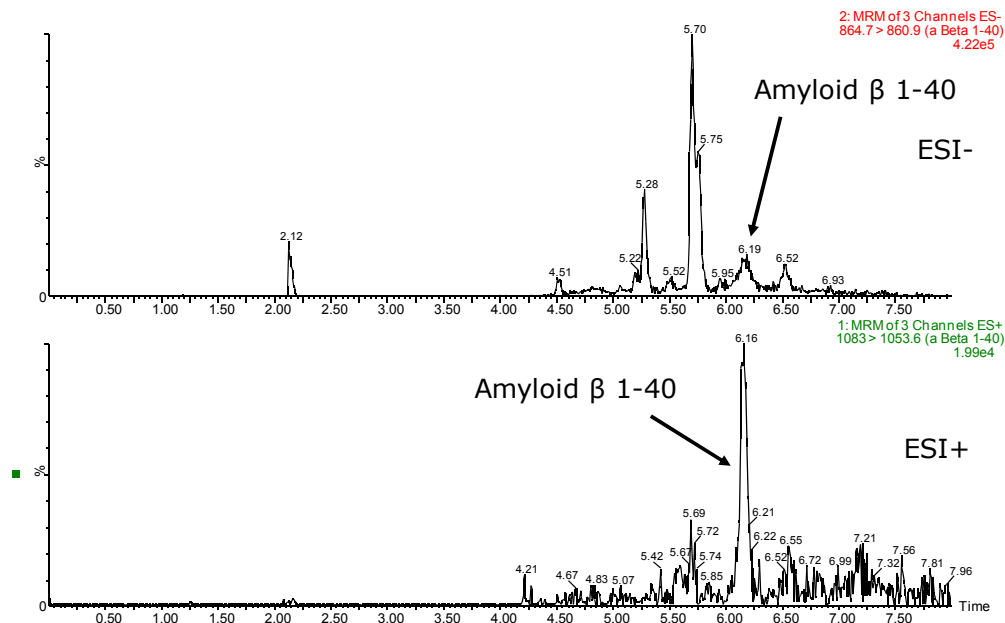


Figure 4.12 Comparison of LC-MS/MS analysis of Aβ₁₋₄₀, extracted from human plasma, using negative ionization (top) and positive ionization (bottom)

Basal levels of Aβ₁₋₃₈, Aβ₁₋₄₀, and Aβ₁₋₄₂ were determined by analyzing six independent extractions from three sources of pooled human CSF and a pooled lot of cynomolgous monkey CSF. These results are summarized in Figure 4.13. Mean basal ng/ml levels of Aβ from 3 human CSF pools were: Aβ₁₋₃₈: 1.64, 2.17 and 1.26; Aβ₁₋₄₀: 3.24, 3.63 and 2.55; Aβ₁₋₄₂: 0.50, 0.63 and 0.46 ng/mL, respectively. Levels for the monkey pool were 1.7, 3.7, and 0.7 ng/mL for Aβ₁₋₃₈, 1-40, and 1-42, respectively. Representative chromatograms of basal levels of Aβ₁₋₄₂ extracted from 3 pooled lots of human CSF and one pooled lot of monkey CSF are shown in Figure 4.14.

Amyloid Beta 1-38

| Replicate # | Human CSF Pool 1 ng/mL | Human CSF Pool 2 ng/mL | Human CSF Pool 3 ng/mL | Cyno CSF Pool 1 ng/mL |
|----------------|---------------------------|---------------------------|---------------------------|--------------------------|
| 1 | 1.58 | 2.35 | 1.01 | 1.71 |
| 2 | 1.65 | 2.10 | 1.37 | 1.61 |
| 3 | 1.61 | 2.46 | 0.95 | 1.95 |
| 4 | 1.66 | 1.94 | 1.61 | 1.54 |
| 5 | 1.82 | 2.16 | 1.47 | 1.68 |
| 6 | 1.49 | 2.00 | 1.17 | 1.64 |
| Mean | 1.64 | 2.17 | 1.26 | 1.69 |
| Std. Deviation | 0.11 | 0.20 | 0.26 | 0.14 |
| % CV | 6.7 | 9.4 | 20.7 | 8.3 |

Amyloid Beta 1-42

| Replicate # | Human CSF Pool 1 ng/mL | Human CSF Pool 2 ng/mL | Human CSF Pool 3 ng/mL | Cyno CSF Pool 1 ng/mL |
|----------------|---------------------------|---------------------------|---------------------------|--------------------------|
| 1 | 0.52 | 0.62 | 0.42 | 0.67 |
| 2 | 0.42 | 0.66 | 0.48 | 0.62 |
| 3 | 0.54 | 0.64 | 0.53 | 0.62 |
| 4 | 0.47 | 0.57 | 0.35 | 0.66 |
| 5 | 0.48 | 0.57 | 0.49 | 0.70 |
| 6 | 0.56 | 0.71 | 0.51 | 0.69 |
| Mean | 0.50 | 0.63 | 0.46 | 0.66 |
| Std. Deviation | 0.05 | 0.05 | 0.07 | 0.03 |
| % CV | 10.4 | 8.7 | 14.7 | 5.1 |

Amyloid Beta 1-40

| Replicate # | Human CSF Pool 1 ng/mL | Human CSF Pool 2 ng/mL | Human CSF Pool 3 ng/mL | Cyno CSF Pool 1 ng/mL |
|----------------|---------------------------|---------------------------|---------------------------|--------------------------|
| 1 | 3.08 | 4.03 | 2.54 | 3.70 |
| 2 | 3.39 | 3.78 | 2.59 | 3.99 |
| 3 | 3.29 | 3.60 | 2.58 | 3.52 |
| 4 | 2.88 | 3.53 | 2.61 | 3.96 |
| 5 | 3.13 | 3.23 | 2.51 | 3.28 |
| 6 | 3.66 | 3.62 | 2.49 | 3.59 |
| Mean | 3.24 | 3.63 | 2.55 | 3.67 |
| Std. Deviation | 0.27 | 0.27 | 0.05 | 0.27 |
| % CV | 8.3 | 7.3 | 1.9 | 7.3 |

Figure 4.13 Summary of basal levels of A β ₁₋₃₈, A β ₁₋₄₀, and A β ₁₋₄₂ extracted from three lots of pooled human CSF and a single lot of pooled monkey CSF.

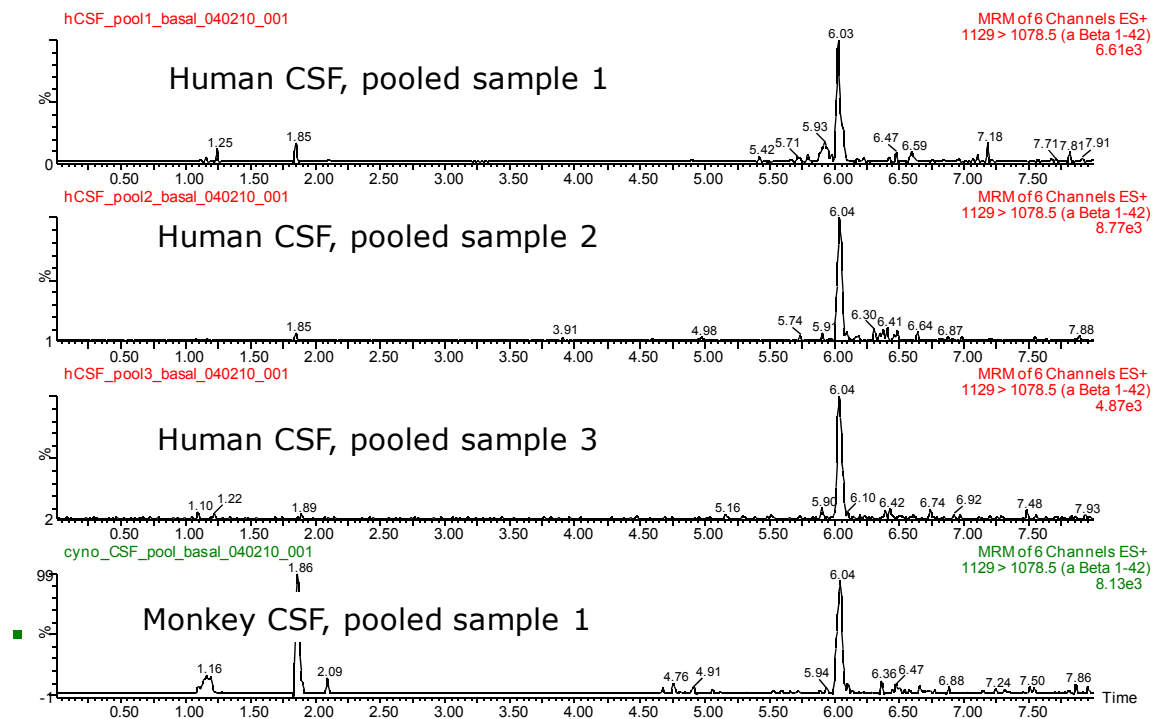


Figure 4.14 Representative chromatogram of A β ₁₋₄₂ extracted from 3 pooled lots of human CSF and one pooled lot of monkey CSF

A β peptide concentrations were significantly different ($p < 0.05$) using a t-test comparison for the 3 pooled CSF sources except for CSF pool one and three in the A β ₁₋₃₈ and A β ₁₋₄₂ fractions. This demonstrated some variability in commercial sources of CSF that are representative of the normal population. The coefficient of variation (CV) was less than 20% for all replicates within the pooled CSF sources.

Quality control samples prepared in human CSF matrix were used to assess intra-sample precision and reproducibility. QC samples were prepared in triplicate in the three separate human CSF pools and one monkey pool, as previously described, at 0.2, 0.8, 2, and 6 ng/ml. The concentrations were determined by subtracting average basal levels from the

CSF source to provide the corresponding QC level and are represented in Tables 4.2A through 4.2D.

| Amyloid β 1-38 | | | | | | |
|---------------------------|----------|-----------------------------|-------------------|------|-----------------------------------|------------------|
| Over-spike Conc. ng/mL | QC Conc. | Mean Calculated Conc. | Std. Deviation | % CV | Number of Replicates Passed | Mean Accuracy |
| 0.2 | 1.88 | 2.00 | 0.13 | 6 | 2/3 | 106.6 |
| 0.8 | 2.48 | 2.40 | 0.20 | 8 | 3/3 | 96.9 |
| 2 | 3.68 | 3.59 | 0.09 | 2 | 3/3 | 97.7 |
| 6 | 7.68 | 7.43 | 0.63 | 8 | 3/3 | 96.7 |
| Amyloid β 1-40 | | | | | | |
| Over-spike Conc. ng/mL | QC Conc. | Mean Calculated Conc. | Std. Deviation | % CV | Number of Replicates Passed | Mean Accuracy |
| 0.2 | 3.44 | 3.29 | 0.25 | 8 | 3/3 | 95.7 |
| 0.8 | 4.04 | 3.61 | 0.25 | 7 | 3/3 | 89.3 |
| 2 | 5.24 | 4.70 | 0.39 | 8 | 2/3 | 89.8 |
| 6 | 9.24 | 8.84 | 0.33 | 4 | 3/3 | 95.6 |
| Amyloid β 1-42 | | | | | | |
| Over-spike Conc. ng/mL | QC Conc. | Mean Calculated Conc. | Std. Deviation | % CV | Number of Replicates Passed | Mean Accuracy |
| 0.2 | 0.698 | 0.71 | 0.06 | 8 | 3/3 | 101.3 |
| 0.8 | 1.298 | 1.26 | 0.18 | 15 | 2/3 | 97 |
| 2 | 2.498 | 2.35 | 0.17 | 7 | 2/3 | 94 |
| 6 | 6.498 | 5.53 | 0.18 | 3 | 2/3 | 85 |

Table 4.2A Summary of QC statistics for A β peptides in human CSF pool 1

| Amyloid β 1-38 | | | | | | |
|------------------------|----------|-----------------------|----------------|------|-----------------------------|---------------|
| Over-spike Conc. ng/mL | QC Conc. | Mean Calculated Conc. | Std. Deviation | % CV | Number of Replicates Passed | Mean Accuracy |
| 0.2 | 2.41 | 2.29 | 0.21 | 9 | 3/3 | 96.7 |
| 0.8 | 3.01 | 2.69 | 0.24 | 9 | 2/3 | 89.3 |
| 2 | 4.21 | 3.92 | 0.10 | 3 | 3/3 | 93.2 |
| 6 | 8.21 | 7.52 | 0.44 | 6 | 3/3 | 91.6 |
| Amyloid β 1-40 | | | | | | |
| Over-spike Conc. ng/mL | QC Conc. | Mean Calculated Conc. | Std. Deviation | % CV | Number of Replicates Passed | Mean Accuracy |
| 0.2 | 3.83 | 3.72 | 0.15 | 4 | 3/3 | 98.5 |
| 0.8 | 4.43 | 4.24 | 0.01 | 0 | 3/3 | 95.7 |
| 2 | 5.63 | 4.98 | 0.29 | 6 | 3/3 | 88.4 |
| 6 | 9.63 | 8.42 | 0.29 | 3 | 2/3 | 87.4 |
| Amyloid β 1-42 | | | | | | |
| Over-spike Conc. ng/mL | QC Conc. | Mean Calculated Conc. | Std. Deviation | % CV | Number of Replicates Passed | Mean Accuracy |
| 0.2 | 0.828 | 0.86 | 0.08 | 9 | 3/3 | 103.8 |
| 0.8 | 1.428 | 1.32 | 0.12 | 9 | 3/3 | 92.4 |
| 2 | 2.628 | 2.28 | 0.30 | 13 | 2/3 | 90 |
| 6 | 6.628 | 5.64 | 0.15 | 3 | 2/3 | 85.2 |

Table 4.2B Summary of QC statistics for A β peptides in human CSF pool 2

| Amyloid β 1-38 | | | | | | |
|------------------------|----------|-----------------------|----------------|------|-----------------------------|---------------|
| Over-spike Conc. ng/mL | QC Conc. | Mean Calculated Conc. | Std. Deviation | % CV | Number of Replicates Passed | Mean Accuracy |
| 0.2 | 1.49 | 1.36 | 0.07 | 5 | 3/3 | 90.9 |
| 0.8 | 2.09 | 1.84 | 0.12 | 6 | 3/3 | 88.2 |
| 2 | 3.29 | 3.29 | 0.32 | 10 | 3/3 | 99.9 |
| 6 | 7.29 | 7.70 | 0.48 | 6 | 3/3 | 105.6 |
| Amyloid β 1-40 | | | | | | |
| Over-spike Conc. ng/mL | QC Conc. | Mean Calculated Conc. | Std. Deviation | % CV | Number of Replicates Passed | Mean Accuracy |
| 0.2 | 2.75 | 2.36 | 0.02 | 1 | 2/3 | 85.8 |
| 0.8 | 3.35 | 3.05 | 0.02 | 1 | 2/3 | 91.2 |
| 2 | 4.55 | 3.93 | 0.01 | 0 | 3/3 | 86.4 |
| 6 | 8.55 | 8.21 | 0.50 | 6 | 3/3 | 96.0 |
| Amyloid β 1-42 | | | | | | |
| Over-spike Conc. ng/mL | QC Conc. | Mean Calculated Conc. | Std. Deviation | % CV | Number of Replicates Passed | Mean Accuracy |
| 0.2 | 0.66 | 0.66 | 0.07 | 11 | 3/3 | 98.8 |
| 0.8 | 1.26 | 1.15 | 0.06 | 5 | 3/3 | 90.7 |
| 2 | 2.46 | 2.40 | 0.12 | 5 | 3/3 | 97.5 |
| 6 | 6.46 | 5.99 | 0.70 | 12 | 3/3 | 92.6 |

Table 4.2C Summary of QC statistics for A β peptides in human CSF pool 3

| Amyloid β 1-38 | | | | | | |
|------------------------|----------|-----------------------|----------------|------|-----------------------------|---------------|
| Over-spike Conc. ng/mL | QC Conc. | Mean Calculated Conc. | Std. Deviation | % CV | Number of Replicates Passed | Mean Accuracy |
| 0.2 | 1.92 | 1.95 | 0.04 | 2 | 3/3 | 101.6 |
| 0.8 | 2.52 | 2.56 | 0.30 | 12 | 3/3 | 101.4 |
| 2 | 3.72 | 3.69 | 0.43 | 12 | 3/3 | 99.2 |
| 6 | 7.72 | 7.35 | 0.25 | 3 | 3/3 | 95.3 |
| Amyloid β 1-40 | | | | | | |
| Over-spike Conc. ng/mL | QC Conc. | Mean Calculated Conc. | Std. Deviation | % CV | Number of Replicates Passed | Mean Accuracy |
| 0.2 | 3.87 | 3.73 | 0.24 | 6 | 3/3 | 96.3 |
| 0.8 | 4.47 | 4.15 | 0.17 | 4 | 3/3 | 92.8 |
| 2 | 5.67 | 4.94 | 0.23 | 5 | 3/3 | 87.1 |
| 6 | 9.67 | 8.34 | 0.12 | 1 | 3/3 | 86.2 |
| Amyloid β 1-42 | | | | | | |
| Over-spike Conc. ng/mL | QC Conc. | Mean Calculated Conc. | Std. Deviation | % CV | Number of Replicates Passed | Mean Accuracy |
| 0.2 | 0.861 | 0.81 | 0.06 | 7 | 2/3 | 93.7 |
| 0.8 | 1.461 | 1.38 | 0.14 | 10 | 3/3 | 94.6 |
| 2 | 2.661 | 2.36 | 0.14 | 6 | 2/3 | 88.7 |
| 6 | 6.661 | 5.89 | 0.05 | 1 | 2/3 | 88.5 |

Table 4.2D Summary of QC statistics for A β peptides in cynomolgous monkey CSF pool 1

Mean accuracy values for A β ₁₋₃₈, A β ₁₋₄₀, and A β ₁₋₄₂ in all three pooled human CSF sources were within 15% of expected values demonstrating high method precision and accuracy. As is typical for endogenous compounds, determination of the LLOQs for each analyte is based on the lowest concentration that can be accurately and precisely quantified. In this particular case, the LLOQs in human CSF were better than or equal to 0.1 ng/ml, based on the lowest point in the standard curve.

4.4 Discussion

Interest in quantifying peptides and proteins to help elucidate biological processes in disease and during therapeutic programs has increased steadily over the past decade. This current work was precipitated by the need for a high-throughput and cost effective assay that could accurately and reproducibly quantify A β peptides in the CSF of human donors. Current quantitative assessments of A β species in biological fluids have relied heavily on immunological methods such as Western blots and ELISA. However, these assays require highly specific antibodies and reagents that can result in assays with limited dynamic ranges, various matrix interferences and dilution linearity problems[34]. Non-commercial immunoassays are especially subject to high intra- and inter-assay variability since they are not subject to more stringent manufacturing controls. Combinations of these factors make immunoassays more labour intensive and often challenging to validate in support of clinical studies. The assay described here utilized an SPE and UPLC-MS/MS workflow. Recent advances in SPE mixed-mode sorbents have facilitated improvements in assay selectivity and analyte recovery and this has been helped by the fact that mass spectrometry platforms have improved significantly in recent years. Not only does LC-MS give a higher throughput than ELISA based methods, the ability to simultaneously quantify a heterogeneous population of A β species by mass spectrometry is advantageous because it reduces the sample requirements associated with running duplicate ELISA assays, minimizes reagent consumption and in this case is more economical. Furthermore, the greater accuracy and precision of LC-MS/MS methods relative to affinity-based methods should allow for more definitive differentiation of subtle changes between normal and AD populations. Immunoprecipitation liquid chromatography mass spectrometry (IP-LC/MS) is another

popular enrichment method, which also relies on antibodies[35]. Based on this work, antibody enrichment or immunochemical assays are not necessary to accurately quantify $A\beta_{1-38}$, $A\beta_{1-40}$, and $A\beta_{1-42}$ in human CSF.

Selectively lowering or enhancing the clearance of $A\beta$ peptides has emerged as a therapeutic strategy for the treatment of Alzheimer's [36]. The diagnostic power of $A\beta$ peptides as well as other Alzheimer's biomarkers depends on the pre-analytical handling of the CSF sample, the assay platform and the test group[37]. Goda et al. describe sample pretreatments with acetic acid to minimize non-specific interactions of $A\beta$ peptides with surfaces and proteins but their recovery was 80% or less [38, 39]. As $A\beta$ species have a propensity for aggregation, poor solubility and also nonspecifically bind to proteins / surfaces, the CSF samples were pre-treated with a denaturant and phosphoric acid to minimize enzyme activities, non-specific protein interactions as well as to induce charge prior to SPE. Using this methodology the recovery was approximately 90% for the three $A\beta$ species investigated. The key to obtaining high recovery was attributed to meticulously altering and optimizing the elutropic composition and ion-pair strength of SPE solvents until the optimal combination (75% ACN/10% NH_4OH) was established, delivering the best recovery. Proteins, salts and other endogenous components within CSF typically interfere with quantification in both immuno-based and MS-based assays, thus requiring highly selective sample preparation. Mixed-mode SPE was chosen for this application primarily due to the selectivity benefit derived from dual, orthogonal retention mechanisms on a sorbent which has both reversed-phase and ion-exchange properties. While high $A\beta$ recovery was achieved, it is not entirely clear if this methodology incorporates only free $A\beta$ or total free $A\beta$; since total free $A\beta$ includes species bound to proteins. As the analyte

recovery is high (>90%) and QC samples are within acceptable coefficients of variation, it is believed that the assay is quantifying total and free A β , but this was not examined further.

Recent advancements in mass spectrometry technologies, both in sensitivity and capability, have allowed deeper large- biomolecule investigation and facilitated the development of more robust LC-MS methodologies for their quantification. While LC-MS is an appealing platform for quantifying A β peptides, it is not without challenges. A β peptides have an isoelectric point of ~ 5.2 , are large and contain various acidic, neutral and basic amino acid residues. A β peptides can ionize negatively or positively during electrospray and produce multiply charged species. During flow injection optimization with standards in negative ion mode, the major observed mass transition from fragmentation of A β was loss of water. While negative ion mode produces an intense transition ion, it does not produce the additional ions needed for assay selectivity when working in complex matrices. In contrast the positive-ion mode electrospray MS fragmentation ions produced an abundance of b- and y-ions but overall intensity was lower than negative ion MS. Others noted similar observations; positive ion electrospray was selective for A β analysis in matrix, but collision cell fragmentation resulted in an overall loss of sensitivity due to mass-charge issues and fragmentation signal dilution[30, 35, 40].

Dillen et al. recently reported a negative ion mode assay with similar sensitivity to the described method. However, their coefficient of variation for low QC's was approximately 40% using an MS system with limited scanning capabilities[40]. The MS platform used in this work allowed the simultaneous detection and quantification of three A β species and their internal standards without sacrificing accuracy or precision. Dillen et al. also described challenges associated with choosing an appropriate surrogate matrix and

reported that artificial CSF might not be a good substitute. Matrix interferences and recovery problems were also observed in this study when working in artificial CSF, but the addition of 5% rat plasma improved detection and reproducibility and increased recovery to 90% or greater. Reduced SPE recovery in artificial CSF without carrier protein is most certainly due to the hydrophobic nature of A β peptides and their propensity to stick to surfaces especially in aqueous solution. In addition, this work takes advantage of highly selective sample preparation based on mixed-mode SPE and the added specificity obtained using positive ion MS to enable the use of artificial CSF as a surrogate matrix. A surrogate matrix for A β quantification is ideal because it is cost effective, more readily available than CSF and does not require data manipulation such as standard addition or background subtraction for absolute quantification experiments.

An accumulation of reports put together by Bates et al highlight published A β_{1-42} peptide concentrations in the CSF healthy and AD human donors[27]. The A β_{1-42} range in healthy subjects is reported as 75 - 2000 pg/ml. The large discrepancy in A β_{1-42} concentrations is also apparent within the AD population (100-2000 pg/ml). When these studies are viewed as a whole, it does not appear that control A β_{1-42} is significantly different than AD groups since the reported range of A β_{1-42} levels are so vast in CSF. However within a test group of control vs. AD patients, A β_{1-42} is significantly different[41, 42]. Since published concentrations of A β_{1-42} and other A β peptide species are routinely analyzed or enriched by immuno-assays, reported A β concentrations are subject to assays with high coefficient of variation leading to misrepresentation of A β levels. In the LC-MS based experiments described herein, relative A β peptide levels trended similarly between pooled CSF lots, but significant differences in A β peptide levels between CSF lots were observed.

This observation is interesting because it shows high heterogeneity in pooled CSF lots, similar to that reported by other groups. However, one might expect less A β variability between population groups using this described method as it has a tight coefficient of variation (< 15%) that cannot be duplicated with ELISA which can be 25% or greater.

Although this work pertains to quantification of A β ₁₋₃₈, A β ₁₋₄₀, and A β ₁₋₄₂ in human CSF, a similar approach could be used for smaller human A β peptides or nonhuman primate[43]. Rat A β could also be measured but masses and fragmentation patterns will need consideration[44].

More recently, efforts have focused on extending application of this work to take advantage of a more sensitive MS platform to improve detection limits and reduce required sample size. By replacing the original MS platform (Xevo TQ MS) with a more sensitive “next generation model” (Xevo TQ-S) triple quadrupole mass spectrometer the preliminary data showed a 5-fold improvement in detection limits using four-times less sample (50 μ l instead of 200 μ l.) Using 50 μ l aliquots, QC samples were successfully quantified down to 40 pg/mL, with CVs less than 5%. A summary of QC and standard curve statistics using 50 μ l of sample and the newer MS system are compiled in Tables 4.3 and 4.4.

| | QC 0.04 ng/mL | QC 0.075 ng/mL | QC 0.15 ng/mL | QC 0.2 ng/mL | QC 0.8ng/mL | QC 2 ng/mL | QC 6 ng/mL |
|---|------------------|-------------------|------------------|-----------------|----------------|---------------|---------------|
| Amyloid β 1-38 Human CSF 1 and 2 | 2.3 | 5.8 | -3.2 | 7.3 | 14.8 | 5.1 | 13.1 |
| Amyloid β 1-40 Human CSF 1 and 2 | -0.8 | -3.2 | -1.9 | 2.5 | -2.6 | -4.2 | -3.8 |
| Amyloid β 1-42 Human CSF 1 and 2 | 1.3 | 13.4 | -3.6 | 5.6 | 2.0 | -0.6 | -0.2 |

Table 4.3 Average QC values for A β peptides extracted from 50 μ L human plasma (N=3 in each of two pooled lots) and detected using a Waters Xevo TQ-S MS

| Name | Type | Std. Conc | RT | Area | IS Area | Response | Conc. | %Dev |
|--------------------------|----------|-----------|------|---------|---------|----------|-------|------|
| blank artificial CSF | | | 5.73 | 19.7 | 7.0 | | | |
| 50 pg/mL artificial CSF | Standard | 0.05 | 5.71 | 230.4 | 3620.5 | 0.06 | 0.06 | 14 |
| 100 pg/mL artificial CSF | Standard | 0.1 | 5.71 | 390.8 | 3585.1 | 0.11 | 0.11 | 8.1 |
| 250 pg/mL artificial CSF | Standard | 0.25 | 5.71 | 778.3 | 3737.3 | 0.21 | 0.22 | -12 |
| 350 pg/mL artificial CSF | Standard | 0.35 | 5.71 | 1267.3 | 3693.8 | 0.34 | 0.37 | 6.2 |
| 500 pg/mL artificial CSF | Standard | 0.5 | 5.71 | 1494.7 | 3566.8 | 0.42 | 0.46 | -8.5 |
| 750 pg/mL artificial CSF | Standard | 0.75 | 5.71 | 2733.5 | 4152.0 | 0.66 | 0.73 | -3.1 |
| 1 ng/mL artificial CSF | Standard | 1 | 5.71 | 3166.8 | 3792.5 | 0.84 | 0.93 | -7.4 |
| 5 ng/mL artificial CSF | Standard | 5 | 5.72 | 14773.9 | 3148.3 | 4.69 | 5.27 | 5.4 |
| 7.5 ng/mL artificial CSF | Standard | 7.5 | 5.72 | 24576.9 | 3877.0 | 6.34 | 7.12 | -5 |
| 10 ng/mL artificial CSF | Standard | 10 | 5.72 | 33343.3 | 3662.5 | 9.10 | 10.24 | 2.4 |

Table 4.4 Representative standard curve statistics for A β ₁₋₄₂ from 50 to 10,000 pg/mL extracted from 50 μ L artificial CSF

4.5 Additional Investigations in Support of Candidate Reference Method Development and Progression

As described in the introduction to this chapter, since the completion and initial publication of this work in 2011, a collaboration between the Alzheimer's Association (AA) and the Global Biomarker Standardization Committee (GBSC) was created in order to develop and progress a candidate reference method for quantification of A β ₁₋₄₂ using LC/MS. The assay developed here was employed to participate in both a round robin and a ring trial study, towards that end. Four labs were expected to partake in the initial round robin study. The aim of which was to have each lab quantify unknowns using their respective versions of the method put forth in this research. The results of this round robin have been submitted as a short communication to the Journal of Alzheimer's and Dementia. Although all labs employed the extraction scheme described in this chapter and largely the LC and MS conditions, there were some slight variations amongst the labs, primarily the nature of the surrogate matrix and the use of 1D versus 2D chromatography. This led to a separate study in our labs aimed at comparing the assay variables and summarizing the

results. This allows the evaluation of the intra-lab variability of these differences relative to the inter-lab variability of the same.

To investigate the influence of surrogate matrix, three different surrogates will be compared to standard addition using human CSF. The three surrogates are as follows: artificial CSF + 5% rat plasma by volume, (the original surrogate, deemed matrix 1), artificial CSF + 4 mg/mL BSA (roughly equivalent protein content in a 5% by volume plasma solution, deemed matrix 2) and a homemade artificial CSF salt solution (containing NaCl, KCl, CaCl₂, MgCl₂, Na₂HPO₄, and NaH₂PO₄) containing 4 mg/mL human serum albumin, 0.05 mg/mL IgG, and 0.8 mg/mL glucose (deemed matrix 3). The latter matrix attempts to mimic human CSF with the addition of appropriate proteins and sugar. Human CSF will be referred to as matrix 4. Standard curves were prepared in each of the four matrices as detailed in the experimental section of this chapter, and used to quantify basal levels of the three A β peptides in normal, non-diseased pooled human CSF. In addition, quantification using the four matrices was carried out on two LC/MS platforms: the standard 1D platform described in the experimental section and a multidimensional platform (referred to as “2D”) which includes at-column-dilution (ACD) and a trap and back elute component. ACD enables the injection of a larger volume than our initial work. Trapping of the peptides is achieved with a 2.1 X 20mm XBridge C18 column. As this trapping configuration does not provide orthogonality, but simply re-focusing capability, significant additional clean-up is not expected, though a modest degree may occur. (A more detailed description and schematics of the analytical configuration can be found in Chapter 5 where this platform provides significant benefits to the quantification of intact insulins in human plasma). A summary of the results from this investigation is presented in Table 4.5. A

representative chromatogram of a 50 pg/mL sample analyzed on an LC/MS system equipped with either a 1D or 2D ACQUITY UPLC is shown in Figure 4.15.

Baseline Concentrations (ng/mL) of Abeta 1-42 in Normal Pooled Human CSF (BioChemed)

| | 2D | 2D | 2D | 2D | 1D | 1D | 1D | 1D |
|----------|---------|---------|---------|---------|---------|---------|---------|---------|
| | Matrix1 | Matrix2 | Matrix3 | Matrix4 | Matrix1 | Matrix2 | Matrix3 | Matrix4 |
| Analyst1 | 0.42 | 0.41 | 0.45 | 0.41 | 0.45 | 0.43 | 0.47 | 0.47 |
| | 0.39 | 0.38 | 0.41 | 0.40 | 0.45 | 0.43 | 0.47 | 0.43 |
| Analyst2 | 0.40 | 0.39 | 0.43 | 0.39 | 0.43 | 0.42 | 0.45 | 0.41 |
| | 0.39 | 0.39 | 0.42 | 0.38 | 0.45 | 0.43 | 0.47 | 0.43 |
| | | | | | | | | |
| Average | 0.42 | | | | | | | |
| Std Dev | 0.03 | | | | | | | |
| CV | 6.19 | | | | | | | |

%CV by Variable

| | 2D | 1D | Matrix 1 | Matrix 2 | Matrix 3 | Matrix 4 |
|------|-----|-----|----------|----------|----------|----------|
| % CV | 4.5 | 4.0 | 5.8 | 5.4 | 5.0 | 6.3 |

Table 4.5 Summary of basal A β ₁₋₄₂ levels in human CSF, as determined from standard curves prepared in four different matrices (three surrogates compared to human CSF) and analyzed on LC/MS platforms utilizing either a 1D or a 2D LC system

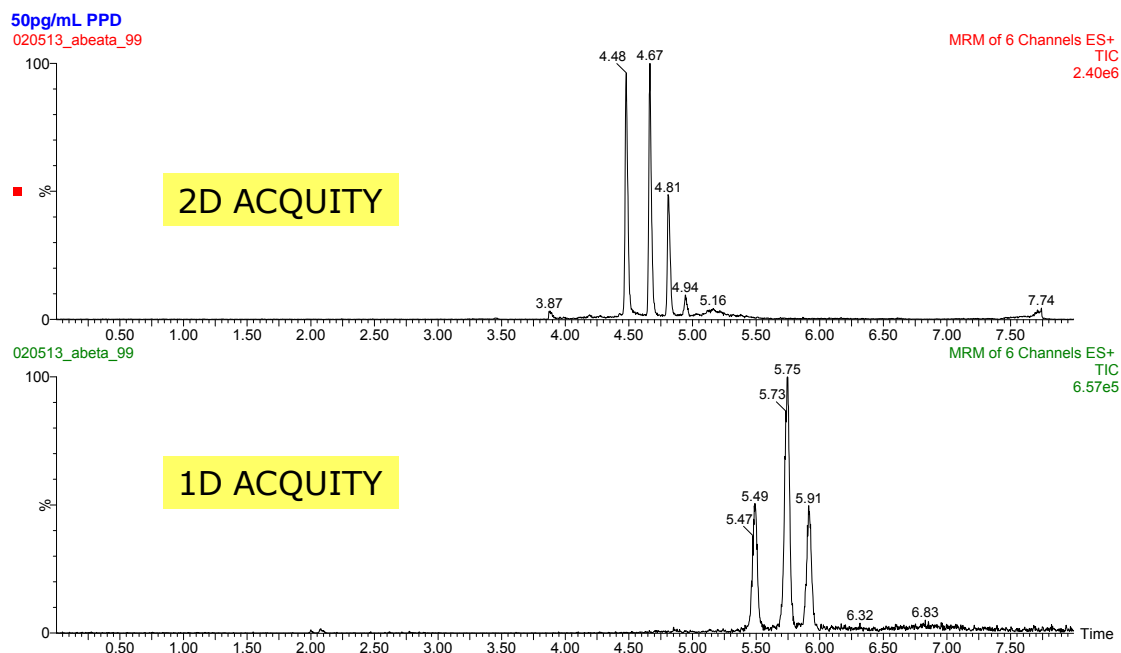


Figure 4.15 Comparison of 50 pg/mL A β peptides separated using either a 1D or 2D ACQUITY UPLC system; 30 μ L of sample are injected in the 2D system and 15 μ L on the 1D system

The data clearly validate the use of any one of the three possible surrogate matrices or standard addition using human CSF for quantification of A β ₁₋₄₂, on either a 1D or 2D LC platform. The overall CV of the measurements, incorporating all variables, is only 6%, indicating that highly precise and consistent measurement is achieved regardless of standard curve matrix or analytical platform. The precision within the measurements, by independent variable, is also excellent, averaging 4-6%. The primary benefit of the multi-dimensional LC system is to enable the injection of larger volumes of extract without breakthrough. The final injection solvent for amyloid peptides, using the extraction scheme outlined in the experimental section, contains approximately 37.5% organic and 5% ammonium hydroxide. During initial method development, it was discovered that it was not possible to inject more than 10-15 μ L of extract without substantial breakthrough on the standard 1D configuration.

Use of ACD and subsequent focusing on the trap column facilitated injections of $>45\ \mu\text{L}$, resulting in significant sensitivity improvements. This cursory examination of the benefits of multi-dimensional chromatography warrant a more thorough study of its value in peptide quantification and therefore are examined in greater detail in the subsequent chapter of this thesis.

4.6 Conclusions

In spite of the acknowledged obstacles to high sensitivity, the highly selective measurement of $\text{A}\beta$ peptides was achieved using LC-MS without affinity-based purification.

The methodology described above allowed the simultaneous quantification of multiple $\text{A}\beta$ species in CSF. This LC-MS/MS assay approaches the sensitivity of ELISA or IP LC-MS/MS methods, but is higher throughput and more cost effective. Quantification of multiple $\text{A}\beta$ species in pooled CSF from a heterogeneous control population was possible with this method using mixed-mode solid-phase extraction, sub-2 micron particle column technology and positive ion MRM to achieve an accurate, precise and quantitative assay that can be validated to support studies in large cohorts of clinical samples. As new strategies emerge for AD treatment, accurate and reproducible quantification of known and unknown $\text{A}\beta$ species will play a crucial role in understanding amyloid disease progression and intervention. The method described herein shows promise for adaptation to quantify additional $\text{A}\beta$ peptides as well.

4.7 References

1. Organization, W.H. *Dementia: a Public Health Priority*. in *World Health Organization*. 2012. Geneva.
2. Association, A.s., *Latest Facts and Figures*, 2014.
3. Andreasen, N., et al., *EValuation of csf-tau and csf-a β 42 as diagnostic markers for alzheimer disease in clinical practice*. Archives of Neurology, 2001. 58(3): p. 373-379.
4. Christoffer, R., et al., *Fluid biomarkers in Alzheimer's disease – current concepts*. Molecular Neurodegeneration, 2013. 8(1): p. 20-20.
5. Kang, J.H., et al., *Clinical utility and analytical challenges in measurement of cerebrospinal fluid amyloid-beta(1-42) and tau proteins as Alzheimer disease biomarkers*. Clin Chem, 2013. 59(6): p. 903-16.
6. Kang, J.H., et al., *Simultaneous analysis of cerebrospinal fluid biomarkers using microsphere-based xMAP multiplex technology for early detection of Alzheimer's disease*. Methods, 2012. 56(4): p. 484-93.
7. Pannee, J., et al., *A selected reaction monitoring (SRM)-based method for absolute quantification of Abeta38, Abeta40, and Abeta42 in cerebrospinal fluid of Alzheimer's disease patients and healthy controls*. J Alzheimers Dis, 2013. 33(4): p. 1021-32.
8. Parnetti, L., et al., *Performance of abeta1-40, abeta1-42, total tau, and phosphorylated tau as predictors of dementia in a cohort of patients with mild cognitive impairment*. J Alzheimers Dis, 2012. 29(1): p. 229-38.

9. Mapstone, M., et al., *Plasma phospholipids identify antecedent memory impairment in older adults*. Nature Medicine, 2014. 20: p. 415-418.
10. Hye, A., et al., *Plasma proteins predict conversion to dementia from prodromal disease*. Alzheimer's & Dementia, 2014. July: p. 1-9.
11. Leinenbach, A., et al., *Mass Spectrometry-Based Candidate Reference Measurement Procedure for Quantification of Amyloid-beta in Cerebrospinal Fluid*. Clin Chem, 2014. 60(7): p. 987-94.
12. Mattsson, N., et al., *Reference measurement procedures for Alzheimer's disease cerebrospinal fluid biomarkers: definitions and approaches with focus on amyloid beta42*. Biomark Med, 2012. 6(4): p. 409-17.
13. Andreasson, U., et al., *Multiplexing and multivariate analysis in neurodegeneration*. Methods, 2012. 56(4): p. 464-470.
14. Andreasson, U., et al., *Analytical aspects of molecular Alzheimer's disease biomarkers*. Biomarkers in medicine, 2012. 6(4): p. 377-389.
15. Chen, J., M. Wang, and I.V. Turko, *Quantification of amyloid precursor protein isoforms using quantification concatamer internal standard*. Analytical Chemistry, 2012. 85(1): p. 303-307.
16. Kim, J.S., et al., *Detection and quantification of plasma amyloid-beta by selected reaction monitoring mass spectrometry*. Anal Chim Acta, 2014. 840: p. 1-9.
17. Korecka, M., et al., *Qualification of a surrogate matrix-based absolute quantification method for amyloid-beta(4)(2) in human cerebrospinal fluid using 2D UPLC-tandem mass spectrometry*. J Alzheimers Dis, 2014. 41(2): p. 441-51.

18. Mawuenyega, K.G., et al., *Amyloid-beta isoform metabolism quantitation by stable isotope-labeled kinetics*. Anal Biochem, 2013. 440(1): p. 56-62.
19. Watanabe, K.-i., et al., *A new methodology for simultaneous quantification of total- $A\beta$, $A\beta$ x-38, $A\beta$ x-40, and $A\beta$ x-42 by column-switching LC/MS/MS*. Analytical and bioanalytical chemistry, 2012. 402(6): p. 2033-2042.
20. Glenner, G.G. and C.W. Wong, *Alzheimer's disease: initial report of the purification and characterization of a novel cerebrovascular amyloid protein*. Biochem Biophys Res Commun, 1984. 120(3): p. 885-90.
21. Seubert, P., et al., *Isolation and quantification of soluble Alzheimer's beta-peptide from biological fluids*. Nature, 1992. 359(6393): p. 325-7.
22. Thompson, L.K., *Unraveling the secrets of Alzheimer's beta-amyloid fibrils*. Proc Natl Acad Sci U S A, 2003. 100(2): p. 383-5.
23. Clark, C.M., et al., *Use of florbetapir-PET for imaging beta-amyloid pathology*. JAMA, 2011. 305(3): p. 275-83.
24. Dubois, B., et al., *Research criteria for the diagnosis of Alzheimer's disease: revising the NINCDS-ADRDA criteria*. Lancet Neurol, 2007. 6(8): p. 734-46.
25. Hardy, J. and D.J. Selkoe, *The amyloid hypothesis of Alzheimer's disease: progress and problems on the road to therapeutics*. Science, 2002. 297(5580): p. 353-6.
26. Lemere, C.A., et al., *Alzheimer's disease abeta vaccine reduces central nervous system abeta levels in a non-human primate, the Caribbean vervet*. Am J Pathol, 2004. 165(1): p. 283-97.

27. Bates, K.A., et al., *Clearance mechanisms of Alzheimer's amyloid-beta peptide: implications for therapeutic design and diagnostic tests*. Mol Psychiatry, 2009. 14(5): p. 469-86.
28. Ida, N., et al., *Analysis of heterogeneous A4 peptides in human cerebrospinal fluid and blood by a newly developed sensitive Western blot assay*. J Biol Chem, 1996. 271(37): p. 22908-14.
29. Motter, R., et al., *Reduction of beta-amyloid peptide₄₂ in the cerebrospinal fluid of patients with Alzheimer's disease*. Ann Neurol, 1995. 38(4): p. 643-8.
30. Oe, T., et al., *Quantitative analysis of amyloid beta peptides in cerebrospinal fluid of Alzheimer's disease patients by immunoaffinity purification and stable isotope dilution liquid chromatography/negative electrospray ionization tandem mass spectrometry*. Rapid Commun Mass Spectrom, 2006. 20(24): p. 3723-35.
31. Takeda, S., et al., *Plasma beta-amyloid as potential biomarker of Alzheimer disease: possibility of diagnostic tool for Alzheimer disease*. Mol Biosyst, 2010. 6(10): p. 1760-6.
32. Villemagne, V.L., et al., *Blood-borne amyloid-beta dimer correlates with clinical markers of Alzheimer's disease*. J Neurosci, 2010. 30(18): p. 6315-22.
33. Mawuenyega, K.G., et al., *Decreased clearance of CNS beta-amyloid in Alzheimer's disease*. Science, 2010. 330(6012): p. 1774.
34. Bidlingmaier, M. and C.J. Strasburger, *Growth hormone assays: current methodologies and their limitations*. Pituitary, 2007. 10(2): p. 115-9.

35. Ford, M.J., et al., *Qualitative and quantitative characterization of the amyloid beta peptide (Abeta) population in biological matrices using an immunoprecipitation-LC/MS assay*. J Neurosci Methods, 2008. 168(2): p. 465-74.
36. Findeis, M.A., *The role of amyloid beta peptide 42 in Alzheimer's disease*. Pharmacol Ther, 2007. 116(2): p. 266-86.
37. Welge, V., et al., *Combined CSF tau, p-tau181 and amyloid-beta 38/40/42 for diagnosing Alzheimer's disease*. J Neural Transm, 2009. 116(2): p. 203-12.
38. Goda, R., et al., *Development of a pretreatment method for amyloid beta-protein analysis based on the effect of acetic acid on the dissolution of plasma polypeptides*. Biomed Chromatogr, 2008. 22(11): p. 1279-87.
39. Lanz, T.A. and J.B. Schachter, *Solid-phase extraction enhances detection of beta-amyloid peptides in plasma and enables Abeta quantification following passive immunization with Abeta antibodies*. J Neurosci Methods, 2008. 169(1): p. 16-22.
40. Dillen, L., et al., *A screening UHPLC-MS/MS method for the analysis of amyloid peptides in cerebrospinal fluid of preclinical species*. Bioanalysis, 2011. 3(1): p. 45-55.
41. Lewczuk, P., et al., *Neurochemical diagnosis of Alzheimer's dementia by CSF Abeta42, Abeta42/Abeta40 ratio and total tau*. Neurobiol Aging, 2004. 25(3): p. 273-81.
42. Moonis, M., et al., *Familial Alzheimer disease: decreases in CSF Abeta42 levels precede cognitive decline*. Neurology, 2005. 65(2): p. 323-5.

43. Podlisny, M.B., D.R. Tolan, and D.J. Selkoe, *Homology of the amyloid beta protein precursor in monkey and human supports a primate model for beta amyloidosis in Alzheimer's disease*. Am J Pathol, 1991. 138(6): p. 1423-35.
44. Yamada, T., et al., *Complementary DNA for the mouse homolog of the human amyloid beta protein precursor*. Biochem Biophys Res Commun, 1987. 149(2): p. 665-71.

Chapter 5

Investigation into Intact Insulin Quantification Using Single or Multidimensional Chromatography and Reversed-phase or Mixed-mode SPE

This Chapter is based on the following publications:

Development of a Fast Method for Direct Analysis of Intact Synthetic Insulins in Human Plasma: the Large Peptide Challenge

Erin E. Chambers, Cristina Legido-Quigley, Norman Smith and Kenneth J Fountain

Bioanalysis, 5 (1), 2013, pages 65-81

and

Multidimensional LC-MS/MS Enables Simultaneous Quantification of Intact Human Insulin and Five Recombinant Analogs in Human Plasma

Erin E. Chambers, Kenneth J. Fountain, Norman Smith, Leah Ashraf, Janaka Karalliedde, David Cowan, and Cristina Legido-Quigley

Analytical Chemistry, 86, 2014, pages 694-702

This chapter will be presented in two sections. The first establishes proof of concept for direct quantification of four intact insulins in human plasma. This section describes the fundamental research endeavours aimed at overcoming the challenges of working with large peptides such as insulin and proposes a starting point methodology. The second section builds on the proof of concept work by incorporating multidimensional LC and more specific sample preparation to extend the number of insulins in the assay and to improve assay sensitivity and specificity. The second section also presents results from a blind study of 22 diabetic patients on combination therapies and a unique insulin overdose case, thereby demonstrating successful application of the final assay.

Section I: Initial Proof of Concept Investigation

5.1 Introduction

Over recent years the proportion of new drug entities (NDEs) being developed has seen increased interest in large biomolecules such as proteins and peptides. Of these biopharmaceuticals, insulin is one of the oldest and perhaps best known, and to this day, remains one of the primary treatments for diabetes [1, 2]. In addition to recombinant human insulin, a number of closely-related analogs with improved pharmacokinetics have been developed, resulting in several long, fast, and intermediate acting versions. Insulin glargine and insulin detemir are two popular long-acting analogs, effectively stabilizing blood glucose for 24 and 16 hours, respectively [3]. Glargine is homologous to insulin except for the substitution of glycine for asparagine at position 21 of the A-chain and the addition of two arginines to the C-terminus of the B-chain. Structures and sequences of insulins are shown in Figure 5.1.

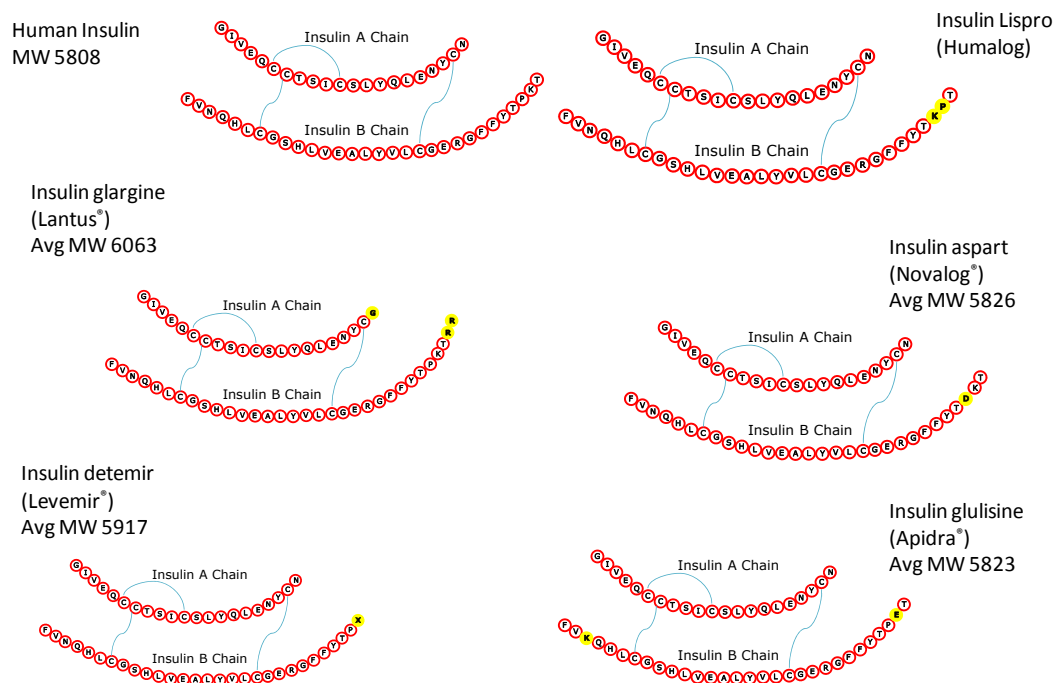


Figure 5.1 Amino acid sequences and structures for human insulin and five analogs

These changes shift the isoelectric point (pI) from 5.4 (pI of endogenous insulin) to approximately 6.7. This results in reduced solubility at physiological pH which causes formation of a microprecipitate when the acidic solution is injected. It is the slow release of the drug from this precipitate that elongates the half-life of glargine. It is believed that these sequence changes also increase the natural propensity of insulin to form hexamers, which further prolongs bioavailability. Detemir is modified through acetylation and addition of a fatty acid chain to lysine 29 on the B-chain. In addition to increased hexamer formation, detemir rapidly binds to human albumin, slowing its release into the bloodstream. Insulin glulisine and insulin aspart are two widely prescribed fast acting analogs. The sequence modifications and amino acids substitutions shown in Figure 5.1 result in significantly

reduced hexamer formation, which yields bioavailability within approximately 10-15 minutes [4].

As control of both short-term, meal-time and long-term basal levels of blood glucose are critical, many diabetic patients are prescribed a combination of these analogs for the maintenance of near-normal glycemic profiles.

To date, most biological measurement of insulins has been carried out using ligand-binding assays (LBAs). For example, in 2007, there were at least 12 different commercial assays for human insulin[5], including radio-immunoassays (RIAs) and enzyme-linked immunosorbent assays (ELISAs). The short comings of LBAs in general are exemplified in human insulin assays and are well documented[5-10]. Of these, perhaps one of the greatest challenges for accurate quantification of insulins and analogs using LBAs is cross-reactivity. Performance of LBAs, in particular the degree of cross-reactivity between and amongst analogs as well as with endogenous insulin, is entirely dependent on the choice of specific monoclonal antibody that comprises the commercial reagent. Numerous papers exist detailing the different cross-reactivities of “commercially available” insulin kits with analogs [5-10]. It is not uncommon to observe 50-100% cross-reactivity of most of the kits with one or more analogs. It has also been shown that the degree of cross-reactivity can be concentration dependent[7]. Furthermore, there appears to be high variability between commercial assays. Manley et al reported that when different assays were used to quantify the same samples, results differed by as much as 2-fold [7].

Since patients will often take a combination of these analogs to stabilize blood glucose, it is important to have an analytical methodology capable of simultaneously differentiating *and* quantifying the various analogs. When trying to determine

pharmacokinetic parameters for a discrete insulin analog by LBA, it can be near impossible to quantify the absorption endpoint due to basal levels of other analogs present, which react equally with the assay. Use of multiple assays has been described [4] to obtain concentrations for individual analogs, using subtraction or multiplication factors based on known cross-reactivity.

Interest in insulin analog quantification extends beyond diabetes treatment and monitoring. Due to the suspected performance enhancing properties of insulin, the use of insulins in non-diabetic athletes has been prohibited by both the International Olympic Committee (IOC) and the World Anti-Doping agency (WADA)[11]. There is therefore a need to be able to screen for and unambiguously identify any of the insulin analogs possibly used in sports doping. Methods which quantify and differentiate amongst the analogs are also needed in the identification of the specific insulin responsible for wrongful death cases or in the study of hypoglycemia. Finally, patent protection for many of the current formulations will expire by 2017 (Figure 1.1). As such, the development of bioequivalence methods for these compounds is already actively in progress. These methods need to be very accurate and precise to meet regulatory requirements; they should also be capable of facile implementation in conventional bioanalysis laboratories.

Coinciding with the increased development of biologically based therapies, there has been an increase in the use of LC-MS/MS for quantification of biopharmaceuticals. LC-MS/MS has been the technique of choice for small molecule quantification for many years, and as such, is the platform that dominates most discovery-stage, pre-clinical and clinical bioanalytical laboratories[12, 13]. It now shows promise in overcoming the shortcomings of LBAs for large molecule quantification in biofluids. As previously discussed, in contrast

to LBAs, LC-MS/MS assays offer a higher degree of accuracy and precision, high specificity, the ability to multiplex, broader linear dynamic range, fast development times and freedom from reagent reproducibility and reliability issues. LC-MS based approaches are not without their challenges. Chapters 1 and 2 have outlined these challenges, examined them in detail and proposed solutions where possible.

To date a few LC-MS methods exist for the quantification of insulin and its analogs[11, 14-24]. Many methods employ a multi-step affinity purification and/or multidimensional or nano-flow chromatography to achieve adequate specificity and sensitivity. Though most methods quantify the intact insulin, some require reduction of disulfide bonds in order to release the A and B chains[25]. In the latter case, the B chain was used to represent the intact molecule. The most sensitive of these methods was developed for urine sample analysis and employed a sample prep process taking several hours and involving a 4-step SPE isolation followed by an 8-step immunoaffinity chromatography (IAC) method, and finally an additional 4-step SPE clean up prior to LC/MS analysis[11]. The subsequent overall analytical run time was 40 minutes. A similar three- stage, multi-step sample prep method was also described for insulin quantification in serum[17]. In this methodology up to 4 mL of serum was required, and the analytical run time was 15 minutes. Additional serum methods have been developed using nano-flow or 2D LC. Here the sample volume required was up to 1 mL (serum) and run times ranged from 10 to 40 minutes[23, 25]. A very sophisticated approach for quantifying human insulin uses 3D nano-LC, an overnight immunoprecipitation (IP) extraction, and in-house prepared anti-peptide columns[22]. This approach however, is not suitable for high throughput bioanalysis.

A common requirement with methods that employ some form of sample preparation is evaporation and reconstitution of the extracted sample prior to LC-MS analysis. This increases the analyte concentration and allows the injection solvent to be optimized. For many peptides, this evaporation step is associated with significant adsorptive losses. In addition, the minimum run time recorded is 10 minutes and the average sample prep time is several hours to overnight. These characteristics are not suited for the routine bioanalytical laboratory where it is typical to process several hundred samples each day and to require that the data be available by start of business the following day.

Section I of this chapter describes the efforts to develop a simple LC-MS method utilizing 250 μ L of plasma for the simultaneous differentiation and rapid quantification of 4 synthetic insulin analogs. In addition, the sample prep described herein requires significantly less sample than previously published methods and can be accomplished in under 30 minutes for a 96-well plate, an average of 6-10 times faster than current methods achieving detection limits in the hundreds of pg/mL range. The reduction in sample prep time is achieved through a combination of eliminating evaporation and significantly reducing the complexity and number of steps required for the sample clean-up. Finally, the method employs conventional analytical flow LC and triple quadrupole MS, a common comfortable platform for the vast majority of bioanalytical scientists. This has the advantages of much shorter run times, greater system robustness, and is more readily implemented by the typical bioanalytical laboratory chemist than nano-LC.

5.2 Experimental

5.2.1 Chemicals and Reagents

Lantus[®] (insulin glargine) and Apidra[®] (insulin glulisine), both manufactured by Sanofi-Aventis, were used as formulated. Levemir[®] (insulin detemir) and NovoLog[™] (insulin aspart), both manufactured by Novo Nordisk, were also used as formulated. Normal, non-diseased human plasma was purchased from Lampire Biological Labs, Pipersville, PA. Rat plasma was purchased from Equitech Bio, Kerrville, TX. Water for mobile phase and sample preparation was obtained from a Milli-Q lab water system, (Millipore, Billerica, MA). Acetonitrile, methanol, and formic acid (concentrated solution, 99%) were purchased from Fisher Scientific (Fair Lawn, NJ). All other chemicals and reagents were purchased from Sigma (St. Louis, MO) unless otherwise stated.

5.2.2 Preparation of samples, calibration standards and quality control samples

The concentration of the insulin analog in each formulation was first converted from IU/mL into mg/mL in order to facilitate dilution calculations. For all formulations, respective insulin analogs are present at 100 IU/mL. For Lantus, Apidra, and NovoLog, 100 IU is equal to 3.638, 3.49, and 3.5 mg insulin glargine, insulin glulisine, and insulin aspart, respectively, per mL. (These values were taken from product inserts). For Levemir, 100 U insulin detemir is equivalent to 14.2 mg. This value was obtained from the European Medicines Agency webpage containing product information for Levemir (http://www.ema.europa.eu/docs/en_GB/document_library/EPAR_-_Product_Information/human/000528/WC500036662.pdf).

A diluent consisting of 30/10/60 MeOH/CH₃COOH/H₂O plus 0.05% rat plasma was prepared. The various insulin formulations were diluted serially in the above diluent and then combined to generate a working solution containing the four analogs, each at a concentration of 1 µg/mL. Separate working solutions were produced for preparation of quality control samples and standards. Bovine insulin was used as the internal standard (IS) and was prepared in the above diluent at a concentration of 500 ng/mL to be used for spiking. For standard curve and quality control (QC) samples, spiking solutions of pooled insulin analogs were made through serial dilution of the 1 µg/mL stock. For each intended standard curve point and each QC level, 1 mL of control human plasma was spiked with an appropriate volume of the appropriate concentration of analyte spiking solution (combined insulin solutions), and 20 µL of 500 ng/mL IS spiking solution. Standard curve points were prepared at 0.2, 0.5, 1, 5, 10, and 25 ng/mL in human plasma. Quality control samples were prepared in human plasma at 0.35, 0.75, 2, 8, and 20 ng/mL. Blank human plasma samples were also extracted for determination of limit of detection (LOD). A 250 µL aliquot of each sample was diluted with 250 µL of 10 mM TRIS base and vortex mixed. The resultant 500 µL sample was extracted by SPE.

5.2.3 Solid-phase extraction conditions

Samples were extracted using an Oasis[®] HLB µElution plate (Waters Corp., Milford, MA). The plate was conditioned with 200 µL of methanol followed by 200 µL of water. The 500 µL pre-treated standard curve, blank, and quality control samples were loaded onto the SPE plate and washed with 200 µL of 1% acetic acid in 5% methanol in water. Insulin analogs were eluted with two separate 25 µL aliquots (collected together) of 10% acetic

acid in 60% methanol. The eluates were then diluted with 50 μ L water and placed in the autosampler for analysis.

5.2.4 Chromatographic Conditions

A 20 μ L aliquot of the diluted SPE eluate was injected onto an ACQUITY UPLC CSH C18 column (2.1 x 50 mm, 1.7 μ m) using a Waters ACQUITY I-Class UPLC system equipped with a flow-through needle (FTN) autosampler. Samples were kept cooled at 10°C and the column temperature was maintained at 60°C. Mobile phase A consisted of 0.1% formic acid (by volume) in water and mobile phase B consisted of 0.1% formic acid (by volume) in acetonitrile. Insulin analogs were eluted using a linear gradient from 20% B to 65% B over 2 min at 0.25 mL/min, which was directly introduced into the MS, without splitting. Mobile phase B was then ramped from 65 to 98% over 0.1 min and held for 0.5 min to clean the column. This was followed by an equilibration at initial conditions. Total cycle time was 3.5 minutes.

5.2.5 Mass spectrometry and Software

For each peptide and the IS, collision induced dissociation (CID) products of multiply charged precursors were detected in positive ion multiple reaction monitoring (MRM) mode using a Waters Xevo™ TQ-S mass spectrometer (Milford, MA). The electrospray voltage, source temperature, desolvation temperature and desolvation gas flow rate were 3.0 kV, 150 °C, 500 °C and 1000 L/Hr respectively. MRM transitions and charge states for each peptide and the IS as well as their respective cone voltages and collision energies are summarized in Table 5.1. MassLynx instrument control software was used for data acquisition. All peak area integration, regression analysis and sample quantification

was performed using TargetLynx. Peak area ratios (PARs) of the insulin analogs and the bovine insulin internal standard were determined and calibration curves generated for each of the analogs. Insulin analog concentrations in QC samples were determined from their PARs against their respective calibration lines.

| Specific Insulin | MRM Transition | Cone Voltage (V) | Collision Energy (eV) |
|------------------|-----------------|------------------|-----------------------|
| Glargine | 1011->1179 | 60 | 25 |
| | 867->984 | 60 | 18 |
| Lispro | 1162-> 217 | 50 | 40 |
| | 968.5->217 | 50 | 40 |
| Detemir | 1184-> 454.4 | 60 | 20 |
| | 1184-> 1366.3 | 60 | 20 |
| Aspart | 971.8 -> 660.8 | 60 | 18 |
| | 971.8 -> 1139.4 | 12 | 18 |
| Glulisine | 1165 -> 1370 | 14 | 22 |
| | 1165 -> 346.2 | 14 | 22 |
| Bovine (IS) | 956.6 -> 1121.2 | 60 | 18 |
| Human insulin | 1162 -> 226 | 50 | 40 |
| | 968.5->217 | 50 | 40 |

Table 5.1 MS conditions for human insulin, 5 analogs, and the internal standard bovine insulin; highlighted transitions correspond to the primary quantitative transition, other transitions are confirmatory

5.3 Results and Discussion

5.3.1 Development of sample pre-treatment and solid-phase extraction

Obtaining adequate specificity and recovery for insulin analogs in human plasma matrix is not a trivial task. As with all peptides, insulins are zwitterionic and their behaviour is difficult to predict. They also need to be separated from thousands of other, potentially isobaric, peptides found in a sample. Experimentation during development of this method

found that many of the recovery and poor reproducibility issues encountered with insulins are related to non-specific binding (NSB), protein binding, and solubility. Careful and systematic evaluation of various pretreatment options as well as wash and elution compositions was critical to the overall specificity and high recovery of the method. In all cases described herein, extraction efficiency was determined by comparing average peak areas from a 1 or 10 ng/mL mixture of peptides in matrix after the described extraction procedure to average area counts from blank SPE extracted matrix which was then spiked post-extraction at 1 or 10 ng/mL. Initial extraction studies were performed with insulin glargine only. Other analogs were added once preliminary method development was complete. An experiment comparing reversed-phase SPE to protein precipitation (PPT) methods confirmed that the endogenous background from samples extracted with simple precipitation was too high to allow quantification in the sub-ng/mL range. This is not surprising as it is identical to the findings during teriparatide method development described in Chapter 3. In order to concentrate the samples without evaporation, a step that often leads to adsorptive losses for peptides, method development was performed in 96-well μ Elution plates as discussed in Chapter 2. These plates are characterized by high loading capacity and low elution volumes, facilitating as much as a fifteen-fold concentration without dry-down. To simplify interpretation of retention behaviour, a polymeric reversed-phase only SPE (Oasis HLB) was evaluated, rather than mixed-mode sorbents, using the generic SPE screening protocol described in Chapter 2, which had been developed specifically for peptides. It was necessary to make minor changes to the generic protocol based on knowledge of insulin properties. These included diluting the sample with TFA (to improve solubility) and reducing the organic content of the elution solvent from 75%

acetonitrile (+ 1% TFA) to 50% acetonitrile (+1% TFA). The latter change was made based on the fact that the insulins elute with <50% acetonitrile from the LC column. Large peptides such as insulin precipitate at lower concentrations of organic than smaller peptides do (Chapter 2), as such, the reduction and change in organic concentration was intended to reduce the likelihood of precipitation as well. This basic method yielded a reasonable insulin glargine recovery of 70%, however specificity was poor. In an attempt to improve specificity, similar methodologies were tested on mixed-mode anion and cation exchange sorbents, resulting in equal or lower recovery and little benefit to specificity. At this stage, in order to minimize uncontrolled variables potentially contributed by unexpected interactions with mixed-mode sorbents, further development proceeded with the reversed-phase sorbent only and focused on optimization of the pre-treatment and wash solutions to reduce interferences while improving and maximizing recovery. Plasma pre-treatment was optimized first in order to eliminate protein-binding, adjust pH, and selectively retain insulins relative to undesired plasma components. Various acidic pre-treatments were assessed including TFA, H₃PO₄, FA and precipitation with HCl or TCA. There was no improvement in specificity using any of these pre-treatments, and of these options, the TFA dilution still provided the best recovery. In order to change the retention characteristics of the insulins, the samples were diluted with 10 mM TRIS base at approximately pH 9- 9.5. Not only did recovery improve significantly (insulin glargine recovery was >95%) but the endogenous background was reduced. The combination of reduced background and increased recovery resulted in a 50% increase in signal. Chromatograms from the final eluates from samples pretreated with TFA (Figure 5.2B, top panel) contained a broad, intense interference peak at 5.76 minutes that was absent in the eluates from samples

pretreated with TRIS (Figure 5.2A, top panel). These samples were further analyzed using full scan MS to elucidate the nature of the peak. Spectra were summed from 5.5 to 6.25 minutes samples from both pre-treatments, and the resultant data are shown in the bottom panels of Figures 5.2A and 5.2B. Deconvolution of the protein envelope in the samples pretreated with TFA produced an intact MW of approximately 66,400, providing putative identification as human serum albumin (HSA). HSA is typically present at approximately 35-50 mg/mL and must be efficiently removed and separated from the insulin analytes. Pretreatment with TRIS efficiently achieved this goal, as evidenced by the absence of the large protein peak at 5.76 minutes.

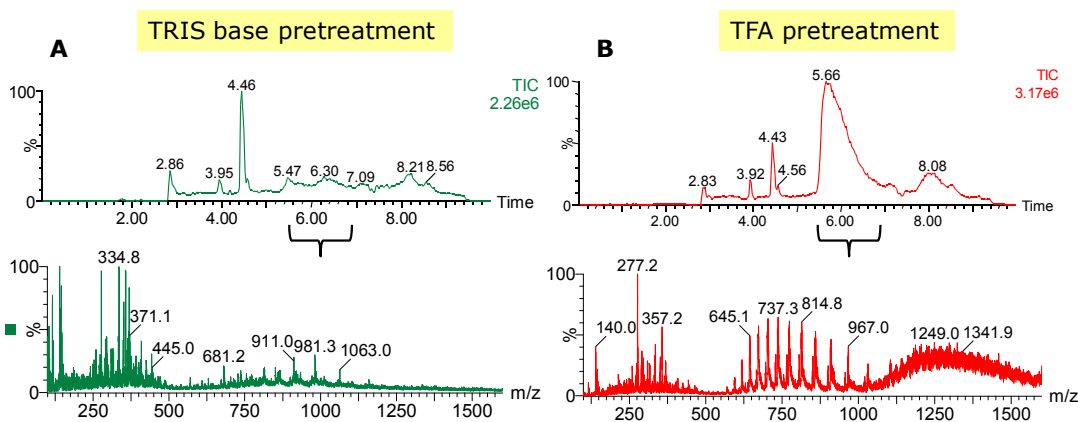


Figure 5.2 LC chromatograms of final SPE eluates resulting from plasma samples initially pretreated with TRIS (panel A, top) or TFA (panel B, top) prior to SPE; bottom panels are summed spectra from 5.5 to 6.25 minutes

The experiments in Chapter 2 highlight the importance of screening of various injection solvents. This is particularly important for peptide compounds as it may provide valuable information pertaining to solubility, which can heavily influence carryover, linearity, sensitivity and peak shape. The information resulting from this investigation showed that the combination of methanol and acetic acid produced the sharpest and most

intense chromatographic peaks for insulin analogs. The composition of the final SPE elution solvent was derived from these results. Specifically, the final elution solvent was changed to methanol and acetic acid, resulting in an additional 50% increase in signal for insulin glargine relative to that seen using the original TFA/ACN based elution solvent. The proportion of methanol (60%) was derived from the chromatographic elution profile for glargine plus an additional 10% to ensure adequate recovery off of the SPE sorbent, which was believed to be more retentive than the chromatographic column. The final acetic acid content (10%) was optimized. Lower percentages yielded lower recovery for some of the insulin analogs. It is possible that the high concentration of acetic acid required is related to modifier strength. Just as formic acid is a weaker modifier than TFA (and thus higher concentrations are typically required), acetic acid is a weaker modifier than formic acid, requiring even higher concentrations to disrupt secondary interactions with the sorbent and improve recovery. An additional theory is that insulin solubility is also improved by increasing acetic acid content in the elution solvent. Tuning solutions prepared with identical organic content and different modifiers (formic versus acetic acid) were compared in terms of peak response, and the acetic acid modified solution yielded a two-fold increase in the area of the solution compared to that obtained with formic acid. One possible explanation is that the acetic acid somehow improves solubility for insulin relative to formic acid or that ionization efficiency is improved under acetic acid conditions.

Using the method described in the experimental section, final absolute recoveries of glargine, detemir, glulisine, aspart and bovine insulin (the internal standard) from human plasma were 84, 62, 87, 83, and 94%, respectively. Although absolute recovery for glargine was ~10% higher using ACN and TFA in the SPE elution solvent, area counts were ~50%

lower than when acetic acid and methanol were used to elute the analytes. This is possibly due to improved selectivity of the acetic acid/methanol based elution solvent, resulting in a reduction in co-eluting interferences, ultimately yielding higher area counts even if the absolute recovery was lower. The lowest recovery was obtained for insulin detemir, which elutes significantly later chromatographically than the other analogs. This suggests that a higher organic composition in the final SPE eluate might increase detemir recovery. Increasing the organic content might also elute more interferences, however. To evaluate this theory, various extraction conditions were tested. The organic solvent content of the SPE eluent was changed from 60% to 80% methanol; the same was tried using isopropanol or acetonitrile. These failed to increase recovery for detemir. The additional organic content merely served to elute an additional, closely related isobaric interference from the SPE bed, which was evident in the subsequent LC/MS analysis and MRM data for detemir. Consequently, the methanol composition was maintained at 60%.

Larger format SPE plates were also evaluated with larger sample volumes. The necessity to evaporate and reconstitute eluates from these larger plates resulted in insulin losses of up to 50%, presumably due to NSB to the collection plates during dry down. This phenomenon was studied extensively by Pezeshki et al, where they found up to 40% loss during dry down for a variety of peptides under different conditions[26]. A second experiment was attempted wherein 20 μ L of DMSO was added to the eluate prior to evaporation to keep the sample from going to complete dryness. Peptide losses were still evident and the chromatographic peak shape deteriorated due to the presence of DMSO, rendering this an unattractive option. These experiments confirmed the value of the μ -plates

to simultaneously extract and concentrate the samples without evaporation and reconstitution.

5.3.2 Mass Spectrometry of Insulin Analogs

Peptides such as the insulin analogs, which are not only large ($>4000\text{Da}$), but also stabilized by multiple disulfide bridges, can make it particularly difficult to optimize the MS detection conditions using the traditional small molecule approaches. The determination of optimal MS parameters for these compounds highlights several major differences between peptide and small molecule tuning processes. Though it is best practice to tee the analyte stream into the LC effluent for MS optimization, this may not always be carried out, for a variety of reasons. For small molecule tuning, neither the actual flow rate at which tuning occurs nor the % of the acidic modifier in the solvent (typically) impacts the observed precursor m/z . One usually expects $M+1$, $M-1$, or adducts from solvents or cations. However, for peptides, both flow rate and organic/modifier composition dramatically influence not only the specific multiply charged precursors formed, but also their relative abundances. Data obtained from experiments conducted during this study, highlighted differences between a simple infusion of human insulin at $10\text{ }\mu\text{L/min}$ and teeing into the mobile phase at $200\text{ }\mu\text{L/min}$ (Figure 5.3). The most abundant and highest intensity precursor ion (a common choice for obtaining optimal assay sensitivity), is distinctly different depending on the tuning condition. For example, at $10\text{ }\mu\text{L/min}$, the highest intensity precursor is the $4+$ precursor at $m/z\ 1452$, while the $5+$ precursor at $m/z\ 1162$ is most intense at $200\text{ }\mu\text{L/min}$. Interestingly, this phenomenon is not observed for all peptides, making it difficult to explain. A theory was proposed in Chapter 2 relating to dilution within the droplet. An additional theory is that initial droplet size at nano/micro flow is smaller

than at analytical flow, reducing the surface available for charge residence, thus reducing the number of charges present/accessible to the peptides within the droplet.

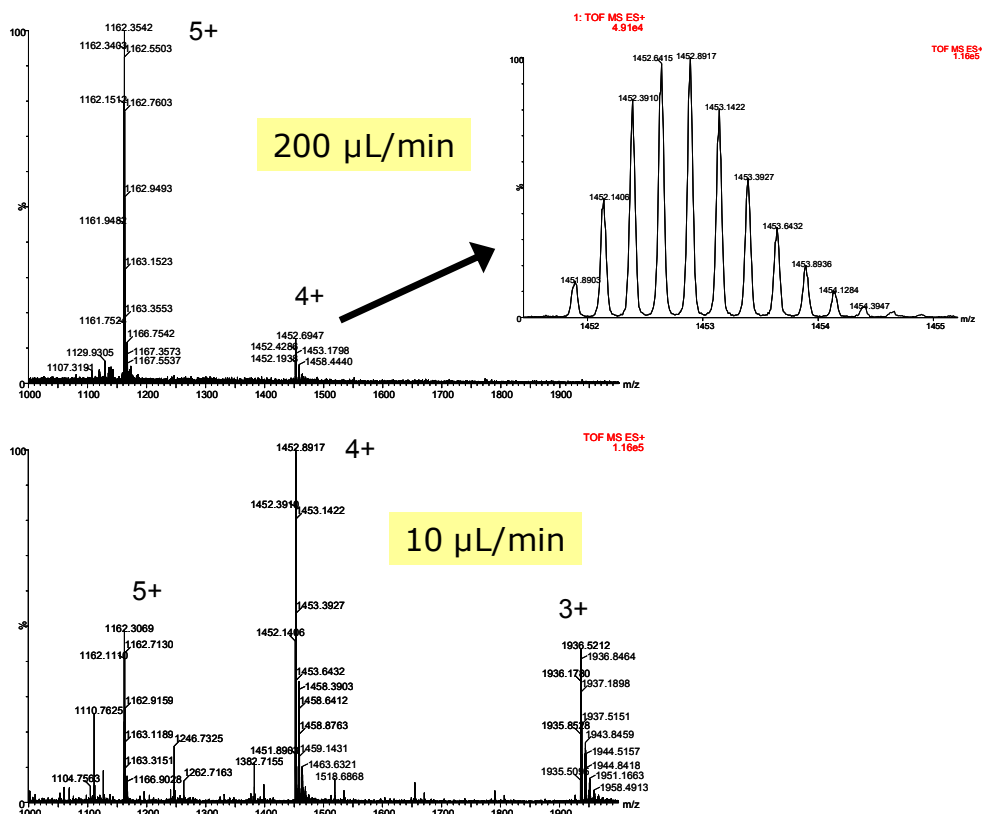


Figure 5.3 MS spectra for human insulin at either 200 $\mu\text{L}/\text{min}$ (top) or 10 $\mu\text{L}/\text{min}$ (bottom)

While one typically relies on a single precursor to generate fragments for small molecule analyses, there are advantages to selecting multiple precursors to attempt fragmentation of a peptide analyte. Not only do the various charge states fragment differently, but it can also be difficult to predict the specificity of a particular MRM when the sample is derived from a biological matrix. Furthermore, there exists some question as to whether or not the relative abundance of the various charge states changes during analysis and with concentration (this phenomenon was seen by Darby et al[14]), driving the

recommendation (Chapter 2) to monitor and possibly sum MRMs arising from distinct precursors. An MS spectrum for each of the analogs is displayed in Figure 5.4. Each analog yields a unique selection and pattern of precursors, despite their closely related nature. For each analog, the two or three most abundant precursors were chosen for fragmentation.

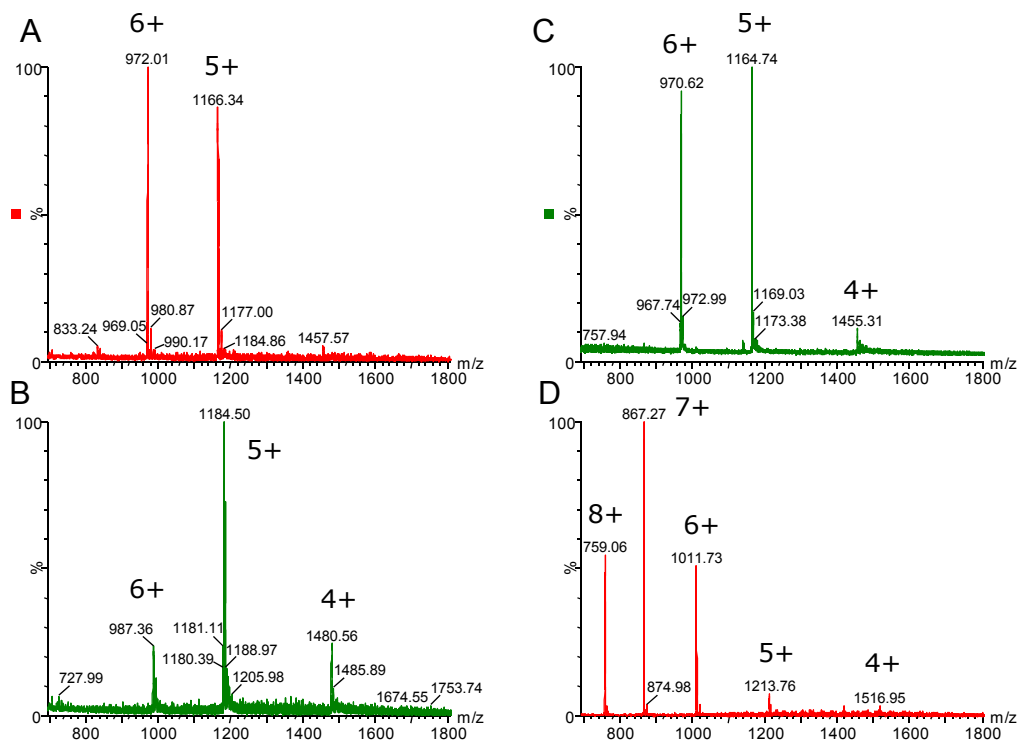


Figure 5.4 MS spectra for insulin aspart (A), detemir (B), glulisine (C) and glargine (D)

Collision induced dissociation (CID) of the chosen precursors was performed over the range of m/z 100-1800. Both the 6+ and 7+ insulin glargine precursors yielded multiple possible fragments, whereas only the 6+ charge state of insulin aspart and the 5+ of glulisine and detemir resulted in fragment ions with sufficient intensity for meaningful quantification. Representative MSMS spectra for each insulin analog, at its optimum collision energy, is shown in Figure 5.5. Fragments chosen for quantification are highlighted with an asterisk.

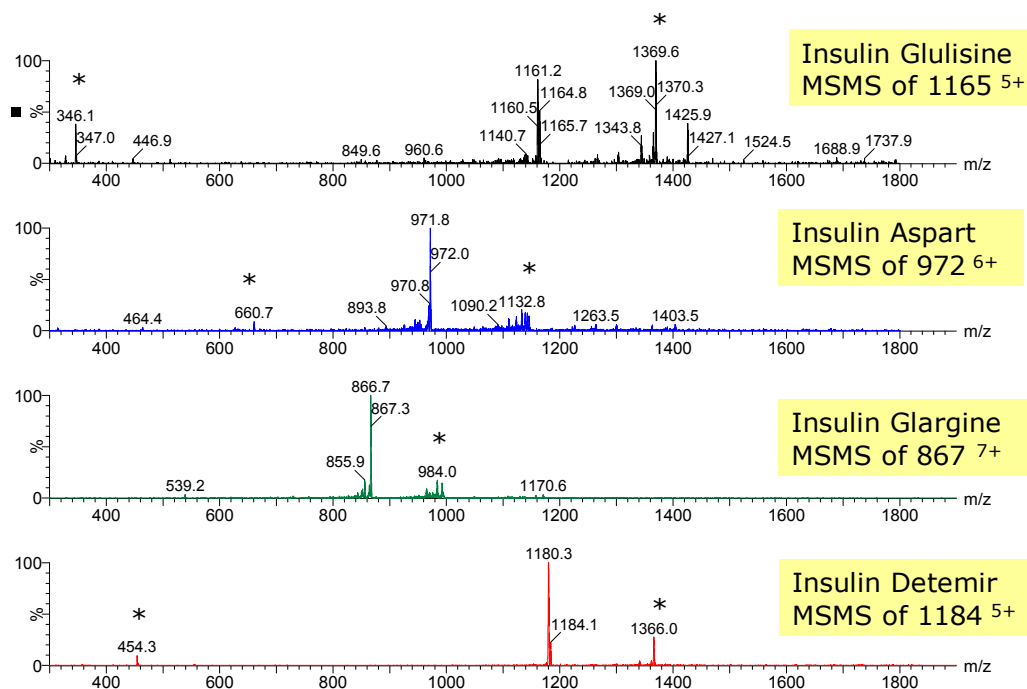


Figure 5.5 Representative MSMS spectra for insulin analogs

Under nominal mass MS resolution conditions, there is overlap between the isotope patterns of the 5+ and 6+ multiply charged precursors of aspart and glulisine (see Figure 5.4). This was previously reported by Thomas et al[27], and may lead to a lack of specificity if unique fragments are not chosen. These same precursors also overlap with human insulin. However, certain fragments arising from human insulin (at m/z 561, 653, and 226) were determined to be unique. At higher collision energies, each of the insulin analogs readily produces immonium ion fragments which exhibit high intensities. Most yield an intense peak m/z 136, for example, corresponding to a tyrosine immonium ion. These spectra are simpler than the MSMS spectra for the insulins at their optimal, lower collision energies. The higher energy spectra are dominated by a single intense fragment at m/z 136 (Figure 5.6, bottom), rather than several low intensity fragments (Figure 5.6, top). Though it is

tempting to choose the most intense fragment, the choice of peptide fragment ion is more complicated.

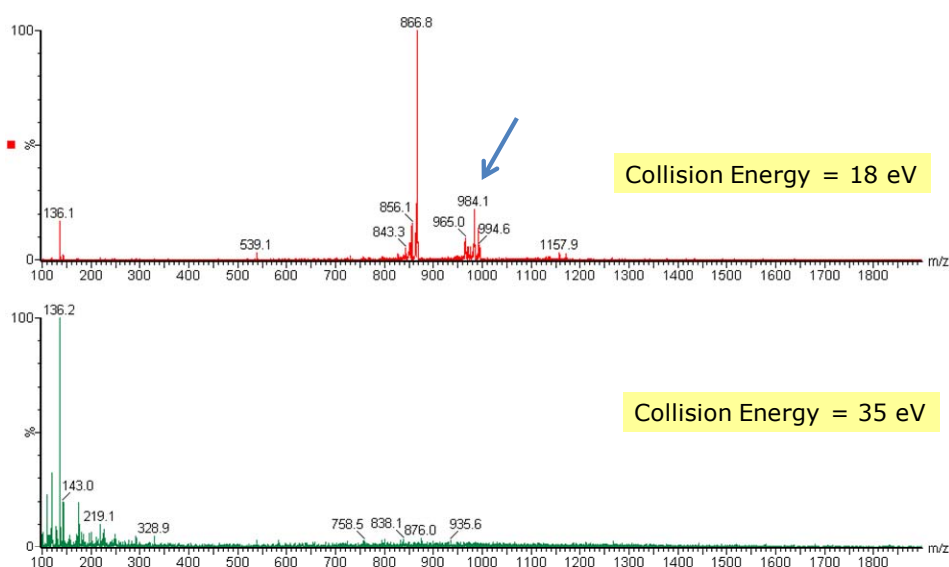


Figure 5.6 MSMS of the 7+ insulin glargine precursor using a collision energy of 18 eV (top) or 35 eV (bottom)

Due to the nominal mass resolution limitations of triple quadrupole instruments, the high concentration of other peptides in the sample (possibly closely related), and the high chemical background associated with low m/z fragments, specificity in the endogenous matrix was the critical deciding factor. The chromatograms for insulin glargine in Figure 5.7 demonstrate the dramatic difference in specificity obtained from a transition based on a lower intensity b or y ion fragment such as m/z 984, versus the higher intensity immonium fragment at m/z 136 seen in Figure 5.6. The mass spectrometer used in this work had a mass range of 50 - 2048 amu on both quadrupoles, facilitating improved sensitivity at higher mass ranges, which enabled the use of fragments such as the m/z 984 for glargine and m/z 1370

for glulisine in quantification. The observed specificity benefit derived from these larger fragments was central to reducing the overall demand on the sample preparation. In this application, it has contributed substantially to the use of a significantly simpler and faster sample prep scheme than previously published methods. In summary, it is recommended that one always choose the highest m/z precursor and/or product ions possible and that immonium and other low m/z ions be avoided.

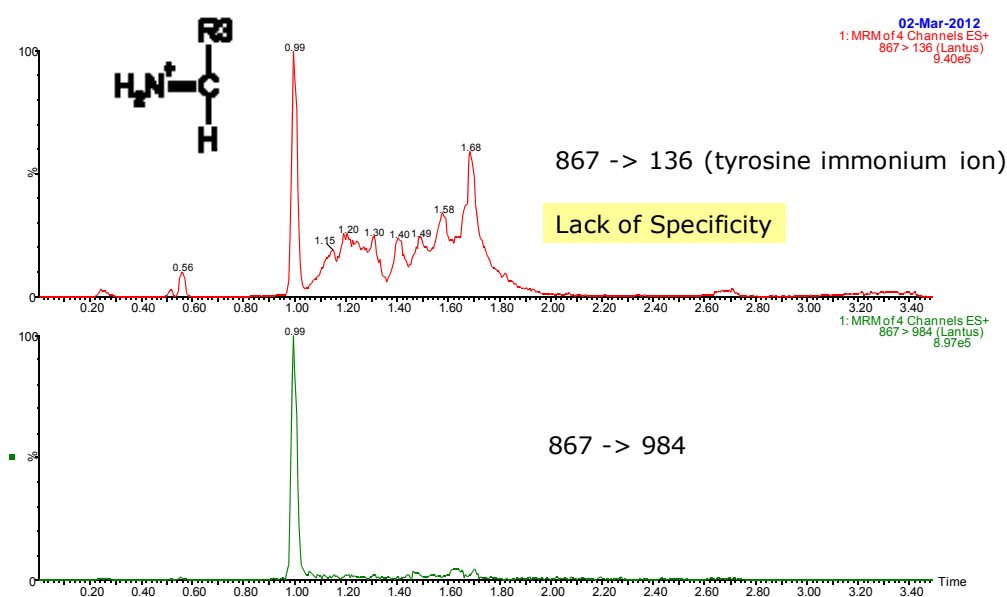


Figure 5.7 Specificity difference for insulin glargine extracted from human plasma observed when monitoring an immonium ion fragment (top) versus the more specific sequence ion at m/z 984 (bottom); inset shows a typical immonium ion structure

5.3.3 Liquid Chromatography

The value of wide (300 Å) pore size LC columns for the separation of peptides has been documented previously[28, 29] and was demonstrated in Chapter 2. These columns produced significantly narrower analyte peak widths, particularly for large peptides. The

data presented in Chapter 2 established that transitioning from columns packed with the typical 3.5 μm particles to the newer $<2\ \mu\text{m}$ particle columns extends the flow rate range for optimal chromatographic performance for larger peptides into the desired bioanalytical range of several hundred $\mu\text{L}/\text{min}$, due to improved efficiency resulting in a broader optimal linear velocity operating range.. Therefore, the initial test conditions for the insulin analysis consisted of LC method development with a C_{18} , 1.7 μm , 300 Å column. Unexpectedly, and specifically for insulin and its analogs, this column produced peaks characterized by severe tailing and widths of approximately 6-8 seconds wide at base. One of the major sources of tailing for peptides is thought to be interaction of the analyte with the stationary phase surface. A recently introduced column chemistry, the Charged Surface Hybrid (CSH) column (described in Chapter 2), claims improved peak shape under formic acid conditions, mimicing performance expected when using TFA under certain conditions. Peptides, historically, have primarily been chromatographed using TFA mobile phases in order to improve peak shape, making this novel column a particularly intriguing option. Figure 5.8 shows that this charged surface column improved the peak shape for insulin versus a traditional C_{18} column.

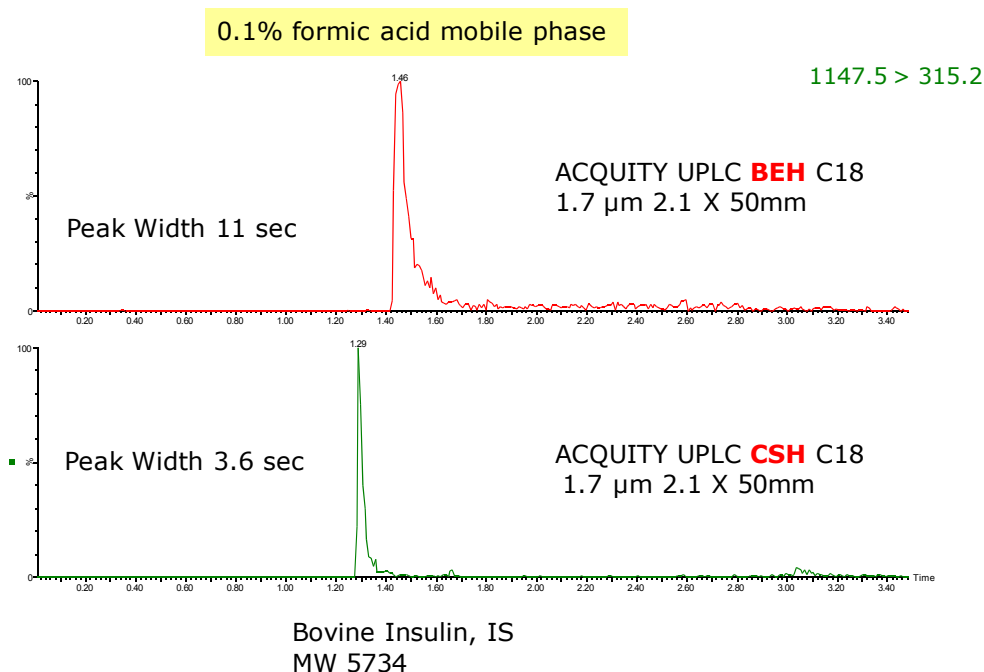


Figure 5.8 Chromatographic separation of bovine insulin using a traditional C18 300Å (ACQUITY UPLC BEH 300 C18) column (top) and a charged surface (ACQUITY UPLC CSH C18) column (bottom)

In general, the isoelectric points (pI) for most insulin analogs are in the 5-7 range, making them positively charged under the low pH mobile phase conditions employed. The observed improved peak shapes could be due to the stationary phase also being positively charged, in this way minimizing secondary interactions through charge repulsion. During the method development process, various organic solvents and modifiers as well as LC flow rates were tested in order to obtain the best peak shape and sensitivity. As the best SPE recovery (and presumably, solubility) of the insulin analogs was obtained using methanol and acetic acid, this combination was tested and investigated as an LC mobile phase. Experimental results yielded reduced MS sensitivity and broad LC peaks. It is possible that acetonitrile improves MS ionization and/or that acetic acid is not as good a buffer as formic acid, or finally that the mobile phase pH is not as low with acetic acid as it is when using

formic, resulting in a change in peak shape. However, acetic acid and methanol *were* incorporated into the sample manager wash solvents, and were effective at eliminating carry-over.

Initial LC method development was performed using solvent-only standards in methanol/acetic acid. Chromatographic performance was unpredictable, with peak areas varying as much as 50-200% injection to injection. The Insulin peaks were also undetectable in many of the injections. In addition, serial dilution of a high level standard yielded poor linearity, particularly at lower concentrations. This behaviour is symptomatic of non-specific binding (NSB), which is a common attribute of many peptides, particularly larger ones containing lengthy hydrophobic regions. In Chapter 2, it was demonstrated that addition of a carrier protein can be an effective way to minimize NSB. In this case, for simplicity, 0.05% rat plasma was added to the sample diluents (described in the experimental section), resulting in improved linearity in solvent standards. NSB can also occur between peptide analytes and the chromatographic columns. To alleviate this effect, LC columns may have to be “pre-treated” in order to obtain the best performance for biomolecules such as insulin. Figure 5.9 highlights the difference between injections of insulin onto a column which has been subject only to solvent standards versus the same column after 9 injections of protein precipitated plasma. The plasma components presumably coat the column surface and effectively minimize NSB. These changes resulted in reproducible peak areas and a broad linear dynamic range in solvent standards as well as an easily achievable LLOQ of 50 pg/mL for solvent standards.

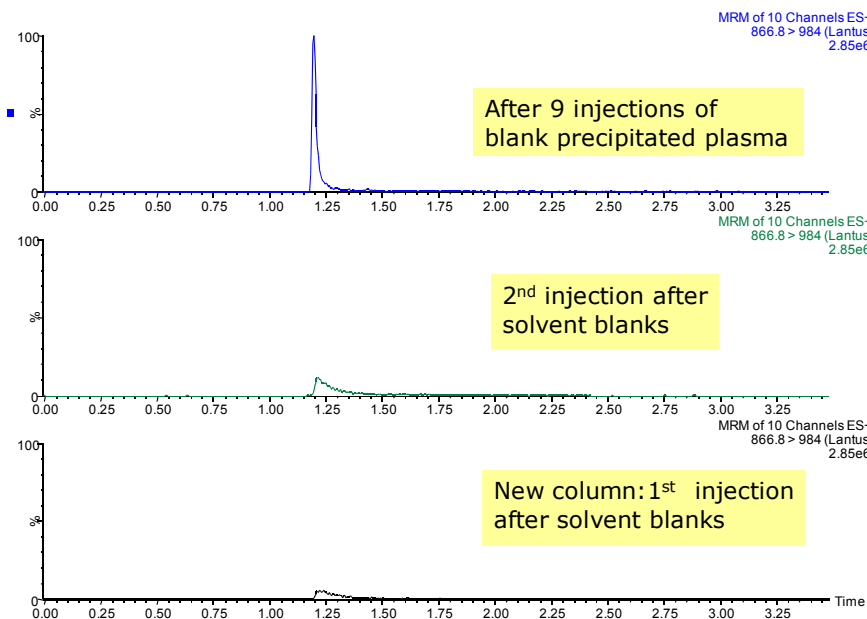


Figure 5.9 Change in chromatographic performance for insulin glargine from the first two injections (bottom and middle panels) and after injections of precipitated plasma (top)

The optimized separation conditions were formic acid (0.1%) in water and acetonitrile at a flow rate of 0.25 mL/min (shown in Figure 5.10) where retention times for the various analogs and IS range from 1.17 to 1.74 minutes. Peaks widths were ≤ 2.8 seconds wide at base for all insulin analytes and Gaussian peak shapes were obtained. Table 2 summarizes representative peak statistics from solvent-based standard curves for several insulin analogs. All curves were linear with 1/x weighting and r^2 values were >0.993 .

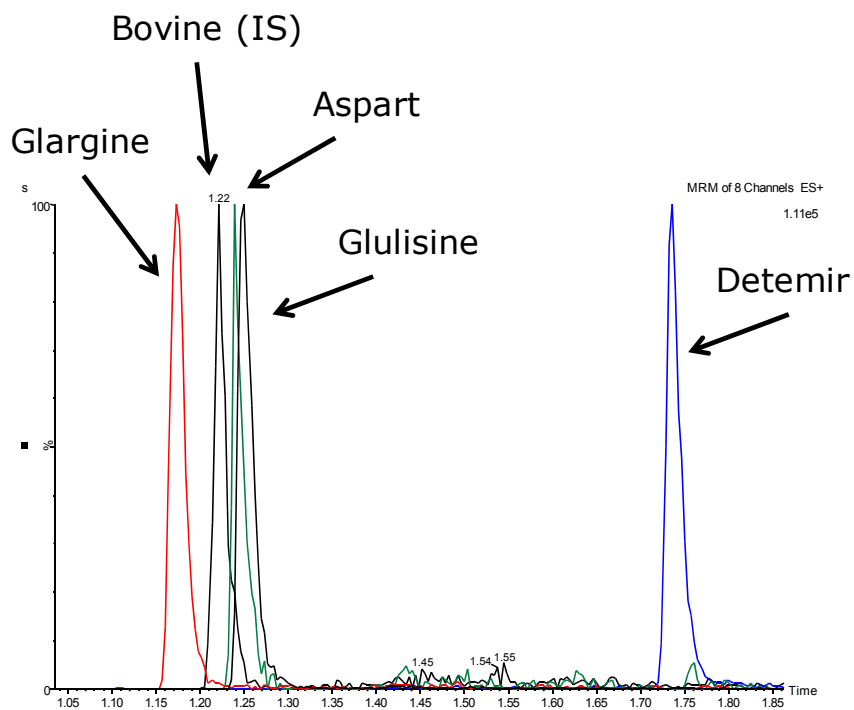


Figure 5.10 Chromatographic separation of insulin analogs using the final gradient conditions described in section 5.2.4

| Name | Expected Conc (ng/mL) | Area | Calc. Conc. (ng/mL) | %Dev |
|-----------|-----------------------|-----------|---------------------|------|
| 50 pg/mL | 0.05 | 246.6 | 0.045 | -9.5 |
| 100 pg/mL | 0.1 | 563.7 | 0.101 | 1 |
| 200 pg/mL | 0.2 | 1090.0 | 0.194 | -3.2 |
| 500 pg/mL | 0.5 | 2642.8 | 0.467 | -6.7 |
| 1 ng/mL | 1 | 5544.9 | 0.977 | -2.3 |
| 2 ng/mL | 2 | 11120.5 | 1.957 | -2.1 |
| 5 ng/mL | 5 | 28094.9 | 4.942 | -1.2 |
| 10 ng/mL | 10 | 61467.9 | 10.811 | 8.1 |
| 20 ng/mL | 20 | 117881.6 | 20.731 | 3.7 |
| 50 ng/mL | 50 | 298668.7 | 52.523 | 5 |
| 100 ng/mL | 100 | 625570.8 | 110.009 | 10 |
| 500 ng/mL | 500 | 2764219.3 | 486.092 | -2.8 |

A

| Name | Expected Conc. (ng/mL) | Area | Calc. Conc. (ng/mL) | %Dev |
|-----------|------------------------|-----------|---------------------|-------|
| 50 pg/mL | 0.05 | 483.06 | 0.051 | 2.4 |
| 100 pg/mL | 0.1 | 777.31 | 0.094 | -6.4 |
| 500 pg/mL | 0.5 | 3748.09 | 0.522 | 4.3 |
| 1 ng/mL | 1 | 6955.55 | 0.984 | -1.6 |
| 2 ng/mL | 2 | 15881.66 | 2.27 | 13.5 |
| 5 ng/mL | 5 | 38498.98 | 5.528 | 10.6 |
| 10 ng/mL | 10 | 74175.04 | 10.668 | 6.7 |
| 20 ng/mL | 20 | 143202.70 | 20.612 | 3.1 |
| 50 ng/mL | 50 | 308271.28 | 44.393 | -11.2 |
| 500 ng/mL | 500 | 2734696.0 | 393.954 | -21.2 |

B

Table 5.2 Representative standard curve statistics for insulin glulisine (A) and insulin glargine (B) from 50 pg/mL to 500 ng/mL in solvent standards

5.3.4 Human Plasma Standard curve and Quality Control Data

Following the testing in solvent standards, samples were prepared in human plasma. Linear dynamic range and assay accuracy and precision were determined using standard curves and quality control (QC) samples prepared in human plasma spiked with a mixture of the insulin analogs and a fixed concentration of the IS as described. Calibration standards used for quantification of the various insulin analogs ranged from 0.2 to 25 ng/ml. Using a $1/x$ weighting and linear fit, the r^2 values for all curves, for all insulin analogs were > 0.997 . The mean accuracies for all standard curve points extracted from human plasma were 93.4%, 91.6%, 96%, and 95.1% for glargine, detemir, aspart, and glulisine, respectively. QC samples were prepared in triplicate in pooled human plasma, as previously described, at 0.35, 0.75, 2, 8, and 20 ng/ml. The mean accuracies for all QC samples were 94.2%, 94.6%, and 91.5% for glargine, detemir, and glulisine, respectively. Statistics for aspart QC samples were not as accurate nor as precise; this is explained by overall lower area counts and higher endogenous background in extracted plasma samples. To improve this performance, a more specific extraction and/or modified LC strategy will be needed. This will be the subject of Section II of this chapter. Representative standard curve and QC statistics are presented for insulin detemir and glulisine in Tables 5.3 and 5.4, respectively. Representative chromatograms of an extracted plasma blank and insulin glulisine and insulin glargine at the LOD and LLOQ are shown in Figures 5.10 and 5.11, respectively.

| Name | Conc ng/mL | Area | Peak Area Ratio | IS Area | %Dev | Calc Conc ng/mL |
|---------------------|---------------|---------|-----------------------|---------|-------|-----------------------|
| Blank plasma | | 31.5 | | | | |
| 200 pg/mL plasma | 0.2 | 153.3 | 0.012 | 13239.5 | 16.6 | 0.23 |
| 500 pg/mL plasma | 0.5 | 375.6 | 0.03 | 12437.3 | -4.6 | 0.48 |
| 1 ng/mL plasma | 1 | 750.2 | 0.06 | 12419.1 | -12.7 | 0.87 |
| 5 ng/mL plasma | 5 | 4714.5 | 0.399 | 11801.8 | 6.3 | 5.31 |
| 10 ng/mL plasma | 10 | 8984.8 | 0.696 | 12907.3 | -8 | 9.20 |
| 25 ng/mL plasma | 25 | 25007.1 | 1.948 | 12836.3 | 2.4 | 25.60 |
| | | | | | | |
| QC 350 pg/mL plasma | 0.35 | 241.6 | 0.02 | 12200.7 | -2.6 | 0.34 |
| QC 750 pg/mL plasma | 0.75 | 733.6 | 0.058 | 12560.6 | 12.9 | 0.85 |
| QC 2 ng/mL plasma | 2 | 1969.4 | 0.141 | 13954.4 | -3.5 | 1.93 |
| QC 8 ng/mL plasma | 8 | 7486.7 | 0.615 | 12168.7 | 1.8 | 8.14 |
| QC 20 ng/mL plasma | 20 | 20549.6 | 1.616 | 12712.9 | 6.3 | 21.26 |

Table 5.3 Representative standard curve and QC sample statistics (n=3) for insulin detemir from 200 pg/mL to 25 ng/mL in human plasma

| Name | Conc ng/mL | Area | Peak Area Ratio | IS Area | %Dev | Calc Conc ng/mL |
|----------------------|---------------|---------|-----------------------|---------|-------|-----------------------|
| Blank plasma | | 36.9 | | | | |
| 0.2 ng/mL plasma | 0.2 | 230.3 | 0.013 | 17486.8 | 7.4 | 0.22 |
| 0.5 ng/mL plasma | 0.5 | 1017.4 | 0.057 | 17807.0 | 5 | 0.53 |
| 1 ng/mL plasma | 1 | 2068.0 | 0.12 | 17249.8 | -3.2 | 0.97 |
| 5 ng/mL plasma | 5 | 11330.0 | 0.61 | 18563.8 | -11.4 | 4.43 |
| 10 ng/mL plasma | 10 | 23803.2 | 1.396 | 17051.6 | -0.2 | 9.98 |
| 25 ng/mL plasma | 25 | 57342.0 | 3.606 | 15903.8 | 2.3 | 25.58 |
| | | | | | | |
| QC 0.35 ng/mL plasma | 0.35 | 626.1 | 0.035 | 17654.8 | 6.3 | 0.37 |
| QC 0.75 ng/mL plasma | 0.75 | 1700.4 | 0.101 | 16856.5 | 11.2 | 0.83 |
| QC 2 ng/mL plasma | 2 | 4744.9 | 0.31 | 15317.0 | 15.5 | 2.31 |
| QC 8 ng/mL plasma | 8 | 18609.8 | 1.013 | 18366.4 | -9 | 7.28 |
| QC 20 ng/mL plasma | 20 | 47779.3 | 2.828 | 16894.6 | 0.5 | 20.09 |

Table 5.4 Representative standard curve and QC sample statistics (n=3) for insulin glulisine from 0.2 ng/mL to 25 ng/mL in human plasma

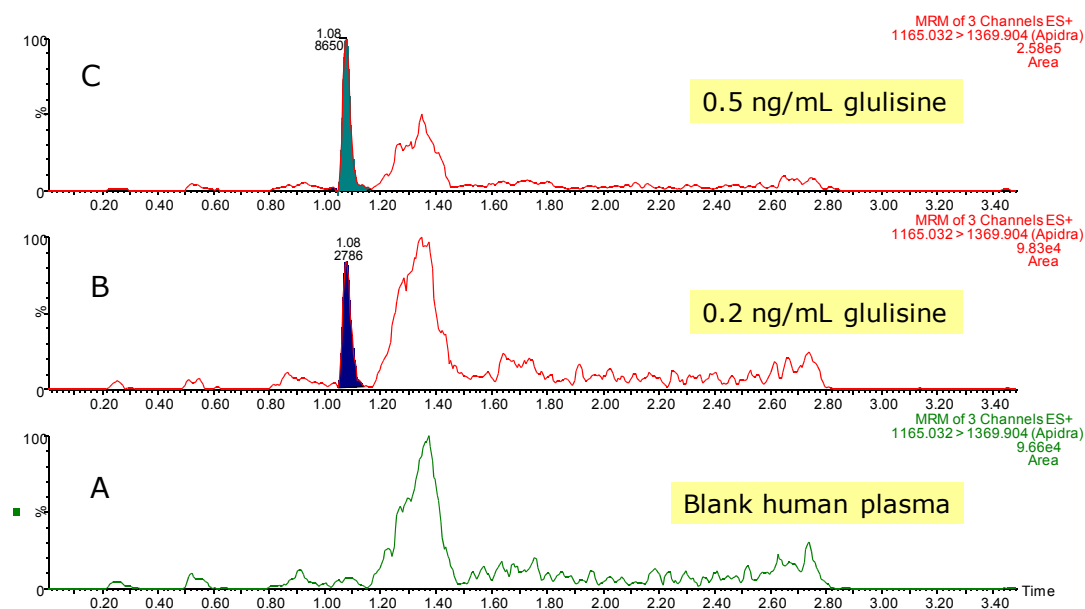


Figure 5.11A Representative chromatogram of insulin glulisine at the LOD (B) and LLOQ (C) in human plasma; blank extracted human plasma is also shown (A)

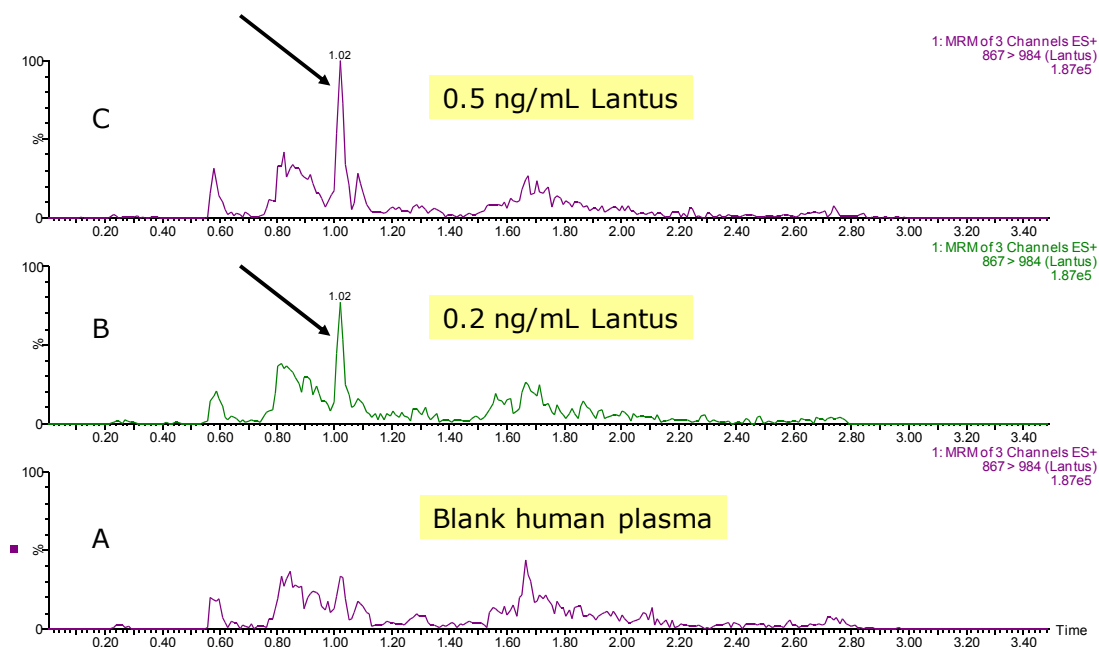


Figure 5.11B Representative chromatogram of insulin glargine at the LOD (B) and LLOQ (C) in human plasma; blank extracted human plasma is also shown (A)

Figure 5.11A clearly shows that a limit of detection, and perhaps even quantification, of 0.2 ng/mL for insulin glulisine is readily achieved using this method. However, for insulin glargine, the data in Figure 5.11B indicates that even detection at 0.2 ng/mL may be difficult to achieve in other sources of plasma matrix due to the high background and closely-eluting interferences. Section II of this chapter focuses on improving detection limits and reducing matrix interferences for all analogs, especially insulin glargine, one of the most widely sold insulin analogs and coincidentally, one in which there is great interest due to patent expiry (Figure 1.1).

5.3.5 Specificity

For a method such as this, where several closely related large peptides (with multiple possible molecular ions) are being analyzed in complex matrix using low resolution mass

spectrometry, the risk of interference from the MRM of one insulin channel into another is high. Therefore, one must assess the contribution of analytes present individually at high concentration, to the response in other channels. In order to evaluate the specificity of the method, samples were fortified individually with one of the four analogs at a concentration of 500 ng/mL, which is 20X the plasma ULOQ of 25 ng/mL. In addition, samples were fortified with human insulin only at 500 ng/mL and 1 µg/mL to assess the impact and potential interference of high levels of endogenous insulin (as might be present in Type 2 diabetics) on assay specificity.

The specificity experiments highlighted several positive attributes as well as certain limitations of this method, if the method were employed as-is. When human insulin is present at 1 µg/mL there is no detectable response in the primary MRMs for Levemir, Lantus and Novolog. There is a low level response (roughly equivalent to 0.5-1 ng/mL) in the 2 MRM transitions for Apidra. This is easily attributable to the overlap of precursor molecular ions experienced under low resolution conditions, coupled to the high sequence homology. In samples containing either Lantus only or Levemir only, the method demonstrated complete specificity as there was no detectable response in the primary channel for any of the other analogs or for human insulin. However, when Apidra or Novolog are present at 20X of the plasma ULOQ of 25 ng/mL, a response close to the LOD is detected in the channels for Novolog and Apidra, respectively, limiting the practical quantification limit for those analytes, if Novolog or Apidra were present at such extreme levels. Furthermore, Novolog, at 500 ng/mL, does trigger a response in the MRM channels for human insulin arising from the 6+ precursor. This presents a challenge as these analytes nearly co-elute under the gradient conditions proposed. The test run here, where individual

analogs are present at such high concentrations, represents an extreme circumstance. When these analogs are present at 2X the plasma ULOQ, the assay is completely specific for all analogs, as well as for human insulin.

5.4 Conclusions from Initial Proof of Concept Studies

With the global incidence of diabetes having grown dramatically over the past decade [30], it is expected that the interest in development of treatment and monitoring options, and thus potentially the identification and quantification of insulins, will be increasingly important to the scientific community. Though there are many distinct advantages to quantifying insulin and other large hydrophobic peptides by LC-MS/MS, this technique presents many analytical challenges including non-specific binding, poor chromatographic peak shape, carry-over, poor linearity, poor reproducibility and poor MS sensitivity. Section I of this chapter has presented proof of concept for a novel method for differentiating and quantifying therapeutic insulin analogs using μ -Elution SPE and UPLC-MS/MS, and highlights the tools and techniques for understanding, identifying, and addressing the challenges associated with large peptide/small protein analysis in the bioanalytical laboratory. The figures throughout this section illustrate these behaviours, many of which may be new to bioanalytical researchers previously focused on small molecule development. Although full validation was not performed, the data show distinct promise for the direct, simultaneous quantification and differentiation of multiple, intact long and fast acting insulin analogs in human plasma. This UPLC-MS/MS analysis can be readily implemented, is simpler, and has a higher throughput than other published LC-MS/MS methods, which are considerably more complex and typically use multi-

dimensional and/or nano LC or time consuming affinity purification. The run time of 3.5 minutes is 5-10X faster than other publications. In addition, this is the first study that simultaneously analyzed several long and fast acting analogs. Although this proof of concept work is not as sensitive as the ultrasensitive IP/nano-LC/high, resolution method recently published by Thomas et al[31] for urine, its speed, simplicity and adequate detection limits make it attractive to high throughput bioanalytical laboratories and provide the foundation for the further research described in Section II of this chapter. In contrast to ligand-binding assays, there is no concern with cross-reactivity between human insulin and the analogs, using the LC/MS method described herein, as this MRM approach readily differentiates the glargine, detemir, and glulisine analogs from endogenous insulin. The primary limitation of the current method is that there is a lack of adequate specificity between glulisine and aspart, when either is present at extremely high concentrations (20X the plasma ULOQ) as they co-elute chromatographically. Fortunately, they are not expected to be present in the sample as both are fast acting analogs and would not likely be co-administered. Furthermore, when aspart is present at 20X the plasma ULOQ, there is a detectable response in the human insulin channels chosen. An additional limitation of the proof of concept study is that it does not include validated quantification of human insulin or the popular analog lispro. Section II will address this limitation.

Section II Improved Sensitivity and Specificity Using Multidimensional LC and Mixed-mode SPE

As mentioned in section 5.1, recombinant human insulin and the many long and fast acting analogs that have been developed represent the primary treatment for insulin dependent Type I and, with an increasing trend, these are also prescribed to Type II diabetes patients. Dosage is normally in combination with oral therapy or after failure of diet or oral agents to exhibit glycemic control [32]. Section I of this chapter presented proof of concept for insulin quantification using LC/MS, however full validation was not performed and human insulin and its most closely related analog, lispro, were not included. In addition, detection limits were not adequate for current research efforts or for monitoring fasting levels. Therefore, alternative techniques were investigated to resolve these shortcomings, the results of which are discussed in Section II.

5.5 Introduction

Several factors highlight interest in quantification methods for insulin and analogs, and justify further development beyond the proof of concept work detailed in Section I of this chapter. The global incidence of diabetes mellitus (DM) continues to increase and therefore also the number of patients requiring daily insulin treatment. Additionally, patent protections have expired or are due to expire shortly[34] for many of the most widely prescribed insulins, leading to a multitude of active research programs to develop additional biosimilars. In addition, the biosimilar market is expected to grow by over 50 % through 2015[35] with insulins and diabetic treatments holding a prominent position. All of these

factors support the strong need to continue research on a viable LC-MS method for insulin quantification, leading to the work presented in Section II. Additionally, as mentioned in Section I, insulin administration has a forensic interest [36] and is of interest to the anti-doping industry[37, 38]. More selective, accurate and more sensitive analytical methods than the assay described in Section I of this chapter are urgently needed for such applications.

Historically, insulins have been analyzed using radioimmunoassay (RIA) or enzyme-linked immunosorbent assay (ELISA). LC-MS analysis of insulins is needed due to the many shortcomings of ELISA and RIA assays. For example problems with lack of standardization, cross-reactivity, limited linear dynamic range, and sample preparation time, are all well documented [18, 39-41]. These factors have driven the development of alternative LC-MS/MS assays and LC-MS method standardization [42]. For insulin analysis specifically, hybrid assays based on immuno-capture followed by LC-MS have been the most effective [11, 18-20, 27, 31, 41] though they lack the simplicity and throughput required for routine testing and bioanalysis.

Arguably the main challenge in developing LC-MS assays for large peptides such as insulin is in achieving detection limits equivalent to gold-standard immunoassays. Factors affecting sensitivity include (but are not limited to) selectivity during the sample preparation step, MS sensitivity (as peptide signal is shared across multiple precursors) and poor transfer into the gas phase. Furthermore, for an insulin assay to be readily implemented into laboratories, it must provide high throughput (several hundred samples a day), adequate dynamic range and utilize a simple sample preparation step.

The most sensitive assays to date have been based on affinity purification, followed by SPE and nano-flow LC. Generally, nano-flow methods do not offer high-throughput and although affinity purification is highly selective it is also less amenable to automation. Moreover a recent report on the development of an insulin analog [43] found that an assay based on immunoaffinity (IA) capture could be subject to anti-drug antibody (ADA) effects. Kelley *et al.* [44] demonstrated the need for assays absent of an IA component which is reliant on ligand-binding.

Section I of this chapter and the resultant publication[39] showed feasibility for the simultaneous measurement of insulins in human plasma using LC-MS/MS. However, targeting human insulin and lispro (Humalog[®]) and the need to achieve detection limits required for clinical samples (i.e. ~ 50 pg/mL.) prompted an entirely new approach. The improved method described in this section is based on six steps. These included precipitation, mixed-mode solid phase extraction, column trapping and back elution, followed by a separation using a fused core C₁₈ column with positively charged surface and MS-MS fragmentation based detection. Figure 5.1 shows the molecular structures for the six insulins, including human insulin and insulin lispro, which were added to the improved analysis described in this section. Section I of this chapter served to highlight and reinforce that each analytical step was going to be crucial to achieve the fasting level sensitivity described herein. Previous reported methods which achieved this sensitivity relied on affinity sample preparation or two separate validations and/or the analysis of human insulin only using the reduced B-chain as a surrogate [11, 18-20, 27, 31, 40, 41].

In order to avoid the use of affinity purification, alternatives were considered. One such option is the use of multidimensional LC. In proteomic analyses, multidimensional LC

has long been a standard tool used to effectively identify peptides, improve peptide mapping coverage, and to separate the complex peptide mixture resulting from various proteolytic digests of a proteome[45]. In the bioanalytical arena multidimensional chromatography has also successfully been implemented to improve assay specificity and sensitivity. For example, Ismaiel *et al.* [46] demonstrated the effective separation and removal of phospholipids to reduce matrix effects and improve sensitivity in an assay for octreotide. Chen et al [40] applied an on-line extraction and parallel column regeneration approach in the analysis of reduced human insulin. Dual reversed-phase (RP) column or RP-HILIC systems, described by Rogatsky *et al.* [47] and Liu *et al.* [48], also reduced matrix effects and improved sensitivity. For these reasons, multidimensional LC seemed a reasonable approach to both improve sensitivity and reduce interferences for intact insulin analysis. In this investigation a multidimensional platform was designed that achieved the selectivity and detection limits needed for the simultaneous analysis of human insulin and five recombinant analogues.

5.6 Experimental for Improved Insulin Assay

5.6.1 Chemicals and Reagents

Lantus[®] (insulin glargine) and Apidra[®] (insulin glulisine), both manufactured by Sanofi-Aventis, were used as formulated. Levemir[®] (insulin detemir) and NovoLog[™] (insulin aspart), both manufactured by Novo Nordisk, were also used as formulated. Humalog[®] (insulin lispro), manufactured by Eli Lilly and Company, was also used as formulated. Human insulin and bovine insulin were purchased from Sigma-Aldrich, St. Louis, MO. A representation of the analog sequences and how they differ from human

insulin is depicted in Figure 5.1. Human plasma was purchased from Biological Specialty Corporation, Colmar, PA. For specificity testing (determination of matrix factors), 6 different lots of normal control human plasma were used. Lots 82111 and 82740 were female, lot 57901 was male, and lots 70193, 57298, and X1803C were pools. Rat plasma was purchased from Equitech Bio, Kerrville, TX. Water for mobile phase and sample preparation was obtained from a Milli-Q lab water system, (Millipore, Billerica, MA). Acetonitrile (ACN), methanol, and formic acid (concentrated solution, 99 %) were purchased from Fisher Scientific (Fair Lawn, NJ). All other chemicals and reagents were purchased from Sigma (St. Louis, MO) unless otherwise stated.

5.6.2 Preparation of samples, calibration standards and quality control samples

For all formulations, the insulin analogs are present at 100 IU/mL. For Lantus[®], Apidra[®], NovoLog[™], and Humalog[®], 100 IU is equal to 3.638, 3.49, 3.5 and 3.5 mg insulin glargine, insulin glulisine, insulin aspart, and insulin lispro, respectively, per mL (values as stated in product inserts). For Levemir[®], 100 IU insulin detemir is equivalent to 14.2 mg. This value was obtained from the European Medicines Agency webpage containing product information for Levemir[®][49]. The lyophilized human insulin was dissolved in 0.01 M HCl to generate a concentrated stock at 1 mg/mL. A diluent consisting of 30/10/60 CH₃OH/CH₃COOH/H₂O v/v/v plus 0.05% rat plasma was prepared. The various insulin formulations or stocks were diluted serially in the above diluent and then combined to generate a working solution containing all six at a concentration of 1 µg/mL. Bovine insulin was used as the internal standard (IS) and was prepared in the above diluent at a concentration of 100 ng/mL to be used for spiking. For standard curve and quality control (QC) samples, human plasma was initially fortified with the combined insulin working

solution to a final concentration of 50 ng/mL of each of the 6 insulins. The 50 ng/mL plasma stock was then diluted with control human plasma to generate appropriate standard curve and QC samples. Standard curve samples were prepared at the following concentrations: 50, 100, 200, 500, 1000, 2000, 5000, and 10,000 pg/mL in human plasma. QC samples were prepared at 150, 750, 2500, and 7500 pg/mL in human plasma. Blank human plasma samples were also extracted for determination of limit of detection (LOD) and lower limit of quantification (LLOQ.)

5.6.3 Sample pre-treatment and solid-phase extraction conditions

Protein precipitation (PPT) pre-treatment:

A 250 μ L aliquot of each patient sample, standard curve point, QC or blank was transferred to an Eppendorf tube and 25 μ L of IS solution was added. Samples were vortexed, followed by addition of 250 μ L of 1:1 (v:v) ACN: CH₃OH containing 1 % acetic acid. Samples were mixed to precipitate and centrifuged at 13,000 rcf for 10 minutes. The supernatant was removed and added to a 2 mL plate containing 900 μ L 5 % NH₄OH in water.

Solid phase extraction (SPE):

The wells of a strong anion exchange (Oasis MAX) μ Elution plate were first conditioned with 200 μ L methanol, followed by equilibration with 200 μ L water. The entire diluted PPT supernatant was loaded onto the extraction plate in two steps of approximately 700 μ L each. Samples were washed with 200 μ L 5 % NH₄OH in water, followed by 200 μ L 5 % methanol and 1 % acetic acid in water. Bovine and human insulin and its analogs were eluted with 2 by 25 μ L 60/30/10 methanol/water/acetic acid and diluted with 50 μ L water.

5.6.4 Collection and Handling of Patient Samples

Venous blood was collected (Ethics number for the study LREC 10/H0802/86 and according to established practice [50, 51]) from 22 patients into commercially available standard anticoagulant-treated (EDTA) tubes. Blood samples were centrifuged at 1500-2000 x g for 15 minutes and plasma was transferred to sterile cryovial storage tubes and stored at -80 °C. On the day of analysis, samples were thawed at room temperature and immediately re-frozen after an appropriate aliquot was removed for analysis.

5.6.5 Chromatographic Conditions

Samples were maintained at 10°C in the autosampler. 30 µL of SPE eluate were chromatographed using an ACQUITY UPLC I-Class with 2D Technology, configured for at-column dilution and trap and back elution, see Figure 5.12. Insulins were first trapped on an XBridge C18 IS, 3.5 µm, 2.1 X 20 mm column and then separated on a CORTECS UPLC C18+ 1.6 µm, 2.1 x 50 mm analytical column. The gradient elution solvents were 0.1 % HCOOH in water (mobile phase A) and 0.1 % HCOOH in acetonitrile (mobile phase B.) The trapping/loading solvent was 85:15 mobile phase A:B with a flow rate of 0.1 mL/min. The dilution solvent was 100 % mobile phase A with a flow rate of 0.3 mL/min. With the valve in position 1, the sample was loaded onto the head of the trap column for 2 minutes with the combined flow of the trapping and dilution solvents, the valve was then switched to position 2 and the analytes were back-eluted onto the analytical column maintained at 60 °C, with a linear gradient from 15 to 40 % B over 4 minutes at 0.25 mL/min.

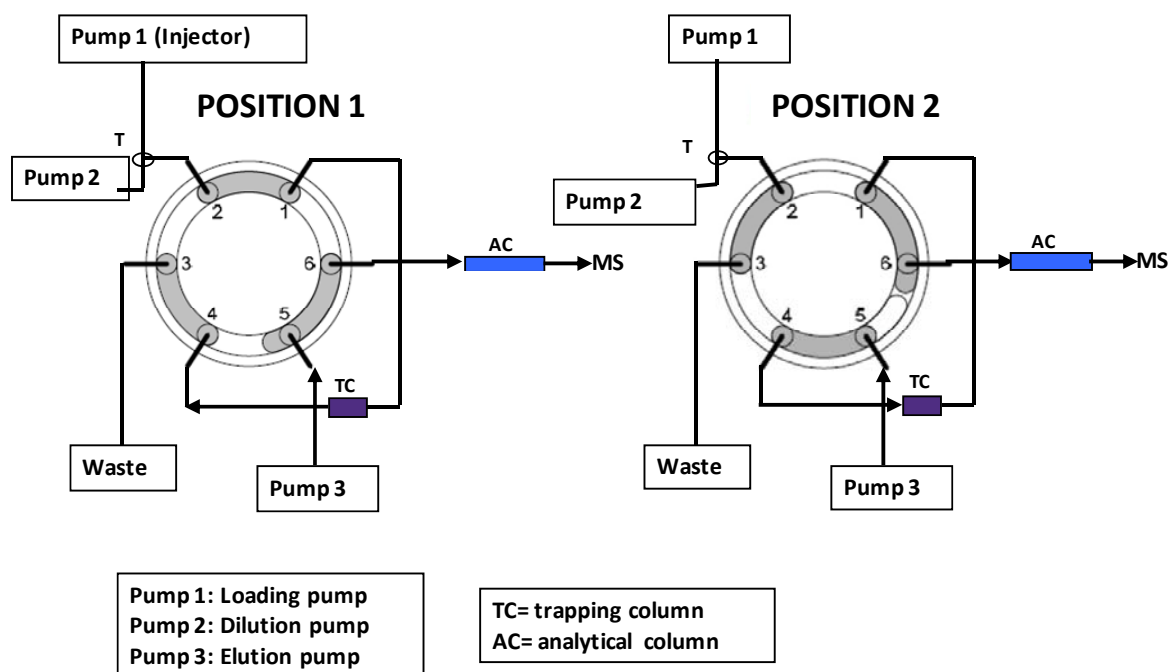


Figure 5.12 ACQUITY UPLC 2D valve diagram for at-column-dilution (ACD) and trap and back elute chromatography

5.6.6 Mass spectrometry and Software

For each peptide and the IS, collision induced dissociation (CID) products of multiply charged precursors were detected in positive ion multiple reaction monitoring (MRM) mode using a Waters Xevo™ TQ-S mass spectrometer (Milford, MA). The electrospray voltage, source temperature, desolvation temperature and desolvation gas flow rate were 3.0 kV, 150 °C, 500 °C and 1000 L/Hr, respectively. Primary and secondary MRM transitions used for quantification and qualification, respectively, for each peptide and the IS as well as their respective cone voltages, collision energies, precursor charge states, and fragment identification (where known) are summarized in Table 5.1. MassLynx instrument control software, version 4.1, was used for data acquisition. All peak area

integration, regression analysis and sample quantification was performed using TargetLynx. Peak area ratios (PARs) of the insulin analogs and the bovine insulin internal standard were determined and calibration curves generated for each of the analogs. Insulin analog concentrations in QC samples were determined from their PARs against their respective calibration lines. Calibration curves, prepared in human plasma, were constructed by applying a 1/concentration weighted linear regression model. All QC sample concentrations were then calculated from their PARs against their respective calibration lines.

5.7 Results and Discussion

5.7.1 Sample pre-treatment and extraction

Section I of this chapter described a simple reversed-phase SPE sample preparation method. This method however, did not reduce endogenous background enough to allow for the achievement of adequate detection limits nor the quantification and differentiation of human insulin and insulin lispro. Therefore, a more selective sample preparation method needed to be devised. The data in Chapter 2 established that protein precipitation (PPT) may be used to selectively eliminate high abundance proteins. It was theorized that this might improve specificity for insulin analysis. To test this, a protein precipitation step was investigated prior to SPE to both clean-up the sample and disrupt protein binding. Both acetonitrile (ACN) and methanol (MeOH) with and without acetic acid, formic acid, or NH_4OH were evaluated for insulin recovery. In addition, both 1:1 and 2:1 ratios of organic to plasma were tested. In all cases, recovery was significantly lower when a 2:1 ratio was used. It is believed that the higher ratio results in insulin loss due to partial precipitation of the insulins as previously described [29] and as observed in the teriparatide analysis

described in Chapter 3. The combination of a mixture of ACN and methanol, modified with acetic acid, provided the best recoveries (80-100 %) for the insulins from human plasma. Figure 5.13 summarizes results from all pre-treatment conditions evaluated, and supports the final choice of pre-treatment. In general, recovery is about twice as high when a 1:1 ratio of organic to plasma was used in precipitation than when a 2:1 ratio was used. This is consistent with observations in Chapter 2, where a similar study was performed for teriparatide analysis. There was no specific trend relating to the use of acidic or basic modifier as neither consistently produced higher recoveries than the other. SPE eluates with and without the PPT pre-treatment were examined for cleanliness, and it was found that PPT pre-treatment prior to SPE, reduced background by as much as 80 % during various chromatographic segments, demonstrating its importance.

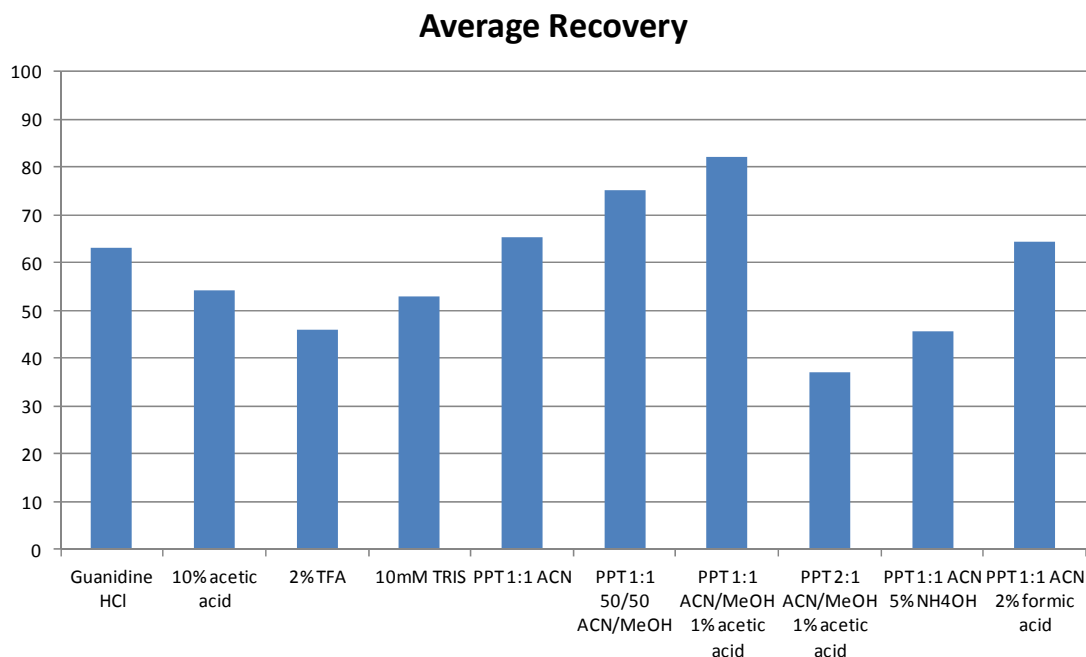


Figure 5.13 Average insulin recovery using different precipitation and pretreatment conditions

The reversed-phase SPE described in Section I of this chapter was sufficient to extract four insulin analogs (glargine, glulisine, detemir, and aspart) from human plasma[39]. This approach however was inadequate for comprehensive, sensitive insulin analysis as the remaining endogenous background was very high and quantification of human insulin and lispro below 1 ng/mL was not possible. RP clean-up achieved detection limits in the range of 200-500 pg/mL for the analogs. However, for clinical applications these insulins should be accurately quantified down to levels of ~ 50 pg/mL., as demonstrated by pharmacokinetic profiles [3, 52-54] and known fasting insulin levels [55]. Mixed-mode (MM) sorbents have been shown not only to reduce matrix effects, but also to provide significantly more selective elutions [56]. Data in Chapter 2 emphasized the importance of its use for peptide extractions. Strong anion exchange (SAX) was chosen as insulins were negatively charged at high pH (≥ 9). Low pH (≤ 3) was also investigated with cation exchange resins, however experiments with both weak and strong mixed-mode cation exchange sorbents yielded reduced recovery when compared to the SAX sorbent. Since an LLOQ of 50 pg/mL was readily achieved on the SAX-MM sorbent, this phase was chosen.

5.7.2 Mass Spectrometry of Insulin and Analogs

Peptides are challenging molecules to analyze by LC/MS, however, many of the guidelines summarized in Chapter 2 were applied to the development of this new method. Flow rate impacted the relative abundance of precursors formed, so fine-tuning of the fragmentation at the utilized chromatographic flow rate was performed. First, CID of several of the highest intensity precursors from each insulin was optimized as not all precursors fragmented to the same extent. Specificity of the MRM transition in the final

extracted sample could not be predicted, and was critical to the success of the assay. Therefore at least three to four transitions for each of the insulins were monitored and intensity optimized. Considering the guideline developed in Chapter 2, of particular interest were the higher m/z precursor/fragment pairs, specifically those where the fragment m/z was higher than its precursor. This unique combination most often produced signal with the greatest specificity and lowest background in extracted samples. The MRM transitions for glulisine, detemir, and aspart that were identified in Section I of this chapter were adequate to achieve the required sensitivity using the modified extraction procedure and multidimensional chromatography described in this section. For glargine, the use of MRM m/z 867->984 produced a low level interference detected in several lots of plasma during our specificity testing, therefore an alternative m/z 1011->1179 was tested and chosen, achieving a quantification limit of 50 pg/mL (8.25 fmol/mL). This interference was not found during the proof of concept work as only a single lot of plasma was used in testing. The discovery of the interference in m/z 867-> 984 underlines the importance of specificity testing in multiple lots/sources of biological matrix and also serves to further highlight the importance of higher m/z precursor/fragment pairs.

The primary focus rested on differentiation between human insulin and lispro, and the identification of the most specific precursor and fragment pairs. Human insulin and lispro produce the same precursor pattern (Figure 5.14) and share almost complete overlap in their fragmentation profiles due to a simple reversal in the positions of amino acids 28 and 29 in the B chain (see Figure 5.1).

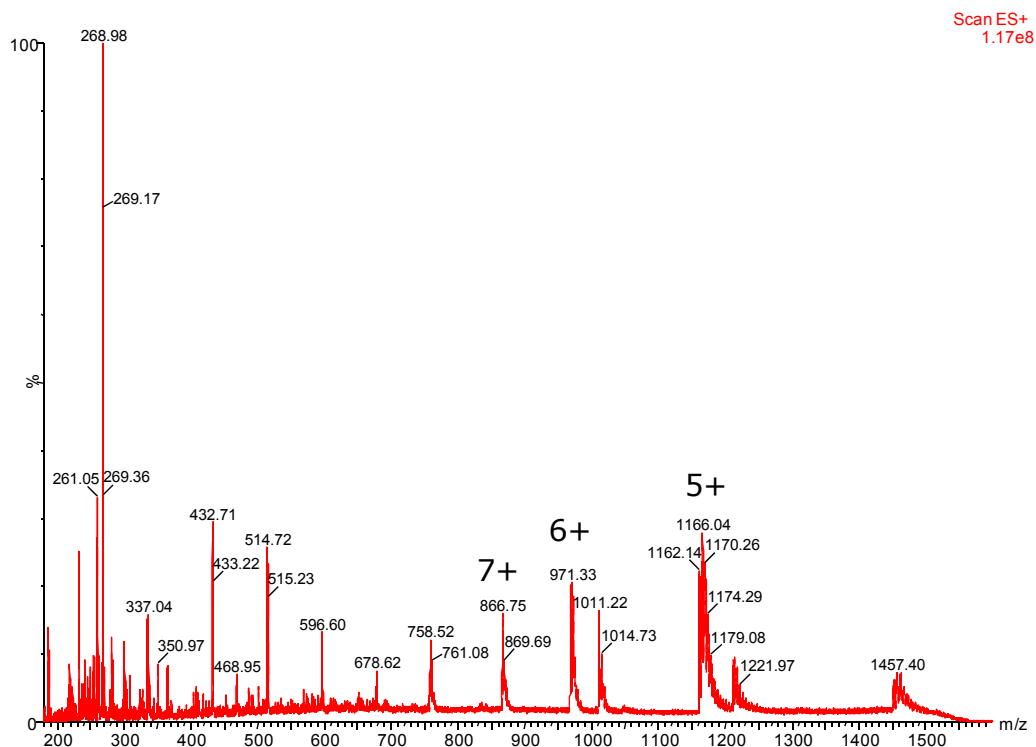


Figure 5.14 MS spectra for human insulin; insulin lispro produces the same precursor mass profile

A single low molecular weight fragment differentiated the two, with human insulin yielding a diagnostic fragment at m/z 226 and lispro producing a characteristic fragment at m/z 217, both arising from cleavage at the last 2 amino acids in the B chain. MSMS spectra are shown in Figure 5.15; fragments used for quantification are highlighted with an asterisk. Although lispro produces a very low level of the $m/z = 226$ product at high concentrations, it did not interfere with this assay under the analytical conditions.

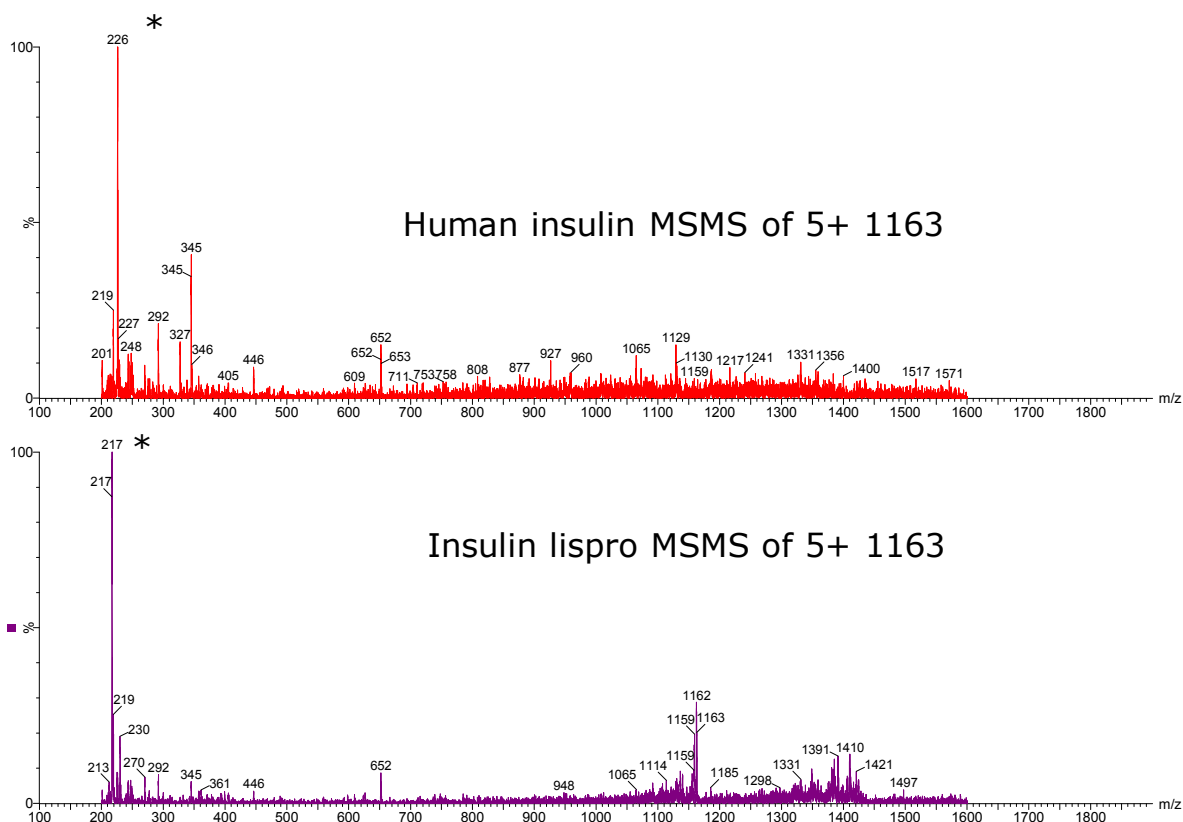


Figure 5.15 MSMS spectra for human insulin and insulin lispro

Higher MS background, which is generally observed when monitoring fragments below $\sim m/z$ 300 (for peptides), made sample preparation and chromatography crucial. In Chapter 2, Figure 2.15 is evidences the value of choosing a higher m/z *precursor*, even if a low m/z *fragment* must be used. In Figure 2.15, although the absolute intensity of the 969 \rightarrow 217 MRM is higher than that of 1163 \rightarrow 217, the signal to noise is greater in the latter case. This effect is magnified further in the presence of matrix. When the influence of precursor choice was examined in human plasma, as Figure 5.16 demonstrates, higher specificity was obtained when the 5+ precursor (m/z 1162, panel A) was chosen versus the 6+ at m/z 968 (panel B).

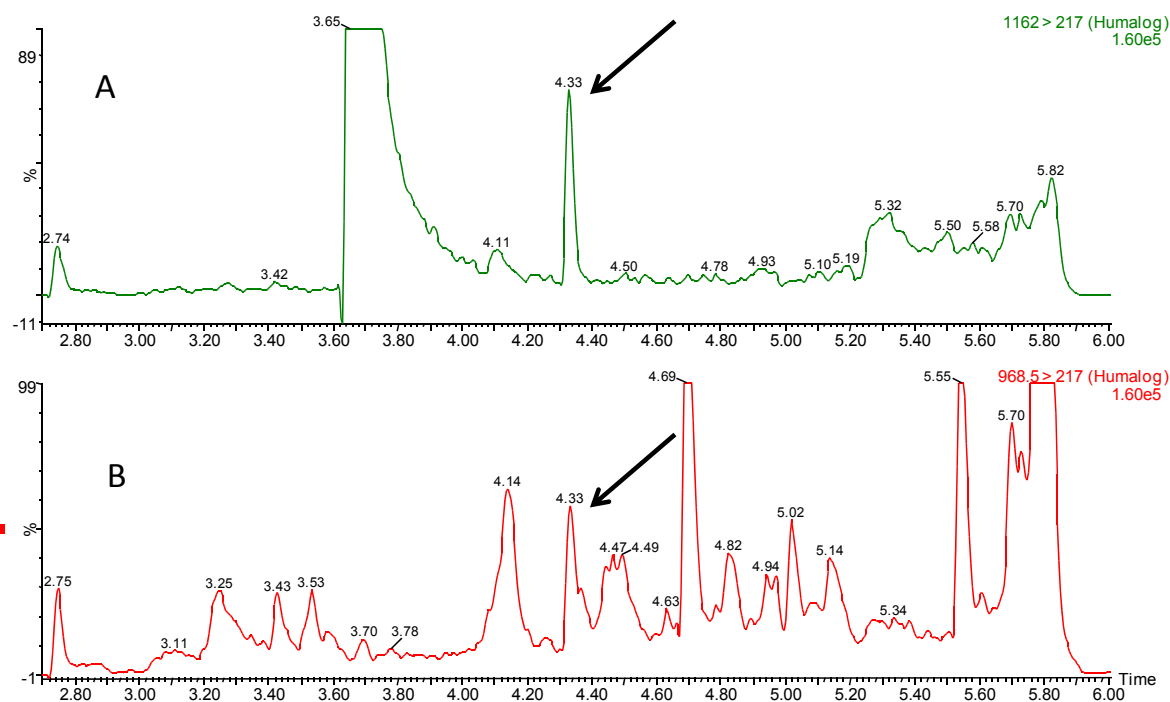


Figure 5.16 Effect of precursor choice on specificity of insulin lispro in extracted human plasma: m/z 1162->217 (A) and m/z 968->217 (B); arrow indicates lispro peak

With the exception of human insulin and lispro, which are only distinguished by mass spectrometry, all other insulins were differentiated from each other and identified based on both retention time and MRM transition. Identity was further confirmed using retention time match to within 2 % and MRM peak area ratio match of the sample against an authentic standard run in the same batch. Figure 5.17 compares extracted ion chromatograms for insulin glargine and lispro detected in patient 20 with the standard run in the same batch. Retention times in the patient sample are identical to the calibration standard. This is in accordance with the criteria required by the World Anti-Doping Agency to evidence the administration of an insulin in a sports sample[38].

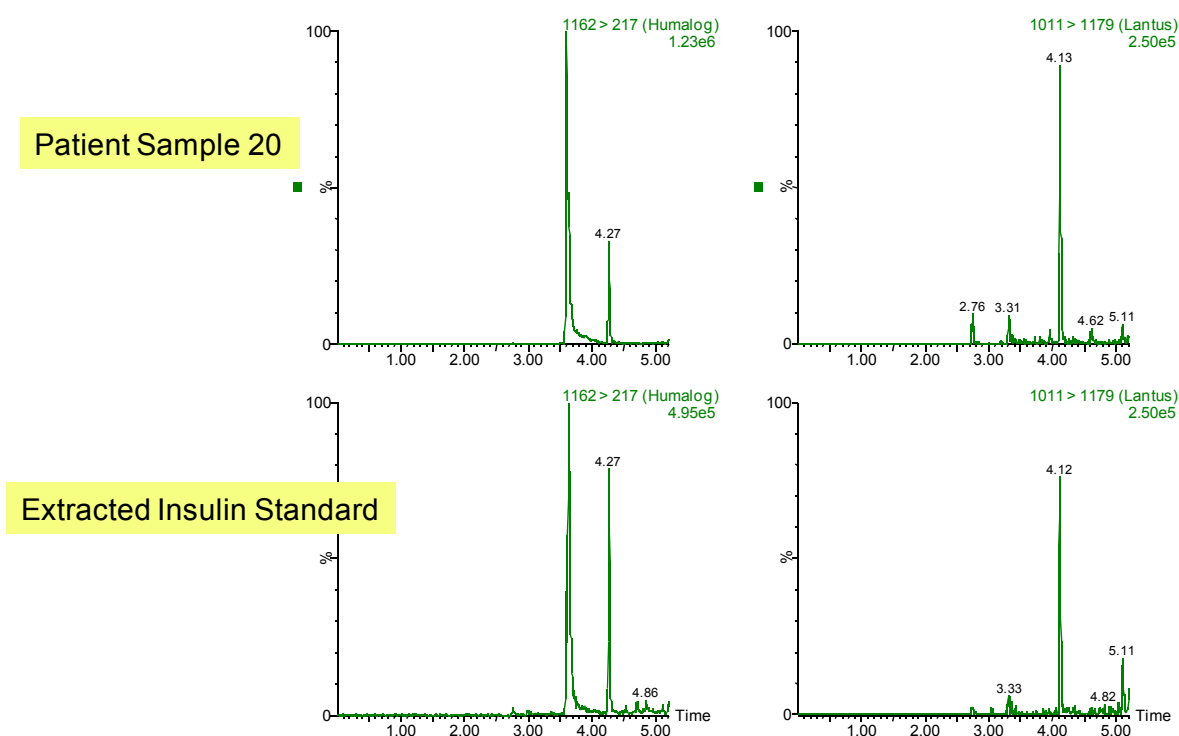


Figure 5.17 Comparison of extracted ion chromatograms for insulin lispro, RT 4.27 (left) and glargine, RT 4.12 (right) from patient sample 20 (top) and an extracted insulin standard (bottom)

5.7.3 Liquid Chromatography

Unlike small molecules, larger peptides and small proteins like insulin suffer from poor mass transfer. Thus, using a column packed with solid-core particles allowed for sharper peak shapes at the higher flow rates typically needed for bioanalytical studies [57, 58]. For insulin and analogs specifically, a column packed with particles containing a low level positive surface charge gives superior peak shapes [39] as shown in Chapter 2. Furthermore, $<2\ \mu\text{m}$ particle column employed uses a flow rate of several hundred $\mu\text{L}/\text{min}$ with high peak capacity[59]. Gilar *et al.* [60] demonstrated a marked increase in peak capacity for peptides using $1.8\ \mu\text{m}$ particles. The CORTECS C_{18}^+ column employed here

combined solid-core particle technology, a low level positive surface charge, and sub-2 μm particles. Using this column, insulin peaks were typically 4 to 4.5 seconds wide at base. In addition, to the narrow peaks 9-40 % higher area counts were observed with the superficially porous, positively charged columns, for the 6 insulins, than when an equivalent fully porous particle column with a positively charged surface was tested. These observations are derived from the data in Figure 5.18. This data is consistent with the column testing performed in Chapter 2.

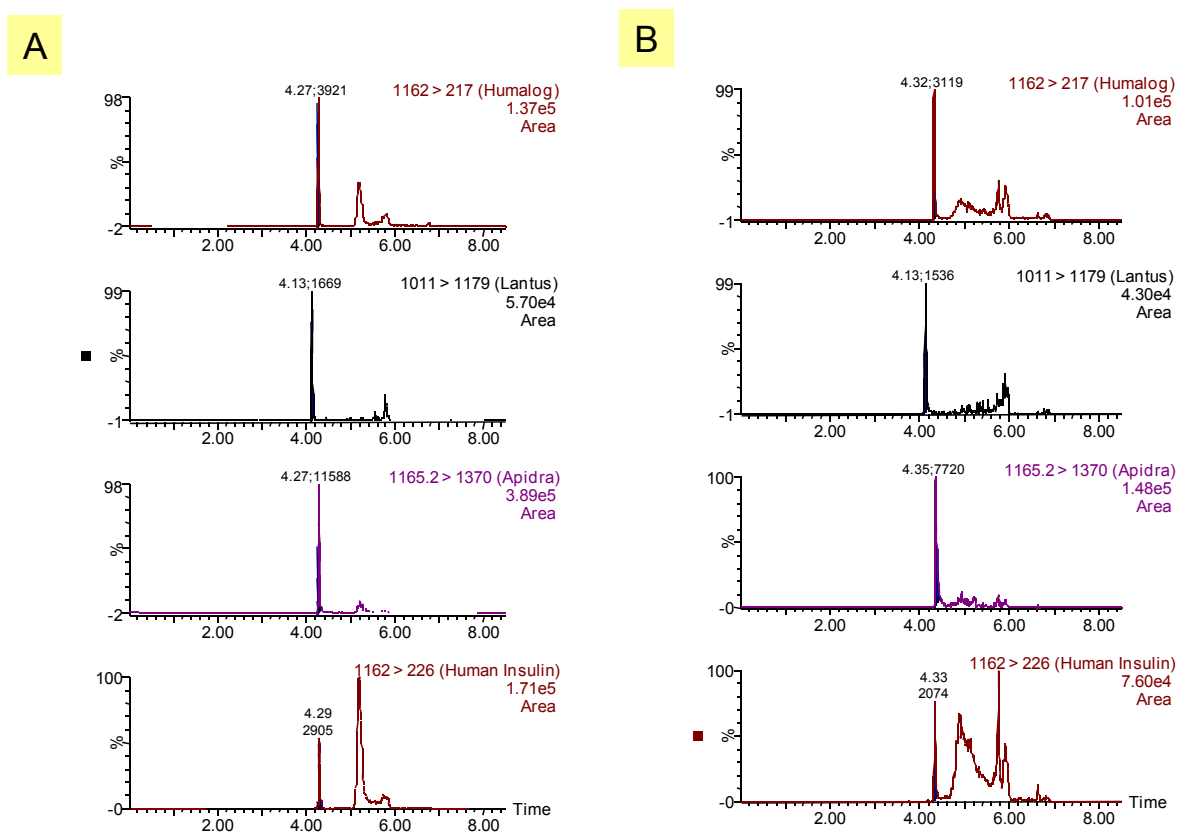


Figure 5.18 A representative comparison of peak areas for insulin and analogs chromatographed on sub-2 μm solid core charged-surface C_{18} columns (A) versus fully porous charged-surface C_{18} columns (B). Peak annotation includes area and retention time

The final separation for human insulin, its analogs, and the internal standard (IS), bovine insulin, is shown in Figure 5.19. Human insulin, lispro, glulisine, aspart and the IS nearly or completely co-elute, while glargine and detemir are both well separated from each other and from all other insulins. Experiments performed on several columns, mobile phases and gradients all failed to eliminate these co-elutions. As this was the case, the 50 mm column and 3 minute gradient (20-65 % B) were used to improve throughput. Though a longer column may have improved resolution between the insulins, good sensitivity and adequate specificity were obtained on the 50 mm column. Ideally one might strive to resolve human insulin and insulin lispro, but the increase in run time that would accompany a 150 mm length column, for example, was not deemed an acceptable trade-off.

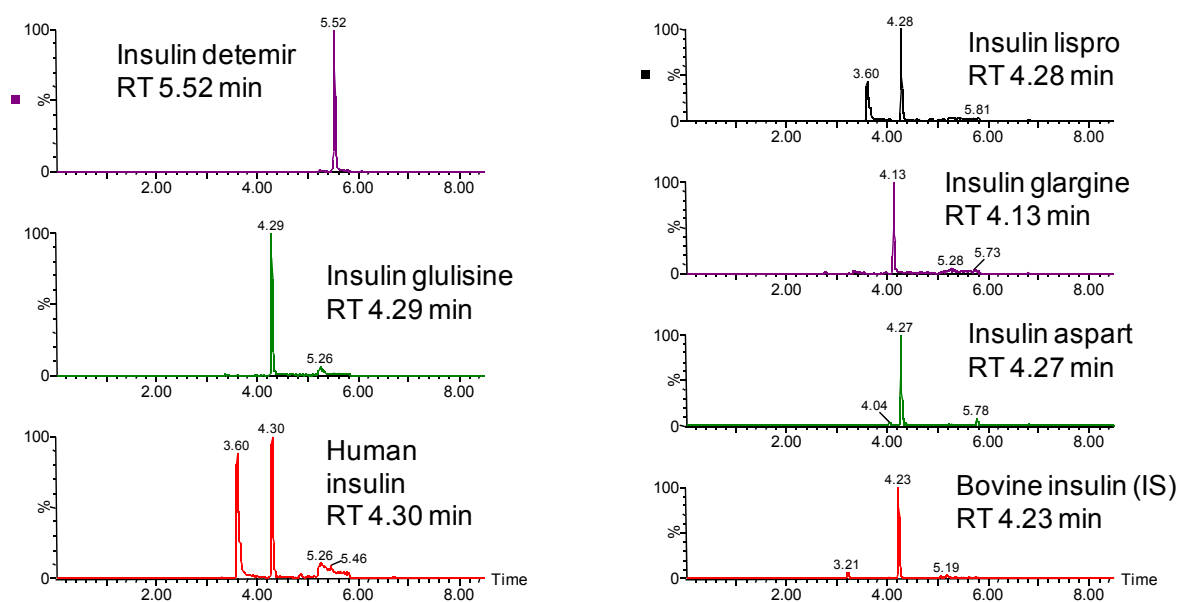


Figure 5.19 UPLC-MS/MS Chromatograms of human insulin, insulin analogs, and bovine insulin (IS)

A multidimensional system provided the increased selectivity and reduced background necessary to use low molecular weight fragments for human insulin and lispro as well as to achieve the required lower detection limits for all insulin analogs. Initially, it was hypothesized that a heart-cut configuration (two analytical columns and selected window fractionation) would provide the best method. However, several column chemistries, (C4, C8, 300Å C18) and two pHs (pH 3 and pH 11) were tested for the first dimension analytical column. Poor sensitivity was observed at high pH and the insulin analogs did not elute closely enough together, under any condition, to perform an efficient fractionation from the first column to the second. If detemir were eliminated from the mix, a true heart-cut separation may have been possible. Detemir requires significantly more organic (than the other analogs or human insulin) to elute from both the proposed and tested first dimension and certainly the second dimension chromatographic columns, rendering the use of a narrow fractionation window impossible. For these reasons, an alternative multidimensional LC strategy was employed.

The use of at-column dilution (ACD) onto a 2.1 X 20 mm XBridge C18 column facilitated the higher injection volume of 40 µL and allowed for lower limits of detection. The trapping was followed by back-elution of the insulins under optimized conditions which provided an initial reversed-phase (RP) separation. During trapping, the initial organic mobile phase composition and valve switch timing were of particular importance. Trapping under lower or higher organic composition conditions reduced sensitivity, possibly due to incomplete elution or retention, respectively. Detemir sensitivity was particularly affected when samples were loaded under reduced organic (<15 %) conditions. To improve recovery for detemir the sample was continually eluted from the trap column during 5.5 minutes.

5.7.4 Human Plasma Standard Curve and Quality Control Data: Sensitivity, Linearity, Accuracy and Precision

All curves were linear using the 1/x regression. A summary of standard curve performance for all insulins can be found in Table 5.5.

| Analyte | Std. Curve Range pg/mL | Std. Curve Range fmol/mL | r ² , linear fit, 1/x weighting | Average % accuracy of all points | Max/min Accuracy | Retention Time (min) |
|-------------------|---------------------------|--------------------------------|--|--|---------------------|-------------------------|
| Insulin lispro | 50-10,000 | 8.6-1720 | 0.998 | 99.99 | 90.1 | 4.28 |
| Insulin glargine | 50-10,000 | 8.25-1650 | 0.996 | 99.98 | 85.1 | 4.13 |
| Human insulin | 50-10,000 | 8.6-1720 | 0.996 | 100 | 108.7 | 4.30 |
| Insulin detemir | 200-10,000 | 33.8-1690 | 0.998 | 96.4 | 87.0 | 5.52 |
| Insulin glulisine | 50-10,000 | 8.6-1720 | 0.995 | 100 | 91.5 | 4.29 |
| Insulin Aspart | 100-10,000 | 17.16-1716 | 0.995 | 100 | 114.4 | 4.27 |

Table 5.5 Standard curve ranges, r² values, and mean accuracy for curve points for all compounds

For human insulin, the basal concentration in pooled or individual control plasma was determined by calculating the x-intercept. The basal level of human insulin (average 1940 pg/mL) was then added to the spiked concentration for all standard curve and QC samples, to enable accurate quantification. The lower limit of quantification (LLOQ) was 50 pg/mL (8.3-8.6 fmol/mL) for human insulin, glargine, glulisine, and lispro. A representative LC/MS chromatogram for insulin glargine at the LLOQ and the low QC (150 pg/mL) as compared to blank extracted plasma is shown in Figure 5.20. Similar data for

insulin lispro and glulisine are shown in Figures 5.21 and 5.22, respectively. These figures clearly show the performance improvement using the modified method. A comparison of Figures 5.11 and 5.20 verify that greater than a 10-fold improvement in sensitivity was achieved, from an LLOQ of 500 pg/mL to a 50 pg/mL LLOQ for insulin glargine. A similar comparison of Figures 5.10 and 5.22 exhibit the same performance improvement for insulin glulisine. The analysis of insulin lispro, while not possible using the methods in the proof of concept study, was accurately and precisely quantified, achieving an LLOQ of 50 pg/mL, when the improved method was applied. Quantification of both human insulin and insulin lispro at low levels such as these was made possible primarily through a significant reduction in endogenous background. This was accomplished through a combination of improved sample preparation (including the use of mixed-mode SPE instead of reversed phase only SPE and protein precipitation to remove albumin and other interferences) and trapping, focusing, and isolating the analytes on a trap column prior to the analytical separation. The LLOQs for aspart and detemir were 100 pg/mL (17.2 fmol/mL) and 200 pg/mL (33.8 fmol/mL), respectively. All curves were linear with r^2 values >0.995 using $1/x$ weighting. The mean accuracy for all standard curves points, for all analytes was $>96\%$.

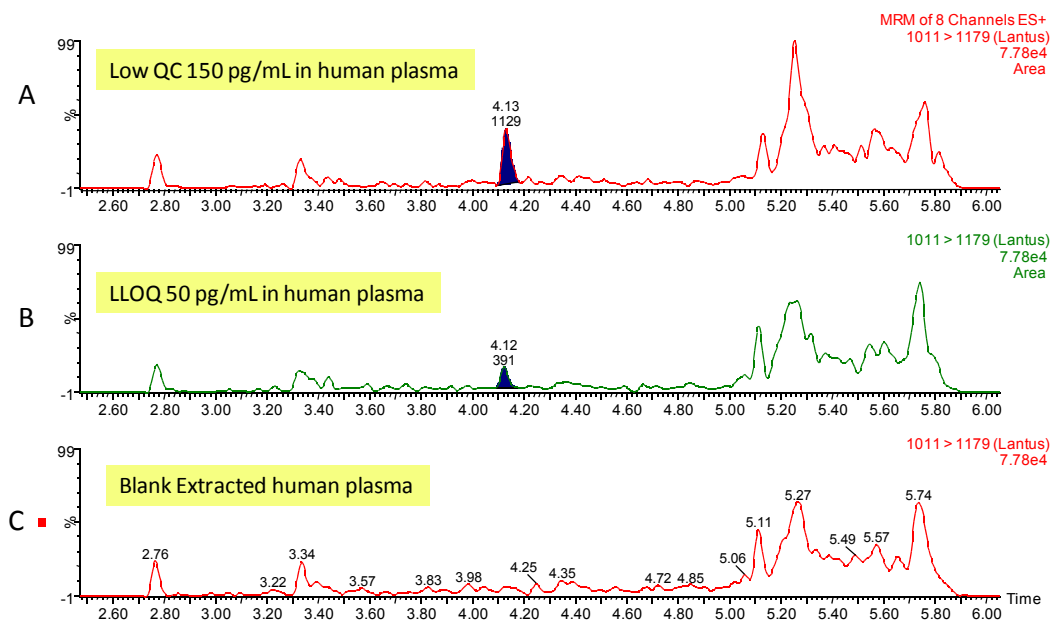


Figure 5.20 LC-MS/MS extracted ion chromatograms for insulin glargine (Lantus) in human plasma at the low QC (A) and LLOQ (B) as compared to blank extracted human plasma (C).

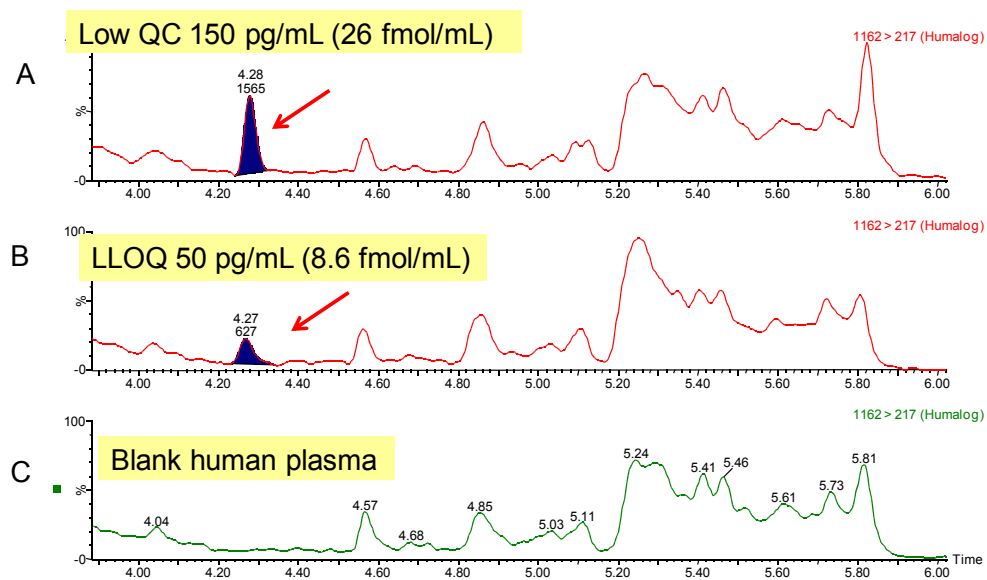


Figure 5.21 LC-MS/MS extracted ion chromatograms for insulin lispro (Humalog) in human plasma at the low QC (A) and LLOQ (B) as compared to blank extracted human plasma (C)

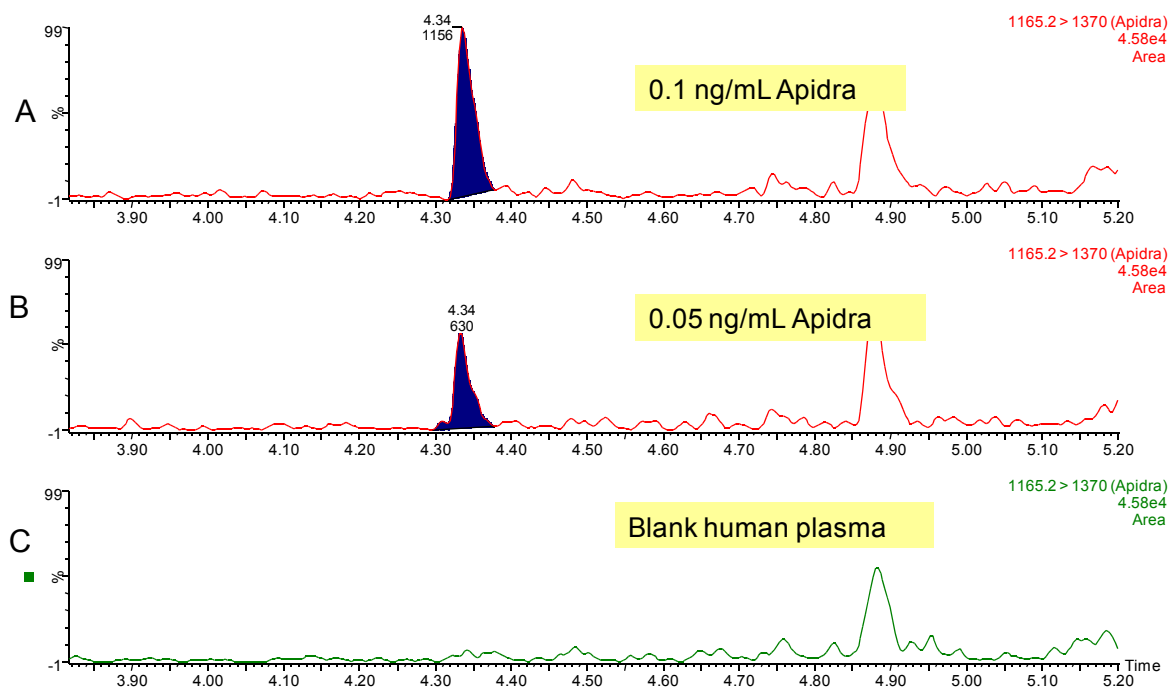


Figure 5.22 LC-MS/MS extracted ion chromatograms for insulin glulisine (Apidra) in human plasma at 100 pg/mL (A) and LLOQ (B) as compared to blank extracted human plasma (C)

Inter- and intra-day accuracy and precision were calculated for all QC samples. Representative summary statistics for insulin glargine, lispro, and human insulin can be found in Tables 5.6, 5.7 and 5.8, respectively. All other analogs exhibited similar performance. For insulin glargine, inter- and intra- day accuracy ranged from 95-103 % and 95-112 %, respectively. For insulin lispro, the same ranges were 96-103 % and 97-110 %. Human insulin inter- and intra-day accuracies were 92-104 and 90-101 %, respectively. QC sample precision was excellent with average inter- and intra- day values ranging from 2.5 to 8.3 %. These values comfortably meet regulatory criteria for bioanalytical method validation for chromatographic assays[61-63].

Insulin Glargine

Inter-day n=9

| QC conc. (pg/mL) | Mean Calc. Conc. | Std Dev | % CV | Mean Accuracy |
|---------------------|---------------------|---------|------|------------------|
| 150 | 150.1 | 18.7 | 12.4 | 102.7 |
| 750 | 718.4 | 47.3 | 6.6 | 95.8 |
| 2500 | 2369.3 | 131.2 | 5.5 | 94.8 |
| 7500 | 7648.5 | 511.3 | 6.7 | 102.0 |

Intra-day n=3

| QC conc. (pg/mL) | Mean Calc. Conc. | Std Dev | % CV | Mean Accuracy |
|---------------------|---------------------|---------|------|------------------|
| 150 | 167.4 | 16.6 | 9.9 | 111.6 |
| 750 | 757.7 | 62.4 | 8.2 | 101.1 |
| 2500 | 2378.0 | 184.9 | 7.8 | 95.1 |
| 7500 | 7949.5 | 257.9 | 3.2 | 106.0 |

Table 5.6 . Inter- and intra-day accuracy and precision for QC samples for insulin glargine.

Insulin Lispro

Inter-day n=9

| QC conc. (pg/mL) | Mean Calc. Conc. | Std Dev | % CV | Mean Accuracy |
|---------------------|---------------------|---------|------|------------------|
| 150 | 144.0 | 17.5 | 12.2 | 96.0 |
| 750 | 721.8 | 32.3 | 4.5 | 96.2 |
| 2500 | 2447.1 | 202.9 | 8.3 | 97.9 |
| 7500 | 7697.5 | 634.8 | 8.2 | 102.6 |

Intra-day n=3

| QC conc. (pg/mL) | Mean Calc. Conc. | Std Dev | % CV | Mean Accuracy |
|---------------------|---------------------|---------|------|------------------|
| 150 | 164.6 | 14.9 | 9.1 | 109.8 |
| 750 | 748.2 | 19.8 | 2.6 | 99.8 |
| 2500 | 2417.6 | 230.4 | 9.5 | 96.7 |
| 7500 | 8215.4 | 243.1 | 3.0 | 109.5 |

Table 5.7 Inter- and intra-day accuracy and precision for QC samples for insulin lispro.

Human Insulin Avg basal level was 1937 pg/mL
Inter-day n=9

| QC conc. (pg/mL) | Mean Calc. Conc. | Std Dev | % CV | Mean Accuracy |
|---------------------|---------------------|---------|------|------------------|
| 150 | 1915.1 | 125.4 | 6.5 | 92.0 |
| 750 | 2542.5 | 141.0 | 5.5 | 94.8 |
| 2500 | 4326.0 | 146.7 | 3.4 | 97.6 |
| 7500 | 9819.0 | 960.3 | 9.8 | 104.0 |

Intra-day n=3 Basal level was 1872 pg/mL

| QC conc. (pg/mL) | Mean Calc. Conc. | Std Dev | % CV | Mean Accuracy |
|---------------------|---------------------|---------|------|------------------|
| 150 | 2056.5 | 16.7 | 0.8 | 90.2 |
| 750 | 2506.3 | 46.6 | 1.9 | 99.3 |
| 2500 | 4269.8 | 206.4 | 4.8 | 101.3 |
| 7500 | 10233.2 | 265.2 | 2.6 | 100.3 |

Table 5.8 Inter- and intra-day accuracy and precision for QC samples for human insulin.

5.7.5 Specificity

Matrix factors and CVs of matrix factors for all analogs were calculated in 6 separate sources of normal control human plasma (see the experimental section for details) as outlined in the 2007 AAPS white paper [61]. The CVs of the matrix factors were 12.3, 11.6, 11.8, 9, and 7.7 % for insulin detemir, glargine, aspart, glulisine, and lispro, respectively, well below the recommended criteria of <15% CV[64].

In addition, a study was performed to assess the impact of relatively high levels of human insulin, such as one might expect to find in type II diabetic patients, on the assay specificity. This is particularly important for two reasons. First, not all insulins are chromatographically resolved from one and another. Second, due to the use of a nominal mass instrument (triple quadrupole) and the high degree of sequence homology between the

analogs themselves, and with human insulin, there exists the possibility of MS overlap in some of the transitions. For this test, plasma samples were fortified to a final concentration of 5 ng/mL with all of the analogs. A subset of these samples was also spiked with human insulin at 200 times greater concentration, to a final concentration of 1 µg/mL human insulin. All samples were then pretreated, extracted and quantified. There was no significant change in area counts for any of the analogs when human insulin was present in high concentration.

5.7.6 Analysis of Patient Samples

Twenty-two venous blood samples were collected from patients and were comprised of patients with Type I and one Type II diabetes (on a variety of individual and combination insulin therapies) as well as normal controls. In a blind study, human insulin and/or its analogs were detected in the samples and calculated concentrations are shown and summarized in Table 5.9. The analysis revealed that most patients received a combination of long and fast acting analog treatments. (No patient was treated with insulin glulisine). In all but a single case, insulin detection was in agreement with dosing regimes. In two instances, insulin glargine was administered but detected below LLOQ. Below LLOQ detection was perhaps due to the low circulating levels of glargine and the sample collection time relative to dosing as glargine is dosed once a day. Perhaps more importantly, glargine is rapidly enzymatically converted into its major metabolite M1[65], which is likely to be the primary reason that glargine itself was not detected in all dosed subjects. Patient #1 received insulin aspart, however it was not detected by the assay. As aspart reaches peak serum levels within

an hour post dose[66] and rapidly declines from that point, it is also possible that sampling time relative to dosing was a the factor for the detection failure.

Patient 22 represents the sole case where detection did not correlate with recorded dosing. Levemir was detected, however dosing records indicated that only Lantus and Humalog were dosed.

Low levels of human insulin, an average of approximately 200 pg/mL, were detected in most Type I diabetic patients. In patient #4, a Type II diabetic, 4490 pg/mL human insulin was detected. A shortcoming of this method was highlighted by Patients # 9 and 19 who were dosed with Insulatard® and Humulin®, respectively. These two insulins were detected as “human insulin” since this current assay does not distinguish these recombinant forms from the endogenous insulin with which they have an identical peptide sequence. A possible future modification to this method would be to add C-peptide, the precursor to endogenous human insulin. Its presence or lack thereof would enable identification of human insulin (C-peptide present) or one of the recombinant forms (C-peptide absent).

| | Conc. (pg/mL) | Conc. (pg/mL) | Conc. (pg/mL) | Conc. (pg/mL) | Conc. (pg/mL) | Conc. (pg/mL) |
|-----------|------------------|-------------------|--------------------|-------------------|---------------|--------------------|
| Sample ID | Humalog (lispro) | Lantus (glargine) | NovoRapid (aspart) | Levemir (detemir) | Human insulin | Apidra (glulisine) |
| 1 | | 115 | n/d | | 206 | |
| 2 | 855 | | | 9402 | 253 | |
| 3 | | 597 | 1813 | | 341 | |
| ¥4 | | | 4056 | | 4486 | |
| 5 | | n/d | 118 | | 188 | |
| 6 | | 147 | 702 | | 222 | |
| 7 | 615 | 49 | | | 231 | |
| 8 | | 212 | 1229 | | 247 | |
| ⌘9 | | | | | 5567 | |
| 10 | | | 178 | 3960 | 391 | |
| 11 | | | 2439 | 116106 | 283 | |
| 12 | 266 | § 31 | | | 181 | |
| 13 | | 138 | 1546 | | 189 | |
| 14 | 451 | | | 125 | 213 | |
| 15 | | | | | 218 | |
| 16 | | | 289 | 32280 | 209 | |
| 17 | | n/d | 455 | | 191 | |
| 18 | 828 | § 34 | | | 234 | |
| ⌘19 | | | | | 1342 | |
| 20 | 1494 | 1526 | | | 598 | |
| 21 | | | 1024 | | § | |
| 22 | 1478 | 131 | | *657 | 296 | |

n/d = dosed, but not detected

* = detected but not on dose sheet

§ = below LLOQ

¥ = type II diabetic

⌘ = dose with Insulatard® and Humulin®

Table 5.9 Calculated concentrations of human insulin and/or its analogs detected in patient samples.

Note: for those values that fall outside of the reported concentration range, samples were diluted as required and appropriate dilution QC's prepared

5.8 Conclusions on the Use of Multidimensional LC and Improved Sample Preparation for Insulin Quantification

Using analytical scale chromatography and a 96-well SPE sample prep, this method simultaneously quantifies human insulin and 5 analogs with high throughput, and reaches detection limits which are equivalent to those previously achieved using immuno-precipitation and nano-scale chromatography.

The method is divided in six steps. Protein precipitation (1:1) with 1 % acetic acid acetonitrile:methanol resulted in 80-100 % recovery with minimal insulin precipitation. Mixed-mode strong anion SPE provided an additional layer of selectivity and facilitated the use of the low m/z MS fragments that were necessary to distinguish human insulin and lispro. The use of multidimensional trapping and back dilution with a XBridge C18 trap column and further separation on a sub-2 μm solid-core, charged-surface column provided significantly improved sensitivity and efficiency for insulin analogs enabling quantification limits down of 50 to 200 pg/mL (8.3-33.8 fmol/mL or 1.4-5.6 $\mu\text{IU/mL}$) for the 6 insulins, extracted from 250 μL human plasma.

All FDA criteria[64] for accuracy and precision of the method were achieved for this assay. Average accuracies for standard curve points and QC samples were >92 %, with most being close to 99 %. Inter- and intra-day precision for all QC samples was better than 7.5 %. CVs of matrix factors across 6 lots of human plasma were <15 %, further supporting the selectivity of the method. Furthermore, qualitative identification criteria were met showing that, with further validation, this is a possible method for forensic and sports anti-doping analysis.

To obtain the required level of specificity and sensitivity for rapid and routine multi-insulin analysis in plasma, many independent factors from the various analytical stages were studied and carefully optimized. For clarity, an overall summary of the final analytical workflow, detailing specific contributions of the various individual technical components to this method, is summarized in Figure 5.23.

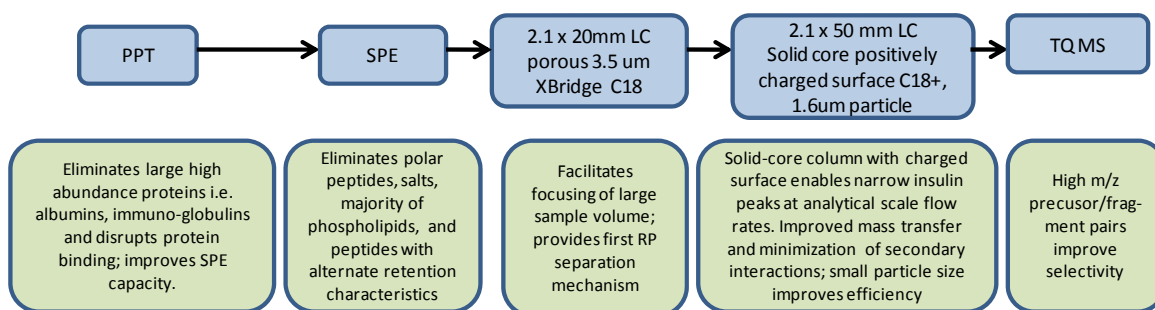


Figure 5.23 Overall method workflow: contribution of individual steps to final performance

5.9 References

1. LaSalle, J.R. and R. Berria, *Insulin therapy in type 2 diabetes mellitus: a practical approach for primary care physicians and other health care professionals*. J Am Osteopath Assoc, 2013. 113(2): p. 152-62.
2. Presswala, L. and J. Shubrook, Clinical Diabetes, 2011. 29(4): p. 151-153.
3. Porcellati, F., et al., *Comparison of Pharmacokinetics and Dynamics of the Long-Acting Insulin Analogs Glargine and Detemir at Steady State in Type 1 Diabetes*. Diabetes Care, 2007. 30(10): p. 2447-2452.
4. Lindström, T., C.A. Hedman, and H.J. Arnqvist, *Use of a Novel Double-Antibody Technique to Describe the Pharmacokinetics of Rapid-Acting Insulin Analogs*. Diabetes Care, 2002. 25(6): p. 1049-1054.
5. Marcovina, S., et al., *Standardization of Insulin Immunoassays: Report of the American Diabetes Association Workgroup*. Clinical Chemistry, 2007. 53(4): p. 711-716.
6. Glenn, C. and A. Armston, *Cross-reactivity of 12 recombinant insulin preparations in the Beckman Unicel DxI 800 insulin assay*. Annals of Clinical Biochemistry, 2010. 47(3): p. 264-266.
7. Manley, S.E., et al., *Comparison of 11 Human Insulin Assays: Implications for Clinical Investigation and Research*. Clinical Chemistry, 2007. 53(5): p. 922-932.
8. Moriyama, M., et al., *Performance Evaluation and Cross-Reactivity from Insulin Analogs with the ARCHITECT Insulin Assay*. Clinical Chemistry, 2006. 52(7): p. 1423-1426.

9. Owen, W.E. and W.L. Roberts, *Cross-Reactivity of Three Recombinant Insulin Analogs with Five Commercial Insulin Immunoassays*. Clinical Chemistry, 2004. 50(1): p. 257-259.
10. Sapin, R., et al., *Elecsys Insulin Assay: Free Insulin Determination and the Absence of Cross-Reactivity with Insulin Lispro*. Clinical Chemistry, 2001. 47(3): p. 602-605.
11. Thevis, M., et al., *Doping Control Analysis of Intact Rapid-Acting Insulin Analogues in Human Urine by Liquid Chromatography–Tandem Mass Spectrometry*. Analytical Chemistry, 2006. 78(6): p. 1897-1903.
12. Ackermann, B.L., M.J. Berna, and A.T. Murphy, *Recent advances in use of LC/MS/MS for quantitative high-throughput bioanalytical support of drug discovery*. Curr Top Med Chem, 2002. 2(1): p. 53-66.
13. Jemal, M., *High-throughput quantitative bioanalysis by LC/MS/MS*. Biomed Chromatogr, 2000. 14(6): p. 422-9.
14. Darby, S.M., et al., *A Mass Spectrometric Method for Quantitation of Intact Insulin in Blood Samples*. Journal of Analytical Toxicology, 2001. 25(1): p. 8-14.
15. Kippen, A.D., et al., *Development of an Isotope Dilution Assay for Precise Determination of Insulin, C-peptide, and Proinsulin Levels in Non-diabetic and Type II Diabetic Individuals with Comparison to Immunoassay*. Journal of Biological Chemistry, 1997. 272(19): p. 12513-12522.
16. Nowicka, J., et al., *Comments on 'Measuring insulin in human vitreous humour using LC-MS/MS' by Thevis et al.* Drug Testing and Analysis, 2012: p. n/a-n/a.

17. Rodríguez-Cabaleiro, D., et al., *Pilot Study for the Standardization of Insulin Immunoassays with Isotope Dilution–Liquid Chromatography/Tandem Mass Spectrometry*. Clinical Chemistry, 2007. 53(8): p. 1462-1469.
18. Thevis, M., A. Thomas, and W. Schänzer, *Mass spectrometric determination of insulins and their degradation products in sports drug testing*. Mass Spectrometry Reviews, 2008. 27(1): p. 35-50.
19. Thevis, M., et al., *Measuring insulin in human vitreous humour using LC-MS/MS*. Drug Testing and Analysis, 2012. 4(1): p. 53-56.
20. Thomas, A., et al., *Mass Spectrometric Identification of Degradation Products of Insulin and Its Long-Acting Analogues in Human Urine for Doping Control Purposes*. Analytical Chemistry, 2007. 79(6): p. 2518-2524.
21. Van Uytfanghe, K., et al., *New liquid chromatography/electrospray ionisation tandem mass spectrometry measurement procedure for quantitative analysis of human insulin in serum*. Rapid Communications in Mass Spectrometry, 2007. 21(5): p. 819-821.
22. Porter, K., et al., *Validation of an Immunoprecipitation and Immunoaffinity LC/MS/MS Assay for Intact Human Insulin*, in ASMS2012: Vancouver, BC.
23. Magnes, C., et al., *Strategies for Quantification of Insulin and Insulin analogues by LC MS/MS*, J. Research, Editor.
24. Ho, E.N.M., et al., *Doping control analysis of insulin and its analogues in equine urine by liquid chromatography–tandem mass spectrometry*. Journal of Chromatography A, 2011. 1218(8): p. 1139-1146.

25. Chen, Z. and N. Clarke, *Quantitative Analysis of Insulin by Liquid Chromatography-Tandem Mass Spectrometry*, in *MSACL2012*: San Diego, CA.
26. Pezeshki, A., et al., *Adsorption of peptides at the sample drying step: Influence of solvent evaporation technique, vial material and solution additive*. *Journal of Pharmaceutical and Biomedical Analysis*, 2009. 49(3): p. 607-612.
27. Thomas, A., et al., *Sensitive and fast identification of urinary human, synthetic and animal insulin by means of nano-UPLC coupled with high-resolution/high-accuracy mass spectrometry*. *Drug Testing and Analysis*, 2009. 1(5): p. 219-227.
28. Chambers, E., D. Diehl, and J. Wheaton, *Simplifying Peptide Bioanalysis*. *LCGC: chromatography online*, 2010. The Application Notebook.
29. Ewles, M. and L. Goodwin, *Bioanalytical approaches to analyzing peptides and proteins by LC-MS/MS*. *Bioanalysis*, 2011. 3(12): p. 1379-1397.
30. Zimmet, P., K.G. Alberti, and J. Shaw, *Global and societal implications of the diabetes epidemic*. *Nature*, 2001. 414: p. 782-798.
31. Thomas, A., et al., *Immunoaffinity purification of peptide hormones prior to liquid chromatography-mass spectrometry in doping controls*. *Methods*, 2012. 56(2): p. 230-235.
32. Krein, S.L., et al., *Quality improvement strategies for type 2 diabetes*. *Journal of the American Medical Association*, 2006. 296(22): p. 2680.
33. *International diabetes federation*. Available from: www.diabetesatlas.org/content/diabetes-and-impaired-glucose-tolerance.
34. www.drugpatentwatch.com. 2013.

35. Cai, X.-Y., A. Wake, and D. Gouty, *Analytical and bioanalytical assay challenges to support comparability studies for biosimilar drug development*. *Bioanalysis*, 2013. 5(5): p. 517-520.
36. Marks, V., *Murder by insulin: suspected, purported and proven - a review*. *Drug Testing and Analysis*, 2009. 1((3-4)): p. 162-176.
37. (WADA), W.A.-D.A., *The 2013 Prohibited List 2013*. 2013.
38. Agency, W.A.-D., *Minimum Required Performance Limits for Detection of Prohibited Substances*. Technical Document TD2010MRPL.
39. Chambers, E.E., et al., *Development of a fast method for direct analysis of intact synthetic insulins in human plasma: the large peptide challenge*. *Bioanalysis*, 2012. 5(1): p. 65-81.
40. Chen, Z., et al., *Quantitative Insulin Analysis Using Liquid Chromatography–Tandem Mass Spectrometry in a High-Throughput Clinical Laboratory*. *Clinical Chemistry*, 2013.
41. Hess, C., et al., *Simultaneous determination and validated quantification of human insulin and its synthetic analogues in human blood serum by immunoaffinity purification and liquid chromatography-mass spectrometry*. *Analytical and Bioanalytical Chemistry*, 2012. 404(6-7): p. 1813-1822.
42. Jones, A.R., et al., *Guidelines for reporting the use of column chromatography in proteomics*. *Nature Biotechnology*, 2010. 28(7): p. 654-654.
43. Blackburn, M., et al., *Quantitation of a therapeutic insulin analogue by immuno-affinity extraction – LC-MS/MS*, in *European Bioanalytical Forum 5th Open Meeting* 2012: Barcelona, Spain.

44. Kelley, M., et al., *Theoretical Considerations and Practical Approaches to Address the Effect of Anti-drug Antibody (ADA) on Quantification of Biotherapeutics in Circulation*. The AAPS Journal, 2013. 15(3): p. 646-658.
45. Issaq, H.J., et al., *Multidimensional separation of peptides for effective proteomic analysis*. Journal of Chromatography B, 2005. 817(1): p. 35-47.
46. Ismaiel, O.A., et al., *Determination of octreotide and assessment of matrix effects in human plasma using ultra high performance liquid chromatography–tandem mass spectrometry*. Journal of Chromatography B, 2011. 879(22): p. 2081-2088.
47. Rogatsky, E., et al., *Sensitive Quantitative Analysis of C-Peptide in Human Plasma by 2-Dimensional Liquid Chromatography–Mass Spectrometry Isotope-Dilution Assay*. Clinical Chemistry, 2006. 52(5): p. 872-879.
48. Liu, A., J. Tweed, and C.E. Wujcik, *Investigation of an on-line two-dimensional chromatographic approach for peptide analysis in plasma by LC–MS–MS*. Journal of Chromatography B, 2009. 877(20–21): p. 1873-1881.
49. http://www.ema.europa.eu/docs/en_GB/document_library/EPAR_-_Product_Information/human/000528/WC500036662.pdf, 2013.
50. Karalliedde, J., et al., *Valsartan improves arterial stiffness in type 2 diabetes independently of blood pressure lowering*. Hypertension, 2008. 51: p. 1617-1623.
51. Dessapt, C., et al., *Circulating vascular progenitor cells in patients with type 1 diabetes and microalbuminuria*. Diabetes Care, 2010. 33: p. 875-877.
52. Lepore, M., et al., *Pharmacokinetics and pharmacodynamics of subcutaneous injection of long-acting human insulin analog glargine, NPH insulin, and ultralente*

- human insulin and continuous subcutaneous infusion of insulin lispro*. Diabetes, 2000. 49(12): p. 2142-2148.
53. Lilly, E. *Humalog Package Insert*. 2013; Available from: <http://pi.lilly.com/us/humalog-pen-pi.pdf>.
 54. Porcellati, F., et al., *Pharmacokinetics and Pharmacodynamics of the Long-Acting Insulin Analog Glargine After 1 Week of Use Compared With Its First Administration in Subjects With Type 1 Diabetes*. Diabetes Care, 2007. 30(5): p. 1261-1263.
 55. Bowsher, R.R. and W.L. Nowatzke, *Insights in regulated bioanalysis of human insulin and insulin analogs by immunoanalytical methods*. Bioanalysis, 2011. 3(8): p. 883-98.
 56. Chambers, E., et al., *Systematic and comprehensive strategy for reducing matrix effects in LC/MS/MS analyses*. Journal of Chromatography B, 2007. 852(1–2): p. 22-34.
 57. Kirkland, J.J., et al., *Fused-Core Particle Technology in High-Performance Liquid Chromatography: An Overview*. Journal of Pharmaceutical Analysis, (0).
 58. Wagner, B.M., et al., *Superficially porous silica particles with wide pores for biomacromolecular separations*. Journal of Chromatography A, 2012. 1264(0): p. 22-30.
 59. *Characterization of Protein Therapeutics Using Mass Spectrometry* 2013: Springer.
 60. Gilar, M., et al., *Two-dimensional separation of peptides using RP-RP-HPLC system with different pH in first and second separation dimensions*. Journal of Separation Science, 2005. 28(14): p. 1694-1703.

61. Bansal, S. and A. DeStefano, *Key elements of bioanalytical method validation for small molecules*. The AAPS Journal, 2007. 9(1): p. E109-E114.
62. FDA, *Guidance for Industry: Bioanalytical Method Validation*, C.a. CVM, Editor 2001.
63. FDA and CDER, *Guidance for Industry Bioequivalence Studies with Pharmacokinetic Endpoints for Drugs Submitted Under an ANDA*. 2013.
64. *Guidance for Industry Bioanalytical Method Validation*, C. FDA, CVM, Editor 2001: Rockville, MD.
65. Bolli, G.B., et al., *Plasma Exposure to Insulin Glargine and Its Metabolites M1 and M2 After Subcutaneous Injection of Therapeutic and Supratherapeutic Doses of Glargine in Subjects With Type 1 Diabetes*. Diabetes Care, 2012. 35(12): p. 2626-2630.
66. <http://www.novologpro.com/pharmacology/mechanism-of-action.aspx>, 2013.

Chapter 6

Preliminary Investigations into the Benefits of Integrated Microscale LC for Peptide Quantification

6.1 Introduction

Chapter 1 established that the two major hurdles that LC/MS faces relative to the gold-standard ligand binding assays for the quantification of peptides and proteins in biofluids are sensitivity and sample volume requirements. Chapter 2 of this thesis identified and developed screening methods and guidelines aimed at addressing these very issues in LC/MS analyses. The subsequent chapters applied these principles to quantify several therapeutic and endogenous peptides. However, sample volumes of 100-300 μL were still required and although detection limits described in Chapters 3-5 were adequate for the intended application, a niche remains to be filled whereby available sample volumes are limited to $\leq 100 \mu\text{L}$ and frequently $\leq 50 \mu\text{L}$.

The demand for low sample volume assays is derived from two primary trends. Over the past few years, the bioanalytical industry has seen an increasing interest in microsampling. At the same time, the use of LC/MS in biomarker discovery and validation studies has increased. Both of these trends share a common key requirement, to obtain higher sensitivity from smaller sample volumes.

Microsampling has emerged as an attractive option to traditional methods [1-3] for several reasons. Smaller rodent animal models (i.e. mice versus rats) are being used and there is a strong desire to reduce overall animal usage both from a financial and humanitarian perspective. Naturally, researchers prefer to euthanize as few animals as possible. Also genetically modified rodents (“knock-out” models) used in specific disease testing are extremely costly (in the region of \$5000). The ability to re-use these animals facilitates the investigation of disease models. In addition, if the sample volume required

can be sufficiently minimized, a full PK profile can be obtained from a single animal in contrast to the previous practice of obtaining composite profiles whereby each time point was represented by an animal[2]. This ultimately improves the quality and reproducibility of PK data obtained from rodent models.

Extensions into pediatrics and/or inhaled dose forms or biomarker validation studies where the matrix may be in limited supply such as with exhaled breath condensate[4], also require that assays be developed which require the least amount of sample possible.

One has only to look at the field of proteomics to see that a common way to maximize sensitivity for very small sample volumes is through the use of low flow LC such as nano or capillary flow. Therefore, a natural extension of the work presented in all preceding chapters is to assess the value of low flow LC in further improving sensitivity whilst reducing sample volumes in bioanalytical methods/studies for peptides. In theory, if the particle size and column length are kept constant, reducing the column diameter should significantly increase sensitivity if the same sample volume is injected. This increase in sensitivity is directly related to the ratio of the square of the 2 column diameters i.e. d_1^2/d_2^2 where d_1 is the diameter of the larger column and d_2 is the diameter of the smaller column. In addition to the improvement due to scale[5], low flow LC provides also greater sensitivity versus analytical scale due to reduced matrix effects[6, 7], and improved ionization efficiency[8]. The benefits of capillary scale LC at the 300 μ m scale for the analysis of a small molecule candidate pharmaceutical was demonstrated by Fraser et-al [9], here they demonstrated that a full PK profile could be obtained from a single rodent.

This chapter will investigate the practical aspects of adapting the highly optimized analytical scale methods presented in Chapters 3 and 5 to an integrated microfluidic LC/MS

device. In addition, the interest in diabetes research also prompted an assessment of the value of this technology for the analysis of glucagon. Finally, several small cyclic peptides, representing biosimilars and an endogenous hormone were subjected to the same approach.

6.2 Experimental

6.2.1 Source of Reagents and Preparation of Stock Solutions

Teriparatide and human insulin and its analogs were prepared as described in sections 3.2.1 through 3.2.3 and 5.6.1 through 5.6.3, respectively. Glucagon, desmopressin, octreotide and vasopressin were purchased from Sigma Aldrich (St. Louis, MO). Glucagon stock solutions were prepared in 70/30 water/methanol plus 1% acetic acid and 0.05% rat plasma (added as carrier protein), by volume. Desmopressin, octreotide, and vasopressin stock solutions were prepared in 80/20 water/acetonitrile plus 1% formic acid and 0.05% rat plasma added by volume.

6.2.2 Sample preparation

Human plasma samples were spiked with peptide(s) to an initial starting concentration of 50 ng/mL. Standard curves and QC samples were prepared through serial dilutions of the 50 ng/mL plasma standard with additional control, non-diseased sterile human plasma.

6.2.3 Liquid Chromatography

Analytical scale (2.1 mm ID) chromatographic methods for teriparatide, insulin and analogs, and the cyclic peptide mixture (desmopressin, vasopressin, and octreotide) are described in Chapters 3, 5 and 2, respectively. At the 2.1 mm ID scale, glucagon was

separated on a Waters 1.6 μm CORTECS C18+ 2.1 mm X 50 mm column. The column temperature was 60°C. A gradient from 15-50% organic mobile phase over 3 minutes at a flow rate of 0.25 mL/min. resolved glucagon from interferences and produced the best peak shape and intensity. Mobile phases consisted of 0.1% formic acid in either water (mobile phase A) or acetonitrile (mobile phase B). The injection volume was 25-30 μL on the 2.1 mm ID column.

All microscale LC separations were performed using a Waters ACQUITY M-Class pump and sample manager, equipped with an optional trap valve manager. Mobile phases A and B were comprised of aqueous formic acid 0.1% (v/v) and acetonitrile respectively, for all compounds. In each instance, the analytical separation device was preceded by a 300 μm X 50mm Symmetry C18 trap column. The trapping configuration is depicted in Figure 6.1. Glucagon and the insulins were separated on 150 μm X 100 mm BEH (bridged hybrid) 130Å 1.7 μm integrated microfluidic devices using the gradient conditions described in Tables 6.1A and 6.1B. Teriparatide was separated on a 150 μm X 50 mm BEH 130Å 1.7 μm integrated microfluidic device using the gradient detailed in Table 6.1C. Desmopressin, octreotide, and vasopressin were separated on a 150 μm X 50 mm HSS T3 (silica-based) 130Å, 1.8 μm integrated microfluidic device using the gradient in Table 6.1D. All separations performed on the microfluidic devices were carried out at 75° C, whilst the experiments on the Waters 1.6 μm CORTECS C18+ 2.1 mm X 50 mm column were performed at 60 °C. Higher temperature was used at microscale to help eliminate carryover.

| Time (min) | Flow Rate (μL/min) | Composition A (%) | Composition B (%) | Curve |
|------------|--------------------|-------------------|-------------------|---------|
| 0.00 | 2.00 | 85 | 15 | Initial |
| 6.00 | 2.00 | 55 | 45 | 6 |
| 6.50 | 2.00 | 15 | 85 | 6 |
| 8.50 | 2.00 | 15 | 85 | 6 |
| 9.50 | 2.00 | 85 | 15 | 6 |

Table 6.1A Gradient conditions for microscale analysis of glucagon

| Time (min) | Flow Rate (μL/min) | Composition A (%) | Composition B (%) | Curve |
|------------|--------------------|-------------------|-------------------|---------|
| 0.00 | 2.50 | 75 | 25 | Initial |
| 5.00 | 2.50 | 45 | 55 | 6 |
| 6.00 | 2.50 | 5 | 95 | 6 |
| 8.00 | 2.50 | 5 | 95 | 6 |
| 9.00 | 2.50 | 75 | 25 | 6 |

Table 6.1B Gradient conditions for microscale analysis of insulins

| Time (min) | Flow Rate (μL/min) | Composition A (%) | Composition B (%) | Curve |
|------------|--------------------|-------------------|-------------------|---------|
| 0.00 | 2.00 | 85 | 15 | Initial |
| 5.00 | 2.00 | 55 | 45 | 6 |
| 6.00 | 2.00 | 5 | 95 | 6 |
| 8.00 | 2.00 | 5 | 95 | 6 |
| 9.00 | 2.00 | 85 | 15 | 6 |

Table 6.1C Gradient conditions for microscale analysis of teriparatide

| Time (min) | Flow Rate (μL/min) | Composition A (%) | Composition B (%) | Curve |
|------------|--------------------|-------------------|-------------------|---------|
| 0.00 | 3.00 | 98 | 2 | Initial |
| 5.00 | 3.00 | 50 | 50 | 6 |
| 5.50 | 3.00 | 50 | 50 | 6 |
| 7.00 | 3.00 | 10 | 90 | 6 |
| 8.00 | 3.00 | 10 | 90 | 6 |
| 9.00 | 3.00 | 98 | 2 | 6 |

Table 6.1D Gradient conditions for microscale analysis of desmopressin, vasopressin, and octreotide

6.2.5 Sample Preparation

Teriparatide, insulin and analogs, and desmopressin, vasopressin, and octreotide were extracted according to the optimized SPE protocols described in Chapters 3, 5, and 2, respectively. Extracted sample volumes ranged from 25-100 μL of spiked human plasma. Human plasma samples spiked with glucagon were treated with a protease inhibitor cocktail and aliquots were extracted on a mixed-mode strong anion exchange, low sorbent bed volume 96-well plate. The protocol was as follows: wells were conditioned with 200 μL methanol and then equilibrated with 200 μL water. 200 μL sample was diluted 1:1 with 5% (v:v) ammonium hydroxide in water and then loaded into the wells of the 96-well plate. Samples were washed with 200 μL 5% ammonium hydroxide in water, followed by 200 μL 10% acetonitrile in water. Glucagon was eluted with 2 X 25 μL 65:25:10 acetonitrile:water:acetic acid and the final eluate was diluted with 50 μL water prior to injection.

6.3 Results and Discussion

6.3.1 Chromatographic Method Development

If microscale LC is to be implemented in a routine bioanalytical laboratory, one must first identify the column ID which is best suited for balancing the sensitivity and throughput requirements. To make a decision it was important to fully understand the sensitivity gains that were possible scaling chromatography from the microbore 2.1 mm format to the nanoflow format. A test was performed whereby a mixture of small molecules (lidocaine, propranolol, dextromethophan, fluconazole, alprazolam and verapamil) was injected (N=3) at various chromatographic scales. Figure 6.2 summarizes the sensitivity

enhancement for the series of small molecules in relation to a 2.1mm separation performed on an Acquity UPLC instrument. The same volume and concentration of the sample were injected on each column format. The data show that as the column dimension is reduced from 2.1 mm to 1 mm ID a modest two-fold gain may be realized. A 300 μm capillary may yield approximately a four-fold gain. (While Rainville et al[2] showed a 20-30X gain using a prototype 300 μm ceramic device, this was performed on a highly optimized research-grade source that is not commercially available). The 150 μm dimension appears to be an inflection point where the observed sensitivity gain begins to increase non-linearly with reduced flow rate. For this series of molecules a 4-30-fold gain was observed. Finally, a common nanoflow format of 75 μm ID provided the greatest average gain of \sim 50-fold. In general, none of the observed sensitivity increases corresponded to the expected gains, it is believed that this is largely due to extra column band broadening (which is exaggerated as the column ID is reduced) and packing efficiency differences. However, from these data, it was determined that the best balance between throughput and sensitivity can be achieved using 150 μm ID columns. Although the 75 μm ID column scale provides the greatest absolute improvements in sensitivity, the flow rates employed ($<1 \mu\text{L}/\text{min}$) result in excessively long run times of between 30 minutes to several hours. This does not yield acceptable throughput for a bioanalytical lab desiring to process an entire 96-well plate during a 24 hour period. While flow rates, and thus run times are faster when 300 μm and larger ID columns are used, the sensitivity gains are marginal when compared to those obtained from 150 μm ID columns. Flow rates of 2-5 $\mu\text{L}/\text{min}$, common for 150 μm columns, still allow for run times that are $\leq 10\text{-}12 \text{ min.}$, resulting in acceptable throughputs.

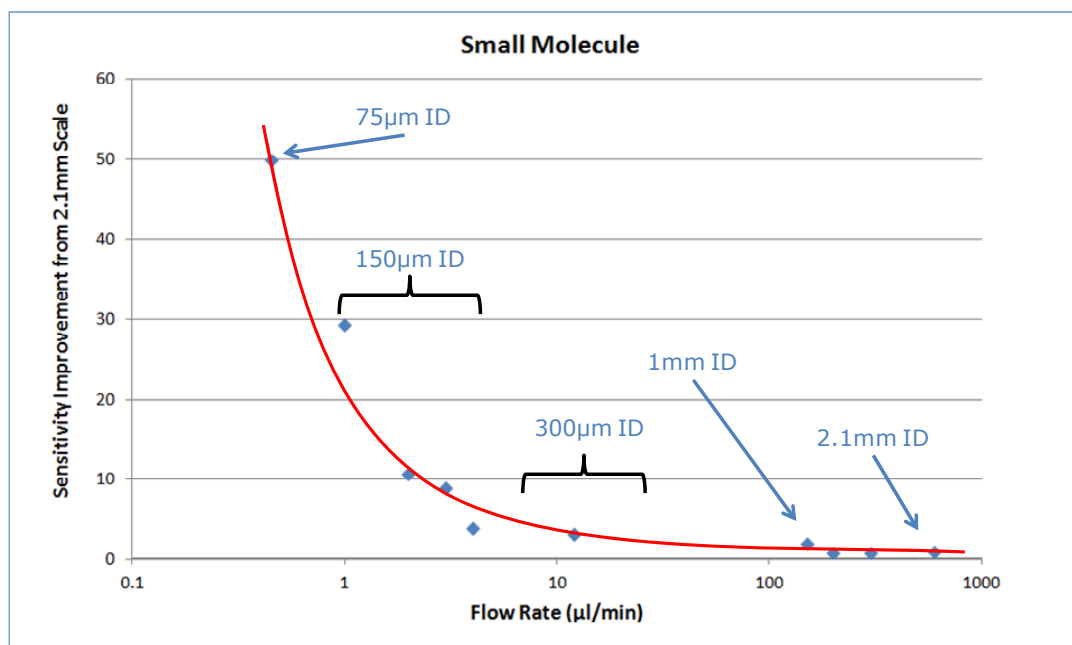


Figure 6.2 Average increase in sensitivity for a group of small molecules injected (constant volume and concentration) at various chromatographic scales from 2.1 mm to 75 μm ID. Figure reproduced with permission from Waters Corporation and James Murphy.

The aim of the work presented in this chapter was to determine whether microscale LC could be successfully implemented for bioanalytical methods for peptides. Specifically, the key question was whether its use could provide any incremental benefit in terms of sensitivity and/or reduction in sample volume requirements for methods which were *already* highly optimized and exhibited ultra-high sensitivity. In theory, decreasing the diameter of the chromatographic column (all else being equal) should improve sensitivity if an equal sample load is injected. Theoretically, the increase is a result of the ratio of the squares of the column diameters. For example, scaling from a 2.1 mm ID to a 150 μm ID column should yield a 196X increase in signal. There are, however, several factors affecting the results and the ability to fully realize this benefit from a practical standpoint. Firstly, injection volumes such as those used in Chapters 3 and 5 for teriparatide and insulin

analysis were 30 and 35 μL , respectively. This represents approximately one-fifth of the column volume of a 2.1 mm X 50mm column. This same volume injected onto a 150 μm ID column of the same length would correspond to approximately 203 times the column volume. The larger the injection volume is, relative to the column volume, the more chromatographic performance is affected by solvent composition, over-loading, and band spread. Secondly, the ability to achieve the predicted sensitivity increase also assumes that columns are packed equally as efficiently. While most 2.1 X 50 mm columns used in this study produced plate counts of approximately 9000-11000, 150 μm microfluidic devices of the same l/dp were tested in another laboratory and shown to produce plate counts closer to 3000-5000. In his book on HPLC columns and theory[5], Uwe Neue described how reducing the column diameter in order to increase sensitivity has its limitations due to injection volume/solvent effects and bandspread related processes.

The first step in transferring from 2.1mm ID scale to 150 μm was to determine the optimum flow rate, gradient time, and gradient profile. It was hypothesized that an appropriate geometric scale would provide the best starting point. However, using the insulin method as an example, scaling the flow rate and gradient time from 2.1 mm (0.25 mL/min, 4 minute gradient from 15-40% organic mobile phase) to 150 μm scale resulted in unnecessarily long run times (in excess of 30 min) and a flow rate of 1.3 $\mu\text{L}/\text{minute}$. These conditions were rapidly discarded due to a failure to meet throughput requirements. There was concern though that increasing the flow rate or gradient slope to reduce run time would degrade peak performance. This was not, in fact, the case. As a first test, the flow rate was increased to either 2 or 3 $\mu\text{L}/\text{min}$ and the gradient steepness reduced to 5 minutes in duration. Neither of these changes decreased performance, but rather resulted in improved

sensitivity and narrower peak widths. It seemed appropriate to use the same gradient profile as was used in the analytical separation as a starting point. For example, the analytical separation of insulin was achieved by linearly ramping the organic composition from 15-40% in 4 minutes, therefore the initial micro-scale conditions relied on separation at 2, 2.5 or 3 $\mu\text{L}/\text{min}$ using the same 15-40% B ramp. While this indeed produced excellent peak shapes, 2-3 seconds wide at base for all 6 of the insulins tested, optimal sensitivity was reached at the 2.5 $\mu\text{L}/\text{min}$ flow rate and by methodically adjusting the starting and ending mobile phase compositions in conjunction with gradient slope. Final conditions for insulin analysis included a linear gradient ramp from 25-55% B in 5 minutes.

The data in Chapter 2 suggest that either a 300Å pore size or positively charged surface columns might provide a further enhancement in sensitivity. Therefore three 150 μm X 50 mm columns were compared under constant gradient conditions to rapidly confirm column choice. The results are shown in Figure 6.3.

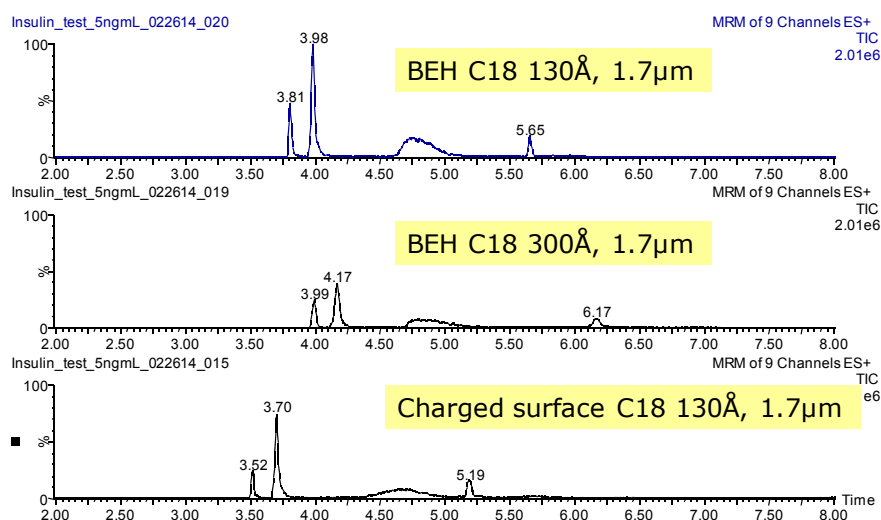


Figure 6.3 Comparison of insulin separation on 50mm x 150 μm ID columns packed with various stationary phases. The first peak in each chromatogram is insulin glargine, the second peak contains human insulin and insulin lispro, aspart, and glulisine. The last peak is insulin detemir.

The outcome was somewhat surprising in that, under microflow conditions, neither pore size nor surface charge had a positive influence. In fact, Figure 6.3 indicates that the best peak shape for all insulins and the greatest intensity were realized on a traditional hybrid C18, 130Å column. While peak shape for most insulins was comparable across the stationary phases compared, optimal peak shape for the most retentive insulin, detemir, was obtained on the BEH C18, 130Å. This stationary phase also produced sensitivity that was 50% greater than the BEH C18 300Å, and 20-50% greater than the charged surface C18, 130Å phase. The difference in behaviour between 2.1 mm scale and the microflow conditions used here can be explained quite simply by the difference in gradient slope. That is to say that the microflow conditions employed a steeper gradient (approximately 14.15 column volumes over the linear ramp time) than the 2.1 mm ID gradient (5.8 column volumes over the linear ramp). This steeper gradient would likely be expected to result in the narrower peaks that were observed.

A similar approach was taken to optimize methods for teriparatide and glucagon. The final flow rates (2 µL/min) and gradient profiles (15-45% B) were the same for each and were derived from their 2.1 mm scale methods.

Not surprisingly, a faster flow rate of 3 µL/min. could be used for the small peptide mixture without compromising performance. As these peptides are all significantly more polar than any of the larger peptides previously tested, a stationary phase designed for polar retention (high strength silica) was evaluated against the BEH C18 130Å that provided optimal performance for the larger peptides. The results are shown in Figure 6.4. Peak shape for vasopressin (the most polar and earliest eluting molecule) is improved significantly

using the high strength silica column, therefore this column was chosen for sample analysis.

Performance for desmopressin is comparable between the columns.

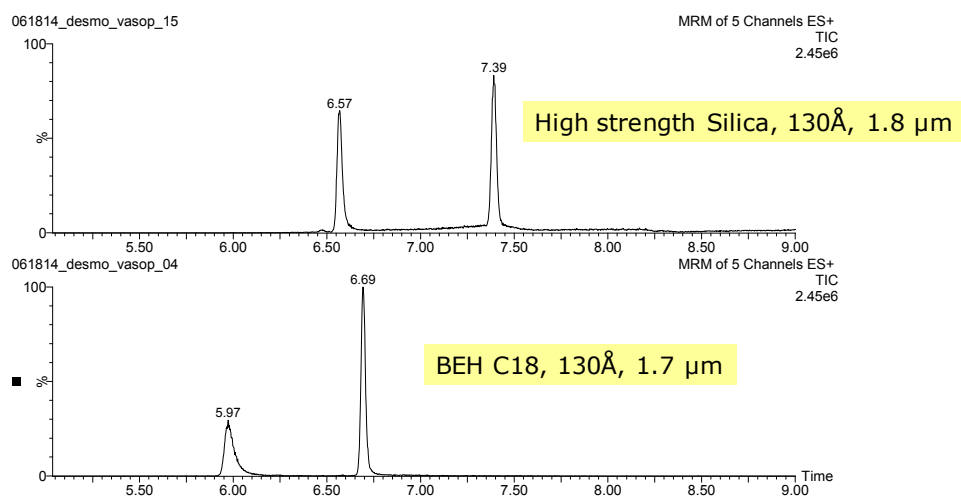


Figure 6.4 Comparison of vasopressin (first peak) and desmopressin (second peak) separation on 150 μm ID columns packed with two stationary phases.

The next step in development was to optimize injection volume. Although theory predicts nearly a 200-fold gain in increase in sensitivity if the injection volume is constant, this did not prove to be the case in actual practice. For the small molecule performance summarized in Figure 6.2, a 4-30-fold gain was observed. The same test was performed for glucagon and insulin. The results are shown in Figures 6.5A and 6.5B. The outcome of these tests in solvent standards was a 5-7-fold increase in sensitivity from microscale LC, relative to analytical scale. This data is consistent with what was observed for small molecules. Neither approaches the theoretical predictions. This is believed to be due to a combination of factors: worse efficiency values for the microscale columns, a lack of understanding of the role MS plays in influencing the observed gains, and other column related phenomena. It is not yet understood whether the fact that the ceramic channels into which stationary phase

is packed are square on the 150 μm columns, versus the cylindrical geometry that characterizes 2.1 mm columns, plays a role. One may also question whether the nature of the column hardware contributes in an unexpected way; for example are there interactions between the ceramic material and the peptides which are absent in stainless steel hardware? Unlike optical detection where the theoretical increase may be achieved more readily, when working with mass spectrometry, there are simply too many confounding factors on both sides (2.1 mm ID and microflow scale) to have a simplistic, numerical and geometric comparison between the two. It has become a multivariant problem for which we do not know all of the contributing factors.

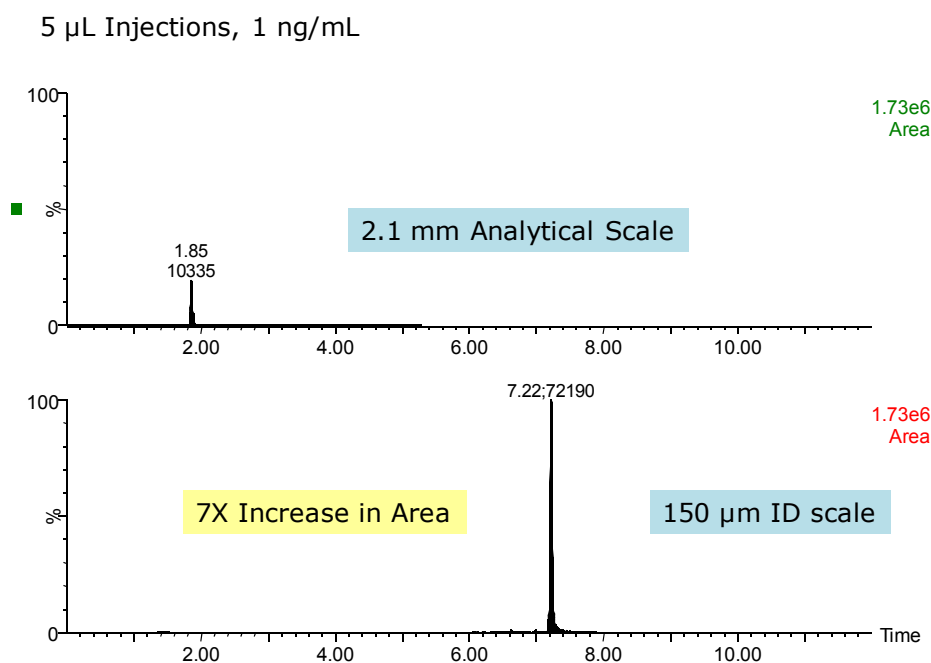


Figure 6.5A Comparison of a 5 μL injection of a 5 ng/mL standard of glucagon at analytical scale (top) and microscale (bottom)

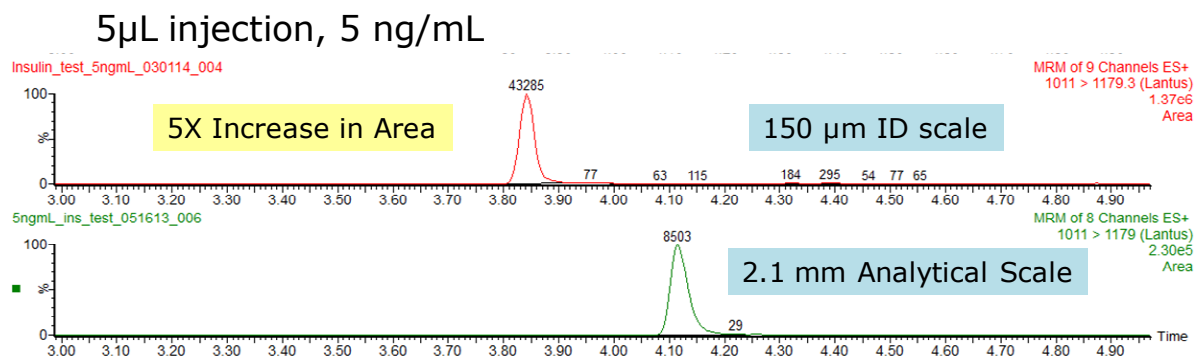


Figure 6.5B Comparison of a 5 μ L injection of a 5 ng/mL standard of insulin glargine at analytical scale (bottom) and microscale (top)

Although an increase of 5-7-fold from a 5 μ L injection is certainly a positive step, most optimized and high sensitivity bioanalytical methods have the advantage of larger injection volumes to help achieve the required detection limits. Therefore it becomes important to understand the practical injection volume limitations of the integrated microscale system. To this end, 5, 10, or 15 μ L extracted human plasma samples containing glucagon were injected onto the microscale LC/MS system. The results are shown in Figure 6.6. The data verify that peak area increases linearly up to a 15 μ L injection. This is actually rather remarkable when one considers that this would be the equivalent of injecting up to 3 mL of extracted plasma on a 2.1 mm ID scale column. The presence of the trap column is critical for re-focusing the peptides and removing residual protein. The former is largely responsible for achieving narrow peak widths in spite of large volumes of aggressive injection solvents, the latter safeguards the 150 μ m ceramic tile from over-pressuring due to excess protein load.

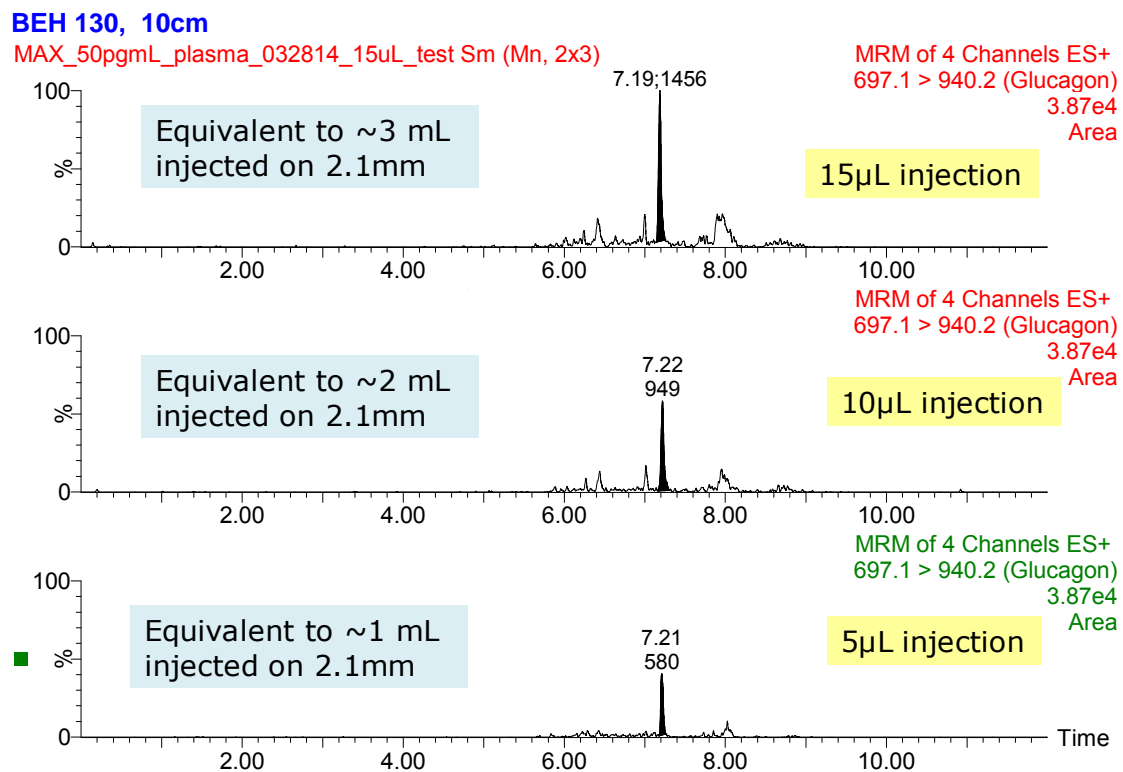


Figure 6.6 Injections of 5, 10 or 15 µL of human plasma extract containing 50 pg/mL glucagon

6.3.2 Sensitivity, Linearity, Accuracy and Precision

Using the sample preparation methods previously described, detection limits and additional validation tests were performed on human plasma samples. For each peptide tested, sample volume was minimized as much as possible without losing sensitivity relative to that achieved by the analytical scale method. A comparison of the final analytical and microscale methods for teriparatide and glucagon are shown in Figures 6.7A and 6.7B, respectively. In each case, the cumulative benefit of chromatographic scale, reduction in sample volume, and reduction in injection volume is significant, yielding an approximately 30-fold improvement for teriparatide and a 15-fold improvement for glucagon. The final method for insulins resulted in a 15-fold overall improvement in sensitivity, also derived

from reducing sample volume, reducing injection volume, and changing chromatographic scale. While the quantification limits for insulin glargine and insulin glulisine were 50 pg/mL from 250 μ L of plasma (30 μ L injection) at the analytical scale (2.1mm), an LLOQ of 25 pg/mL was readily obtained from 100 μ L of plasma using a 10 μ L injection at microscale (Figures 6.8A and 6.8B).

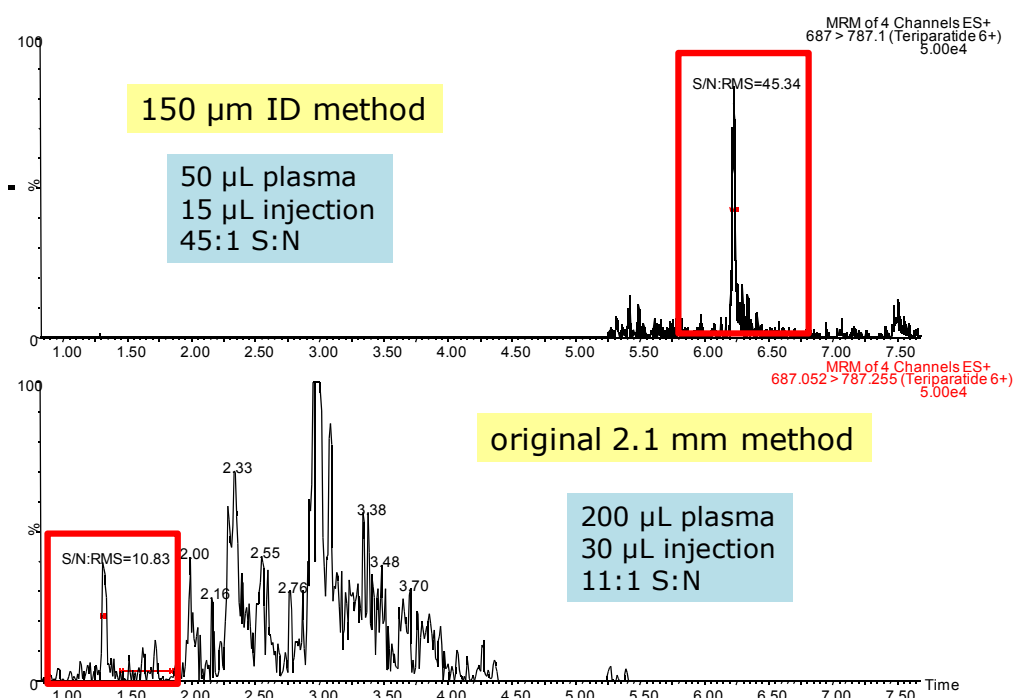


Figure 6.7A Comparison of the analysis of a 20 pg/mL teriparatide extracted plasma sample using either analytical (bottom) or microscale (top) chromatography

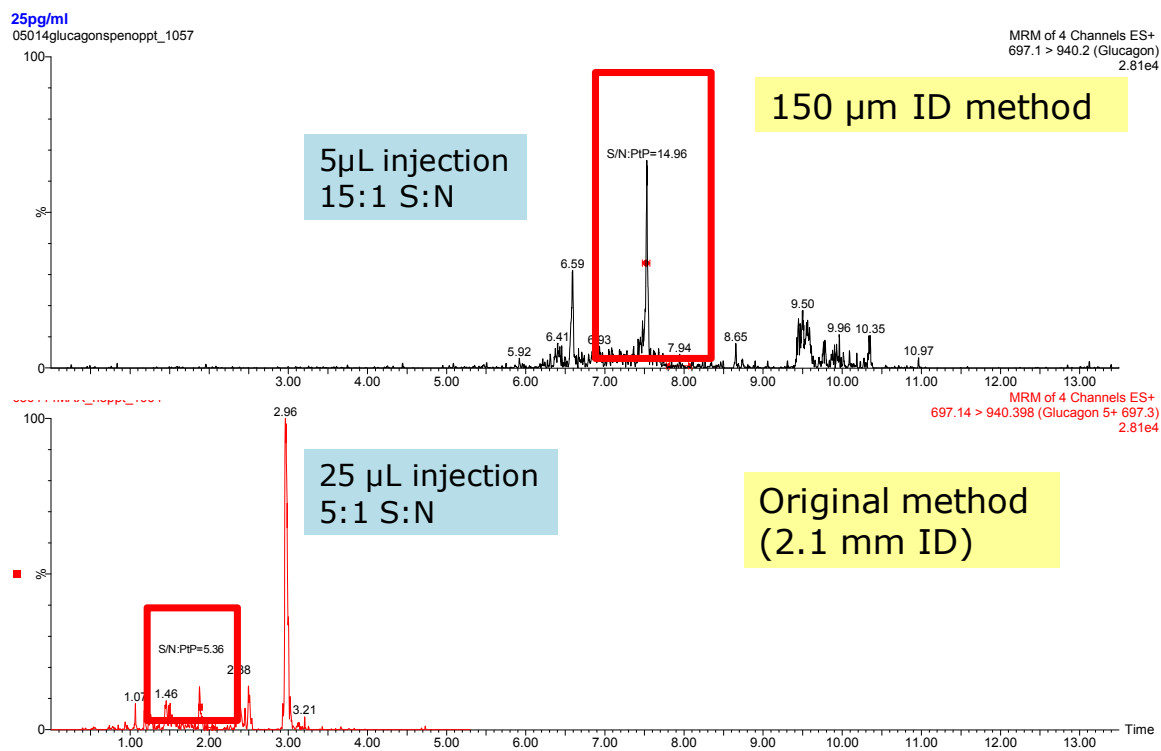


Figure 6.7B Comparison of the analysis of a 25 pg/mL glucagon extracted plasma sample using either analytical (bottom) or microscale (top) chromatography

BEH 130, 10cm, 100uL

2

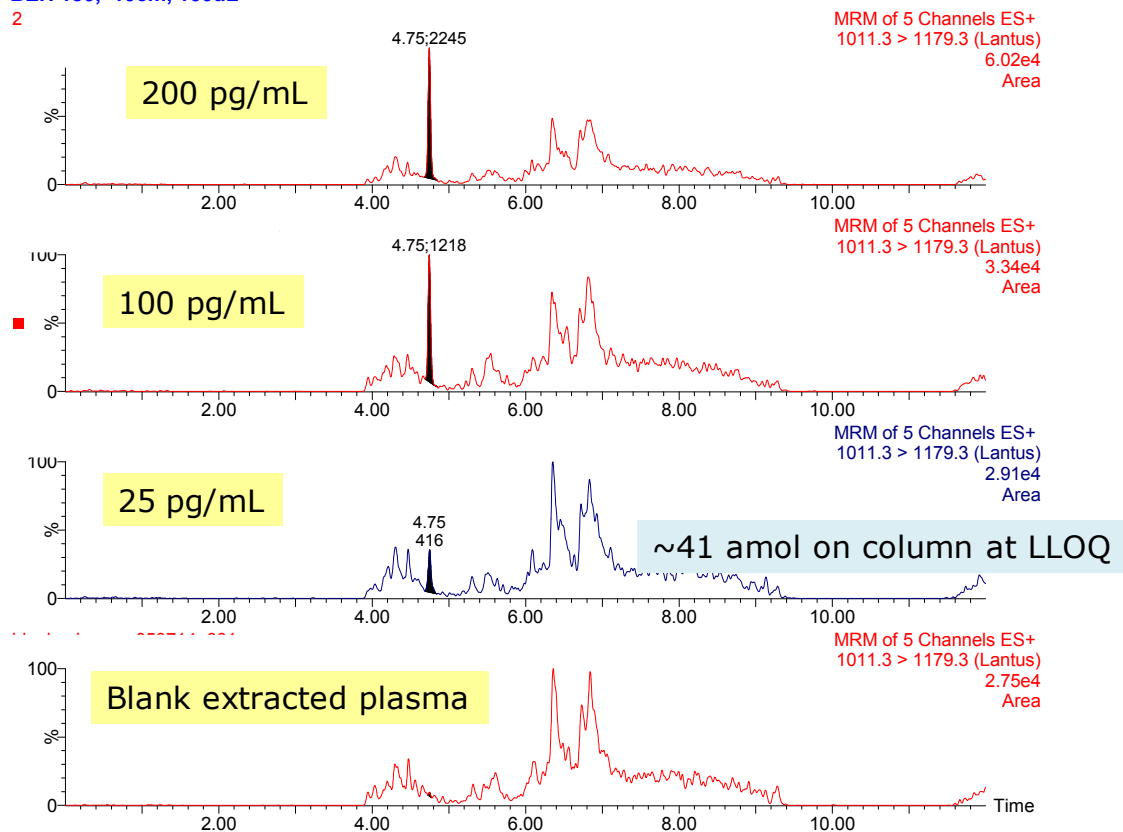


Figure 6.8A Representative chromatograms of insulin glargine at 25, 100, and 200 pg/mL compared to blank extracted plasma, separated on a 150 μ m column

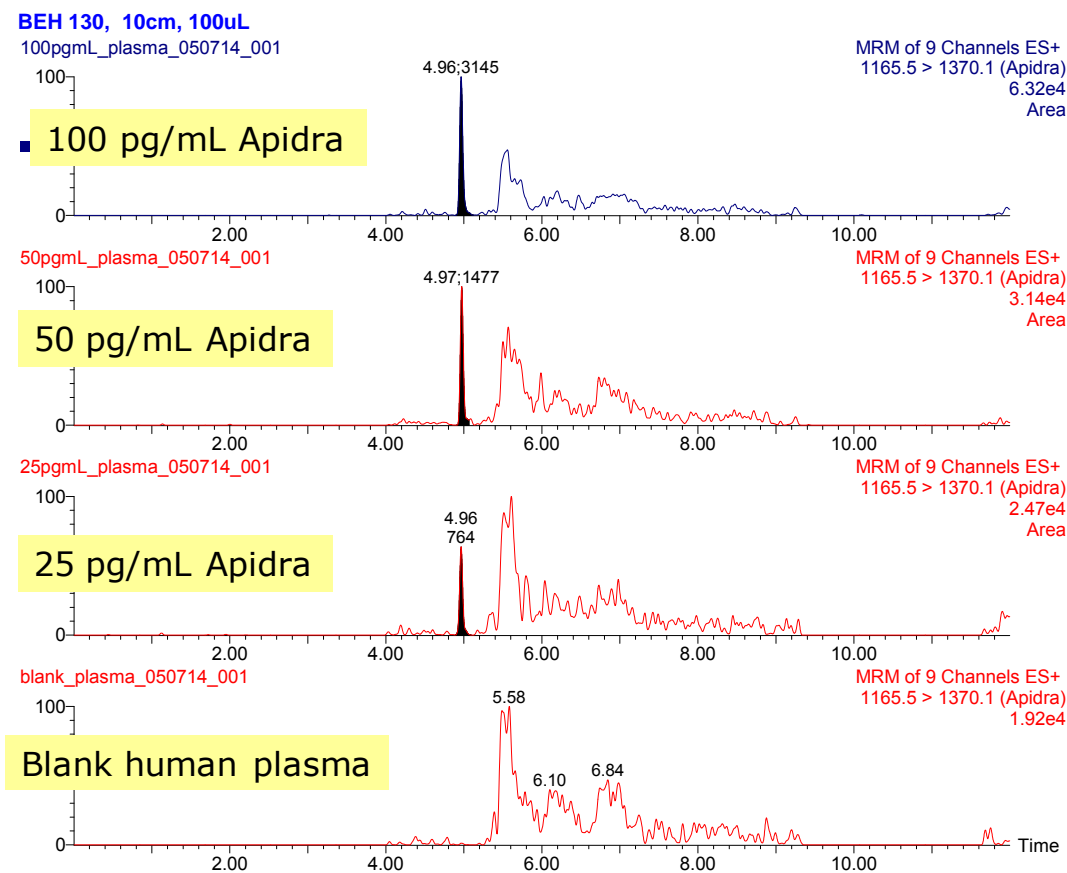


Figure 6.8B Representative chromatograms of insulin glulisine at 25, 100, and 200 pg/mL compared to blank extracted plasma, separated on a 150 μ m column

Analysis of desmopressin, vasopressin and octreotide presented the best example of maintaining sensitivity whilst significantly reducing sample volume. Chapter 2 described an optimized analytical scale method for desmopressin which achieved an LOD of 1 pg/mL from 500 μ L of plasma. Figure 6.9 (bottom panel) clearly shows that similar detection limits can be obtained from only 25 μ L of plasma using the 150 μ m ID column. A detection limit of 1 pg/mL was reached for desmopressin, vasopressin, and octreotide if 100 μ L of plasma was extracted. This is shown in Figures 6.10A-C.

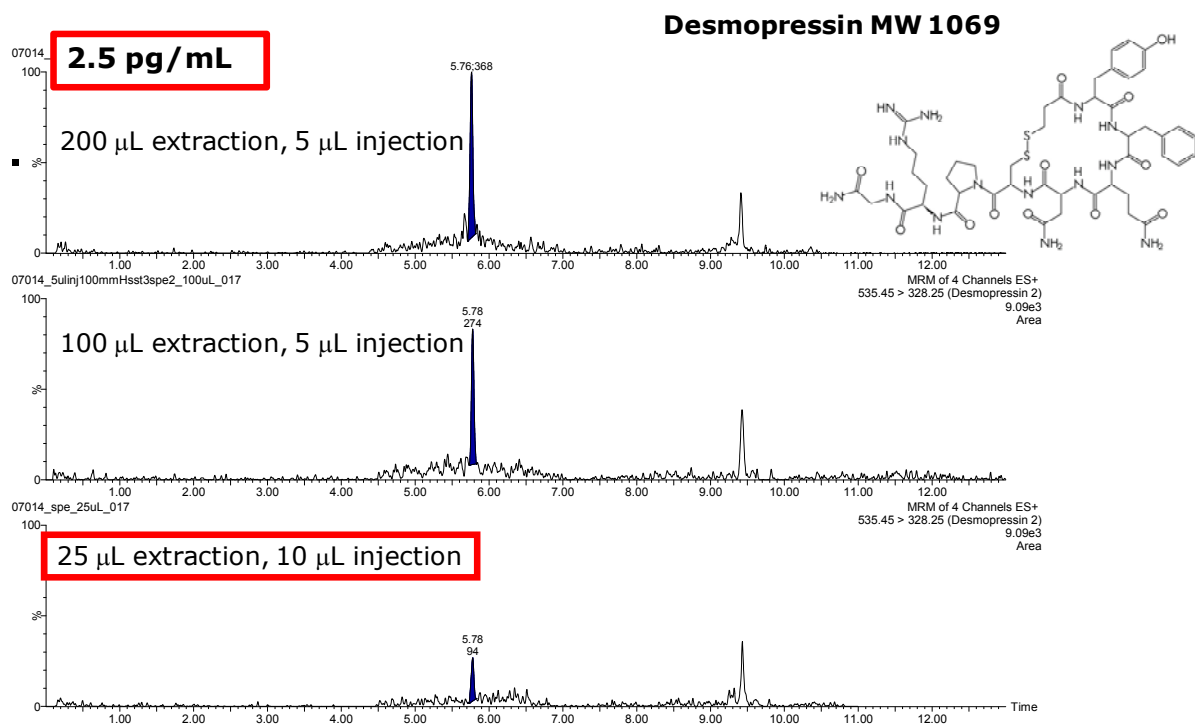


Figure 6.9 Separation of 2.5 pg/mL desmopressin from 25, 100, and 200 µL human plasma

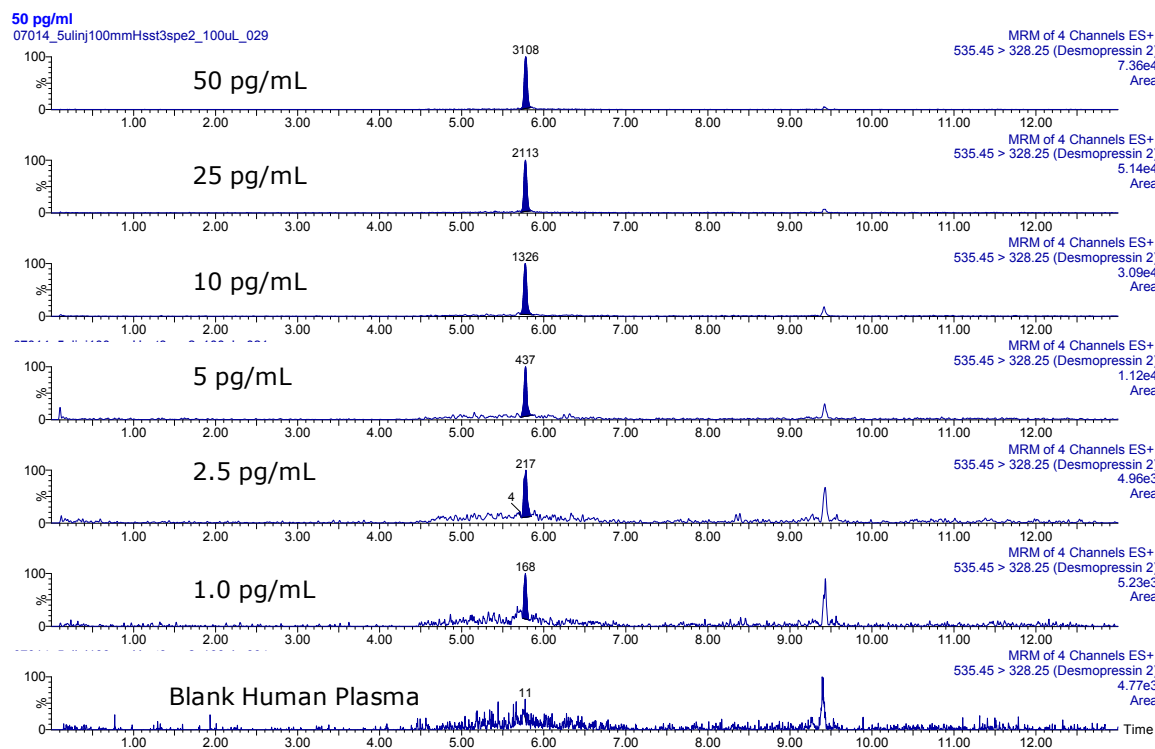


Figure 6.10A Separation of desmopressin at various concentrations, extracted from 100 μ L human plasma

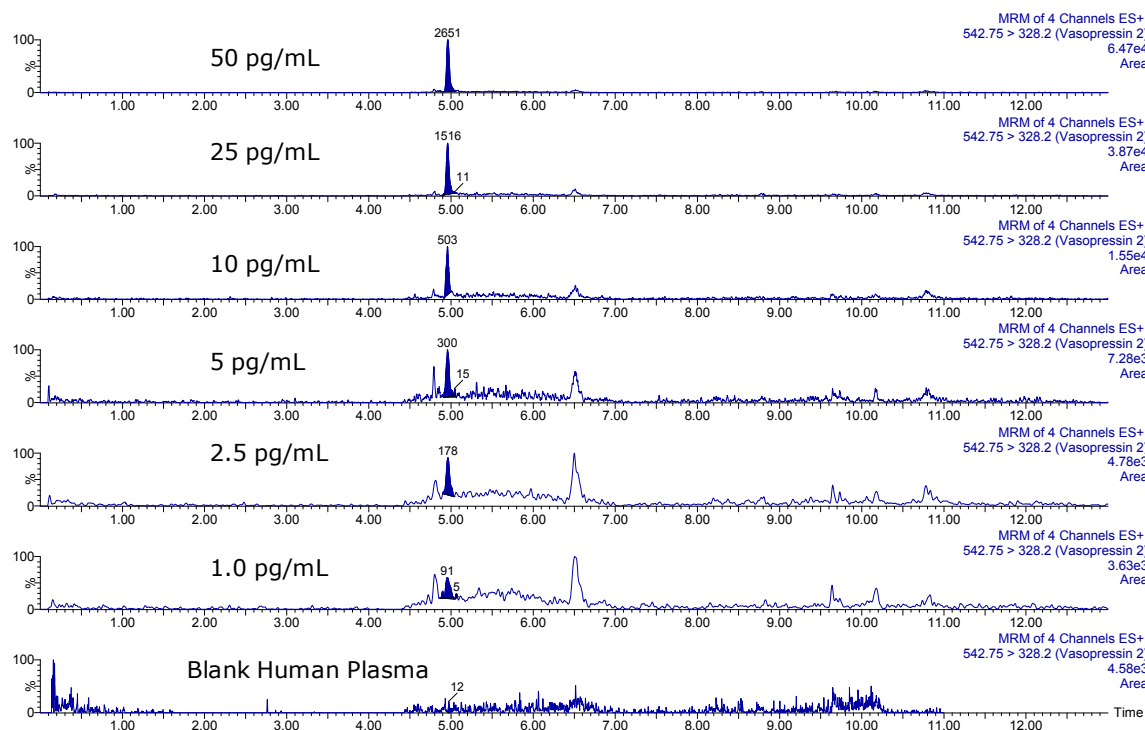


Figure 6.10B Separation of vasopressin at various concentrations, extracted from 100 μ L human plasma

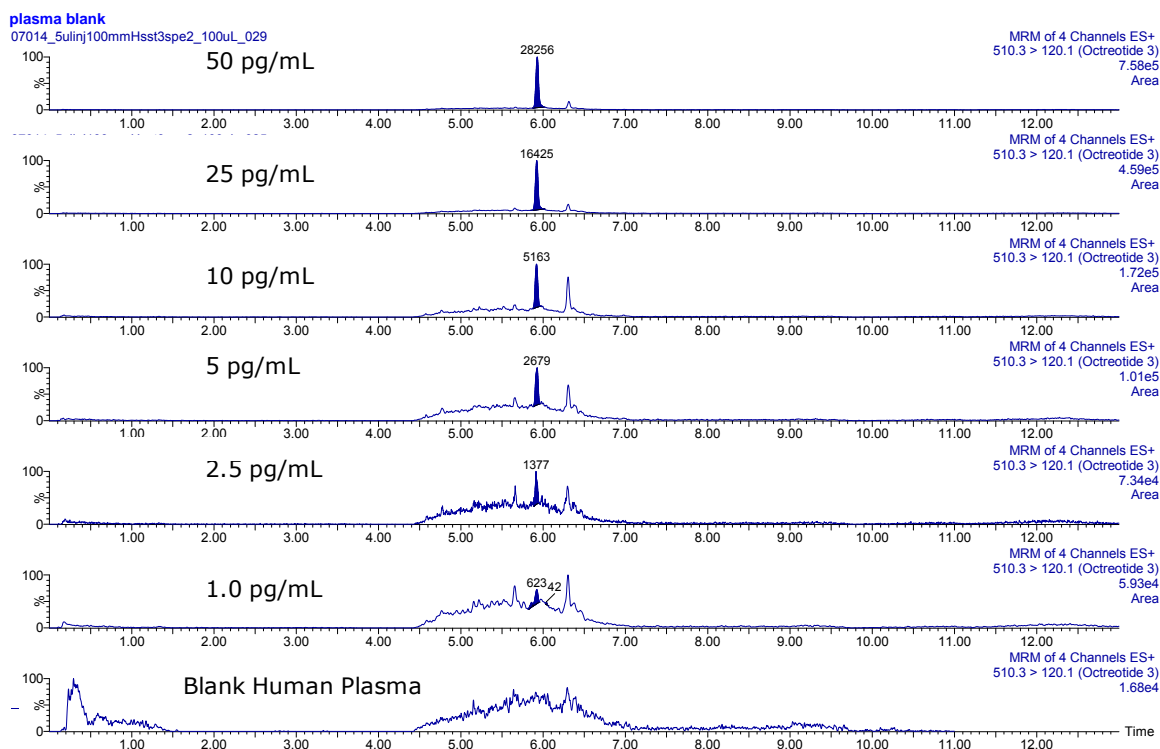
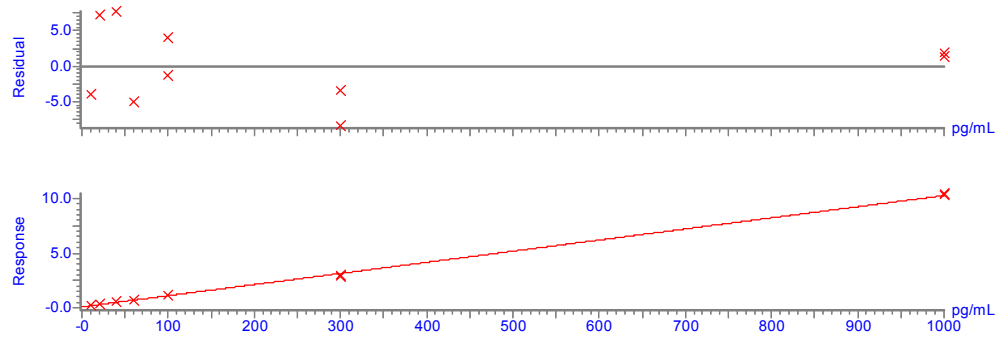


Figure 6.10C Separation of octreotide at various concentrations, extracted from 100 µL human plasma

With sensitivity established, the linear dynamic range and accuracy of the method must also be demonstrated. Stock fortified human plasma was diluted down with additional human plasma to yield final concentrations of the peptides ranging from 1 to 10,000 pg/mL. Samples were then extracted according to the method prescribed for each analyte. The linear dynamic ranges for teriparatide, glucagon, and most insulins were 1-1000, 12.5-1000, and 25-10,000 pg/mL, respectively. For the small cyclic peptides, the range was 1-2000 pg/mL. Representative standard curves for teriparatide, glucagon, and insulin gargine are shown in Figures 6.11A-C. Representative statistics for glucagon, insulin glargine, and the three cyclic peptides are summarized in Tables 6.2- 6.4. With rare exception, all calculated concentrations were within 15% of expected for all points, and within 20% of expected at the LLOQ.

Compound name: Teriparatide 687
 Correlation coefficient: $r = 0.999254$, $r^2 = 0.998508$
 Calibration curve: $0.010184 * x + 0.0879951$
 Response type: Internal Std (Ref4), Area * (IS Conc. / IS Area)
 Curve type: Linear, Origin: Exclude, Weighting: 1/x, Axis trans: None



Teriparatide Extracted from 50 μ L Human Plasma: 10-1000 pg/mL
 Linear fit and broader range than analytical

Figure 6.11A Representative standard curve for teriparatide extracted from 50 μ L human plasma, from 10-1000 pg/mL

Compound name: Glucagon 1040
 Correlation coefficient: $r = 0.998699$, $r^2 = 0.997400$
 Calibration curve: $42.6771 * x + -120.577$
 Response type: External Std, Area
 Curve type: Linear, Origin: Exclude, Weighting: 1/x, Axis trans: None

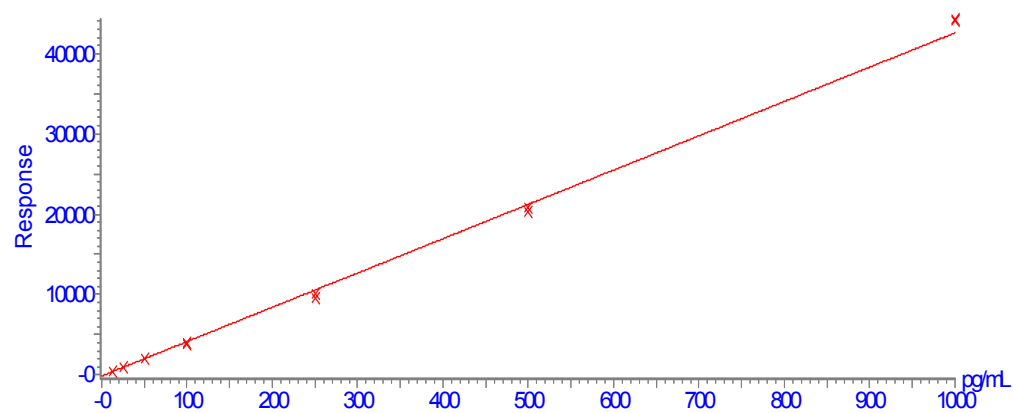


Figure 6.11B Representative standard curve for glucagon extracted from 200 μ L human plasma, from 12.5-1000 pg/mL

Compound name: Lantus
 Correlation coefficient: $r = 0.995564$, $r^2 = 0.991147$
 Calibration curve: $0.000398185 \cdot x + -0.00299844$
 Response type: Internal Std (Ref 2), Area * (IS Conc. / IS Area)
 Curve type: Linear, Origin: Exclude, Weighting: $1/x$, Axis trans: None

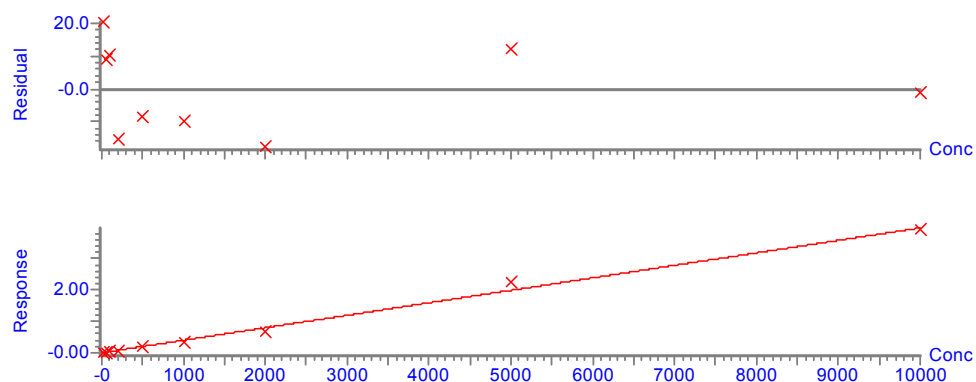


Figure 6.11C Representative standard curve for insulin glargine extracted from 50 μ L human plasma, from 25-10000 pg/mL

| Std. Conc pg/mL | Area | Calc. Conc. pg/mL | %Dev | Accuracy |
|--------------------|-------|-------------------------|------|----------|
| Blank | - | - | - | - |
| Blank | - | - | - | - |
| 12.5 | 469 | 13.8 | 10.5 | 89.5 |
| 12.5 | 461 | 13.6 | 9 | 91 |
| 25 | 982 | 25.8 | 3.3 | 96.7 |
| 25 | 959 | 25.3 | 1.1 | 98.9 |
| 50 | 2005 | 49.8 | -0.4 | 100.4 |
| 50 | 2080 | 53.5 | 6.9 | 93.1 |
| 100 | 3958 | 95.6 | -4.4 | 104.4 |
| 100 | 3733 | 90.3 | -9.7 | 109.7 |
| 250 | 10142 | 240.5 | -3.8 | 103.8 |
| 250 | 9481 | 225 | -10 | 110 |
| 500 | 20893 | 492.4 | -1.5 | 101.5 |
| 500 | 20184 | 475.8 | -4.8 | 104.8 |
| 1000 | 44244 | 1039.5 | 4 | 96 |
| 1000 | 44094 | 1036 | 3.6 | 96.4 |

Table 6.2 Representative standard curve performance statistics for glucagon extracted from human plasma

| Name | Type | Std. Conc. pg/mL | Retention Time | Area | IS Area | Conc. | %Dev |
|------------------|----------|---------------------|-------------------|--------|---------|-------|-------|
| Blank Plasma | | | 4.75 | 41 | | | |
| 25 pg/mL plasma | Standard | 25 | 4.75 | 279 | 31017 | 30 | 20.4 |
| 50 pg/mL plasma | Standard | 50 | 4.75 | 620 | 33096 | 55 | 9.2 |
| 100 pg/mL plasma | Standard | 100 | 4.75 | 1313 | 32043 | 111 | 10.5 |
| 200 pg/mL plasma | Standard | 200 | 4.75 | 2199 | 34167 | 169 | -15.4 |
| 500 pg/mL plasma | Standard | 500 | 4.75 | 5515 | 30733 | 458 | -8.4 |
| 1 ng/mL plasma | Standard | 1000 | 4.74 | 11575 | 32504 | 902 | -9.8 |
| 2 ng/mL plasma | Standard | 2000 | 4.75 | 20828 | 31912 | 1647 | -17.7 |
| 5 ng/mL plasma | Standard | 5000 | 4.76 | 59151 | 26498 | 5614 | 12.3 |
| 10 ng/mL plasma | Standard | 10000 | 4.76 | 112246 | 28524 | 9890 | -1.1 |
| | | | | | | | |
| QC 1 | QC | 150 | 4.76 | 2013 | 33144 | 160 | 6.7 |
| QC 2 | QC | 750 | 4.76 | 9477 | 33670 | 714 | -4.7 |
| QC 3 | QC | 2500 | 4.76 | 28692 | 31598 | 2288 | -8.5 |
| QC 4 | QC | 7500 | 4.75 | 90793 | 27901 | 8180 | 9.1 |

Table 6.3 Representative standard curve and QC performance statistics for insulin glargine extracted from human plasma

| Desmopressin Plasma Concentration (pg/mL) | Area | Calculated Desmopressin Concentration (pg/mL) | Mean Accuracy | Vasopressin Plasma Concentration (pg/mL) | Area | Calculated Vasopressin Concentration (pg/mL) | Mean Accuracy | Octreotide Plasma Concentration (pg/mL) | Area | Calculated Octreotide Concentration (pg/mL) | Mean Accuracy |
|--|--------|--|------------------|---|--------|---|------------------|--|---------|--|------------------|
| 1.0 | 215 | 0.95 | 94.8 | 1.0 | 107 | 0.98 | 98.9 | 1.0 | 668 | 1.06 | 106.0 |
| 2.5 | 319 | 2.58 | 103.5 | 2.5 | 193 | 2.50 | 99.9 | 2.5 | 1474 | 2.38 | 95.3 |
| 5.0 | 453 | 4.70 | 94.3 | 5.0 | 344 | 5.15 | 103.1 | 5.0 | 3017 | 4.91 | 98.1 |
| 10.0 | 898 | 11.75 | 117.5 | 10.0 | 646 | 10.50 | 104.8 | 10.0 | 5820 | 9.50 | 95.0 |
| 25.0 | 1965 | 28.63 | 114.5 | 25.0 | 1551 | 26.38 | 105.6 | 25.0 | 16404 | 26.82 | 107.3 |
| 50.0 | 3363 | 50.70 | 101.5 | 50.0 | 2781 | 48.05 | 96.1 | 50.0 | 29385 | 48.08 | 96.2 |
| 100.0 | 6376 | 98.35 | 98.4 | 100.0 | 5454 | 95.08 | 95.1 | 100.0 | 59131 | 96.77 | 96.8 |
| 250.0 | 15625 | 244.60 | 97.9 | 250.0 | 13751 | 241.10 | 96.5 | 250.0 | 149267 | 244.34 | 97.8 |
| 500.0 | 33594 | 528.68 | 105.7 | 500.0 | 28805 | 506.05 | 101.2 | 500.0 | 304504 | 498.48 | 99.7 |
| 1000.0 | 62242 | 981.60 | 98.2 | 1000.0 | 55252 | 971.53 | 97.2 | 1000.0 | 584899 | 957.52 | 95.8 |
| 2000.0 | 126145 | 1991.95 | 99.6 | 2000.0 | 115450 | 2030.98 | 101.5 | 2000.0 | 1251918 | 2049.51 | 99.7 |

Table 6.4 Representative standard curve performance statistics desmopressin, vasopressin, and octreotide extracted from human plasma

6.4 Conclusions

The data in this chapter firmly establish that LC/MS using integrated microscale LC can finally obtain the sensitivity of ligand binding assays whilst consuming only a minimum volume of sample. Sensitivity gains of 15-30-fold were realized when comparing final results from 2.1 mm ID LC/MS methods to those attained on a 150 μ m ID integrated microfluidic device LCMS system. The data acquired using this platform easily met recommended accuracy and precision guidelines[10-12] and analysis speed was adequate for high throughput bioanalytical assays. Use of integrated microscale LC shows promise for quantification of peptides from sample volumes as low as 25 μ L, facilitating single animal PK models and biomarker discovery research.

6.5 References

1. Chappell, D.L., et al., *An ultrasensitive method for the quantitation of active and inactive GLP-1 in human plasma via immunoaffinity LC–MS/MS*. *Bioanalysis*, 2013. 6(1): p. 33-42.
2. Rainville, P.D., et al., *Addressing the challenge of limited sample volumes in in vitro studies with capillary-scale microfluidic LC–MS/MS*. *Bioanalysis*, 2011. 3(8): p. 873-882.
3. Zhou, H., et al., *Measurement of apo(a) kinetics in human subjects using a microfluidic device with tandem mass spectrometry*. *Rapid Communications in Mass Spectrometry*, 2013. 27(12): p. 1294-1302.
4. Montuschi, P., *LC/MS/MS analysis of leukotriene B4 and other eicosanoids in exhaled breath condensate for assessing lung inflammation*. *Journal of Chromatography B*, 2009. 877(13): p. 1272-1280.
5. Neue, U., *HPLC Columns Theory, Technology and Practice* 1997: Wiley-VHC.
6. Johnson, J., P. Rainville, and J. Murphy, *Taking Advantage of Significant Reductions in Ion Suppression Using IonKey/MS Compared to Standard-flow LC/MS*, in *White Paper* 2013, Waters Corporation.
7. Karas, M., *Journal of the American Society for Mass Spectrometry*, 2003. 14: p. 492-500.
8. Covey, T., *Mass Spectrometry Reviews*, 2009(28): p. 870-897.

9. Fraser, I.J., et al., *The Use of Capillary HPLC with Electrospray Mass Spectrometry for the Analysis of Small Volume Blood Samples from Serially Bled Mice to Determine the Pharmacokinetics of Early Discovery Compounds*. Rapid Communications in Mass Spectrometry, 1999. 13: p. 2366-2375.
10. Bansal, S. and A. DeStefano, *Key elements of bioanalytical method validation for small molecules*. The AAPS Journal, 2007. 9(1): p. E109-E114.
11. FDA, *Guidance for Industry: Bioanalytical Method Validation*, C.a. CVM, Editor 2001.
12. FDA and CDER, *Guidance for Industry Bioequivalence Studies with Pharmacokinetic Endpoints for Drugs Submitted Under an ANDA*. 2013.

Chapter 7

Final Conclusions and Recommendations for Future Work

7.1 Final Conclusions

The focus of this research project was to improve the specificity and sensitivity of LC/MS such that it could be applied to the quantification of therapeutic and endogenous peptides. Traditional ligand binding assays (LBAs) have dominated quantitative methods for large molecules such as these, however they suffer serious shortcomings. For example, LBAs suffer from lack of standardization, variable reagents, matrix effects, poor linear dynamic range, inability to multiplex, cross reactivity and long development times. In spite of these apparent weaknesses, LBAs remain the technique of choice over LC/MS, in part due to their ability to achieve extremely low detection limits, fast analysis speeds and to minimize sample consumption. These shortcomings being amongst the LC/MS hurdles surmounted in this thesis.

The work presented in Chapter 2 encompassed LC, MS, and sample preparation in 3 sections. Each section aimed to study and identify the optimal conditions for peptide quantification. The initial investigation focused on the role that chromatographic particle size, pore size, stationary phase chemistry and particle porosity play in attaining optimal peptide separations. Relative to traditional 3.5 μm and larger particles, sub 2- μm size particles significantly extended the flow rate range under which efficient peptide separations can be performed, thus enabling the increased throughput required in bioanalytical laboratories to be achieved. In addition, the study determined that for fully porous stationary phases, both larger pore sizes (i.e. 300Å) and a positive surface charge may improve chromatographic peak shape and thus intensity, especially for peptides >2000 Da. The data showed that columns packed with newer solid-core particles also provide excellent peak shape for peptides both large and small, using flow rates which allow for adequate

throughput. The work in Chapter 2 also established the importance of temperature, flow rate, gradient slope, and mobile phase modifier selection on assay performance. This prompted the consideration to increase temperature, decrease flow rate, reduce gradient steepness and possibly add a modifier such as TFE to mobile phase B, all if greater sensitivity and/or reduced carry-over were desired. The sample preparation section examined multiple techniques in detail, and compared and contrasted all on the basis of specificity and recovery. None were deemed suitable as is, using a basic protocol designed for small molecules. This necessitated the development of an SPE method specifically for peptides, which simultaneously screened two complementary mixed-mode sorbents. The value of the ability of mixed mode sorbents to impart orthogonality onto the method selectivity as a whole was demonstrated. In addition, the use of a low-bed volume 96-well plate format allowed for concentration of the analyte without risk of adsorption related losses. Although a wide-pore sorbent prototype was tested, this served only to retain more serum albumin at the expense of the recovery of low-level peptides of interest, and therefore was not pursued. Experiments described in the mass spectrometry section resulted in concrete rules for choosing precursor and product ions. These included the recommendation to choose the highest precursor/product pairs possible, avoid immonium ions, monitor multiple MRM transitions during method development, and the importance of tuning at the chosen chromatographic flow rate was also noted, amongst other recommendations. The rules derived in this MS research became the foundation for the current scoring algorithm applied in the Waters mass spectrometry automated tuning software. Chapter 2 concluded with a comprehensive set of rules and guidelines which will facilitate the efficient

development of highly specific and sensitive methods by any researcher- novice or otherwise.

Chapter 3 implemented the strategies and recommendations from Chapter 2 to develop an assay to quantify the osteoporosis drug teriparatide. This presented a unique case where adequate recovery could not be obtained on mixed-mode sorbents as desired. Therefore, reversed-phase only SPE was used. On its own, this technique was not specific enough to enable detection at the low concentration levels required (based on dosing and systemic exposure). Extensive evaluation of various pre-treatment options resulted in the inclusion of a carefully controlled protein precipitation step to eliminate high abundance proteins such as albumin and immunoglobulins as well as other interferences. The result was a validated assay with detection limit of 15 pg/mL (3.6 pMolar) teriparatide from 200 μ L of human plasma, which permits analysis of PK samples, previously performed by radio immunoassay, by LC/MS.

Solutions for addressing non-specific binding, aggregation, and protein binding were a key part of successful quantification of amyloid β peptides, putative Alzheimer's disease biomarkers, in Chapter 4. An extensive study of surrogate matrices resulted in the identification of a surrogate based on artificial CSF containing 5% rat plasma. A parallelism study was carried out which confirmed equivalency to human CSF. The use of a guanidine HCl denaturation step increased recovery to >90% for a series of amyloid peptide isoforms studied in Alzheimer's research. This higher recovery ensured that all the amyloid peptide was accounted for and facilitated the achievement of ultra-low detection limits in human cerebrospinal fluid. This, in conjunction with exceptional accuracy and precision, made the assay an optimal platform for Alzheimer's research. In fact, this work ultimately became the

foundation for a method being progressed towards a candidate reference method for amyloid β_{1-42} through a joint effort between the Alzheimer's Association and the Global Biomarker Standardization Committee[1].

Chapter 5 presented the development of a method for simultaneous quantification of 6 intact insulins using multidimensional LC and a dual stage sample preparation scheme which included mixed-mode SPE. The final assay is the most sensitive and comprehensive LC/MS method to date. In fact it is more sensitive and significantly faster than a nano-flow LC method using affinity purification and multiple SPE processes, firmly supporting the value of the guidelines established in Chapter 2. The first section of Chapter 5 focused on overcoming the challenges that plague large peptides in particular. At almost 6000 Da, insulins actually sit on the border between large peptides and small proteins. The focus was on developing an LC/MS method which could simultaneously quantify human insulin and 5 analogs, intact, without reduction to individual chains. MS sensitivity is particularly low for large peptides such as insulin, especially for those having two amino acid chains which are stabilized by multiple disulfide bridges. This placed a greater burden on the LC and sample preparation processes to deliver the sensitivity required. A two-stage sample clean-up similar to that of teriparatide, was developed. This approach demonstrated the advantages of using both finely tuned protein precipitation and mixed-mode SPE for the quantification of these analytes. This was coupled to further on-line clean-up, at column dilution to minimize solvent effects and therefore maximize injection volume, and high m/z MRM transitions to aid specificity. Final detection limits of 50 pg/mL (8.6 fmol/mL or 8.6 pMolar) were achieved for various insulins extracted from human plasma. This allowed for detection of fasting insulin levels and identification and quantification of human insulin and analogs in a

blind study of Type I and Type II diabetic volunteers on a variety of multi-dosing regimes. The assay described in the chapter easily met regulatory guidelines for validated bioanalytical methods.

Chapter 6 addressed the issue of sample consumption, filling the final remaining gap between LC/MS assays and LBAs for routine peptide quantification. This was accomplished by employing an integrated microflow LC system to both reduce sample volume requirements and provide an incremental increase in sensitivity over what was described in earlier chapters. This chapter detailed the process and challenges encountered during scaling of analytical scale (2.1 mm ID) methods for teriparatide, insulins, and glucagon to 150 μ m ID scale. The analysis of several small cyclic peptides was also presented. In all cases, both of the primary objectives were attained. Although the “theoretical” increase in sensitivity of 196-fold was not achieved, the chapter presented the practical side of adjusting to this chromatographic scale, including the influence of injection volume, solvent effects, and optimization. Moreover, it set appropriate expectations for adapting highly optimized analytical scale methods, such as those presented in Chapters 3 and 5 where injection volumes of 30-35 μ L were common, through to microscale. In comparison with the standard LC/MS 2.1 mm chromatographic scale, sensitivity increases of 15-30X were realized. For the smaller cyclic peptides, integrated microscale LC enabled a 20-fold reduction in plasma volume required. The work described in this chapter paves the way for peptide analysis from dried blood spots, rodent species, and pediatric patients. These studies also demonstrated the utility of microscale LC in biomarker discovery research where sample available for bioanalysis is limited due to the multitude of tests that must be performed on that sample.

In summary, this thesis has shown that, following the guidelines developed herein, LC/MS can provide both the sensitivity and specificity to enable direct, ultra high sensitivity quantification of therapeutic and endogenous peptides in biological fluids for biomarker research, drug development and monitoring, or forensic/doping applications.

7.2 Recommendations for Future Work

During the course of this research several areas of possible future focus were identified which have the potential to provide even greater sensitivity gains and /or specificity improvements over what has been achieved to date.

1. Research aimed at establishing/confirming a correlation between CSF and plasma amyloid beta levels would require a more specific method for amyloid quantification by LC/MS than that described in Chapter 4. Therefore, it may be useful to combine mixed-mode SPE with 2D chromatography for amyloid beta peptides in plasma. This would include analysis in the first dimension using a low pH mobile phase followed by heart-cutting the amyloid fraction onto a second analytical dimension using a high pH mobile phase.
2. Another option that may prove beneficial for improving sensitivity for amyloid peptides would be the use of a microflow LC/MS system. Current low flow systems have limited pH stability primarily due to the presence of fused silica in the system construction, whose polyimide coating dissolves at elevated pH. Analysis would have to be performed at a $\text{pH} \leq 10$, which is lower than the current analysis, however, this is worth investigating.

3. The microflow experiments described in Chapter 6 showed great promise for ultra-high sensitivity peptide quantification, particularly in cases where sample volume is limited. These benefits may be further augmented through the use of 2D microflow. This could include two analytical dimensions such as HILIC/ RP, low pH/high pH, or other configurations.
4. Recently, the sensitivity of accurate mass instrumentation has approached that of triple quadrupole instruments. Significant background signal reduction is possible by employing accurate mass detection through the extraction of very narrow mass range windows. This combined with mixed-mode SPE or other pre-fractionation techniques may result in adequate/improved detection limits. A further extension of this could include ion mobility to improve selectivity.
5. While traditional C18 (both silica and hybrid particles) and charged surface stationary phases were evaluated in Chapter 6 for use in microflow separations, all were fully porous particles. Chapter 5 demonstrated the incremental benefit of solid core particles for insulin quantification. It would be interesting to investigate any benefit that might be derived from their use at microflow scale.
6. Chapter 6 established that the theoretical increase in sensitivity scaling from a 2.1 mm ID to a 150 μ m ID column should be 196-fold, if all else were equal. The average improvement actually obtained ranged from 5-30-fold, this is significantly different from the theoretical value. An investigation into why the theoretical increase is not realized might highlight parameters/processes that could improve this performance.

7. Finally, Chapter 2 described an orthogonal and highly selective sample preparation strategy based on mixed-mode SPE. A study which assesses the benefits of HILIC or pure ion exchange SPE for the pre-fractionation of therapeutic, endogenous biomarker peptides or proteins (including monoclonal antibodies and antibody drug conjugates) prior to analysis by LC/MS may produce a useful alternative sample preparation technique.

7.3 References

1. Pannee, J., et al., *Round robin test on quantification of A β 42 in CSF by mass spectrometry*. Alzheimer's & Dementia, 2014. submitted manuscript.